P A L A C K Ý U N I V E R S I T Y I N O L O M O U C

F A C U L T Y O F S C I E N C E

DEPARTMENT OF BOTANY & LABORATORY OF GROWTH REGULATORS

Jan F. Humplík

A ROLE OF ABSCISIC ACID IN TOMATO (*SOLANUM LYCOPERSICUM* L.) EARLY SEEDLING DEVELOPMENT

Ph.D. THESIS

Ph.D. PROGRAM OF BIOLOGY – BOTANY

Supervisor: Doc. RNDr. Martin Fellner, Ph.D.

Supervisor specialist: Véronique Bergougnoux, Ph.D.

Olomouc

2015

DECLARATION

I hereby declare that the work presented in this manuscript is my own and was carried out entirely with help of literature and aid cited in the manuscript.

In Olomouc on

BIBLIOGRAPHICAL IDENTIFICATION

Author's first name and surname: Jan Humplík

Title: A role of abscisic acid in tomato (*Solanum lycopersicum* L.) early seedling development

Type of thesis: Ph.D. thesis

Department: Department of Botany

Supervisor: Doc. RNDr. Martin Fellner, Ph.D.

Supervisor specialist: Véronique Bergougnoux, Ph.D.

The year of presentation: 2015

Abstract:

This Ph.D. thesis is dedicated to physiological effects of abscisic acid (ABA) during early development of tomato seedlings. More specifically, it is focused on the influence of ABA on hypocotyl elongation. The aims of the thesis are:

1. Systematic study of the ABA metabolic changes during early development of tomato seedlings.
2. Physiological study of the effects of endogenous ABA in the early development especially in the growth of hypocotyl of etiolated seedlings.
3. Cellular and molecular study of potential mechanisms of ABA action in the growth of etiolated tomato hypocotyls.

First experiments were performed to analyze changes in the endogenous ABA content during seed imbibition, germination, etiolated and de-etiolated growth of tomato seedlings. It was observed that after dramatic decrease of ABA during seed germination in the dark, the ABA content increases again after the radicle protrusion. Interestingly, this increase in ABA was double-fold higher in the etiolated seedlings in comparison to the same aged seedlings that were grown after germination in blue-light. The corresponding pattern was observed also in the expression of key gene for ABA biosynthesis in tomato *LeNCED1*. Further, the effect of ABA-deficiency in the growth of etiolated hypocotyl was studied using two mutants *sitiens* and *notabilis* that are impaired in different steps of ABA biosynthesis. The reduced hypocotyl growth in the mutants was observed when compared to the wild-types (WTs). When the exogenous ABA (100 nM) was added to the mutants their hypocotyl growth was improved to the WTs levels. The treatment of WT by ABA has no effect on hypocotyl elongation up to concentration of 1 µM, higher concentration led to the growth inhibition. The effect of ABA-deficiency was also mimicked by using of inhibitor of ABA biosynthesis fluridone that caused reduced hypocotyl elongation in etiolated WT seedlings. Detailed analysis of the mutant *sitiens*

showed that ABA-deficiency led to the reduced growth of epidermal cells in etiolated hypocotyl. Since important factors in cell expansion are endopolyploidic cycles, the flow-cytometry analysis of DNA content was performed. The importantly reduced number of endoreduplicating cells was observed in the *sitiens* mutant in comparison with the WT. In parallel, the reduced expression of the cyclin-dependent kinases inhibitory proteins (ICK/KRPs) that affect the rate of endoreduplication in plants was observed in mutant hypocotyls. When the exogenous ABA was applied, these cellular and molecular parameters were improved to the levels of WT. In other experiments it was shown that ABA-deficiency caused overproduction of certain cytokinin metabolites and highly increases overall cytokinin content. Cytokinins support cell division but inhibit DNA endoreduplication and cell expansion, causing the inhibition of hypocotyl growth. The subsequent analysis of cytokinins showed important increase especially in isopentenyladenine metabolites in de-etiolated WT seedlings. De-etiolation was induced by blue-light that is strong inducer of plant photomorphogenesis. Based on the results, we concluded that in dark conditions ABA supports the growth of etiolated hypocotyls via inhibition of cytokinin biosynthesis and stimulation of DNA endoreduplication and cell expansion. Conversely, cultivation of seedlings in light conditions leads to the inhibition of ABA synthesis, stimulation of cytokinins (especially of isopentenyladenine metabolites) and to subsequent reduction in the DNA endoreduplication and cell expansion that finally leads to the inhibition of hypocotyl growth. Thus endogenous abscisic acid should not be considered as general inhibitor of plant growth, since a least in tomato early seedling development it works as a growth promoter.

Keywords: abscisic acid, blue-light, cytokinins, de-etiolation, endopolyploidy, endoreduplication, etiolated growth, hypocotyl, *notabilis*, photomorphogenesis, seedling development, *sitiens*, skotomorphogenesis, *Solanum lycopersicum* L., tomato

Number of pages: 116

Number of appendices: 1

Language: English

BIBLIOGRAFICKÁ IDENTIFIKACE

Jméno a příjmení autora: Jan Humplík

Téma: Úloha kyseliny abscisové v raném vývoji semenáčku rajčete (*Solanum lycopersicum* L.)

Druh práce: doktorská disertační

Katedra: Katedra botaniky

Školitel: Doc. RNDr. Martin Fellner, Ph.D.

Školitel specialista: Véronique Bergougnoux, Ph.D.

Rok obhájení práce: 2015

Abstrakt:

Disertační práce je věnována fyziologickým účinkům kyseliny abscisové (ABA) v raném vývoji semenáčků rajčete, konkrétně jejím vlivem na prodlužování hypokotylů. Cíle této práce jsou:

1. Systematická studie metabolických změn ABA v průběhu rané ontogeneze semenáčků rajčete a jejich ovlivnění světlem.

2. Studium fyziologických účinků změněné hladiny ABA na vývoj semenáčků rajčete.

3. Zkoumání možných mechanismů účinků ABA na buněčné a molekulární úrovni.

První typ experimentů se zabýval změnou hladiny ABA v průběhu bobtnání, klíčení, etiolovaného a světelného růstu semenáčků rajčete. Bylo zjištěno, že po počátečním prudkém poklesu hladiny ABA v průběhu klíčení, dochází po vyklíčení k nárůstu hladiny endogenní ABA v semenáčcích. Tento nárůst byl přibližně dvojnásobně větší u etiolovaných rostlin ve srovnání se stejně starými rostlinami, které po vyklíčení ve tmě byly přeneseny na modré světlo. Obdobná reakce byla zjištěna i u exprese klíčového biosyntetického genu pro ABA *LeNCED1*. Dále byl hodnocen růst dvou etiolovaných mutantů rajčete *sitiens* a *notabilis*, mutovaných v rozdílných krocích biosyntézy ABA. Bylo pozorováno, že mutované semenáčky, mají zkrácený růst hypokotylu. Pokud byla k mutantům přidána exogenní ABA (100 nM) růst hypokotylu mutovaných rostlin se zcela vyrovnal růstu nemutované kontroly. Na nemutované semenáčky (WT) neměla exogenní aplikace v koncentracích do 1 µM žádný vliv, vyšší koncentrace vedly k inhibici jejich růstu. Vliv nedostatku ABA na růst etiolovaných hypokotylů, byl rovněž studován aplikací inhibitoru biosyntézy ABA fluridonu, který také vedl k inhibici růstu. Detailní analýza mutanta *sitiens* ukázala, že nedostatek ABA vede k inhibici expanze epidermálních buněk hypokotylu. Jelikož jedním z významných faktorů ovlivňujících buněčnou expanzi jsou endopolyploidizační cykly, byla provedena analýza obsahu DNA v buňkách hypokotylu mutantních a WT rostlin pomocí průtokové cytometrie. Zde byl pozorován významný pokles počtu endoreduplikujících buněk u mutanta *sitiens* ve srovnání s WT. Zároveň byla prokázána

snížená exprese genů kódujících inhibitory cyklin-dependetních kináz (ICK/KRP), které endoreduplikaci podporují. Po aplikaci exogenní 100nM ABA došlo ke srovnání zmíněných parametrů na úroveň WT. V dalších experimentech bylo zjištěno, že nedostatek ABA vede k výrazné nadprodukci některých cytokininových metabolitů. Cytokininy podporují buněčné dělení na úkor endoreduplikace a vedou tak k inhibici buněčné expanze a následně také k inhibici růstu hypokotylu. Na základě získaných výsledků, byl vyvozen závěr, že ve tmě ABA přispívá k růstu etiolovaných hypokotylů, tím že inhibuje biosyntézu cytokininů, podporuje endoreduplikaci DNA a buněčnou expanzi. Naopak, za světelných podmínek dochází k inhibici syntézy ABA a ke zvýšené syntéze cytokininů, k inhibici buněčné expanze ve prospěch dělení a diferenciace buněk. Endogenní kyselina abscisová by tedy neměla být generalizována jako inhibitor růstu, jelikož minimálně v podmínkách raného vývoje semenáčků rajčete působí jako stimulátor.

Klíčová slova: kyselina abscisová, modré světlo, cytokininy, de-etiolace, endopolyploidie, endoreduplikace, etiolovaný růst, hypokotyl, *notabilis*, photomorphogeneze, vývoj semenáčku, *sitiens*, skotomorphogeneze, *Solanum lycopersicum* L., Rajče jedlé

Počet stran: 116

Počet příloh: 1

Jazyk: anglický

O. A. M. D. G.

Dedicated to my wife and my sons.

ACKNOWLEDGEMENTS

At a first I would like to thank to my supervisors Dr. Véronique Bergougnoux and Dr. Martin Fellner for their supervision, helpful advices and valuable discussions during the laboratory practice as well as during the writing of manuscripts and this thesis. I wish to acknowledge all my colleagues from the Laboratory of Growth Regulators, namely Prof. Miroslav Strnad, Dr. Lukáš Spíchal, Dr. Ondřej Novák, Dr. Aleš Pěnčík, Dr. Jakub Rolčík, Ms. Jana Balarynová, Mrs. Jana Kundratová for their help and support in the discussion of the results and in the laboratory practice. I am grateful to Mrs. Renáta Plotzová and Mrs. Věra Chytilová for their excellent technical assistance and help with the experiments.

I am thankful to my family for their big patience and support during my doctoral study, without them I would never finish my work.

CONTENT

ABBREVIATIONS

AAO	abscisic aldehyde oxidase
ABA	abscisic acid
aba2	*abscisic acid deficient 2*
ABA-GE	ABA-glucosyl ester
ABI	ABA Insensitive
ABRE	ABA response element
ABRE	ABA response element
ACC	1-aminocyclopropane-1-carboxylic acid
ARF	Auxin Response Factor
BL	blue light
BRs	brassinosteroids
CDK	Cyclin-Dependent Kinase
CE	Coupling Element
Chl	chlorophyll
ChlH	chloroplast-localized Mg^{2+} chelatase
CKs	cytokinins
CRY	cryptochrome
*c*Z	*cis*-Zeatin
*c*Z9G	*cis*-Zeatin-9-N-glucoside
*c*ZOG	*cis*-Zeatin-O-glucoside
*c*ZR	*cis*-Zeatin riboside
*c*ZRMP	*cis*-Zeatin riboside-5'-monophosphate
*c*ZROG	*cis*-Zeatin riboside-O-glucoside
DAG	days after germination
DHZ	Dihydrozeatin
DHZ7G	Dihydrozeatin-7-N-glucoside
DHZ9G	Dihydrozeatin-9-N-glucoside
DHZOG	Dihydrozeatin-O-glucoside
DHZR	Dihydrozeatin riboside
DHZRMP	Dihydrozeatin riboside-5'-monophosphate
DHZROG	Dihydrozeatin riboside-O-glucoside
DLH	digital length of hypocotyl
DMSO	dimethyl sulfoxide
DREB	Drought Response Element Binding
ein	*ethylene insensitive*
ERF	Ethylene response factor
ETR	Ethylene receptor
flc	*flacca*
FR	far-red light
FT	Flowering Locus T

GAMyb	GA-induced transcription factor
GARE	GA response element
GAs	gibberellins
gin1	*glucose insensitive 1*
GPA	heterotrimeric G-proteins
GTG	G-protein coupled receptor
GTGs	G-protein coupled receptors
HAI	Highly ABA Induced
HIRs	high-irradiance responses
HY5	long hypocotyl 5
IAA	indole-3-acetic acid (natural auxin)
ICK/KRP	Inhibitor of CDK/KIP-related protein
iP	isopentenyladenine
iP	isopentenyladenine
iP7G	isopentenyladenine-7-N-glucoside
iP9G	isopentenyladenine-9-N-glucoside
iPR	isopentenyladenine riboside
iPRMP	isopentenyladenine riboside-5'-monophosphate
JA	jasmonic acid
LFR	low-fluence responses
LOG	Lonely-Guy
MEP	2-C-methyl-D-erythritol-4-phosphate
MS	Murashige and Skoog medium
MVA	mevalonate
NAA	1-naphthaleneacetic acid (synthetic auxin)
NCED	9-cis-epoxycarotenoid dioxygenase
not	*notabilis*
NPQ	non-photochemical quenching
OST	Open Stomata
Pfr	far red-light absorbing form of phytochrome
PHOT	phototropin
PHY	phytochrome
PHYA	phytochrome A
PHYB	phytochrome B
PIF	Phytochrome Interacting Factor
PLD	Phospholipase D
PP2C	Protein Phosphatase 2C
Pr	red-light absorbing form of phytochrome
PSB	Plant Signaling and Behavior journal
PYL	Pyrabactin Resistant-Like

PYR/PYL/RCARs	Pyrabactin Resistant/Pyrabactin Resistance-1 like/Regulatory Component of ABA receptor
PYR1	Pyrabactin Resistant 1
RCAR	Regulatory Component of ABA Receptor
RGR	relative growth rate
RL	red light
SAM	shoot apical meristem
SDR	Short-chain Dehydrogenase/Reductase
sit	*sitiens*
SnRK2	SNF1-Related protein Kinase 2
SOM	SOMNUS gene
STS	silver thiosulphate
*t*Z	*trans*-Zeatin
*t*Z7G	*trans*-Zeatin-7-N-glucoside
*t*Z9G	*trans*-Zeatin-9-N-glucoside
*t*ZMP	*trans*-Zeatin riboside-5'-monophosphate
*t*ZOG	*trans*-Zeatin-O-glucoside
*t*ZR	*trans*-Zeatin riboside
*t*ZROG	*trans*-Zeatin riboside-O-glucoside
VAL	VP1/ABI3-like
VFLRs	very low-fluence responses
VP	Viviparous
WT	wild-type
ZEP	zeaxanthin epoxidase
Φ_{NPQ}	quantum yield of regulatory light-induced non-photochemical quenching
Φ_{P}	actual quantum yield of PSII photochemistry for a light adapted state
Φ_{Po}	maximal quantum yield of PSII photochemistry for a dark-adapted state

1. INTRODUCTION

The early seedling development occurring immediately after seed germination represents a very unique biological situation – the true metamorphosis. In this process the heterotrophic organism that is fully dependent on its storage reserves completely reprograms and rebuilds its modus of life to became autotrophic, "light-consuming entity." Even more than 200 years ago a great poet and natural philosopher Johann Wolfgang Goethe was fascinated by the transformation power of the plants and described the first ontogenetic steps in his essay *The Metamorphosis of the Plants* (*Versuch die Metamorphose der Pflanzen zu erklären*):

> *Bursts from the seed so soon as fertile earth*
> *Sends it to life from her sweet bosom, and*
> *Commends the unfolding of the delicate leaf*
> *To the sacred goad of ever-moving light!*
> *Asleep within the seed the power lies,*
> *Foreshadowed pattern, folded in the shell,*
> *Root, leaf, and germ, pale and half-formed.*
> *The nub of tranquil life, kept safe and dry,*
> *Swells upward, trusting to the gentle dew,*
> *Soaring apace from out the enfolding night.*
> *Artless the shape that first bursts into light—*
> *The plant-child, like unto the human kind—*
> … (Goethe 1790).

From the time of Goethe the modern science did tremendous progress in the revealing of substantial actions leading to the establishment of mature plant. Despite these progresses there are still many particular questions in plant physiology that are waiting for solutions or at least reliable hypotheses. One of them is the role of the abscisic acid (ABA) – important regulator of plant growth – in the etiolated (skotomorphogenic) growth, de-etiolation and photomorphogenesis. The role of ABA in the growth of young seedlings is often deduced from the effects of exogenous ABA treatment on adult plants, especially in the stress conditions. As shown in the review part, these studies usually conclude that ABA plays inhibitory role in the plant growth from the germination stage to the mature plant. On the contrary, there is important number of reports concluding opposite growth-promoting effects of especially endogenous ABA in adult plants. These contradictions should induce an impulse for scientific community to focus on this field of plant physiology and to bring new light to the essential processes of early development of plants. Thus, this doctoral thesis is dedicated to early seedling growth and tries to answer the question whether the naturally occurring (endogenous) ABA plays the stimulatory or inhibitory role in this process. The doctoral thesis is composed as compilation of published reports together with unpublished literature review and some newer results intended for publication in close future. Among the literature review the core of the thesis form chapters 6 and 7 (published also in *PlosOne* and *Plant Signaling &*

Behavior) and chapter 8. After the thesis conclusion, in the Appendix part, other publications of the author that are not directly related to topic of the thesis but belong to the field of plant physiology are attached as well.

2. AIMS AND SCOPE

Although the topic of the thesis covers wide part of plant development we focused mainly on the "earliest" part of seedling life – the etiolated growth. The etiolated growth (skotomorphogenesis) provides a good model to study ABA role because it is characterized by enormous hypocotyl elongation. Thus it could be easily correlated with effects of changed ABA content. Some experiments were also performed in contrasting conditions of blue-light that is a strong inhibitor of hypocotyl growth. Until recently the role of ABA and more specifically endogenous ABA in these processes was poorly investigated and particular mechanism of ABA action was unknown.

The main aims of this doctoral thesis were:

1. Systematic study of the ABA metabolic changes during early development of tomato seedlings.

2. Physiological study of the effects of endogenous ABA in the early development especially in the growth of hypocotyl of etiolated seedlings.

3. Cellular and molecular study of potential mechanisms of ABA action in the growth of etiolated tomato hypocotyls.

3. LITERATURE REVIEW

3.1. Brief history of ABA physiology research

The abscisic acid was discovered in 60s of the last century while searching for compounds that promote leaf abscission. The compound isolated was originally named abscisin II and was found also to inhibit oat cotyledon growth (Ohkuma et al. 1963). In the same time, dormin was isolated as inducer of bud dormancy. The chemical characterization revealed the identical structure of abscisin II and dormin, and the compound was renamed as abscisic acid (Cornforth et al. 1965). Paradoxically but interestingly, recent studies reported that leaf abscission is indirectly regulated by ABA, which regulates ethylene production required for the abscission (Cutler et al. 2010). ABA was found to antagonize gibberellins (GAs) resulting in the inhibition of seed germination (Thomas et al. 1965). The role of ABA in plant water relations can probably be considered as the most important role of ABA in plant growth and development. The regulation of stomatal conductance is impaired in ABA-deficient mutants, which developed wilty phenotype even under well-watered conditions (Quarrie 1987). Exogenous treatment with ABA rescued the wilty phenotype in tomato *flacca* mutant and caused stomatal closure in *Xanthium* (Imber and Tal 1970; Jones and Mansfield 1970). It is commonly admitted that ABA is an inhibitor of plant growth but growing evidence accumulates that ABA has a stimulatory effect on growth. Indeed, in high water potential the shoot growth of ABA-deficient maize *viviparous* mutant was reduced compared to the wild-type (Saab et al. 1990). Further work on ABA-deficient tomato mutants demonstrated that ABA rather maintains than inhibits shoot growth in well-watered adult plants (reviewed in Sharp 2002).

3.2. ABA occurrence, biosynthesis, and catabolism.

ABA is represented in all kingdoms except *Archaea*, suggesting its old evolutionary origin and its biosynthesis was evidenced in plant-associated bacteria, fungi, cyanobacteria, algae, lichens, higher plants, protozoa, sponges and even in mammals - human granulocytes (Hauser et al. 2011). ABA belongs to the group of isoprenoids, also called terpenoids. ABA has a chiral centre (C-1'). Whereas two enantiomers S-(+)-ABA and R-(−)-ABA, are formed during chemical synthesis, only the S-configuration naturally occurs in plants (Todoroki 2014). However, both isomers show similar hormonal activities (Lin et al. 2005), suggesting that the synthetic R-isomer mimics the endogenous hormone (Todoroki 2014).

ABA derives from isopentenyl pyrophosphate. The isopentenyl pyrophosphate can be produced by two pathways: the mevalonate (MVA) pathway occurring in the cytosol and 2-C-methyl-d-erythritol-4-phosphate (MEP) pathway which takes place into plastids. Whereas in some phytopathogenic fungi ABA is produced directly from farnesyl dipshosphate issued from the MVA pathway (direct pathway), in plants ABA originates from the cleavage of carotenoids

that are synthesized by MEP pathway within the plastids (indirect pathway). MEP is converted into isopentenyl pyrophosphate, precursor of geranyl diphosphate and geranylgeranyl diphosphate. Geranylgeranyl diphosphate is precursor of a huge amount of important metabolites such as chlorophylls, plastoquinones, but also hormones such as gibberellins and ABA as derivatives of carotenoids. The first ABA specific synthesis step is the oxidative cleavage of the carotenoids violaxanthin and neoxanthin into xanthoxin by the 9-cis-epoxycarotenoid dioxygenase enzyme (NCED). Xanthoxin was discovered as a plant growth inhibitor (Taylor and Burden 1970). The *cis*-xanthoxin is transported to the cytosol where it is subsequently converted into abscisic-aldehyde by the short-chain dehydrogenase/reductase (SDR). The last step of ABA synthesis in plants is the oxidation of abscisic aldehyde an abscisic aldehyde oxidase (AAO) enzyme (Nambara and Marrion-Poll 2005; Schwartz and Zeewaart 2010). The simplified scheme of ABA metabolism is depicted in Figure 1.

The inactivation of ABA is mediated by two different processes: hydroxylation and conjugation. Three forms of hydroxylated ABA (C-7´, C-8´, and C-9´) retaining a substantial biological activity can be found, but the hydroxylation leads to the subsequent degradation steps. The principal hydroxylation occurs on the methyl-group in C-8´position of the ring-structure. This reaction is catalysed by a cytochrome P450 monooxygenase (CYP707A); 8´-hydroxy ABA is spontaneously isomerized to phaseic-acid. Nevertheless, because 2% of 8'-hydroxy ABA is not isomerized *in vitro*, it is assumed that an enzymatic reaction is catalyzing this reaction *in vivo*. A soluble reductase mediates the conversion of phaseic-acid into dihydrophaseic acid. Another process of ABA inactivation is its conjugation with glucose. The carboxyl and hydroxyl groups of ABA are potential targets of conjugation. The most common conjugate is ABA-glucosyl ester (ABA-GE), which is physiologically inactive but might serve to transport ABA in long-distance signalling. This hypothesis is supported by the fact that ABA-GE can be converted into active ABA through a one-step hydrolysis mediated by β-glucosidases. Two β-glucosidases were characterized in Arabidopsis: AtBG1 and AtBG2, localized in endoplasmic reticulum and vacuole, respectively (Xu et al. 2014). Apart from glucosyl ester, other conjugates with the hydroxyl groups of ABA and its hydroxylated catabolites were also reported (Schwartz and Zeewaart 2010).

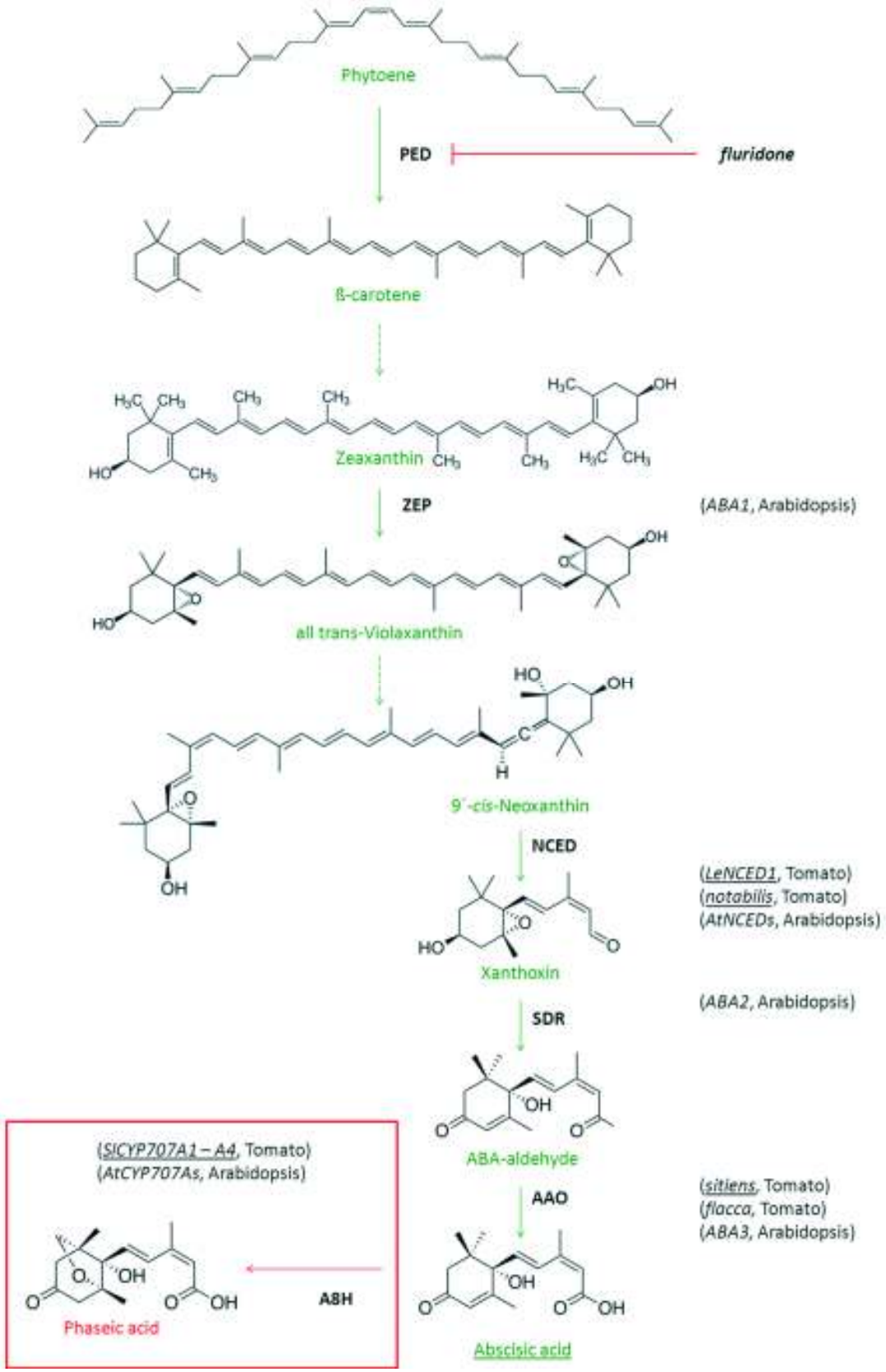
Phytoene
PED
fluridone
ß-carotene
Zeaxanthin
ZEP
(ABA1, Arabidopsis)
all trans-Violaxanthin
9´-cis-Neoxanthin
NCED
(LeNCED1, Tomato)
(notabilis, Tomato)
(AtNCEDs, Arabidopsis)
Xanthoxin
(ABA2, Arabidopsis)
SDR
ABA-aldehyde
(SlCYP707A1 – A4, Tomato)
(AtCYP707As, Arabidopsis)
(sitiens, Tomato)
(flacca, Tomato)
(ABA3, Arabidopsis)
AAO
A8H
Phaseic acid
Abscisic acid

Figure 1. Simplified scheme of ABA biosynthesis and catabolism.
Selected enzymatic steps in ABA biosynthesis are shown. The names of the genes encoding the enzymes that catalyze each step in tomato and Arabidopsis are indicated; the names of genes examined in this work are underlined. The conversion of phytoene to ß-carotene is mediated by phytoene desaturase (PED); this step is blocked by fluridone. Zeaxanthin epoxidase (ZEP) catalyzes the synthesis of violaxanthin, which is then converted to neoxanthin. The subsequent synthesis of xanthoxin is catalyzed by 9-cis-epoxycarotenoid dioxygenase (NCED), which is encoded in the gene *LeNCED1* in tomato and disrupted in *notabilis* mutant. Whereas the previous steps occur in plastids, xanthoxin is transported to the cytosol where it is converted to the abscisic aldehyde by short-chain dehydrogenase/reductase (SDR). The final step of ABA biosynthesis is the oxidation of abscisic aldehyde to ABA by an abscisic aldehyde oxidase (AAO), which is encoded in gene that is disrupted in the *sitiens* tomato mutant. ABA degradation (shown in the red frame) is mediated by ABA 8´-hydroxylase (A8H, cytochrome P450 monooxygenase) whose product spontaneously isomerizes to phaseic acid. The genes encoding ABA 8´-hydroxylase in tomato are *SlCYP707A1 – SlCYP707A4*. Dashed arrows represent missing steps in the pathway. These schemes are modified according to Kitahata and Asami (2011).

3.3. ABA signalling in higher plants

It is widely accepted that hormone signal perception starts with binding of hormone molecule to the extracellular or intracellular receptor that triggers downstream signalling cascade to activate final physiological response (Wang and Zhang 2014). Thus the hormone receptor should fulfil these two criteria: hormone binding and activation of signalling cascade (Venis 1985). Although numerous ABA signalling components were identified by forward genetics (Leung and Giraudat 1998), screening for ABA receptor was unsuccessful. This is perhaps that loss-of-function ABA-receptor mutants are lethal or provide only non-altered phenotype due to high redundancy (McCourt and Creelman 2008). As alternative approaches, the cellular and biochemical screening for ABA-binding proteins revealed the presence of ABA-binding sites at the plasma-membrane, but also in the cytosol (reviewed in Wang and Zhang 2014). Recently at least three-classes of receptors or receptor-candidates were identified: i) a plasma membrane-associated GTPases with homology to G-protein coupled receptors (GTGs), ii) a chloroplast-localized Mg^{2+} chelatase (ChlH) subunit, and iii) the soluble PYRABACTIN RESISTANCE/PYRABACTIN RESISTANCE-1 LIKE/REGULATORY COMPONENT OF ABA RECEPTOR (PYR/PYL/RCARs) (reviewed in Cutler et al. 2010). The signalling mechanisms for the first two classes are still not well characterized, but PYR/PYL/RCAR class provides a link between several of the ABA signalling elements and represents the “core signalling pathway” for ABA. The core ABA signalling pathway is provided by network of signalling components including PYR/PYL/RCARs ABA receptors, group A PROTEIN PHOSPHATASE 2Cs (PP2Cs) and members of the SNF1-RELATED PROTEIN PROTEIN KINASE 2 (SnRK2) group of kinases. PYR/PYL/RCARs the only known ABA-receptor, meeting both criteria for receptor (physical interaction and downstream action) was not identified via classic genetic screening, but by using a synthetic ABA analogue, pyrabactin. This compound mimicked the physiological responses obtained with exogenous ABA treatment. The physical interaction between pyrabactin and protein named as PYRABACTIN RESISTANT1 (PYR1) was evidenced (Park et al. 2009). PYR1 belongs to the family

of highly-redundant PYR-like (PYLs) elements (Park et al. 2009; Szostkiewicz et al. 2010; Dupeux et al. 2011; Hao et al. 2011; Zhang et al. 2012; Zhang et al. 2013). The interactions between PYLs and ABI-group of PP2Cs elements were found (Ma et al. 2009; Nishimura et al. 2010) that lead to the alternative name of the group to Regulatory Component of ABA Receptors (RCARs) (Finklestein 2013). PP2Cs ser/thr protein phosphatases were originally identified as ABA-responsive loci, *ABI1* (ABA INSENSITIVE1) and *ABI2* (Leung et al. 1994; Meyer et al. 1994; Leung et al. 1997; Rodriguez et al. 1998). Some of the other identified members of this gene family have no phenotype because of redundancy. Many members of the PP2Cs group were characterized as negative regulators of ABA-response (Sheen 1998; Rubio et al. 2009). On the contrary, the HIGHLY ABA INDUCED (HAI) mutants from the same family were shown to be positive regulators of ABA response during germination, but negative regulators of post-germination drought response (Bhaskara et al. 2012; Lim et al. 2012). The exception is *hai2* that is a negative regulator of ABA response during germination (Kim et al. 2013). The group of the SNF1-RELATED PROTEIN PROTEIN KINASE2 (SnRK2) was identified using thermoimaging to detect leaves with cooler temperature as a consequence of stomata opening (Merlot et al. 2002). The SnRK2 is homologous to the *OST1* (*open stomata*) locus, identified previously in wheat and broad bean (Gomez-Cadenas et al. 1999; Li and Assmann 1996). In Arabidopsis, the overlapping functions in ABA and stress response among the 10 members of the SnRK2 subfamily were demonstrated (Fujita et al. 2009; Nakashima et al. 2009; Fujii et al. 2011). The ABA signalling via PYR/PYL/RCARs receptor represents the most complete general intracellular ABA perception model: when the ABA binds to the PYR/PYL/RCAR protein the activity of PP2C phosphatases is inhibited, allowing the activation of SnRK2 kinases, which in turn phosphorylate bZIP transcription factors leading to the activation of ABA-responsive genes (Fig.2). Although the network provides core of ABA signalling, the model fails to explain the role of many previously identified ABA-regulators, including secondary messengers (Cutler et al. 2010).

In addition to the mentioned intracellular signalling components, some evidences support the hypothesis of an extracellular ABA receptor. In fact, ABA-protein conjugates cannot enter the cell but they can activate ion channels activity or gene expression (Jeannette et al. 1999). Indeed, ABA was found to stimulate the phospholipase D (PLD) activity in plasma membrane-enriched fractions from barley aleurone protoplasts in a GTP-dependent manner, suggesting the existence of an ABA receptor at the plasma membrane linked to PLD activation via G proteins (Ritchie and Gilroy 2000). The membrane-localized G-protein coupled receptor (GTG) was found to bind ABA and interact with heterotrimeric G-proteins (GPA) (Johnston et al. 2007; Pandey et al. 2006). Arabidopsis *gpa1* mutant displayed reduced sensitivity to ABA in guard cell functions (Wang et al. 2001). Nevertheless, the increased sensitivity to ABA in regards to inhibition of germination or root growth suggested different roles of G-proteins in distinct ABA-mediated responses (Pandey et al. 2006). Numerous candidates were suggested to be ABA-receptors, but with the exception of PYR/PYL/RCARs none of them was found to physically bind

ABA. The classical genetic screens fail to identify new receptors perhaps because of high redundancy in the members of ABA receptor pathways (Finkelstein 2013). It also suggests old evolutionary history and physiological importance of ABA perception that is secured by numerous elements of potentially same function.

Apart from the receptors or receptor candidates, numerous ABA signalling intermediates that were not yet implemented into the complex receptor pathways were described. The first identified was *ABA INSENSENSITIVE* group of regulators. Whereas *abi1* and *abi2* were identified to be PP2C phosphatases as described above, other three *abi* mutants were characterized as transcription factors belonging to B3- (*abi3*), APETALA2- (*abi4*) and bZIP- (*abi5*) domain families (Koornneef et al. 1984; Giraudat et al. 1992; Finkelstein 1994; Finkelstein et al. 1998; Finkelstein and Lynch 2000). Originally these regulators were thought to be seed-specific, but later their effects in post-germination development were reported. It was shown that they affect numerous genes in both direction – activation or repression – depending on the targeted gene (Suzuki et al. 2003; Nakabayashi et al. 2005; Koussevitzky et al. 2007; Nakashima et al. 2009; Kerchev et al. 2011; Monke et al. 2012). The Arabidopsis *ABI3* locus was found to be orthologue of *VIVIPAROUS1* (*VP1*) (Suzuki et al. 2001). To the family of B3- belong also *VP1/ABI3-like* (*VAL*) factors and members of *leafy cotyledon* class (*FUS3* and *LEC2*) (Luerssen et al. 1998; Stone et al. 2001; Suzuki et al. 2007). The *VAL* factors regulate many of genes which are regulated by ABI3, but have the opposite effect on their expression (Suzuki et al. 2007). The ABI4 from the APETALA2-domain family is related to the Drought Response Element Binding (DREB) subfamily. Although they often regulate same genes, the action of DREB is ABA-independent. New members of APETALA2 family were identified on the basis of binding to a coupling element (CE1) present in many ABA-regulated promoters. Many of them are closely related to the Ethylene Response Factor (ERF) subfamily (Lee et al. 2010). The ABI5 is a member of highly-conserved bZIP domain family that contains also other members that are regulated by ABA. There are five ABA response element (ABRE) binding factors (Choi et al. 2000; Uno et al. 2000) that share functional overlaps and cross-regulation with others members of the family (Yoshida et al. 2010). Also other transcription factors that are regulated via ABA or involved into the ABA-related stress-induced gene expression were identified: some examples are the MYB and MYC classes (Urao et al. 1993; Abe et al. 1997), the No Apical Meristem/Cup-Shaped Cotyledon, homeodomain-leucine zipper, and WRKY factor families (Rushton et al. 2011).

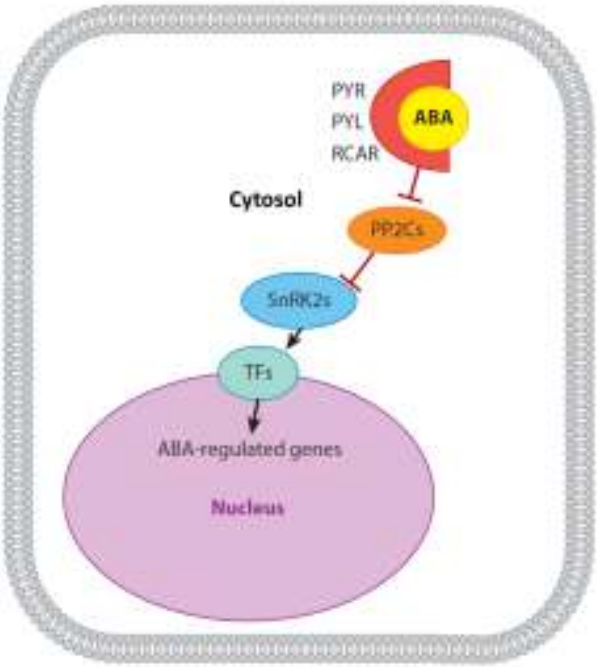

Figure 2. Model of ABA signalling via PYR/PYL/RCAR intracellular receptor.
In the presence of ABA the PYR/PYL/RCAR receptor binds to the PP2C phosphatase to inhibit its action. This leads to the accumulation of phosphorylated SnRK2 proteins and subsequent phosphorylation of transcription factors (TFs) that activate ABA-responsive genes. Figure modified from Cutler et al. 2010.

3.4. Modes of interaction of ABA and plant water status.

Although our work is focused on the role of ABA in "non-stress" conditions especially when considering water accessibility, the vast majority of reports is dedicated to the ABA's role in the plant physiological response to the low soil water content. In most of the papers, ABA action is studied primarily in stress conditions and non-stressed plants serve only as the control, but conclusions are generalized to overall ABA physiology (e.g. Tardieu et al. 2010). Since the shoot growth is very sensitive to the limited water accessibility, the direct connection between shoot growth and ABA acting as "plant water manager" was thought. It should be noted that we are using term "shoot" as general term for vegetative aerial plant organs (leaves and stems in case of dicots or for the leaves in the case of monocots) as it is used in key review of Sharp (2002). The classic theory of the inhibition of leaf and shoot growth under water deficit implies decrease of cell turgor which reduces the driving force for cell expansion (Lockhart 1965). It was reported that leaf growth is reduced by evaporative demand with simultaneous decrease of turgor (Shackel et al. 1987; Bouchabke et al. 2006). Moreover, affecting root hydraulic conductivity correlated with leaf expansion and cell turgor in growing zone (Ehlert et al. 2009). Also, the decreasing leaf elongation rate negatively correlated with increasing ABA content within the maize leaves that underwent progressive soil water deficit (Ben Haj Salah and Tardieu 1997). Conversely, numerous reports concluded that shoot growth inhibition is rather metabolically regulated than directly inhibited by altered water status (reviewed in Sharp 2002). Tardieu and co-authors (2010) considered that ABA interacts with the shoot growth in two different manners: in hydraulic (directly caused by altered shoot water potential) and non-hydraulic (uncoupled from shoot water potential) processes. Whereas, Sharp (2002) presumed a major role of ABA in plant growth non-hydraulic processes, Tardieu et al. (2010) believe in the higher importance of hydraulic processes in the control of leaf growth under water deficit.

However, it was also reported that water deficit or salinity inhibited shoot and leaf growth in spite of maintained turgor in a growing regions as a result of osmotic adjustment (Michelena and Boyer 1982; Termaat et al. 1985; Tang and Boyer 2002). In addition the shoot growth is sometimes so sensitive to soil drying that substantial inhibition of shoot growth can occur before the water potential in aerial parts decrease (Saab and Sharp 1989; Gowing et al. 1990). The non-hydraulic ABA-dependent processes that affect the shoot growth are considered to be some types of hormonal cross-regulation, regulation of cell cycle, or expression of cell wall-expansion related proteins (Tardieu et al. 2010). Although these processes are considered to be too slow to play important roles in the regulation of shoot growth under water deficit, they can play important roles during slower developmental processes (Tardieu et al. 2010). On the contrary, the importance of water conductance for leaf growth was evidenced by pharmacological approach: when aquaporins in a root were chemically blocked the leaf expansion was decreased (Ehlert et al. 2009). Since the expression of aquaporins is regulated

by ABA (Shinozaki et al. 1998) it suggested one hydraulic way through which ABA affects leaf growth.

Another, perhaps a major one comes from the role of ABA in regulation of stomatal conductance. Regulation of stomatal aperture represents the most obvious mechanism of plant water management. The aperture responds to the changes in the air water demand as well as to the soil water content through the complex network of processes that results in modified turgor pressure of guard or adjacent epidermal cells. Guard cells are highly differentiated epidermal cells that forms boundary of small pores in the epidermis of plant aerial organs. Since the epidermal layer is covered by impermeable waxy surface the stomatal pores represent major regulators of gas exchange between plant and atmosphere. The key role of ABA in opening and closing of stomata was studied from 70´s of last century (Jones and Mansfield 1970; Horton 1971; Kriedemann et al. 1972). Even earlier, the abnormal stomatal behaviour was observed in wilty tomato mutants *sitiens, flacca* and *notabilis* (Tal 1966), however at this time it was not known that they were impaired in ABA biosynthesis. Almost 3-times higher stomatal conductance leading to higher transpiration rate and low leaf water potential compared to the WT was shown later in *flacca* mutant (Bradford 1983). Although there is no doubt that ABA is responsible for closing of stomata in the unfavourable water status, the original site of ABA synthesis is not clear (reviewed in Dodd and Davies 2010). Since ABA is not able to pass through the membrane at pH 8, the stomatal response of excised epidermal strips to exogenous ABA was considered to be evidence of extracellular ABA receptor (Hartung and Slovik 1991). However, the injection of ABA into the guard cells also caused closure suggesting the presence of intracellular receptor and symplastic ABA transport (Allan et al. 1994). The “on site” ABA synthesis in guard cells was described as a response to low vapour pressure in atmosphere (Bauer et al. 2013). The effect of ABA in the regulation of leaf growth via affecting stomatal aperture is not clear. Whereas closing of stomatal conductance by exogenous ABA or genetic manipulation led to the inhibition of leaf growth, in drought stressed plant, endogenous ABA can increase leaf expansion via improvement of water relations (Sansberro et al. 2004).

ABA has been considered to be root-sourced long-distance signal of altered soil water status. Zhang and Davies (1991) showed that xylem sap of droughted plants closes the stomata of well-watered leaves. When ABA was removed from the sap, the stomatal pores remained open (Zhang and Davies 1991). However later reports suggested that ABA detected in the leaves during drought probably did not originate from root, but is synthesized directly on site in the leaf (Christmann et al. 2007). It was also shown that in wild-type (WT) sunflower plants that were grafted onto ABA-deficient rootstocks limited soil water content still induced stomatal closure (Fambrini et al. 1995; Holbrook et al. 2002). Since ABA can be synthesized in various tissues, it could be rather presumed that drought-induced ABA originated from outside of the roots, or that increase of ABA in leaves comes from the activation of ABA conjugated with

glucose (Lee et al. 2006) or from releasing of ABA sequestered in alkaline cell compartments (Wilkinson and Davies 2008). Although there are numerous attempts to improve plants drought tolerance via enhanced ABA, their real agricultural benefit is highly questionable as shown in the review by Blum (2015).

3.5. Role of ABA in regulation of plant growth

Because plants grown under abiotic stress (drought or salt) are severely affected in their growth and accumulate high concentrations of ABA, it was admitted that ABA is an inhibitor of plant growth. This idea was supported by the fact that ABA applied exogenously (usually in conncentrations above 1 µM) inhibited growth of well-watered, non-stressed plants (Milborrow 1966; Addicot et al. 1969; Van Volkenburgh and Davies 1983; Zhang and Davies 1990; Creelman et al. 1990; Cramer and Quarrie 2002). Nevertheless, soon after the discovery of ABA, Van Staden and Borman reported that very low ABA concentrations (10^{-8} mg.l^{-1}, i.e. 37.8 fM) led to the increase of biomass production in *Spirodela oligorhiza* (Kurz) Hegelm. When the concentration was increased to 0.1 mg.l^{-1} (i.e. 378 nM) inhibition of *Spirodella* growth occurred (Van Staden and Borman 1969). McWha and Jackson (1976) showed the stimulation of *Lemna polyrhiza* L. (also known as *Spirodela polyrhiza*) growth by ABA (1 nM). In parallel, they reported that nanomolar concentration of ABA (1 to 10 nM) stimulated growth of intact etiolated coleoptiles of oat and wheat (McWha and Jackson 1976). The stimulatory effect of exogenous ABA on the growth of etiolated rice mesocotyls was repeatedly reported (Takahashi 1972; Watanabe and Takahashi 1997; Watanabe et al. 2001). Teltscherová and Seidlová (1977) observed that in *Chenopodium rubrum* L. the same concentration of ABA could have different effect on plant growth depending on the aging of the plant. Thus, high concentration of ABA (100 µM) in watering solution inhibited growth and flowering of 3.5 day-old seedlings, but stimulated the growth and the flowering of older seedlings (Teltscherová and Seidlová 1977). The stimulatory effect of low concentration of ABA *in vitro* cultures of *Spinacia oleracea* calli was reported by Nešković et al. (1977). Nevertheless, the growth promotion was observed only in the presence of high concentration of the artificial cytokinin, kinetin. The stimulatory effect of ABA alone or in combination with auxins (NAA+IAA) was also reported later for tobacco callus cultures (Kochhar 1980).

In several species, ABA-deficient mutants exhibited dwarfism. This is the case for tomato (Taylor and Tarr 1984; Neill and Horgan 1985; Sharp et al. 2000), barley (Mullholand et al. 1996) or Arabidopsis (e.g. LeNoble et al. 2004; Barrero et al. 2005). In Arabidopsis, mutants in four genes encoding proteins involved in different steps of ABA-biosynthesis were described (Schwartz and Zeewaart 2010). The mutant *aba1* impaired in the zeaxanthin epoxidase (ZEP) is characterized by the inhibition of rosette growth; this later was improved by low concentration of ABA (up to 50 nM). The same concentration had no effect on the WT growth. The histological observations revealed that mesophyll cell of the mutant leaves were smaller and their expansion was stimulated by exogenous ABA (Barrero et al. 2005). The Arabidopsis *gin1* (*glucose insensitive 1*)/*aba2* (*abscisic acid deficient 2*) mutant was initially isolated based on its insensitivity to glucose. The mutant exhibited severe growth retardation in cotyledons, rosettes, stems, roots, and siliques in the absence of exogenous sugars and stress conditions. The mutation impairs the short-chain alcohol dehydrogenase/reductase which catalyses the

conversion of the plastid-derived xanthoxin to abscisic aldehyde. Genetic dissection of the mutant clearly indicated that ABA plays an important role in glucose signalling. Moreover, the growth defects were not improved by high humidity conditions, which supported the hypothesis that ABA is responsible for the growth independently of water deficit (Cheng et al. 2002). GIN1/ABA2 acts downstream of the ethylene receptor ETR1 (Zhou et al. 1998), putting to the light the regulation of ABA synthesis and ethylene signalling pathway by glucose (Cheng et al. 2002). In the *aba2/ein1* double mutant where ethylene signalling pathway is also blocked, the root growth was partially improved compared to the single *aba2* mutant, but the shoot growth remained inhibited suggesting uncoupling of ABA effects in shoots and roots (Cheng et al. 2002). It seems that ABA maintains the root-growth mainly via inhibition of ethylene synthesis/action, but in the shoot part another mechanism of ABA action could be expected. In different study, the double mutant *aba2-1*/*etr1-1* (*etr 1-1* is synonymous to *ein1*) shoot growth was only partially improved compared to the single *aba2-1* mutant, suggesting two mechanisms, by which ABA stimulates shoot-growth: i) the inhibition of ethylene synthesis by ABA and ii) ethylene independent mode of ABA action (LeNoble et al. 2004).

In tomato, the wilty ABA-deficient mutants were reported as being shorter and having smaller leaves than the corresponding WTs (Imber and Tal 1970; Bradford 1983; Quarrie 1987). However, these effects were attributed to the inability of the mutants to retain sufficient amount of water. Thus it appeared that the study of the mutants required that they will be grown in the same plant water status as the WT. Three ABA-deficient mutants were identified as *notabilis* (*not*), *flacca* (*flc*) and *sitiens* (*sit*). The *not* mutant is impaired in the NCED enzyme, the key regulatory step of ABA biosynthesis (Burbidge et al. 1999); the *flc* mutant is characterized by impaired molybdenum cofactor sulfurase that is necessary for the activation of the abscisic aldehyde oxidase (Sagi et al. 2002). Finally the s*it* mutant is defective in the abscisic aldehyde oxidase gene involved in the very last step of ABA synthesis (Taylor et al. 1988; Harrison et al. 2011). When *not* and *flc* mutants were grown in controlled humidity conditions such that the leaf water potentials of the mutants were equal to those of WTs, the shorter phenotype of the mutants remained unchanged (Sharp et al. 2000). In consistency with previous observations of Jones et al. (1987) the stems of the mutants initially elongated more rapidly than those of the wild types, but this fast growth was not sustained, and the mutants became shorter at later stages of development. Shoot growth of the mutants substantially recovered after treatment with exogenous ABA, suggesting that ABA promotes shoot growth (Sharp et al. 2000). Ethylene production was doubled in the *flc* mutant compared to the WT, but the inhibition of ethylene action by silver thiosulphate (STS) led only to a partial rescue of shoot and root growth (Sharp et al. 2000). Also, in another study only minor recovery (about 25%) of the shoot growth was observed after spraying with STS (Chen et al. 2003). The growth-inhibition in ABA-deficient tomato mutants was also observed as a side result in other studies (Mäkela et al. 2003; Thompson et al. 2004; Aroca et al. 2008).

Although early physiological studies suggested that ABA is inhibitor of root growth (Pilet 1970; Pilet 1975) this opinion was critically re-evaluated over decade later (Pilet and Saugy 1987). Main interest was then focused on the role of ABA in the growth of roots of plants with reduced water accessibility. When the soybean was hydroponically cultivated at high-water potential and then transferred to low-water potential vermiculite, the shoot growth was severely inhibited, but the elongation of roots was only slightly affected. In parallel, the endogenous ABA increased 5 to 10 times in seedlings growing in reduced water-potential (Creelman et al. 1990). In the maize seedlings similar experiment showed that transfer to low water potential inhibited the shoot growth, but the elongation of primary root continued with concomitant increase of endogenous ABA in the root tip (Saab et al. 1990). Moreover, the application of inhibitor of carotenoid-biosynthesis fluridone to the water-stressed seedlings completely prevented the inhibition of shoot growth but inhibited by 83% the root growth. The same response was observed in the ABA-deficient *vp5* maize seedlings that are impaired in the phytoene-desaturase involved in the same early ABA (carotenoid) biosynthetic step that is blocked by fluridone (Saab et al. 1990). The results were strengthened by study of Tan et al. (1997) who identified maize *vp14* mutant that is impaired in the production of xanthoxin, the main regulatory step of ABA synthesis. The mutant showed importantly reduced root elongation, however no effects on the shoot growth were observed (Tan et al. 1997). These studies suggested that ABA promotes growth of primary root under water-deficiency. On the contrary when ABA content was increased in previously fluridone treated seedlings growing in the normal root water potential (-0.03 MPa) the root growth was significantly inhibited. Also in fluridone untreated seedlings the exogenous ABA led to lower root growth (Sharp et al. 1994). The interaction of ABA with ethylene synthesis was observed in several studies. It has been shown that ethylene is overproduced in water-stressed ABA-deficient plants and that this effect is completely prevented by exogenous ABA together with restoration of root growth. Moreover, the application of ethylene inhibitors improved the root growth of water stressed seedlings (Spollen et al. 2000). The inhibitory effect of exogenous ethylene was shown previously in maize by Moss et al. (1988). When the ethylene inhibitors were applied into water-stressed seedlings with normal ABA-levels, no improvement of root elongation was observed, suggesting that roots at low water potential exhibit an optimal ABA content for growth maintenance (Spollen et al. 2000; Sharp 2002).

As a conclusion we can say that although ABA was initially considered as inhibitor of growth, an increasing number of reports show its growth-promoting effects in physiological experiments. According Tardieu et al. (2010) these contradictions could be explained by differences in the experimental design, developmental and environmental context. Further, it can be considered that each manipulation with ABA content lead to changes in the plant water status (Tardieu et al. 2010). Moreover, leaf growth is defined in different ways in the literature, with different effects of ABA for each definition. Whereas the increase in shoot biomass depends on photosynthesis, respiration or nutrient status, the volumetric expansion of the leaf is largely

independent on these processes on time scales of days to weeks. Although it was suggested that ABA maintain shoot growth via non-hydraulic interaction with ethylene, it was also hypothesized that ABA plays an inhibitory role in the non-hydraulic leaf growth (at least in maize), but may play stimulatory (maintenance) role in hydraulic-dependent leaf growth connected with stomata regulation (short term effect) and tissue hydraulic conductance via increased of root water uptake (Tardieu et al. 2010). Nevertheless, it is noticeable that the results suggesting inhibitory role of ABA are usually provided by studies employing exogenous ABA treatments and/or mutants in ABA-signalling elements. On the contrary experiments based on ABA-deficient mutants most often supported the stimulatory effect of ABA in the shoot growth.

3.6. Role of ABA in other developmental processes

In this chapter the ontogenetic functions of ABA are reviewed. However, since the developmental step called "early seedling development" or "post-germination growth" represents the main topic of the thesis, its review is given in separated chapter (see chapter 3.8.)

3.6.1. Embryogenesis and seed maturation

Although the detectable levels of ABA during early embryogenesis are low, the biosynthetic pathway was shown to be active in Arabidopsis young embryos and maternal tissues, where the transcripts of *AtNCED* and *AtZEP* were expressed (for details about ABA biosynthesis see chapter 3.2). The strong increase of ABA biosynthesis was observed during maturation phase, when the seed reserves are synthesized. Since the carotenoids represent important part of seed reserves the activation of carotenoid synthesis provides increased number of ABA precursors and subsequently ABA itself (Nambara and Marion-Poll 2005). The experiments with ABA-deficient tobacco mutant *Npaba1* and *Npaba2* showed that during early embryogenesis maternal ABA promotes seed growth and prevents seed abortion (Frey et al. 2004). Previously the negative effect of ABA-deficiency on the size of Arabidopsis siliques and ovule fertilization was reported in *aba2/gin1* mutant. The mutants had higher percentage of aborted seeds resulting in low yield (Cheng et al. 2002). Conversely, during late embryogenesis when ABA content increases, the hormone blocks the embryo growth and precocious germination (Raz et al. 2001). The precocious germination – vivipary – is often reported as consequence of ABA deficiency or insensitivity and this effect could be reverted by inhibition of GA synthesis that promotes germination as was shown in maize *viviparous5* (*vp5*) mutant. However, in maize ABA-insensitive *viviparous1* (*vp1*) mutant the obstruction of GA synthesis did not prevent the precocious germination (White et al. 2000).

3.6.2. Seed dormancy and germination

The seed germination is often characterized as three phase process. During the first phase - imbibition- the rapid water uptake is driven mainly by the physical properties of dry seed. The second phase is characterized by lag in weight gain, during which the seed increases metabolic activity and prepares for growth. This phase is "reversible" by re-drying of seed that can even improve the germination potential of some species. The last phase corresponds to the "decision to grow", representing the critical "no-way-back" step. Progression to this phase is regulated by various signals including light and water availability, salinity, temperature, and nutrient status. All of this information must be integrated, and this is mediated by signalling through multiple hormones that either promote (GA, ethylene, brassionosteroids, cytokinins) or inhibit (ABA and jasmonic acid) germination (Finkelstein 2010). As noted previously, ABA is necessary to maintain seed dormancy during late embryogenesis. Seed dormancy is considered

as a block to the completion of germination of an intact viable seed under favourable conditions. A completely non-dormant seed has the capacity to germinate over the widest range of normal physical environmental factors possible for the genotype. However, dormancy of a single seed can have any value between all (maximum dormancy) and nothing (non-dormancy). The normal environment includes proper amounts of water, oxygen and an appropriate temperature; seeds of some species are also sensitive to other factors such as light and/or nitrate. The most important type of seed dormancy is physiological dormancy that is considered to be maintained by active regulatory network (for review see Finch-Savage and Leubner-Metzger 2006). The study of Arabidopsis and tomato ABA-deficient mutants showed that not maternal, but embryo-synthesized ABA is responsible for induction of dormancy during seed maturation. The seed germination is preceded by a dramatic decrease of ABA as a consequence of both inhibition of synthesis and activation of catabolism (Nambara and Marion-Poll 2005).

Whereas in non-dormant seeds ABA originated from embryogenesis stage, the dormant seeds actively produce *de novo* ABA to maintain dormancy during imbibition (Ali-Rachedi et al. 2004). To break the seed dormancy, stimulation of ABA-catabolism is necessary. In Arabidopsis, the cytochrome P450, CYP707A2, plays a major role in it. Transcripts of *CYP707A2* are accumulated in maturating seeds and further increases during seed imbibition reaching the maximum about six hours after start of imbibition and then decrease. The seeds of *cyp707a2* mutant exhibited an extremely dormant phenotype when imbibed without cold stratification. The mutant seeds hold six time higher ABA content during imbibition than the WT seeds (Kushiro et al. 2004). Seed dormancy and germination are regulated by a dynamic balance between ABA and GA. A dormant embryo is characterized by a high ABA:GA ratio together with high ABA sensitivity but low GA sensitivity (Finch-Savage and Leubner-Metzger 2006). The important metabolic process during seed germination is the mobilisation of stored reserves. The reserves are hydrolysed by specific enzymes that are produced in embryo and endosperm. The best characterized is the degradation of stored starch reserves by α-amylase in cereals. The promoters of genes encoding α-amylase contain GA-responding motif GA RESPONSE ELEMENTS (GAREs) that serves as binding site for GA-induced transcription factors (GAMyb). The sensitivity of seed to GA are inhibited by transcription factor VP1 (orthologue to ABI3, for details see chapter 3.3) during late embryogenesis. ABA can also inhibit expression of α-amylase by expression of protein kinase PKABA1 that represses GAMyb transcription factor. In many GA-induced genes the ABA RESPONSE ELEMENTS (ABREs) were identified in their putative promotors, suggesting a direct effect of ABA signalling elements on their expression. This was supported also by parallel analysis of ABA content and *ABI5* expression that are both reduced during seed imbibition prior the elevation of GA-content (Finkelstein 2010).

3.6.3. Floral transition

The floral transition that occurs in the shoot apical meristem (SAM) represents an irreversible change in plant development and its timing is tightly controlled. Several hormonal pathways have been identified to affect floral transition and flowering. Similarly to the growth responses the role of ABA in floral transition is not fully clear: although generally is ABA considered as inhibitor of flowering, in some experiments it appeared to be a promoter. The consensus as to the precise mode of ABA action is lacking (Conti et al. 2014). The exogenous ABA treatment inhibited flowering in Arabidopsis and other species (King and Evans 1977; Blazquez et al. 1998; Domagalska et al. 2010). However the induction of flowering during plant water deprivation that is known as "drought escape" was stimulated by endogenous ABA via upregulating key regulator gene *FLOWERING LOCUS T* (*FT*) (Riboni et al. 2013). The *FT* gene is downregulated by exogenous ABA, but also by ABA-deficiency in the Arabidopsis *abi1-1* mutant (Hoth et al. 2002). The positive effect of root ABA application on flowering was observed in Arabidopsis in study of Koops et al. (2011). Discrepancies in the reports could be explained by circadian fluctuation in ABA levels, gating of ABA signalling as well as tissue specific ABA signalling and transport that can interact with exogenous ABA treatment (Conti et al. 2014). Indeed in the short day plant *Pharabitis nil* exogenous ABA applications during the first part of the inductive short day are inhibitory, while when applications occurs at the end of the night, ABA promotes flowering (Wilmowicz et al. 2011). Teltscherová and Seidlová (1977) observed different effect of exogenous ABA on the growth of *Chenopodium rubrum* L. applied into differentially old seedlings. When the relatively high ABA concentration (100 μM) was added to the watering of 3.5 days old seedlings it led to the inhibition of flowering. When the same concentration was added into the watering of 4.5 to 7 days old seedling, the stimulation of flowering was observed (Teltscherová and Seidlová 1977). Although the ABA deficiency could help to solve the clue, their phenotypes are highly background specific and the effect of endogenous ABA did not recapitulate the results of exogenous treatment in Arabidopsis (Conti et al. 2014). Clearer information are provided by the tomato ABA biosynthetic mutants *not* and *flc* that exhibited extended vegetative phase compared to the WT suggesting a positive role of ABA in flower transition (Carvalho et al. 2011). More reports considering ABA as a promoter of flowering originated from studies with short day plants (Conti et al. 2014). Indeed the stimulatory effects on flowering and yield of maize and sorghum were shown in field experiments by El Antably (1974). Upregulation of ABA biosynthesis in soybean led to the increase of ABA content in SAM followed by induction of floral genes (Wong et al. 2009). The induction of flowering was also observed in long-day wheat plants treated with ABA (Hall and McWha 1981).

3.6.4. Fleshy fruit ripening

Apart from the key role of gaseous hormone ethylene in this process, ABA is widely accepted as important player in the ripening of fleshy fruits. Indeed, ABA is responsible for multiple

events in fruit ripening such as coloration, sugar accumulation, acid decline and flesh softening (Shen and Rose 2014). The key role of ABA was described in ripening of strawberry fruits where exogenous ABA significantly promotes fruit ripening, while the application of ABA-biosynthetic inhibitor fluridone led to the inhibition of this process. Moreover, the silencing of *FaNCED1* biosynthetic gene caused delayed in ripening (Jia et al. 2011). Apart from strawberries, the importance of ABA in fruit ripening was evidenced in other species including persimmon, family of *citrus* or *prunus* species suggesting that ABA is likely a common signalling molecule that modulates many processes in both climacteric and non-climacteric fleshy fruits (for review see Shen and Rose 2014).

3.7. Interaction of ABA and other plant hormones

ABA is known to interact with other plant hormones in regulation of different physiological processes. Cross-talks between ABA and other plant hormones were especially identified in seed dormancy and germination, lateral root formation and regulation of stomatal aperture (Sun and Li 2014).

Auxin and ABA usually act antagonistically (Sun and Li 2014). However a synergistic action of ABA and auxin was shown in the control of seed dormancy in Arabidopsis. When auxin signalling or synthesis was impaired, dormancy was dramatically released; in opposite, when auxin action was increased, seed dormancy was strongly enhanced. Promotion of dormancy by auxin was shown to be dependent on ABA-signalling and vice-versa (Liu et al. 2013). ABA was also shown to induce expression of *AUXIN RESPONSE FACTOR2* (*ARF2*) that is considered to be a central integrator of auxin, ethylene, brassinosteroid and ABA signalling pathways (Wang et al. 2011a). Whereas *arf2* mutants showed enhanced ABA sensitivity in seed germination and primary root growth, the plants overexpressing *ARF2* were less inhibited by exogenous ABA than WT. Moreover, auxin transport in root tips was enhanced by exogenous ABA in *ARF2* overexpressing plants (Wang et al. 2011a). The regulation of polar auxin transport by ABA is probably mediated via ABI4 transcription factor, since the *ABI4* overexpressors showed reduced *PIN1* expression and impaired lateral root formation (Shkolnik-Inbar and Bar-Zvi 2010). Moreover, the mutants in auxin transport proteins, *aux1* and *pin1,* are resistant to ABA-induced repression of embryonic axis elongation (Belin et al. 2009).

Together with auxin, cytokinins (CKs) are important regulators of plant morphogenesis. They are also known to counteract ABA-dependent closure of stomatal pores via modulation of ethylene biosynthesis (Tanaka et al. 2006). However, it was shown that exogenous ABA affects cytokinin signalling in nodulation of alfalfa that was ethylene-independent (Ding et al. 2008). Wang et al. (2011b) reported that CK antagonizes ABA suppression of seed germination by downregulating *ABI5* expression. Moreover the counteracting effects of ABA and cytokinins were observed in several processes during early seedling development, especially in the development of cotyledons. The most studied is the role of ABA and CKs interaction in the maturation of plastids into chloroplasts. Whereas exogenous ABA blocks the plastid maturation, keeping etiolated phenotype, CKs promote cotyledon greening by increasing accumulation of protochlorophylide oxidoreductase enzyme in lupine cotyledons (Kusnetsov et al. 1998). The opposite effects of CKs and ABA in barley leaves were observed. Whereas CK activated, ABA inhibited the transcription of plastid genes and chlorophyll content (Kravtsov et al. 2011; Yamburenko et al. 2013). Recently, Guan et al. (2014) demonstrated that CKs counteracts ABA mediated inhibition of cotyledon greening via CK-dependent degradation of ABI5 protein in Arabidopsis.

The antagonistic interaction between ABA and gibberellins was reported in the seed dormancy and germination as described in the chapter 3.6.2. However, GA importantly affects also other parts of plant life such growth or flowering. It was shown that both ABA and GA stimulate the expression of microRNA159, a regulator of the Arabidopsis MYB33 transcription factor. MYB33 was found to mediate ABA responses during seed dormancy, but GA responses in flowering (Achard et al. 2004; Reyes and Chua 2007). This is an interesting example of integrating hub that is sensitive to differently acting hormones according the plant developmental stage. Recently, Golldack et al. (2013) revealed GA-ABA interplay in plant responses to abiotic stresses. Indeed, they suggested that DELLA and SCL proteins integrate generic GA responses into ABA-dependent abiotic stress tolerance.

The antagonism between ABA and ethylene was shown at the level of biosynthesis, catabolism and signalling (Sun and Li 2014). The important cross-talks of ABA and ethylene in the vegetative growth and early seedling development are described in the chapters 3.5 and 3.8, respectively. Beaudoin et al. (2000) showed that endogenous ethylene promotes seed germination by decreasing sensitivity to ABA. Whereas in seed germination, the antagonism was observed, in root growth, ABA and ethylene act synergistically (Beaudoin et al. 2000; Ghassemian et al. 2000). The over-accumulation of ABA was observed in ethylene insensitive *ein2* mutant (Ghassemian et al. 2000) and vice-versa the ABA-insensitive *hy5* mutant overproduced ethylene (Li et al. 2011) showing that ABA and ethylene inhibit each other biosynthesis. Further, Tanaka et al. (2005) reported that application of ethylene prevented ABA-induced stomatal closure suggesting that ethylene can also inhibit ABA-signalling.

Since both ABA and jasmonic acid (JA) are important players of the plant stress adaptation it is not surprising that they interact at multiple levels. More interestingly is that their cross-talk seems to be antagonistic, suggesting very different strategies of plant responses to abiotic and biotic stresses (Sun and Li 2014). Exogenous ABA supresses the expression of JA-inducible genes and these genes are up-regulated in ABA-deficient *aba1* and *aba2* mutants (Anderson et al. 2004). Moreover, it was shown that plant overexpressing *MYC2* are more sensitive to ABA and the ABA sensitivity was lowered in *myc2* mutant (Abe et al. 2003). Since the MYC2 transcription factor is the major regulator of JA-responses in Arabidopsis it was suggested that MYC2 is an integrating hub of JA-ABA responses (Sun and Li 2014).

3.8. ABA in early seedling development

The early seedling stage of plant growth covers a developmental window from germination, defined as radicle protrusion to the development of the first true leaf that definitively shifts the plant from the heterotrophic (or partially heterotrophic after de-etiolation) to autotrophic stage. The early seedling development represents a fascinating transitional stage when heterotrophic organism is gradually changing into the autotrophic. After germination (of epigeal dicot species), the radicle is forming a root and the hypocotyl rapidly elongates through the soil to bring a hook with cotyledons to the light before the reserves are exhausted. The hook protects the apical meristem from potential mechanical damages caused by soil particles. This fully heterotrophic part of plant life occurs in the dark, so it is called skotomorphogenesis (*skotos* – darkness in Greek) or etiolated growth (*étioler* – from French, meaning bleach or blanch). When the seedling perceives the light, it leads to dramatic changes in seedling physiology that are called photomorphogenesis. The initial redirection of developmental pattern induced by first light exposure is called de-etiolation. At the visible phenotypic level it includes change from dark-grown phenotypes (rapidly-growing hypocotyl, closed apical hook, small, suppressed cotyledons enclosing undeveloped leaf primordia and a pale yellow colour) to the converse pattern of light-grown seedling (inhibited hypocotyl, straightened apical hook, separation and rapid expansion of cotyledons and greening). At the cellular level it includes inhibition of elongation of hypocotyl cells, stimulation of cell expansion in cotyledons and induction of chloroplast development (Quail 2002a).

Light is not only the primary source of energy for photosynthesis but also regulates numerous physiological responses, such as shade avoidance, flowering, germination, tropisms or de-etiolation (Kami et al. 2010). The light is sensed by three main classes of photoreceptors: the phytochromes (PHYA to E), the cryptochromes (CRY1 and 2) and phototropins (PHOT1 and 2), capable of absorbing red/far-red (RL/FR) and blue light (BL), respectively (Quail 2002b). In dark-grown seedlings, phytochrome is present in a RL absorbing form (Pr). Perception of red portion of light spectra leads to the conversion of Pr form to the FR absorbing form of phytochrome (Pfr). The phytochrome responses are divided into three classes according the amount of the inducing light. Very low-fluence responses (VFLRs) can be initiated by the quantity of light as low as 0.0001 $\mu mol.m^{-2}$ and saturation occurs at about 0.05 $\mu mol.m^{-2}$. Similarly, low fluence of RL is capable to induce germination of Arabidopsis seeds or inhibit the growth of etiolated oat mesocotyls. Second category of responses is induced by photon fluences from 1 to 1000 $\mu mol.m^{-2}$. These responses are referred as low-fluence responses (LFR) and they include most of red/far-red photoreversible reactions: e.g. promotion of lettuce seed germination or regulation of leaf movements. Third class of responses is called high-irradiance responses (HIRs) that are induced by continuous exposure to the light of relatively high irradiance. One of the HIRs is inhibition of hypocotyl elongation in etiolated seedlings of lettuce, mustard or petunia. The HIRs are irreversible by FR light (Taiz and Zeiger 2010). In Arabidopsis, five

members of the phytochrome family have been identified (PHYA to E). Individual members of the PHY family differ in the light spectra to which they are most sensitive and/or in their physiological responses. For example both PHYA and PHYB mediate seedling de-etiolation, but PHYA is activated by FR rich signals, whereas PHYB responds more to the red-light-rich signal (Quail 2002a). When etiolated Arabidopsis seedlings are exposed to RL, inhibition of hypocotyl growth starts about 8 minutes later. On a contrary the exposure to BL induces the same reaction in less than 1 minute (approx. 30s), suggesting that phytochromes are rather responsible for latter phases of de-etiolation. Moreover, it was observed that hypocotyl of *phyB* mutant (accumulating functional PHYA) is strongly inhibited by RL for the first 3 hours of light exposure, afterwards the growth rate increases back to that of etiolated seedlings. On the contrary, the *phyA* mutant (containing functional PHYB) is for these 3 hours completely uninhibited by RL, but after this time the growth rate decreases to that of the WT. The double mutant *phyA phyB* was then completely uninhibited along the time of experimentation (about 5 hours) showing a growth rate typical for dark-growing seedling in presence of RL (Parks and Spalding 1999). Using Arabidopsis *cry1* mutant defective in BL-induced de-etiolation, studies have demonstrated that CRY1 is the BL receptor involved in the control of hypocotyl elongation (Cashmore et al. 1999; Lin 2000). Indeed, in the *cry1* mutant seedlings, hypocotyl growth inhibition begins within approximately 30 sec of BL irradiation and reaches the same maximum level displayed by WT seedlings after approximately 30 min of BL treatment. At this point, *cry1* seedling growth accelerates, soon attaining the growth rate observed for dark-grown seedlings. This experiment demonstrated that also BL-mediated hypocotyl inhibition in Arabidopsis occurs in a two genetically independent phases (Parks et al. 1998). When the same method was used on different mutants, the PHOT1 receptor was identified as being involved in the rapid phase of BL-mediated hypocotyl growth inhibition (Folta and Spalding 2001).

The genetic structure of post-germination growth is by default set up to photomorphogenesis and is repressed by dark (Alabadí and Blázquez 2009). The most important molecular mechanism that switches between skoto- and photomorphogensis is the constitutive photomorphogenic 1 (COP1) protein. COP1 is an E3 ubiquitin ligase that mediates the degradation of de-etiolation promoting transcription factors such as HY5 (long hypocotyl 5) protein (Bauer et al. 2004). COP1 and transcription factors are further regulated by multiple phytohormones. Auxin, GAs, brassinosteroids (BRs), ethylene and CKs have been widely established as important players in the regulation of hypocotyl growth during Arabidopsis skoto- and photomorphogenesis (Arsovski et al. 2012). GAs block HY5 accumulation and stimulate etiolated growth by promoting transcription factors of the PHYTOCHROME INTERACTING FACTOR (PIF) protein family (Alabadí et al. 2008). The presence of light reduces GA content, inhibits GA biosynthetic genes expression and also induces expression of genes involved in GA inactivation (Symons and Reid 2003a; Achard et al. 2007). Also auxin stimulates etiolated growth and its action is negatively regulated by light via HY5 pathway (Nemhauser 2008). Mutants impaired in auxin response exhibit de-etiolated phenotype in the darkness

(Woodward and Bartel 2005). Similarly to auxin, BR-deficient or insensitive Arabidopsis mutants develop de-etiolated phenotype in darkness (Clouse et al. 1996; Li et al. 1996) and BR-signalling is inhibited by light through PHYB in rice (Jeong et al. 2007). CKs, another group of phytohormones, play an opposite role to the above mentioned BRs, GAs and auxin. The exogenous application of CKs led to a de-etiolated phenotype of the dark-grown Arabidopsis seedlings (Chory et al. 1994) and CK signalling pathway promotes stabilization of the HY5 protein (Vandenbussche et al. 2007). Recently, the accumulation of isopentenyladenine (iP) after exposure to BL was reported in tomato hypocotyls, suggesting its specific role in de-etiolation (Bergougnoux et al. 2012). The role of the gaseous hormone ethylene in skotomorphogenesis and de-etiolation is not fully elucidated. The probably best described action of ethylene is the triple response. When the ethylene is applied on D-grown seedlings it leads to the development of three typical morphological changes: the hypocotyl is shortened, thickened and apical hook is exaggerated. However in light, ethylene works opposite and stimulates hypocotyl elongation of Arabidopsis seedlings (Smalle et al. 1997). Although the detailed mechanism of this ambivalent action is unknown, the application of the ethylene precursor ACC (1-aminocyclopropane-1-carboxylic acid) on *cop1-4* and *Cop1ox* mutants of Arabidopsis suggested a central role of COP1 in this process (Liang et al. 2012). The overall regulation of skotomorphogenesis depends on various interactions between the different phytohormones. Despite the fact that interplay between above mentioned hormones and ABA is often reported in other physiological responses, it is rather poorly investigated in skoto- and photomorphogenesis.

It has been shown previously that ABA can play a role in post-germination growth. The important observations were performed in etiolated seedlings of monocotyledonous species. The stimulatory effect of ABA in dark-grown rice seedlings by ABA was observed by Takahashi in 1972. Addition of relatively low concentration (up to 1.5 µM) of ABA caused enormous elongation of etiolated rice mesocotyls, but with total inhibition of coleoptile development (Takahashi 1972; Watanabe and Takahashi 1997; Watanabe and Takahashi 1999). Moreover, the mesocotyl growth was repressed by application of fluridone, an inhibitor of the early steps of ABA biosynthesis (Watanabe et al. 2001). Similarly, exogenous ABA stimulated mesocotyl growth of etiolated seedlings of foxtail millet (*Setaria Italica* Beauv.) dwarf mutant. ABA (0.31 µM) also showed additive effect to the GA application in the same specie (Chen and Zhou 1998). In dicots the inhibitory effects of exogenous ABA were reported. In Arabidopsis the treatment with relatively high concentration ABA (20 µM) led to the de-phosphorylation of plasma membrane H^+-ATPase and subsequent inhibition of the growth of etiolated hypocotyl (Hayashi et al. 2014).

3.8.1. Interaction of ABA metabolism and light

The important role of light in regulating ABA synthesis and catabolism was demonstrated in numerous studies. Kraepiel et al. (1994) reported that the phytochrome deficient tobacco *pew*-

1 mutant exhibited higher amount of ABA in seeds and leaves than the WT, suggesting that light has an important role in the regulation of ABA accumulation. In another study, Weatherwax and co-authors (1996) described not only that RL reduced ABA concentration in etiolated *Lemna gibba* but also that dark treatment of previously light-grown Arabidopsis and *Lemna gibba* plants led to a significant increase in ABA content. Symons and Reid (2003a) observed the reduction of ABA in etiolated pea seedlings after 4h of exposure to white light. These last authors proposed that light-mediated decrease of endogenous ABA content may be rather the consequence than the cause of photomorphogenesis (Symons and Reid 2003a; 2003b). Nevertheless, this hypothesis is poorly probable as the involvement of phytochromes in the alteration of ABA content suggests that the connection between light and ABA is a real part of a physiological mechanism. Recently, it was demonstrated that null Arabidopsis mutant in PHYB wilted at the water shortage earlier than WT plants. This was due to *phyB* maintaining open stomata under a reduction in soil water availability. Although *phyB* presented enhanced ABA levels under well-watered conditions, this mutant was less sensitive than the wild type in diminishing stomatal conductance in response to exogenous ABA application. It was revealed that reduced sensitivity of the *phyB* mutant to ABA is caused by low expression of ABA receptor coded by *PYL5*. It was proposed that functional PHYB is important for maintenance of plant sensitivity to ABA (Gonzáles et al. 2012).

In this context, experiments evaluating effect of RL and FR on expression of ABA biosynthetic and catabolic genes during seed germination were conducted. Thus the treatment of photoblastic lettuce seeds by RL decreased ABA content and down-regulated the ABA biosynthetic genes *LsNCED2* and *LsNCED4* (9-cis-epoxycarotenoid dioxygenase), but up-regulated the *LsABA8ox4*, the ABA 8´-hydroxylase gene (Sawada et al. 2008). The lettuce germination is a photoreversible reaction: RL stimulates the germination, but exposure to the FR blocks the germination by increasing seed ABA content (Toyomasu et al. 1998; Seo et al. 2006). The expression of *AtNCED6* was reduced by RL, but not by FR in Arabidopsis seeds. The expression of catabolic *AtCYP7072A* was regulated by light in opposite manner to the *AtNCED6.* Other *AtCYP707A* genes were found to be regulated indirectly by light (Seo et al. 2006). In barley grains, white light as well as BL stimulated the expression of *HvNCED* gene and increased ABA concentration (Gubler et al. 2008). Whereas photoblastic lettuce and Arabidopsis seeds need light to promote germination (Shinomura 1997), in barley light stimulates dormancy (Gubler et al. 2008). Both barley and lettuce seeds need a decrease of ABA to initiate germination, but they use opposite mechanisms based on their light or dark preferences for post-germination growth. The photoreversible reaction in Arabidopsis seed germination is mediated exclusively via PHYB photoreceptor, because in the *phyB* mutant the ABA content was not reduced by RL (Seo et al. 2006). The activation of PHYB by RL causes up-regulation of *ABA1* (ZEP), *AtNCED6* and *AtNCED9*, concurrently with down-regulation of *AtCYP7072A* (Oh et al. 2007; Kim et al. 2008). This process is mediated indirectly via PIL5/PIF1 transcription factor that is a negative regulator of PHYB responses. PIL5 also directly activates

expression of *SOM* (*SOMNUS*) gene. In the *som* mutant the expression levels of *ABA1* and *AtNCED6* are reduced, whereas the level of *CYP707A2* is increased compared to the wild type. As the consequence of this mutation ABA content in *som* seeds is reduced (Kim et al. 2008). The mechanism how the SOM regulates expression of ABA metabolic genes is unknown (Lin and Tang 2014).

To our knowledge, the only systematic study on the skotomorphogenesis of ABA-deficient mutants was performed by Barrero et al. (2008) in Arabidopsis. They observed that growth of etiolated hypocotyl of mutants is inhibited in comparison to the WT. They studied mutants impaired in different steps of ABA biosynthesis: *aba1-101* (ZEP), *aba2-14* (SDR), *aao3-2* (AAO) and *aba3-101* (MoCo sulphurase) mutants (for details about ABA biosynthesis see chapter 3.2). The inhibition of hypocotyl was most pronounced in the early step mutant *aba1-101* (hypocotyl length reached approx. 60% of the WT value), in other genotypes the inhibition was less pronounced but still seeming significant (approx. 75% of the WT value). Unfortunately, authors did not provide any statistical testing of measured data. Since the authors observed highest inhibition in the mutant impaired in early step of biosynthesis that is common for ABA and carotenoids, they surprisingly completely omitted the rest of the mutants and concluded that the effective compound in skotomorphogenesis is not ABA itself but some of its carotenoid precursor (Barrero et al. 2008).

3.8.2. Interaction of ABA signalling and light

Lim et al. (2013) revealed that ABA signalling elements ABI3, ABI5 and GA-induced transcription factor DELLA form a protein complex on the *SOM* promoter in imbibed seeds under high-temperature conditions. The SOM protein activates via unknown mechanism ABA biosynthetic genes (Kim et al. 2008). The ABI5 is a bZIP transcription factor involved in ABA signalling and ABA responses (Finkelstein and Lynch 2000). It was evidenced that ABI5 is regulated by the direct binding of HY5 on its promoter region. Thus HY5 is required for the transcription of some ABA activated genes such as ABI3, RAB18, AtEM1, and AtEM6, in seeds and during seed germination (Chen et al. 2008). HY5 is a target of the COP1-mediated 26S proteasome degradation pathway and is degraded in the dark conditions (Osterlund et al. 2000). The seeds of *hy5* mutant are less sensitive to exogenous ABA in term of germination (Chen et al. 2008) and develop longer hypocotyl in the light conditions compared to WT (Koornneef et al. 1980). Interestingly, when compared to the WT, *abi5* mutant seedlings of Arabidopsis did not show any differences in the hypocotyl growth under D, RL, BL or FR light conditions. Only in *ABI5* overexpressing seedlings the inhibition of hypocotyl elongation was observed in BL, RL and FR, but not in D (Chen et al. 2008). However, the mutation in RPN10 and KEG proteins that stabilize ABI5 protein led to the inhibition of elongation of dark-grown hypocotyls (Smalle et al. 2003; Stone et al. 2006). A similar situation was described for Arabidopsis seedlings with altered expression of *SnRK2.6*. The protein kinase SnRK2.6 was described as an important signalling element of the regulation of stomatal aperture by ABA. In

the *snrk2.6* mutant as well as in the *SnRK2.6* overexpressing seedlings no effects on the growth of etiolated hypocotyl were observed. Only when the growing media was supplemented with 250 nM ABA the inhibition of *SnRK2.6* overexpressing and WT, but not of the *snrk2.6* mutant hypocotyls were observed (Zheng et al. 2010).

It was further reported that the *ABI3* expression was enhanced in etiolated Arabidopsis *phyB* mutant seedlings. ABI3 was down-regulated in etiolated seedlings that were pre-exposed to the RL before germination (Mazzella et al. 2005). When the *GUS* reporter gene was introduced into Arabidopsis under the control of the *ABI3* promoter, the reporter expression was maximum in the cotyledons at the 1st day after germination (DAG), diminished completely at 3rd DAG, but appeared again at the base of cotyledons (top of hypocotyl) on 4th DAG. The expression profile of *ABI3* was reversed by FR, as typical for PHYB-mediated responses. The growth of etiolated hypocotyl was slightly enhanced in *abi3* mutant and down regulated in *ABI3* overexpressing seedlings. Authors suggested a role of ABI3 as component of phytochrome signalling that switches between seed quiescence and photomorphogenesis (Mazzella et al. 2005). Quiescence provides the persistence of the plant in unfavourable environment through the partial or complete arrest of meristematic growth. This arrest is relieved immediately after the environmental limitation has been overcome (Rohde et al. 1999). In the hypothetical model of Mazzella et al. (2005) the etiolated growth is regulated by ABI3 only indirectly via stimulation of quiescence when the etiolated hypocotyl stops elongation and by inhibition of photomorphogenesis. The quiescence should play a role in extreme conditions: when the seedling has a very low probability to reach the light, it will wait until external causes will improve its chance. When the seed germinates deeper in the soil without light the *ABI3* gene is not repressed by phytochrome and support persisting of the quiescence (Mazzella et al. 2005).

3.8.3. Role of ABA in maturation of chloroplasts and stomatal development

Important information on the role of ABA in photomorphogenesis comes from studies dealing with the formation of chloroplast and greening of cotyledons after the exposure of etiolated seedling to the light. It has been shown that the presence of exogenous ABA inhibits, whereas exogenous CKs stimulate cotyledon greening in etiolated lupine (*Lupinus luteus* L.). Exogenous ABA inhibited accumulation of NADPH:protochlorophyllide oxidoreductase that is a key enzyme of the formation of photosystems I and II after light signal (Kusnetsov et al. 1998). ABA also inhibits the etioplast development by controlling the expression of crucial genes in the nucleus (Kusnetsov et al. 1994). It has been reported that ABA effect in the greening process is dependent on the developmental stage of the seedling. In barley ABA inhibited the greening only in three days old seedlings, not in the later stages of etiolated growth (Kravtsov et al. 2011). The exogenous ABA in very high concentration (75 µM) inhibited the expression of barley chloroplast genes (Kravtsov et al. 2011; Yamburenko et al. 2013). In Arabidopsis the complete inhibition of cotyledon greening by exogenous ABA was also reported but at much

more lower concentration (500 nM). The ABA-mediated inhibition of cotyledon greening was antagonized by exogenous CK (6-benzylaminopurine) via degradation of ABI5 protein (Guan et al. 2014). Moreover it was previously shown that ABI3 signalling pathway is necessary to maintain unfolded, yellowish cotyledons containing undifferentiated plastids (Rohde et al. 2000). Surprisingly, when the etiolated Arabidopsis seedlings were pre-treated by ABA (5 to 50 µM) before transfer to the RL, ABA enhanced the cotyledon greening. A similar response was observed in seedlings over-expressing EDL3, an ABA signalling element (Koops et al. 2011). Although it was shown that endogenous CKs promotes seed germination by suppressing ABA effects (Wang et al. 2011b), the antagonism between ABA and BAP was functional in the stage of cotyledon greening, but not during seed germination (Guan et al. 2014), suggesting a developmental specificity of the various compounds or signalling pathways. Another process that is part of photomorphogenesis is stomatal development. Tanaka et al. (2013) showed that stomatal development is retarded in the Arabidopsis ABA-deficient *aba2-2* mutant. The same response was enhanced in the mutant with increased ABA degradation *cyp707a1cyp707a3* or by treatment with exogenous ABA. The stimulation of stomatal development was also observed in the ABA-insensitive *abi1-1* and *abi2-1* mutants (Tanaka et al. 2013).

The role of ABA in etiolated growth and de-etiolation is still poorly understood and does not represent a topic of choice for the scientific community. Moreover the reviewed studies brought contradictory conclusions suggesting once inhibitory and second time stimulatory function of ABA. The aim of this thesis was to unravel the role of ABA during post-germination growth in tomato (*Solanum lycopersicum* L.).

4. MATERIAL AND METHODS

Because the material and method concerning the two published articles (chapters 6 and 7, *PLoSOne* and *PSB* particularly) can be found within the articles, we decided not to repeat them here and to limit the description of methods only for these which are linked to unpublished data in chapter 8.

Plant material and growth conditions

The experiments dealing with the effect of ABA on the relative growth rate (RGR) and application of pyrabactin were performed with the cultivar Rutgers of tomato (*Solanum lycopersicum* L.). For experiments dealing to describe gene expression and endogenous CK content in ABA-deficient mutant, the tomato *sitiens* mutants and its corresponding WT (cv. Rheinlands Ruhm) were used. For the analysis of chlorophyll fluorescence the other two tomato mutants *notabilis* and *flacca* and their WTs (cv. Lukullus and cv. Rheinlands Ruhm) were also used. The CK profiling during etiolated growth and BL-induced photomorphogenesis was performed in the cv. Rheinlands Ruhm. As already mentioned, the *sit* mutant is impaired in the last step of ABA synthesis. The mutant *not* is mutated in the gene coding *LeNCED1* enzyme, a key regulatory step of ABA biosynthesis. The *flc* mutant is impaired in the molybdenum cofactor sulfurase that is necessary for the activation of the AAO the last step of ABA biosynthesis. All mutants consequently produce dramatically less ABA than the corresponding WTs.

To obtain sterile culture, seeds were soaked in 3% sodium hypochlorite (Bochemie, Czech Republic) for 20 min and rinsed extensively with sterile distilled water prior sowing. The seeds were then sown in square Petri dishes (120 x 120 mm) on basal Murashige and Skoog (MS) medium (Murashige and Skoog 1962) supplemented with 0.7% (w/v) agar in square Petri dishes (120 x 120 mm). The pH was adjusted to 6.1 with 1M KOH before autoclaving. The Petri dishes were placed vertically in the dark for 3 days at 23°C to induce germination. For experiments involving BL illumination, the Petri dishes were transferred to a growth chamber (Snijders, The Netherlands) at 23°C with continuous BL illumination provided by fluorescent tubes (TL-D36W/18-Blue, Philips; total photon fluence rate 10 $\mu mol.m^{-2}.s^{-1}$). The light spectrum was measured using a portable spectroradiometer (model LI-1800; Li-COR, NE, USA). For dark conditions, Petri dishes were wrapped in aluminum foil, and placed in the same growth chamber with the same temperature regime.

Hypocotyl growth measurement and relative growth rate (RGR) calculation

Germinated seeds were transferred to new media supplemented or not with abscisic acid or pyrabactin (both from Sigma-Aldrich, MO, USA). Stock solution of pyrabactin was prepared in dimethyl sulfoxide (DMSO) and the same quantity of solvent was added to the control samples; the final concentration of DMSO in media was 0.0004% (v/v). ABA stock solution was prepared in distilled water. Dishes were placed in a growth chamber for two days in the case of analysis of ABA effect on RGR and three days in the experiment with pyrabactin. In order to determine

RGR, Petri dishes were removed from the growth chambers after 24 hours and scanned on desktop scanner, and immediately placed back to the chamber to the dark conditions. The procedure was repeated one day later (48 hours after germination). The high-resolution images were then analyzed for the digital length of hypocotyl (DLH) by ImageJ software (Schneider et al. 2012). The relative growth rate was then calculated according Hoffmann and Poorter (2002) using the following equation: [$lnDLH_{48h} - lnDLH_{24h}$] where the DLH represent the digital length of hypocotyl measured one (24h) or two (48h) days after transfer to the new media supplemented with ABA or control solution. In the study using pyrabactin, after 3 days of growth in culture chamber in the dark, the length of hypocotyls was measured with ruler to the nearest mm; 15 seedlings were measured for each concentration. The statistical analysis was performed using Kruskal-Wallis nonparametric ANOVA test (p<0.05).

Analysis of chlorophyll fluorescence in cotyledons

Seeds were sown into the soil and grown in the growth chamber at 23°C in white LED light (long-day 16/8, total photon fluence rate 300 µmol.m^{-2}.s^{-1}). One week after sowing when the green cotyledons of ABA-deficient *not*, *sit* and *flc* mutants and their corresponding WTs (cv. Lukullus and cv. Rheinlands Ruhm) emerged, the chlorophyll (Chl) fluorescence was analysed after 20 minutes long dark adaptation. The Chl fluorescence was measured by FluorCam unit of PlantScreen phenotyping system (Photon Systems Instruments, Brno, Czech Republic) using standard protocol for kinetic measurement of non-photochemical quenching (NPQ). For details about Chl fluorescence analysis and measuring protocol please see Appendix chapters 10.1 and 10.2 particularly. The theoretical background of Chl fluorescence is reviewed by Lazár (2015). The data are presented as medians of 20 seedlings and statistical significance for particular Chl fluorescence parameters was tested using non-parametric Mann-Whitney *t*-test.

Extraction and quantification of CK

Seedlings were grown on MS medium in the dark or BL as described above. After seed germination all seedlings were transferred onto fresh MS media and cultivated in growth chamber for one or two additional days. De-etiolated seedlings were obtained by transferring Petri dishes under BL after germination; for the dark-grown, etiolated seedlings, Petri dishes were wrapped with aluminum foil and cultivated in the same growth chamber. Afterwards cotyledons, hypocotyls and roots were separated by scalpel and immediately frozen in liquid nitrogen. The elongating zones of hypocotyl, i.e. the 1 cm-long segment situated beneath cotyledons, were excised from independent set of seedlings. The dark-grown samples were harvested under green light while BL-grown samples were harvested under BL illumination of the same intensity as the one used during seedling cultivation. The collected samples were homogenized with a mortar and pestle in liquid nitrogen. 50 mg of the sample were then extracted, purified and analyzed by the same method as described in the article published in *PloSONE* (chapter 6, Humplík et al. 2015a).

Gene expression analysis

Seeds and seedlings were cultivated and harvested as described for ABA quantification. Total RNA was extracted using RNeasy Plant Mini Kit (Qiagen, The Netherlands), with an additional DNaseI treatment (Takara, Japan) for 30 minutes at 37 °C, followed by heat-inactivation at 65°C for 10 minutes. Samples were subjected to phenol:chloroform:isoamyl alcohol (25:24:1) purification. The cDNA synthesis was performed from 0.7 µg total RNA with the PrimeScriptTM 1st strand cDNA Synthesis Kit (Takara, Japan) according to the manufacturer's instructions. RNA was then digested with 5 units of RNaseH (Takara, Japan) for 20 minutes at 37 °C. The cDNAs were purified on a column and eluted with RNase/DNase-free distilled water. qPCR reactions were performed using the SYBR Premix Ex Taq kit (Takara, Japan) and 200 nM of each primer. Three technical repeats were performed for each sample in a two-step temperature program. The initial denaturation at 95 °C for 10 seconds was followed by 45 cycles of 95°C for 5 seconds and 60°C for 20 seconds. The dissociation curve for each sample was monitored during this time. All Ct values were normalized against those for the *PP2Acs* and *Tip41like* genes (Dekkers et al. 2012). The differences in the cycle numbers of the samples during the linear amplification phase, along with the ΔΔCt method, were used to determine fold changes in gene expression. All results are expressed in term of ''fold change''. Relative expression was evaluated using geometrical means calculated from two reference genes in each independent experiment. The quoted values represent the mean relative expressions observed in three independent experiments. The primer sequences are described in Table 1.

Table 1. Sequences of primer combinations.

Gene name		Sequence 5´- 3´
SlKRP2	F	AGATCGACAACCTTAGCACTTC
	R	ACAAGAATCAGAAGCAGAGGG
SlKRP4	F	CTGAGCTTGATGTGTTCTTTGC
	R	GCCTTGTGGTTTCATTGTCG
SlCycD3.1	F	TCTTGAGCTAATGGACACTGC
	R	ATCGAAGATGCTACTGACCATG
SlCycD3.3	F	CAAGGAGAAGGTGGAAGGATG
	R	CTGTTGGACTCCCTGGTAATG
SlLOG1	F	AGGATTGCTGAATGTGGATGG
	R	GACTAGCTCCTTTGACGATGG
SlLOG4	F	CCAAGACACTCATGCCTAGAG
	R	TCCTCAAGTGTGCCATAACC
SlLOG6	F	TGGGAGAGGTTAAAGCAGTTG
	R	AATTCCGAGTTGAGACCACG
PP2Acs	F	CGATGTGTGATCTCCTATGGTC
	R	AAGCTGATGGGCTCTAGAAATC
Tip41like	F	GGTTCCTATTGCTGCGTT
	R	CGAAGACAAGGCCTGAAA

5. BRIEF SURVEY OF PUBLISHED RESULTS

Most of the data obtained in the frame of this doctoral thesis were published in two research journal with peer review: *PloSONE* (Humplík et al. 2015a, chapter 6) and *Plant Signaling and Behavior* (*PSB*, Humplík et al. 2015b, chapter 7). The first publication deals with understanding the role of ABA during early development of tomato using physiological, cytological, molecular and analytical approaches. For this purpose, the etiolated growth of two tomato ABA-deficient mutants was investigated as well as skoto- and photo-morphogenesis in WT tomato with physiological ABA content. The second publication represents an Addendum of the first one, and describes a detailed spatio-temporal analysis of ABA during post-germination development. Despite the fact that a complete description can be found in the article, the most important results are summarized herein. The links to the figures mentioned in this chapter are written in *italic* and reference to the internal figure numbering of published articles (see chapter 6 and 7). The shortcut of the corresponding article is given together with internal figure number.

The two tomato ABA-deficient mutants (*not* and *sit*) were subjected to our analysis. We observed in both that they have significantly shorter hypocotyl than their WT counterpart, when grown in the dark. When different concentrations of ABA (50 nM to 5 µM) were applied, the hypocotyl length of ABA-deficient mutants was significantly stimulated by nM concentration but inhibited by concentrations higher than 1 µM. Whereas higher ABA concentrations inhibited also WT growth, no effect could be observed with low ABA concentrations, suggesting an endogenous ABA content optimal for proper growth (*PloSONE, Fig. 2*). The use of fluridone, an inhibitor of early step of ABA-biosynthesis, lowered endogenous ABA content in hypocotyls of etiolated WT seedlings bellow 50% of the control, concomitant with the inhibition of hypocotyl elongation (*PloSONE, Fig. S3 and S4*). The microscopic analysis showed that hypocotyl cell expansion was decreased in the etiolated *sit* mutant seedlings compared to the WT (*PloSONE, Fig. 4*). Moreover, flow-cytometry analysis of the cells of the growing zone of etiolated hypocotyls revealed that endoreduplication was restrained in the *sit* mutant (*PloSONE, Fig. 6A*). The expression of two genes (*SlKRP1* and *SlKRP3*) encoding CDK inhibitors, important regulator of endoreduplication, was lowered in *sit* mutant compared to the WT (*PloSONE, Fig. 6B*). This correlated with suppressed endoreduplication that occurs via restriction of cell division and contributes to cell expansion.

Since we hypothesized that ABA affects the hypocotyl growth via regulation of cell division, we focused on CKs content. The overall CK content, analysed in whole seedling sampels, was more than two-fold higher in the ABA-deficient *sit* mutant than in the WT (*PloSONE, Fig. 7A*). The molecular analysis showed that in the *sit* mutant the expression of CK biosynthetic gene *SlLOG2* was importantly elevated (*PloSONE, Fig. 7B*). In parallel, endogenous free ABA of the whole WT seedlings was monitored from the time of sowing to early development. The ABA concentration in dark-grown seedlings was almost twice that of BL-grown seedlings which were in photomorphogenesis, as represented by the strong inhibition of hypocotyl growth

(*PloSONE, Fig. 5A*). The accumulation of *LeNCED1* transcripts, encoding key enzyme involved in ABA synthesis, was almost 60% lower in the BL-grown seedlings than in those grown in darkness (*PloSONE, Fig. 5B*). In opposite, BL transiently induced expression of the ABA catabolic gene *SlCYP707A4* (*PloSONE, Fig. 5C*). As stated in the *PloSONE* article, we hypothesize that finely-tuned control of ABA metabolism during skotomorphogenesis promotes hypocotyl growth: ABA acts by stimulating the expression of the CDK inhibitors SlKRP1 and SlKRP3 and by inhibiting CK biosynthesis, both of which ultimately stimulate endoreduplication and cell expansion. While the full mechanisms of ABA action during skoto- and photomorphogenesis remain to be determined, our observations shed new light on the role of ABA during the development of young seedlings, and strongly suggest that at least in some stages of tomato seedling development, ABA stimulates growth.

The spatio-temporal analysis of ABA during tomato seedling development provided us with more detailed data than the previous whole-seedling analysis presented in the *PLoSOne* paper. At the onset of germination, ABA accumulated more in the emerging radicle than in the rest of the seed. During skotomorphogenesis, ABA concentration increased in both hypocotyl and cotyledons to a similar extent after 96 h of cultivation. One day later, a significant increase in ABA content was observed in cotyledons but not in the intact hypocotyl. Nevertheless, a strong increase in ABA content was observed in the growing zone of etiolated hypocotyl. When seedlings were grown under blue-light, ABA accumulation was significantly reduced in the hypocotyl and cotyledons showing similar proportional distribution in particular organs as in the dark except that analysis in hypocotyl growing zone could not be performed (*PSB, Fig. 1*). More results were obtained but were not up to day published. They are presented in the chapter 8 of the present thesis manuscript.

Based on our results, we demonstrated that:

i) ABA acts as stimulator of growth during skotomorphogenesis;

ii) ABA regulates cell expansion; at least a part of the mechanism is the regulation of endopolyploidic cycles;

iii) An interaction exists between ABA and CKs during skotomorphogenesis to support a proper cell expansion.

6. ENDOGENOUS ABSCISIC ACID PROMOTES HYPOCOTYL GROWTH AND AFFECTS ENDOREDUPLICATION DURING DARK-INDUCED GROWTH IN TOMATO (*SOLANUM LYCOPERSICUM* L.)

Published as:

Humplík JF, Bergougnoux V, Jandová M, Šimura J, Pěnčík A, Tomanec O, Rolčík J, Novák O, Fellner M. 2015. Endogenous Abscisic Acid Promotes Hypocotyl Growth and Affects Endoreduplication during Dark-Induced Growth in Tomato (*Solanum lycopersicum* L.). *PLoS One*. 10:e0117793. doi:10.1371/journal.pone.0117793

PLOS | ONE

RESEARCH ARTICLE

Endogenous Abscisic Acid Promotes Hypocotyl Growth and Affects Endoreduplication during Dark-Induced Growth in Tomato (*Solanum lycopersicum* L.)

Jan F. Humplík[1]*, Véronique Bergougnoux[2], Michaela Jandová[3], Jan Šimura[1], Aleš Pěnčík[1], Ondřej Tomanec[4], Jakub Rolčík[1], Ondřej Novák[1], Martin Fellner[1]

1 Laboratory of Growth Regulators & Department of Chemical Biology and Genetics, Centre of the Region Haná for Biotechnological and Agricultural Research, Faculty of Science, Palacký University & Institute of Experimental Botany ASCR, Olomouc, Czech Republic, 2 Department of Molecular Biology, Centre of the Region Haná for Biotechnological and Agricultural Research, Faculty of Science, Palacký University, Olomouc, Czech Republic, 3 Department of Botany, Faculty of Science, Palacký University, Olomouc, Czech Republic, 4 Regional Centre of Advanced Technologies and Materials, Department of Physical Chemistry, Palacký University, Olomouc, Czech Republic

* jan.humplik@upol.cz

Citation: Humplík JF, Bergougnoux V, Jandová M, Šimura J, Pěnčík A, Tomanec O, et al. (2015) Endogenous Abscisic Acid Promotes Hypocotyl Growth and Affects Endoreduplication during Dark-Induced Growth in Tomato (*Solanum lycopersicum* L.). PLoS ONE 10(2): e0117793. doi:10.1371/journal.pone.0117793

Academic Editor: Ricardo Aroca, Estación Experimental del Zaidín (CSIC), SPAIN

Received: July 25, 2014

Accepted: December 31, 2014

Published: February 19, 2015

Data Availability Statement: All relevant data are within the paper and its Supporting Information files.

Funding: This work was supported by the Ministry of Education, Youth and Sports of the Czech Republic grants no. LO1204 and LO1305 (National Program of Sustainability). V. Bergougnoux and M. Fellner were supported by the Operational Programs Education for Competitiveness - European Social Fund, project no. CZ.1.07/2.3.00/20.0165 and project no. CZ.1.07/2.3.00/30.0004, respectively. M. Jandová was supported by internal grants from Palacký University

Abstract

Dark-induced growth (skotomorphogenesis) is primarily characterized by rapid elongation of the hypocotyl. We have studied the role of abscisic acid (ABA) during the development of young tomato (*Solanum lycopersicum* L.) seedlings. We observed that ABA deficiency caused a reduction in hypocotyl growth at the level of cell elongation and that the growth in ABA-deficient plants could be improved by treatment with exogenous ABA, through which the plants show a concentration dependent response. In addition, ABA accumulated in dark-grown tomato seedlings that grew rapidly, whereas seedlings grown under blue light exhibited low growth rates and accumulated less ABA. We demonstrated that ABA promotes DNA endoreduplication by enhancing the expression of the genes encoding inhibitors of cyclin-dependent kinases *SlKRP1* and *SlKRP3* and by reducing cytokinin levels. These data were supported by the expression analysis of the genes which encode enzymes involved in ABA and CK metabolism. Our results show that ABA is essential for the process of hypocotyl elongation and that appropriate control of the endogenous level of ABA is required in order to drive the growth of etiolated seedlings.

Introduction

Abscisic acid (ABA) is very often regarded as an inhibitor of shoot growth e. g. [1], [2], [3]. This is based on the fact that i) ABA accumulates at high concentrations in water stressed plants, correlating with growth inhibition [4], [5], [6] and ii) treatment with exogenous ABA at μM concentrations inhibits shoot growth [7], [5], [8]. However, ABA deficient mutants are

(IGA-PrF-2013-003; IGA-PrF-2014001). The funders had no role in study design, data collection and analysis, decision to publish, or preparation of the manuscript.

Competing Interests: The authors have declared that no competing interests exist.

shorter than the corresponding wild-type (WT) plants, and their growth can be improved by treatment with exogenous ABA. Their reduced growth was attributed to an impaired water balance [9]. The first evidence that ABA could stimulate shoot growth was obtained in a study on etiolated rice seedlings, in which treatment with extremely low concentrations of exogenous ABA stimulated mesocotyl elongation [10]. Later, Saab and co-authors demonstrated that under conditions of high water potential, the ABA-deficient *viviparous* maize mutant exhibited reduced growth compared to WT plants [11]. Similarly, the ABA biosynthesis-impaired *flacca* tomato mutant exhibited reduced shoot growth and elevated ethylene production compared to the WT. The treatment of the *flacca* mutant with exogenous ABA suppressed its excessive ethylene biosynthesis and restored shoot growth to near WT-levels [12]. The inhibition of vegetative growth was also observed in the *Arabidopsis aba1* and *aba2-1* mutants [13], [14], which are defective in different steps of ABA biosynthesis (Fig. 1). It therefore appears that ABA maintains shoot growth rather than inhibiting it, partly by suppressing ethylene synthesis and partly by some ethylene-independent mechanism.

We focused our study on the role of ABA during tomato seedling development, particularly on the growth of hypocotyl. After a seed germinates in the soil, in the absence of light, the seedling undergoes etiolated growth, known as skotomorphogenesis, which is characterized by rapid elongation of the hypocotyl topped by a hook with underdeveloped cotyledons. When the etiolated seedling perceives the light, it begins photomorphogenesis. The transition from skotomorphogenesis to photomorphogenesis, referred to as de-etiolation, involves several developmental changes such as inhibition of the fast hypocotyl growth, activation of the apical meristem, and the development of the cotyledons and plastids [15]. The role of ABA in skotomorphogenesis is poorly documented. Barrero et al. (2008) reported that dark-grown *Arabidopsis aba1* seedlings, deficient in ABA-biosynthesis, had a de-etiolated phenotype [16]. However, since this mutant is also impaired in carotenoid synthesis, the authors concluded that one of ABA's carotenoid biosynthetic precursors was responsible for this effect rather than the ABA itself.

In this work, we investigated the role of ABA during skotomorphogenesis in tomato seedlings (*Solanum lycopersicum* L). Our study was intended to answer the question: Does ABA contribute to the rapid stem growth observed during skotomorphogenesis or does it play a role in growth inhibition observed during tomato de-etiolation? Using physiological and genetic approaches we demonstrated that finely-tuned regulation of ABA homeostasis is required to promote or inhibit growth. Indeed, ABA was found to promote hypocotyl elongation of etiolated ABA deficient tomato seedlings that exhibited a concentration-dependent response. The results were also supported by the analysis of ABA content, and the expression of ABA metabolic genes in contrasting developmental situations. It seems that ABA stimulates cell expansion by enhancing endoreduplication via the elevated expression of cyclin-dependent kinases (CDK) inhibitors and the inhibition of cytokinin biosynthesis.

Materials and Methods

Plant material and growth conditions

The experiments involving ABA quantification, the analysis of the expression of genes involved in ABA metabolism and pharmacological experiments were performed using wild-type tomato (*Solanum lycopersicum* L.) seedlings of the Rutgers cultivar. In all other experiments that focused on the effects of endogenous ABA deficiency, seedlings of the tomato mutants *sitiens* (*sit*) and *notabilis* (*not*) and the corresponding WTs (cv. Rheinlands Ruhm and cv. Lukullus, respectively) were used. The *sit* mutant is defective in the very last step of ABA biosynthesis [17] (Fig. 1) and consequently produces dramatically less ABA than the corresponding WT

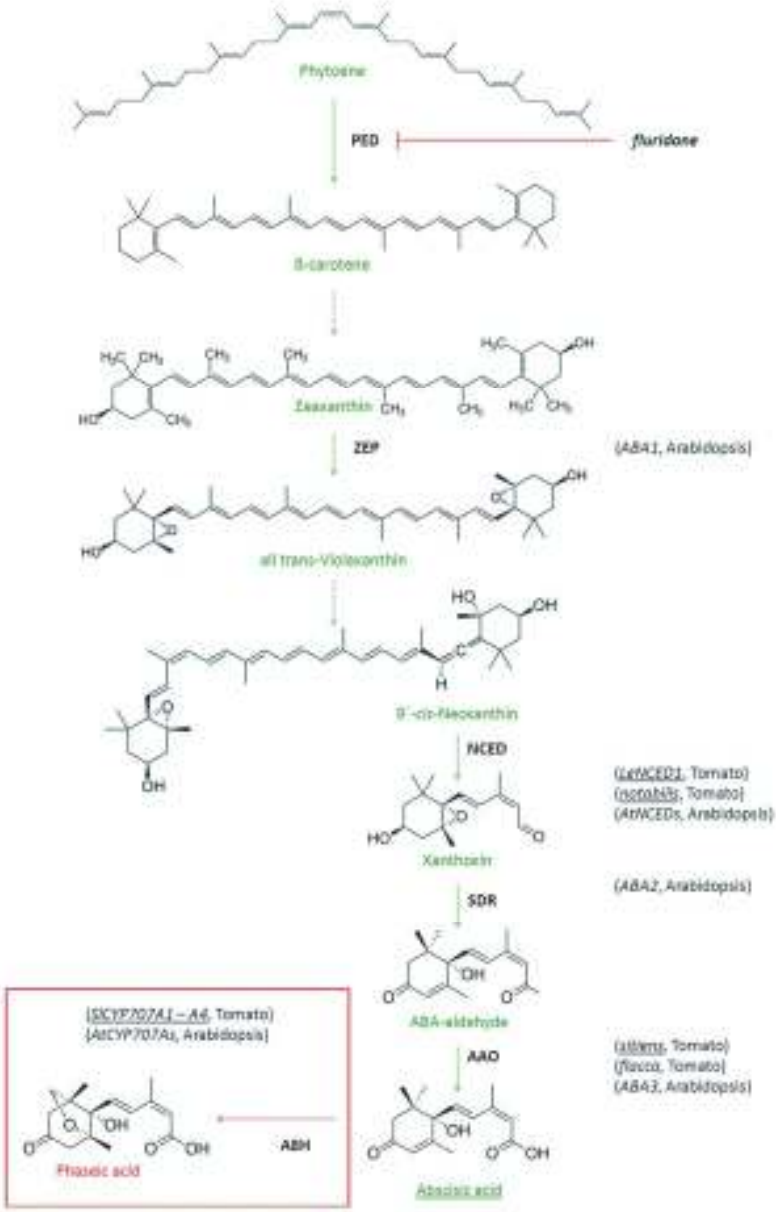

Fig 1. Simplified scheme of ABA biosynthesis and catabolism. Selected enzymatic steps in ABA biosynthesis are shown. The names of the genes encoding the enzymes that catalyze each step in tomato and *Arabidopsis* are indicated; the names of genes examined in this work are underlined. The conversion of phytoene to β-carotene is mediated by phytoene desaturase (PED); this step is blocked by fluridone. Zeaxanthin epoxidase (ZEP) catalyzes the synthesis of violaxanthin, which is then converted to neoxanthin. The subsequent synthesis of xanthoxin is catalyzed by 9-cis-epoxycarotenoid

dioxygenase (NCED), which is encoded in the gene *LeNCED1* in tomato and disrupted in notabilis mutant. Whereas the previous steps occur in plastids, xanthoxin is transported to the cytosol where it is converted to the abscisic aldehyde by short-chain dehydrogenase/reductase (SDR). The final step of ABA biosynthesis is the oxidation of abscisic aldehyde to ABA by an abscisic aldehyde oxidase (AAO), which is encoded in genes that are disrupted in the sitiens and flacca tomato mutants. ABA degradation (shown in the red frame) is mediated by ABA 8'-hydroxylase (ABH, cytochrome P450 monooxygenase), whose product spontaneously isomerizes to phaseic acid. The genes encoding ABA 8'-hydroxylase in tomato are *SlCYP707A1*–*SlCYP707A4*. Dashed arrows represent missing steps in the pathway. These schemes are modified according to Kitahata and co-authors [32] and Nambara and Marion-Poll [70].

doi:10.1371/journal.pone.0117793.g001

[18], [19]. The *not* mutant is impaired in the key regulatory step of ABA biosynthesis, the oxidative cleavage of 9'-*cis*-neoxanthin to xanthoxin [20], and ABA production is also consequently reduced [19], [21].

The seeds were soaked in 3% sodium hypochlorite (Bochemie, Czech Republic) for 20 minutes and rinsed extensively with sterile distilled water prior to sowing. The seeds were then sown on the basal Murashige and Skoog medium [22] supplemented with 0.7% (w/v) agar in square Petri dishes (120 x 120 mm). The pH was adjusted to 6.1 with 1.0 M KOH before autoclaving. The Petri dishes were placed vertically in the dark for 3 days at 23°C to induce germination. For experiments involving blue-light (BL) illumination, the Petri dishes were transferred to a growth chamber (Snijders, The Netherlands) at 23°C with continuous BL illumination provided by fluorescent tubes (TL-D 36W/18-Blue, Philips; total photon fluence rate 10 μmol m^{-2} s^{-1}). The light spectrum was measured using a portable spectroradiometer (model LI-1800; LI-COR, NE, USA). For dark conditions, Petri dishes were wrapped in aluminum foil, and placed in the same growth chamber under the same temperature regime.

Hypocotyl growth measurement

Germinated seeds were transferred to new media that were supplemented as appropriate with abscisic acid or fluridone (both from Sigma-Aldrich, MO, USA) and to new media that were not supplemented with the effectors (control samples). These compounds were added to the medium as 10 mM stock solutions. The stock solution of fluridone was prepared in 10% (v/v) ethanol and the same quantity of solvent was added to the control samples. All samples were placed in a growth chamber for 4 days (96 hours). Hypocotyl length was measured with a ruler and at least 10 seedlings per treatment were measured in each independent experiment. The data of hypocotyl lengths were normalized to the appropriate control samples: the median length of the untreated WT or mutant samples (specified in figure legends) was set as 100% hypocotyl length and all other values were expressed as percentages of this control. The original measured values that were used for data normalization are given in S1 Table. The data are presented as medians and first and third quartiles as they corresponded to the non-parametric statistics. The number of experimental repeats is shown in the figure legends, along with the total number of measured seedlings.

Epidermal cell length measurement

Seedlings of *sit* and WT (cv. Rheinlands Ruhm) were grown in dark on the basal Murashige and Skoog medium for 4 days after transfer as described above. Then a 1 cm segment from the hypocotyl base was excised and immediately fixed in a solution of 4% formaldehyde, 0.5% glutaraldehyde in a 1x MTSB buffer (50 mM PIPES, 5 mM $MgSO_4$, 5 mM EGTA, pH 6.9). Samples were fixed overnight in a vacuum chamber to enhance the penetration of the fixative solution into the hypocotyl tissue. Subsequently samples were washed twice with the 1x MTSB buffer and dehydrated by increasing the concentration of ethanol solution (15%, 30%, 50%, 75%, 90%, 100%). Each dehydration step lasted 20 minutes. Then the 100% ethanol washing was repeated once and samples were incubated overnight. The solution was then replaced by

fresh 100% ethanol solution for storage. Before the analysis hypocotyl segments were mounted on a metal sample holder and ethanol traces evaporated in 3 minutes. Afterwards the sample was immediately transferred to a scanning electron microscope (SEM) and photographed at magnification 100 along the whole length of hypocotyl segment. The epidermal cells were measured in ImageJ software [23] and a non-parametric variant of the t-test (Mann-Whitney test) was applied to prove the significance of the obtained data. The data are presented as medians and first and third quartiles. For each genotype at least 230 cells from three representative hypocotyls were analyzed.

Extraction and quantification of ABA

The seeds and seedlings were cultivated in the dark as described above. For the analysis of ABA, seedlings were harvested at 6, 12, 24, 48, 72, 96 and 120 hours after sowing. To obtain deetiolated seedlings for ABA analysis, the Petri dishes were transferred to BL after seed germination, which occurred 72 hours after sowing. Prior to germination at 72 hours, all seeds were collected; after 72 hours, only germinated seeds were used for analysis. For the analysis in the ABA-deficient mutants, the hypocotyls were excised and frozen immediately in liquid nitrogen. The dark-grown samples were harvested under safety green light while BL-grown samples were harvested under BL illumination. The collected samples were homogenized with a mortar and pestle in liquid nitrogen. For determination of the endogenous levels of ABA, 10 mg of homogenized tissue were extracted by using a phosphate buffer. The sample was then purified by solid-phase extraction on a C8 column as described previously for auxins [24], except in this case [$^2H_6$]ABA was added as an internal standard. After evaporation under reduced pressure, samples were analyzed for free ABA content by UPLC (Acquity UPLC™; Waters, USA) linked to a triple quadrupole mass detector (Xevo TQ MS™, Waters, USA). The same trend in relative ABA content was observed in all biological repeats; however, the number of repeats was not sufficient for statistical analysis. All data are presented as the mean of the relative ABA content, with the value observed for dark-grown samples at the last time point (120 hours) set as 100 arbitrary units (a.u.) for each experimental repeat. The absolute values obtained in the independent repeats are reported in tables S2 Table and S3 Table.

Extraction and quantification of CKs

For the quantification of CKs, the etiolated seedlings of sit and WT were harvested 4 days after their germination. The collected samples were homogenized with a mortar and pestle in liquid nitrogen. Fifty mg of the sample were then extracted in a modified Bieleski buffer (methanol/water/formic acid, 15/4/1, v/v/v) [25]. For the purification of free CKs, two SPE columns were used: a C18 octadecylsilica-based column (500 mg of sorbent, Applied Separations) and an MCX column (30 mg of C18/SCX combined sorbent with cation-exchange properties, Waters) [26]. Analytes were eluted by two-step elution using a 0.35 M aqueous solution of NH_4OH and 0.35 M NH_4OH in 60% (v/v) MeOH. Samples were then evaporated to dryness under reduced pressure at 37°C. An Acquity UPLC System (Waters, Milford, MA,USA), linked to a triple quadrupole mass spectrometer Xevo™ TQ MS (Waters MS Technologies, Manchester, UK) equipped with an electrospray interface was used to determine cytokinin levels. Stable isotope-labeled CK internal standards (0.5 pmol each for CK bases, ribosides, and *N*-glucosides; 1 pmol each for *O*-glucosides and nucleotides) were added to each sample during the extraction step to enable accurate quantification. The final concentration of each analyte was calculated from its peak area in multiple reaction monitoring mode chromatograms, as described by Svačinová and co-authors [27]. The data are presented as mean relative CK contents, with the measured

values for the WT control samples being set to 100 arbitrary units (a.u.) for each experimental repeat. Absolute values for three independent repeats are given in S4 Table.

Analysis of gene expression by RealTime-qPCR

Seeds and seedlings were cultivated and harvested as described for ABA quantification. Total RNA was extracted using an RNeasy Plant Mini Kit (Qiagen, The Netherlands), with an additional round of DNaseI treatment (Takara, Japan) for 30 minutes at 37°C. The DNase I enzyme was then heat-inactivated at 65°C for 10 minutes, after which the samples were subjected to phenol:chloroform:isoamyl alcohol (25:24:1) purification. The cDNA synthesis was performed using 0.7 μg total RNA with the PrimeScript™ 1st strand cDNA Synthesis Kit (Takara, Japan) according to the manufacturer's instructions. The RNA was then digested with 5 units of RNaseH (Takara, Japan) for 20 minutes at 37°C. The cDNAs were purified on a column and eluted with RNase/DNase-free distilled water. qPCR reactions were performed using the SYBR Premix Ex Taq kit (Takara, Japan) and 200 nM of each primer. Three technical repeats were performed for each sample in a two-step temperature program. The initial denaturation at 95°C for 10 seconds was followed by 45 cycles of 95°C for 5 seconds and 60°C for 20 seconds. The dissociation curve for each sample was monitored during this time. All Ct values were normalized against those for the *PP2Acs* and *Tip41like* genes [28]. The differences in the cycle numbers of the samples during the linear amplification phase, along with the $\Delta\Delta C_T$ method, were used to determine fold changes in gene expression. All results are expressed in term of "fold change". Relative expression was evaluated using geometrical means calculated from two reference genes in each independent experiment. The quoted values represent the mean relative expressions observed in three independent experiments. While the number of repeats was not sufficient to prove significance in some samples, we observed the same trends in relative gene expression in all experiments (Tables A–D in S1 File). The primer sequences and gene accession numbers in the SOL genomics network (http://solgenomics.net/) are given in Table 1.

Analysis of ploidy—endoreduplication

The seedlings of *sl0* mutant and WT were grown in the dark as described above. The hypocotyls were harvested and immediately used to determine the level of DNA endoreduplication using a C6 Flow cytometer (Accuri BD, New Jersey, USA) with a blue laser (488 nm). Ten mm-long segments were excised from the upper part of the hypocotyl and cut with a razor blade in a Petri dish containing 350 μl of ice cold LB01 buffer [29]. The suspension of nuclei was then filtered through a 42 μm nylon mesh and stained with propidium iodide (50 $\mu g.ml^{-1}$). For each sample, 5000 particles were measured. A histogram of fluorescence intensity was registered on the FL2 channel using a linear scale. Because the first peak in the histogram corresponded to the G1 (2C) phase of the cell cycle, the ploidy levels of the other peaks were determined by comparison with the position of the G1 peak. The average ratio of the G1 and G2 peak positions was 1.97 (4C) and that of the G1 and G3 positions was 3.69 (8C) with coefficients of variance ranging from 3.7–9.0. For each of the four studied treatments, a total of 10 seedlings were analyzed in three independent experiments.

Statistical analysis

When comparing the results for two samples, the non-parametric variant of the t-test (Mann-Whitney test) was used to assess statistical significance. For multiple-sample experiments, significance was assessed using the non-parametric variant of one-way ANOVA, Kruskal–Wallis test with multiple comparisons post-hoc. The obtained differences were considered as significant when the *p*-value was lower than 0.05 (95% reliability), but in many cases the *p*-values

Table 1. Sequences of primer combinations used in this study.

Gene name	Accession no.	Sequence 5' - 3'	Reference
LeNCED1	SGN-U577478	F: CTTATTTGGCTATCGCTGAACC	[33]
		R: CCTCCAACTTCAAACTCATTGC	
SlCYP707A2	SGN-U583027	F: GCAATGAAAGCGAGGAAAGAG	
		R: TTGTTCGTCAGTGAGTCCTTC	
SlCYP707A3	SGN-U585745	F: GCTCCCAAACCCAATACCTAC	[33]
		R: CAGTTTGGCGAGTTCATTTCC	
SlCYP707A4	SGN-U583028	F: GCTAGTGTCCTTACATGGATCC	[33]
		R: CTCTCATTATCCCCTCTTGCTC	
SlKRP1	AJ441249	F: CAACATTCAGACCCCTGGTT	
		R: CTCCTTTTCTGCACGGGTAA	
SlKRP2	SGN-U320533	F: TTCGTACAAGAGCTAAAACCCTAG	
		R: TGTTTTCGCTTCAAAGCCCAC	
SlLOG2		F: TGTTGGAGAAGTAAGAGCAGTG	[35]
		R: ATGAATGCCTAGTTGAGCCC	
PP2Acs	SGN-U567355	F: CGATGTGTGATCTCCTATGGTC	[28]
		R: AAGCTGATGGGCTCTAGAAATC	
Tip41like	SGN-U584254	F: GGTTCCTATTGCTGCGTT	[28]
		R: CGAAGACAAGGCCTGAAA	

doi:10.1371/journal.pone.0117793.t001

were lower than 0.01 (99% reliability), particular *p*-values are given in figure legends. All statistical analyses were performed using the STATISTICA 12 software (StatSoft, OK, USA). When the number of repeats was not sufficient to prove significance (gene expression and hormone analysis), the original values used for calculation of the means and SE are given in the Supporting information to demonstrate that the data of all replicates in particular experiment showed the same trends.

Results

The effects of ABA deficiency on hypocotyl growth and expansion of hypocotyl cells

The tomato *sit* mutant, which is defective in the last step of ABA biosynthesis, was used as the main tool to investigate the role of ABA in hypocotyl growth. The dark-grown *sit* mutant produced significantly shorter hypocotyls than WT plants grown under identical conditions (Fig. 2A). However, when ABA was added to the growth medium at a concentration of 100 nM, the hypocotyls of the *sit* mutant grew to the same length as those of WT plants. When different concentrations of ABA (50 nM to 5 μM) were applied the hypocotyl length was significantly stimulated by nM but inhibited by concentrations higher than 1μM in the *sit* mutant (Fig. 2B). On the other hand in the WT inhibition only was observed at the highest ABA concentration treatment (Fig. 2C). A similar response was observed in *not* mutant and corresponding WT (cv. Lukullus). The *not* seedlings were significantly inhibited in the hypocotyl growth compared to the WT, but the treatment with 50 nM ABA led to the improvement of the mutant. WT seedlings did not respond to the exogenous ABA treatment (Fig. 2D). In comparison with *sit* mutant, a lower ABA concentration (50 nM) was chosen as most efficient for *not*, based on the previous test of ABA sensitivity (S1 Fig.). ABA contents in *sit* and *not* mutant and corresponding WT hypocotyls were analyzed to see the effects of mutations in our

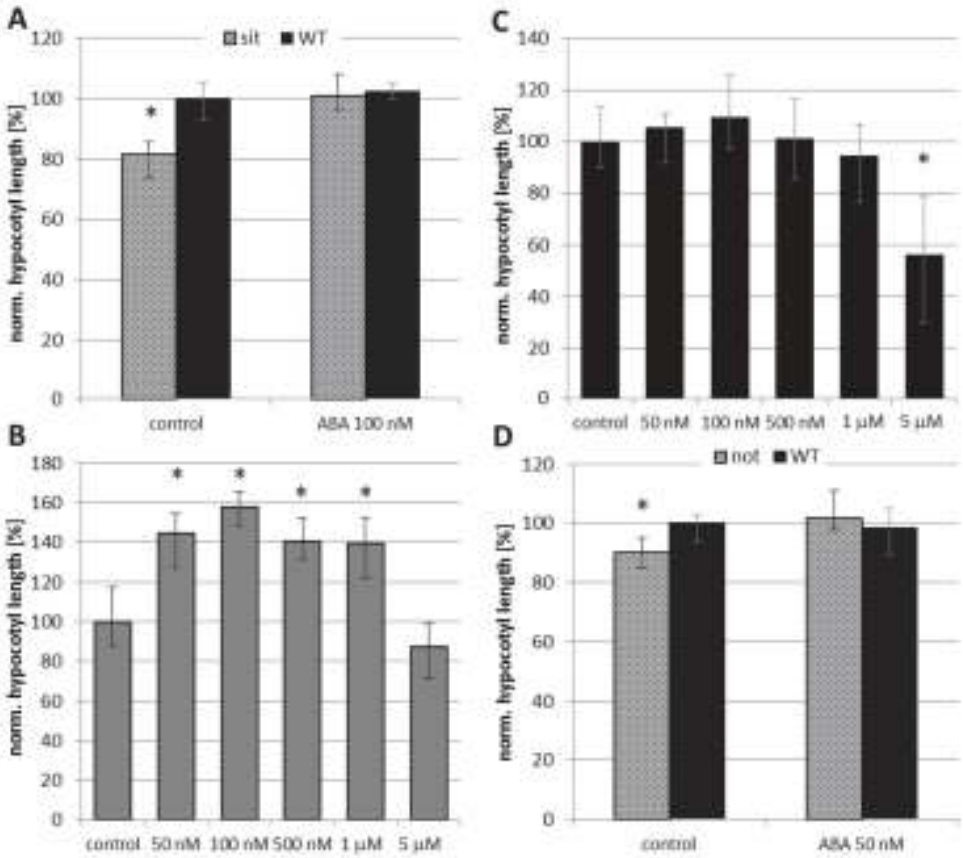

Fig 2. The effects of ABA on the growth of etiolated hypocotyls. A) The effect of ABA-deficiency and exogenous ABA on hypocotyl growth in the *sit* mutant. Germinated seeds of the WT (cv. Rheinlands Ruhm) mutant were transferred to untreated media (control) and media supplemented with 100 nM ABA and grown in the dark for 4 days. The results shown in the figure represent the medians of normalized length of hypocotyls from three independent experiments; the error bars represent the boundaries of the first and third quartiles. The "WT control" was set as 100% hypocotyl length and all other values (medians, quartiles) are expressed as percentages of this value. To prove statistical significance the Mann-Whitney test was performed independently (*sit* versus WT) for control and ABA treated samples. Asterisks denote values that differ significantly (Mann Whitney test; $p < 0.01$, $n = 136$). B) The hypocotyl elongation of the *sit* mutant treated with various concentrations of ABA. Germinated seeds were transferred to untreated media (control) and media supplemented with ABA and grown in the dark for 4 days. The results shown in the figure represent the medians of normalized length of hypocotyls from two independent experiments; the error bars represent the boundaries of the first and third quartiles. The sample "control" was set as 100% hypocotyl length and all other values (medians, quartiles) are expressed as percentages of this value. To prove statistical significance the Kruskal-Wallis ANOVA with multiple post-hoc comparison was performed. Asterisks denote values that differ significantly from "control" sample ($p < 0.01$; $n = 232$). C) The hypocotyl elongation of the WT (cv. Rheinlands Ruhm) treated with various concentrations of ABA. Germinated seeds were transferred to untreated media (control) and media supplemented with ABA and grown in the dark for 4 days. The results shown in the figure represent the medians of normalized length of hypocotyls from two independent experiments; the error bars represent the boundaries of the first and third quartiles. The sample "control" was set as 100% hypocotyl length and all other values (medians, quartiles) are expressed as percentages of this value. To prove statistical significance the Kruskal-Wallis ANOVA was performed. Asterisks denote values that differ significantly from "control" sample ($p < 0.01$, $n = 200$). D) The effect of ABA-deficiency and exogenous ABA on hypocotyl growth in the *not* mutant. Germinated seeds of the WT (cv. Lukullus) mutant were transferred to untreated media (control) and media supplemented with 50 nM ABA and grown in the dark for 4 days. The results shown in the figure represent the medians of normalized length of hypocotyls from one independent experiment. The "WT control" was set as 100% hypocotyl length and all other values (medians, quartiles) are expressed as percentages of this value. To prove statistical significance the Mann-Whitney test was performed independently (*not* versus WT) for control and ABA treated samples. Asterisks denote values that differ significantly (Mann Whitney test; $p < 0.03$, $n = 79$).

doi:10.1371/journal.pone.0117793.g002

experimental conditions. Both mutants showed dramatically lowered endogenous ABA compared to the WT samples (Fig. 3, S3 Table). In order to determine the role of ABA during photomorphogenesis, additional experiments were conducted using seedlings grown under BL illumination, which is known to strongly inhibit hypocotyl growth [30], [31]. The *sit* mutation did not have any discernible effect on hypocotyl growth under continuous BL illumination (S2 Fig.).

In parallel to the studies using mutant lines, we conducted a series of experiments using synthetic inhibitor of ABA biosynthesis. Freshly germinated tomato (cv. Rutgers) seedlings were grown in the dark for four days on a medium supplemented with fluridone (10 μM) and then the length of the hypocotyls was measured. Fluridone is an inhibitor of carotenoid pathway, suppressing early steps of ABA synthesis [32] (for details see Fig. 1). The analysis of ABA content in dark-grown WT hypocotyls showed that fluridone lowered endogenous ABA to the less than 50% of the control samples (S3 Fig.). Fluridone caused significant inhibition of hypocotyl growth in the etiolated seedlings (S4 Fig.). To see how ABA deficiency affected hypocotyl cell elongation the microscopic experiments were performed. The measurement of cell length showed significant inhibition (Mann-Whitney test, p value < 0.05) of cell expansion in the dark-grown *sit* mutant compared to the WT (Fig. 4).

Endogenous ABA levels during germination, skotomorphogenesis and photomorphogenesis

The endogenous free ABA contents of whole WT tomato (cv. Rutgers) seedlings were monitored from sowing to early development. The endogenous ABA levels were highest at the first analyzed time point, i.e. 6 hours after sowing, after which they decreased rapidly until germination, 72 hours after sowing. After germination, the ABA content increased gradually in developing seedlings. De-etiolation and photomorphogenesis were initiated by exposure to BL (constant illumination, 10 $\mu mol.m^{-2}.s^{-1}$). Nevertheless, the ABA concentration in dark-grown seedlings was around twice that in seedlings grown under continuous BL and which had undergone de-etiolation and subsequent photomorphogenesis (Fig. 5A).

To determine whether the differences in ABA seen after germination were due to inhibition of ABA biosynthesis or stimulation of ABA degradation, the expression of genes involved in ABA metabolism was investigated. The gene *LeNCED1* encodes 9-cis-epoxycarotenoid dioxygenase, which is the key enzyme involved in ABA synthesis; its expression over time in dark- and BL-grown seedlings is shown in Fig. 5B. The relative abundance of the transcript was below the limit of detection prior to germination but increased progressively in developing seedlings. In addition, the accumulation of *LeNCED1* transcripts in the BL-grown seedlings was almost 60% lower than in those grown in darkness.

We also investigated the expression of four genes which encode the enzymes involved in ABA catabolism (ABA 8′-hydroxylases SlCYP707A1 to SlCYP707A4) [33]. The *SlCYP707A1* transcript was not detected under our conditions, which suggested that the corresponding enzyme was not involved in seedling development. No significant difference was observed between the dark- and BL-grown seedlings with respect to the expression of either *SlCYP707A2* or *SlCYP707A4* (S4 Fig.). But a BL-induced response was observed in *SlCYP707A3* (Fig. 5C). Indeed, this transcript accumulated gradually and at the same rate in the dark- and BL-grown seedlings during the first 48 hours of the experiment (i.e. the seed imbibition period) and then declined between 48 and 72 hours (the point at which germination occurred). In the dark-grown seedlings, the expression of *SlCYP707A3* then declined further before reaching a low basal level. Conversely, in the BL-grown seedlings, its expression increased dramatically

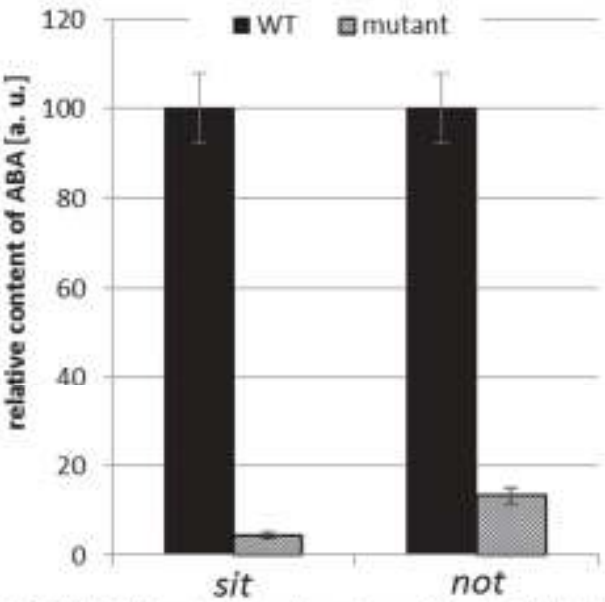

Fig 3. Effect of *sit* and *not* mutations on the endogenous ABA content in etiolated hypocotyls. The dark-grown hypocotyls of *sit* and *not* mutants and corresponding WTs were harvested five days after germination and ABA content was measured. Free ABA levels are reported as relative means [a.u.] ± SE based on two biological repeats. The mutant values are expressed relative to those for corresponding WT, which were assigned a value of 100 a.u.

doi:10.1371/journal.pone.0117793.g003

between 72 and 96 hours before falling again. The developmental stages of tomato germination and post-germination growth considered in this work are shown in Fig. 3D.

The effects of ABA on DNA endoreduplication in etiolated tomato hypocotyls

The results presented above indicated that ABA plays an important role in regulating dark-induced growth. Etiolated hypocotyl growth is primarily due to cell elongation, with cell division only being important in the development of stomata [34]. Moreover, as in *Arabidopsis*, the tomato hypocotyl elongates along a basipetal gradient. Consequently, the upper region of hypocotyl (i.e. the part situated just above the hook and cotyledons) is the active site of elongation [35]. We therefore investigated the effects of ABA on endoreduplication in this part of the seedlings. For this purpose, 10 mm-long segments were excised from the upper parts of the hypocotyls of the etiolated seedlings of both the *sit* mutant and the corresponding WT, and their cell ploidy was measured by flow cytometry. The cell ploidy status was expressed as the ratio of the number of nuclei in the G3 phase to the total number of nuclei [8C/(2C+4C+8C)], where G3 represents nuclei in the endoreduplication cycle (8C). Our data clearly showed that the extent of endoreduplication in hypocotyl segments from dark-grown untreated *sit* mutants was significantly lower than in the corresponding WT samples. Treatment with exogenous ABA

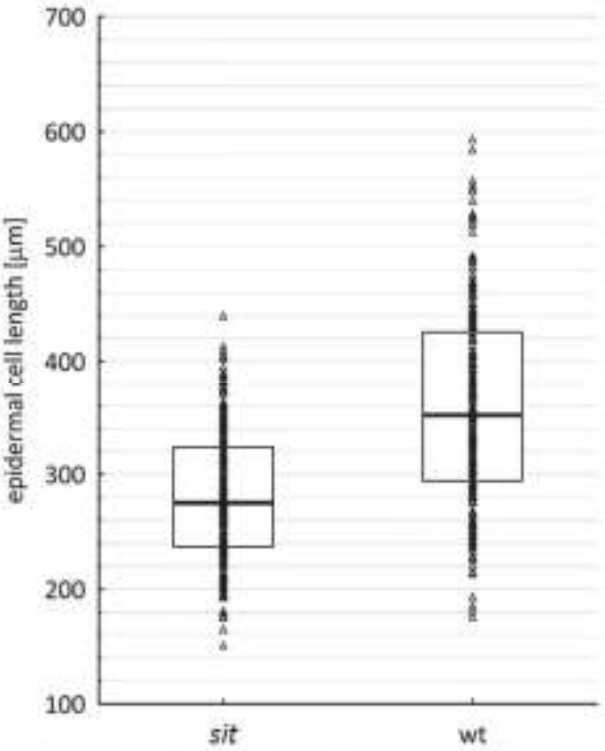

Fig 4. Effect of ABA deficiency on the expansion of hypocotyl cells. The influence of ABA on the elongation of epidermal cells of etiolated hypocotyls in *sit* and WT (cv. Rheinlands Ruhm) was investigated using SEM imaging analysis. Triangles represent all measured values (n = 471) for each genotype. The bars within the boxes indicate the median values in each case, while the boxes' upper and lower boundaries indicate the boundaries of the first and third quartiles. The Mann-Whitney test was used to prove statistical significance ($p < 0.01$).

doi:10.1371/journal.pone.0117793.g004

significantly increased the number of G3-phase nuclei in the *sit* hypocotyls but caused only a slight increase in the WT samples (Fig. 6A).

Endoreduplication is controlled by the activity of cyclin-dependent kinase (CDK) proteins, and it has been reported that the expression of the CDK inhibitor *ICK1* is induced by ABA in *Arabidopsis* [36]. Analyses of the expression of two tomato *ICK1* orthologs, *SlKRP1* and *SlKRP3*, [37], [38] indicated that their transcripts were less abundant in the *sit* mutant than in WT plants. Treatment with ABA stimulated the expression of both genes in *sit*, but had no effect on the WT. The overall *SlKRP1* expression was approximately twice that for *SlKRP3* (Fig. 6B).

The effect of ABA on endogenous cytokinin levels

It was recently demonstrated that cytokinins (CKs) accumulate during de-etiolation, probably due to the accumulation of *SlLOG2* transcripts, which encode an enzyme responsible for the

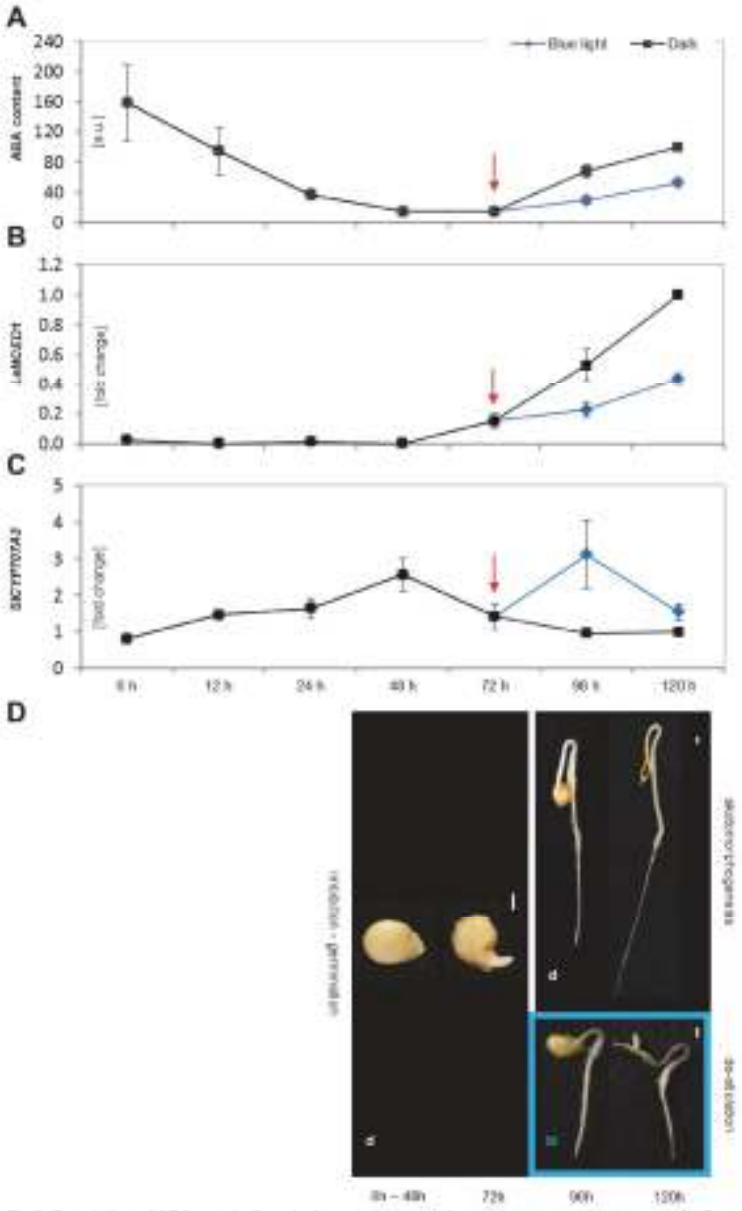

Fig 5. Regulation of ABA metabolism during seed germination and post-germination growth. Free ABA levels are reported as relative means [a.u.] ± SE based on three independent experiments. All values are expressed relative to those for the dark-grown sample at the 120 hours time point, which was assigned a value of 100 a.u. (A). The fold changes in the expression of the LeNCED1 (B) and SlCYP707A2 (C) genes are

reported as the means of three independent experiments ± SE. *Tip41like* and *PP2ACs* were used as housekeeping genes. Relative quantification was performed using the expression levels for the dark-grown sample at 120 hours as a reference. The red arrow marks the point of seed germination. Figure D) shows the different stages of tomato seedling development considered in this work. The first is seed imbibition (6h–48h), which is followed by seed germination (72h). Both of these steps occurred in darkness in all experiments. The seedlings were then separated (96h–120h) into two groups: one was kept in darkness (d) to induce skotomorphogenesis while the other was grown under continuous BL (bl) to induce de-etiolation. White bars indicate a distance of 1 mm.

doi:10.1371/journal.pone.0117793.g005

synthesis of CK free bases. Moreover, it was evidenced that CK accumulation correlated with the inhibition of endoreduplication [35]. To test the hypothesis that CKs and ABA may act antagonistically during de-etiolation, we measured the endogenous CK contents of dark-grown whole WT and *sit* seedlings grown in the presence and absence of exogenous ABA (Fig. 7A; S4 Table). The *sit* seedlings had much higher levels of CK compounds than the WT plants, and treatment with ABA reduced the abundance of CKs in the mutant but not in the WT. In both cases, the seedlings' CK levels correlated with the expression of the *SlLOG2* gene, which was expressed in the hypocotyl segments of the *sit* mutant almost twice as strongly as in the WT. Treatment with exogenous ABA significantly inhibited *SlLOG2* transcript accumulation in the *sit* mutant but had only minor effects on the WT (Fig. 7B).

Discussion

The role of ABA in shoot development has been the subject of debate for some time. While some recent authors still contend that the physiological role of ABA is to inhibit shoot growth [2], [3], [39] there is a growing body of evidence suggesting that it can in fact stimulate shoot growth, or at least contribute to its maintenance [12], [13], [21], [40], [41]. In the present study, the significant inhibition of hypocotyl growth was observed in ABA deficient etiolated seedlings. We found that exogenous ABA stimulated the growth of ABA deficient mutants and had no effect on WTs in nM concentration range. Only a high concentration (5 μM) inhibited WTs growth. As mentioned by Sharp (2002), the interpretation of data related to the application of exogenous ABA are complicated by the uncertain effects of the exogenous treatment [42]. However, our data obtained through treatment with ABA in a wide concentration range suggested that the key factor is plant sensitivity to ABA and homeostatic regulation. It is highly probable that in WT seedlings the number of active ABA receptors corresponds to the signal compound concentration. We can hypothesize that in WT seedlings, the receptors are already saturated by endogenous ABA and the application of exogenous ABA either cannot trigger further response or it can trigger an "over-dose" response that leads to growth inhibition. In ABA deficient seedlings, the endogenous ABA content is too low to activate or saturate the receptors. Thus the *sit* and *not* seedlings are able to respond efficiently to the exogenous ABA treatment. It is important to consider not only the presence or absence, but also the quantity of the signal within the living organism. Then the same compound could evoke opposite responses depending on the concentration used, as has been previously shown for auxin [43] or cytokinins [44]. This can also explain the different sensitivity of *sit* and *not* mutants to ABA. Whereas *sit* seedlings are impaired in the last step of ABA synthesis, the *not* mutation affects the earlier step of conversion of 9′-*cis*-neoxanthin to xanthoxin (LeNCED enzyme). While both mutants produce consistently less ABA than WTs [45], [46], [47], their endogenous ABA content differs (4% and 13% of the WTs for *sit* and *not*, respectively). Thus the difference in sensitivity observed between the two mutants can reflect the difference in their endogenous ABA content. The dose-dependent increase of hypocotyl growth of the mutants suggests that a homeostatic imbalance could be restored by exogenous ABA. Our results suggested that in plants with

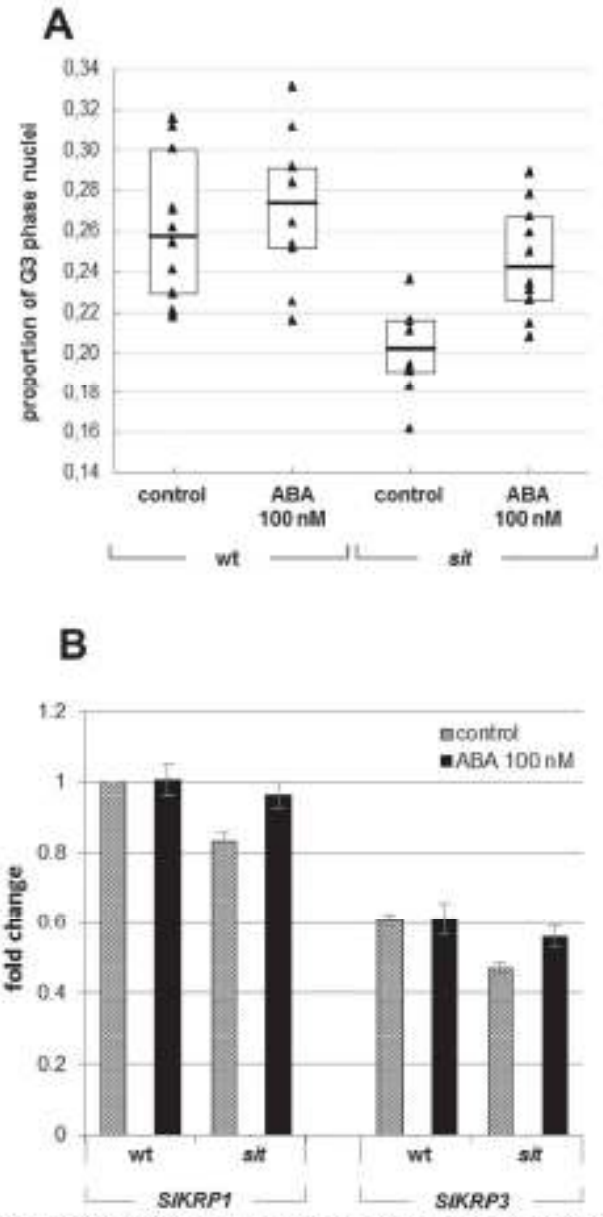

Fig 6. The effects of ABA on endoreduplication. The influence of ABA on nuclear ploidy was investigated using hypocotyl segments of *sit* and WT seedlings grown in darkness on untreated media and media containing 100 nM ABA (A). Triangles represent all measured values (n = 40) for each genotype and

treatment. The bars within the boxes indicate the median values in each case, while the boxes' upper and lower boundaries indicate the boundaries of the first and third quartiles. Three independent experiments were performed. The Kruskal-Wallis ANOVA test with multiple comparisons revealed that only the *sit* control sample differed significantly from the WT control ($p < 0.01$). No other significant differences were found. (B) Analysis of the expression of the *SlKRP1* and *SlKRP2* genes based on the mean of three independent experiments ± SE. *Tip41like* and *PP2ACs* were used as housekeeping genes. All expression values are quoted relative to those for the "WT control" sample.

doi:10.1371/journal.pone.0117793.g006

normal (physiological) ABA levels, additive exogenous ABA will lead to an "over-dose" effect causing growth inhibition, but in the ABA deficient plants the ABA action could be revealed in a more physiological context.

To see the effects of ABA deficiency on the hypocotyl growth the application of ABA biosynthetic inhibitor was performed also as an alternative to genetic approach. Although possible unspecific effects of the chemical treatment should be considered, the application of fluridone led to reduced hypocotyl elongation in dark-grown WT seedlings that further supported the data obtained in genetic experiments. The tomato *sit* mutant was an important genetic tool in this work because it is deficient in the very final step of ABA biosynthesis. Thus, results obtained on this mutant clearly identified the role of ABA in the studied physiological processes. Under conditions with no water stress, the ABA deficient seedlings grown in the dark had significantly shorter hypocotyls than WT plants grown under the same conditions. Previous analysis of the *Arabidopsis aba1* loss-of-function mutant also indicated that ABA may significantly contribute to the process of skotomorphogenesis [16]. However, because the ABA1 enzyme catalyzes an early step in ABA biosynthesis (Fig. 1) whose product is also a precursor of carotenoids, the authors concluded that one of the carotenoid precursors of ABA is required for etiolated growth rather than ABA itself. In the present study, very similar results were obtained with the tomato *sit* mutant, which was deficient in the final step of ABA synthesis, i.e. the conversion of ABA-aldehyde into ABA. Therefore our results strongly suggest that ABA rather than one of its carotenoid precursors promotes the hypocotyl elongation observed during skotomorphogenesis.

Plants defective in ABA signalling are also a good material to investigate the role of ABA during vegetative development. The family of *abscisic-acid insensitive* (*abi*) mutants was the first group of plants discovered with impaired ABA signal transduction [48]. To our knowledge only *abi5* was tested for etiolated hypocotyl elongation and no significant difference was observed between mutant and WT. Even the overexpression of *ABI5* construct in the WT did not change the hypocotyl growth [39]. However, it is hard to determine how the ABA signalling is involved in skotomorphogenesis because of the high level of redundancy between ABA signalling components [49], [50], [51]. In light-grown seedlings a strong inhibition of growth was reported for the *abi8* mutant [52]. Among the ABA receptors the most highly expressed in most developmental stages are PYR1, PYL1, PYL4, PYL8, PYL5, and PYL2. The sextuple mutant showed a strong inhibition of vegetative growth in adult *Arabidopsis* plants [53]. It corresponds to the results obtained with ABA deficient *Arabidopsis* [13] and tomato [12] plants, confirming the importance of proper ABA signalling for maintaining shoot growth.

The postulated correlation between ABA content and tomato hypocotyl growth was further supported by the measurement of endogenous ABA in dark-grown seedlings and in seedlings grown under continuous BL. The dark-grown seedlings undergoing skotomorphogenesis accumulated substantially higher amounts of ABA than those undergoing photomorphogenesis. The fact that seedlings growing under BL still accumulate ABA supports the idea that ABA contributes to the maintenance of steady-state seedling growth. Analyses of the expression of genes involved in ABA synthesis and catabolism suggested that both processes contribute to

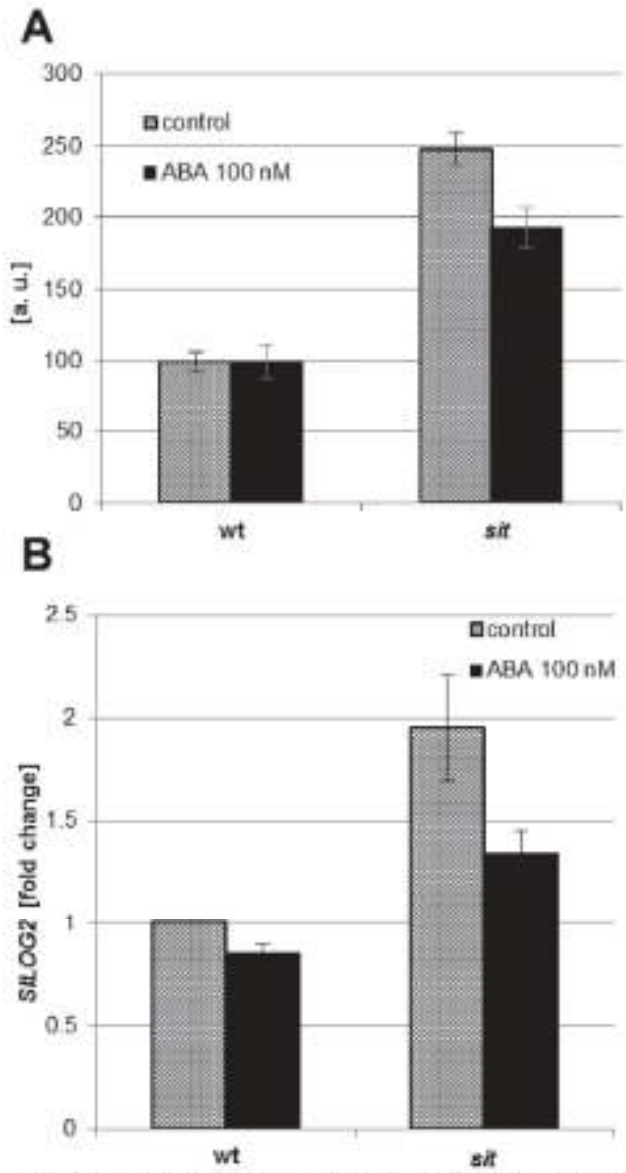

Fig 7. The effects of ABA deficiency on biosynthesis and overall CK levels in etiolated tomato seedlings. Overall CK levels are quoted as the mean of the relative values [a.u.] ± SE for three independent experiments. All measurements are expressed in relation to those for the "WT control" sample, which was assigned a value of 100a.u. (A). The expression of the SlLOG2 gene is presented as the mean of three independent experiments ± SE. *Tip41like* and *PP2ACs* were used as housekeeping genes. Expression was quantified in relation to that of the specified reference genes in the "WT control" sample (B).

doi:10.1371/journal.pone.0117793.g007

the regulation of ABA by light. Thus, the transcript of the *LeNCED1* gene, which is involved in ABA synthesis, was undetectable prior to seed germination (in accordance with the fact that ABA in the tomato seeds was synthesized during their maturation) but accumulated during the development of the young seedlings. The accumulation of *LeNCED1* transcripts in the BL-grown seedlings was considerably lower than in the etiolated seedlings. The differential accumulation of *LeNCED1* transcripts observed between dark- and BL-grown seedlings correlated with their differential accumulation of endogenous ABA. The analysis of catabolic genes revealed that *SlCYP707A1* was not detected in our experimental conditions, consistent with its preferential localization in pollinated ovaries [33]. Under our conditions, *SlCYP707A3* was the only ABA 8'-hydroxylase whose expression differed appreciably between dark- and BL-grown tomato hypocotyls, suggesting that this enzyme plays a role during the onset of photomorphogenesis. Continuous exposure to BL led to a decrease of ABA accumulation in the seedlings, driven by the reduction in synthesis and the strong but transient stimulation of catabolism. This suggests that the BL-induced reduction or limitation of endogenous ABA is important in de-etiolation and the onset of photomorphogenesis. Of course, an analysis of protein levels and enzymatic activities would be required to confirm our conclusions. However, we are not the first to report that light regulates endogenous ABA. Indeed, Kraepiel and co-authors demonstrated that the pea phytochrome-deficient *pcw-1* mutant had a higher content of ABA in its seeds and leaves than the WT, suggesting that light plays an important role in regulating ABA accumulation [54]. Similarly, Weatherwax and co-authors reported that red light reduced the concentration of ABA in etiolated *Lemna gibba* and also that dark treatment of previously light-grown *Arabidopsis* and *Lemna gibba* plants caused significant ABA accumulation [55]. Moreover, Symons and Reid observed reductions in the ABA content of etiolated pea seedlings after 4 hours of exposure to white light [56].

Skotomorphogenesis is characterized by the rapid elongation of the hypocotyl across a basipetal gradient. This elongation is mainly due to cell expansion, with cell division being restricted to the development of stomata [34]. It has been described previously that leaf epidermal cells of the *sit* mutant are significantly reduced [57]. In the present study, we demonstrated that the shorter hypocotyls of the mutants are due to the reduction of cell expansion. Cell expansion is triggered by two processes: an increase in the cell ploidy by endoreduplication and the expansion of the cell itself, which is driven by water uptake [58]. Whereas there is no doubt about the importance of ABA for water regulation, in this study we focused on the possible influence of ABA on endoreduplication. DNA endoreduplication is a consequence of cell multiplication without division, leading to increased ploidy of the cell. Cell division is regulated via the activity of cyclin-dependent kinases (CDKs) which are regulated by cyclin D-type proteins (CYCD). The initiation of endoreduplication requires the suppression of proteins of the CDK B-family. The activity of the CDK-CYC complexes can be blocked by the inhibitor of CDK/KIP-related (ICK/KRP) proteins. The expression of ICK/KRPs stimulated endoreduplication restricts the G2/M transition [59]. Recently, Bergougnoux and co-authors reported that the switch from skoto- to photomorphogenesis is characterized by the inhibition of endoreduplication [35]. Similarly to studies of ABA effects on shoot growth, existing reports concerning the influence of ABA on endocycles are also contradictory. For example, del Castelano and co-authors reported that treatment with high concentrations (μM) of exogenous ABA inhibited endocycles in *Arabidopsis* leaf primordia, but not in root meristems [60]. Conversely, different studies suggested that ABA promoted endoreduplication by up-regulating the expression of *ICK/KRPs* in *Arabidopsis* [36] and in an alfalfa cell suspension culture [61]. In our study, the ABA deficiency of the *sit* mutant correlated to a lower expression of the *SlKRP1* and *SlKRP3* genes compared to the WT, and to reduced endoreduplication. The expression of *SlKRPs* as well as the level of endoreduplication was decreased by about 20% in *sit* compared to the WT,

corresponding to the growth reduction rate observed in this mutant. Such correlation suggests a direct link between endoreduplication and hypocotyl growth. Overall, these results prompted us to hypothesize that the stimulation of endoreduplication is at least one important aspect of the mechanism by which ABA triggers hypocotyl elongation during skotomorphogenesis.

The postulated growth-promoting effect of ABA is supported by the work of Sharp and co-authors [12]. The authors found that under well-watered, non-stressed conditions, the ABA deficient tomato *flacca* mutant exhibited impaired leaf growth and ethylene content two times higher than that of the WT. Exogenous ABA partially restored the mutant's growth and significantly reduced the accumulation of ethylene. This led to the hypothesis that endogenous ABA maintains shoot elongation in adult tomato plants in a non-hydraulic way by restricting ethylene production. Moreover, studies of the ABA-deficient and ethylene-insensitive *Arabidopsis aba2-1/etr1-1* mutant suggested ethylene-independent mechanisms for the maintenance of shoot growth [13], which implies that some other hormone may be responsible for the relevant processes.

Interaction between ABA and other phytohormones is expected to contribute to the control of stem growth during skotomorphogenesis. Aside from its ethylene-suppressing effects, ABA is also known to be antagonistic to gibberellins (GAs) during seed germination. However, GAs stimulate etiolated hypocotyl growth [62] and are rapidly degraded in response to light [56]. It is more likely that CKs counteract the effects of ABA in stimulating hypocotyl growth, in keeping with their established role during plastid development [63]. Recently it was shown in *Arabidopsis* that CK counteracts ABA by degrading the ABI5 protein [64]. The inhibitory effects of CKs on endoreduplication in tobacco and petunia leaves were reported [65]. Recently the negative regulation of endoreduplication by CKs in the *Arabidopsis* shoot apical meristem has been shown by Scofield and co-authors [66]. This response seems to be shoot-specific since the CK-dependent stimulation of endocycling activity in roots has been reported [67]. Here, we focused on ABA-CK interaction as it was found that CKs inhibit endoreduplication and cell expansion during de-etiolation in tomato seedlings [35]. Indeed the he exposure of etiolated tomato seedlings to BL induced the accumulation of CK in the elongating zone of the hypocotyl and the accumulation of *SlLOG2* transcripts; *SlLOG2* encodes an enzyme that is responsible for the synthesis of CK free bases. This is accompanied by the inhibition of endoreduplication, prompting the conclusion that CKs inhibit stem growth by inhibiting endoreduplication and other processes. Our results showed that ABA stimulates endoreduplication and thereby contributes to stem elongation in dark-grown seedlings. This clarifies the previously discussed antagonism between ABA and CKs during seedling development. Indeed, ABA is known to stimulate the accumulation of cytokinin oxidase/dehydrogenase transcripts which encode the proteins responsible for CK degradation [68], while CKs repress the expression of ABA-associated genes [69], [64]. Our data showed that appropriate control of the endogenous ABA balance is necessary to regulate endogenous CK. The insufficient biosynthesis of ABA in the *sit* mutant led to the up-regulation of *SlLOG2* and the concomitant accumulation of endogenous CKs. These effects were partially reversed by treatment with exogenous ABA. Nevertheless, the fact that ABA treatment fully restored the *sit* growth, while the overall amount of CKs was not suppressed to the WT level, raised several questions. These results provided an insight into the interactions between ABA and CKs during skotomorphogenesis, but a more focused study will be required to fully clarify the regulation of CK metabolism.

In conclusion, the results presented here demonstrate that ABA is important for promoting the rapid growth of tomato hypocotyls during skotomorphogenesis. Consistent with previous reports on adult plants we have shown that ABA is necessary to promote growth in young seedlings during the skotomorphogenic stage of development. It seems that this response is masked by homeostasis of endogenous ABA in the WT and can only be observed in ABA

deficient mutants. On the other hand, in the WT seedlings the significant increase in endogenous ABA levels could be observed during fast etiolated growth compared to the growth of de-etiolated seedlings. This shows the importance of ABA for cell elongation. Based on our results, we hypothesize that finely-tuned control of ABA metabolism during skotomorphogenesis promotes hypocotyl growth: ABA acts by stimulating the expression of the CDK inhibitors SlKRP1 and SlKRP3 and by inhibiting CK biosynthesis, both of which ultimately stimulate endoreduplication and cell expansion. While the full mechanisms of ABA action during skoto- and photomorphogenesis remain to be determined, our observations shed new light on the role of ABA during the development of young seedlings, and strongly suggest that at least in some stages of tomato seedling development, ABA stimulates growth.

Supporting Information

S1 Table. The hypocotyl length values used for data normalization.
(PDF)

S2 Table. Absolute quantification of free ABA.
(PDF)

S3 Table. Absolute quantification of free ABA in hypocotyls of ABA-deficient mutants.
(PDF)

S4 Table. Absolute quantification of CK levels.
(PDF)

S1 File. Supporting Information Tables. Table A in S1 File Fold change of *LeNCED1* transcript expression. Table B in S1 File Fold change of *SlCYP707A3* transcript expression. Table C in S1 File Fold change of *SlKRP1* and *SlKRP3* transcript expression. Table D in S1 File Fold change of *SlLOG2* transcript expression.
(PDF)

S1 Fig. The hypocotyl elongation of the *sut* mutant treated with various concentrations of ABA.
(PDF)

S2 Fig. The effect of the *sit* mutation on hypocotyl length in BL-grown seedlings.
(PDF)

S3 Fig. The endogenous ABA content in fluridone treated WT hypocotyls (cv. Rutgers).
(PDF)

S4 Fig. The effect of fluridone on hypocotyl growth in dark-grown seedlings.
(PDF)

S5 Fig. The relative expression of the *SlCYP707A2* and *SlCYP707A4* genes.
(PDF)

Acknowledgments

The authors thank Renáta Plotzová, Jarmila Greplová and Věra Chytilová for their excellent technical support and seed propagation. We thank David Zalabák (Palacký University in Olomouc) for important help with the fixation of hypocotyl segments. We further thank Jan Nauš (Palacký University in Olomouc) for his measurements of the photon fluence rates and Nuria de Diego (Palacký University in Olomouc) for valuable discussion and critical reading of the

manuscript. We thank Tomáš Fürst (Palacky University in Olomouc) for revision of statistical analysis and Dave Richardson (Palacký University in Olomouc) for proof-reading of the manuscript.

Author Contributions

Conceived and designed the experiments: JFH VB. Performed the experiments: JFH MJ JŠ AP OT JR. Analyzed the data: JFH MJ AP JR ON. Contributed reagents/materials/analysis tools: MF. Wrote the paper: JFH VB MF.

References

1. Hansen H, Grossmann K (2000) Auxin-induced ethylene triggers abscisic acid biosynthesis and growth inhibition. Plant Physiol 124: 1437–1448. PMID: 11080315
2. Davies PJ (2010) The plant hormones: their nature, occurrence, and functions. In: Davies PJ, editor. Plant hormones: biosynthesis, signal transduction, action! Dordrecht, The Netherlands: Springer. 9–11 p.
3. Rai MK, Shekhawat NS, Gupta AK, Phulwaria M, Ram K, et al. (2011) The role of abscisic acid in plant tissue culture: a review of recent progress. Plant Cell Tiss Org 106: 179–190.
4. Zhang J, Davies WJ (1990) Does ABA in the xylem control the rate of leaf growth in soil-dried maize and sunflower plants? J Exp Bot 41: 1125–1132.
5. Creelman RA, Mason HS, Bensen RJ, Boyer JS, Mullet JE (1990) Water deficit and abscisic acid cause differential inhibition of shoot versus root growth in soybean seedlings: Analysis of growth, sugar accumulation, and gene expression. Plant Physiol 92: 205–214. PMID: 16667249
6. Munns R, Cramer GR (1996) Is coordination of leaf and root growth mediated by abscisic acid? Opinion. Plant Soil 185: 33–49.
7. Wakabayashi K, Sakurai N, Kuraishi S (1989) Role of the outer tissue in abscisic acid-mediated growth suppression of etiolated squash hypocotyl segments. Physiol Plantarum 75: 151–156.
8. Hayashi Y, Takahashi K, Inoue S-I, Kinoshita T (2014) Abscisic acid suppresses hypocotyl elongation by dephosphorylating plasma membrane H(+)-ATPase in Arabidopsis thaliana. Plant Cell Physiol 55: 845–853. doi: 10.1093/pcp/pcu028 PMID: 24492298
9. Quarrie SA (1987) Use of genotypes differing in endogenous abscisic acid levels in studies of physiology and development. In: Hoad GV, Lenton J R, Jackson MB, Atkin RK, editors. Hormone action in plant development—a critical appraisal. London: Butterworths. pp. 89–105. doi: 10.1111/tpj.12742 PMID: 25624480
10. Takahashi K (1972) Abscisic acid as a stimulator for rice mesocotyl growth. Nat New Biol 238: 92–93.
11. Saab IN, Sharp RE, Pritchard J, Voetberg GS (1990) Increased endogenous abscisic acid maintains primary root growth and inhibits shoot growth of maize seedlings at low water potentials. Plant Physiol 93: 1329–1336. PMID: 16667621
12. Sharp RE, LeNoble ME, Else MA, Thorne ET, Gherardi F (2000) Endogenous ABA maintains shoot growth in tomato independently of effects on plant water balance: evidence for an interaction with ethylene. J Exp Bot 51: 1575–1584. PMID: 11006308
13. LeNoble ME, Spollen WG, Sharp RE (2004) Maintenance of shoot growth by endogenous ABA: genetic assessment of the involvement of ethylene suppression. J Exp Bot 55: 237–245. PMID: 14673028
14. Barrero JM, Piqueras P, González-Guzmán M, Serrano R, Rodríguez PL, et al. (2005) A mutational analysis of the ABA1 gene of *Arabidopsis thaliana* highlights the involvement of ABA in vegetative development. J Exp Bot 56: 2071–2083. PMID: 15983017
15. Arnovski AA, Galstyan A, Guseman JM, Nemhauser JL (2012) Photomorphogenesis. In The Arabidopsis Book. e0147. doi: 10.1199/tab.0147
16. Barrero JM, Rodríguez PL, Quesada V, Alabadí D, Blázquez MA, et al. (2006) The *ABA1* gene and carotenoid biosynthesis are required for late skotomorphogenic growth in *Arabidopsis thaliana*. Plant Cell Environ 31: 227–234. PMID: 17096011
17. Taylor IB, Linforth RST, Al-Naieb RJ, Bowman WR, Marples BA (1988) The wilty tomato mutants flacca and sitiens are impaired in the oxidation of ABA-aldehyde to ABA. Plant Cell Environ 11: 739–745.
18. Tal M, Nevo Y (1973) Abnormal stomatal behavior and root resistance, and hormonal imbalance in three wilty mutants of tomato. Biochem Genet 8: 291–300. PMID: 4701995

19. Neill SJ, Horgan R (1985) Abscisic acid production and water relations in wilty tomato mutants subjected to water deficiency. J Exp Bot 36: 1222–1231.

20. Burbidge A, Grieve TM, Jackson A, Thompson A, McCarty DR, et al. (1999) Characterization of the ABA-deficient tomato mutant notabilis and its relationship with maize Vp14. Plant J 17: 427–431. PMID: 10205899

21. Thompson AJ, Thorne ET, Burbidge A, Jackson AC, Sharp RE, et al. (2004) Complementation of notabilis, an abscisic acid-deficient mutant of tomato: importance of sequence context and utility of partial complementation. Plant Cell Environ 27: 459–471.

22. Murashige T, Skoog A (1962) A revised medium for rapid growth and bio assays with tobacco tissue cultures. Physiol Plantarum 15: 473–497.

23. Schneider CA, Rasband WS, Eliceiri KW (2012) NIH Image to ImageJ: 25 years of image analysis. Nat Methods 9: 671–675. PMID: 22930834

24. Pěnčík A, Rolčík J, Novák O, Magnus V, Barták P, et al. (2009) Isolation of novel indole-3-acetic acid conjugates by immunoaffinity extraction. Talanta 80: 651–655. doi: 10.1016/j.talanta.2009.07.043 PMID: 19836533

25. Hoyerová K, Gaudinová A, Malbeck J, Dobrev PI, Kocábek T, et al. (2006) Efficiency of different methods of extraction and purification of cytokinins. Phytochem 67: 1151–1158. PMID: 16678229

26. Dobrev PI, Kamínek M (2002) Fast and efficient separation of cytokinins from auxin and abscisic acid and their purification using mixed-mode solid-phase extraction. J Chromatogr A 950: 21–29. PMID: 11990994

27. Svačinová J, Novák O, Plačková L, Lenobel R, Holík J, et al. (2012) A new approach for cytokinin isolation from Arabidopsis tissues using miniaturized purification: pipette tip solid-phase extraction. Plant Methods 8: 17. doi: 10.1186/1746-4811-8-17 PMID: 22594941

28. Dekkers BJ, Willems L, Bassel GW, van Bolderen-Veldkamp RP, Ligterink W, et al. (2012) Identification of reference genes for RT-qPCR expression analysis in *Arabidopsis* and tomato seeds. Plant Cell Physiol 53: 28–37. doi: 10.1093/pcp/pcr113 PMID: 21852358

29. Doležel J, Greilhuber J, Suda J (2007) Estimation of nuclear DNA content in plants using flow cytometry. Nat Protoc 2: 2233–2244. PMID: 17853881

30. Parks BM, Cho MH, Spalding EP (1998) Two genetically separable phases of growth inhibition induced by blue light in Arabidopsis seedlings. Plant Physiol 118: 609–615. PMID: 9765547

31. Parks BM, Spalding EP (1999) Sequential and coordinated action of phytochromes A and B during Arabidopsis stem growth revealed by kinetic analysis. P Natl Acad Sci USA 96: 14142–14146. PMID: 10570212

32. Kitahata N, Asami T (2011) Chemical biology of abscisic acid. J Plant Res 124: 549–557. doi: 10.1007/s10265-011-0415-0 PMID: 21461561

33. Nitsch LM, Oplaat C, Feron R, Ma Q, Wolter-Arts M, et al. (2009) Abscisic acid levels in tomato ovaries are regulated by *LeNCED1* and *SlCYP707A1*. Planta 229: 1335–1346.

34. Traas J, Hülskamp M, Gendreau E, Höfte H (1998) Endoreduplication and development: rule without dividing? Curr Opin Plant Biol 1: 498–503. PMID: 10066638

35. Bergougnoux V, Zalabák D, Jandová M, Novák O, Wilsse-Klinkenberg A, et al. (2012) Effect of blue light on endogenous isopentenyladenine and endoreduplication during photomorphogenesis and deetiolation of tomato (Solanum lycopersicum L.) seedlings. PLoS One 7: e45255. doi: 10.1371/journal.pone.0045255 PMID: 23049779

36. Wang H, Qi Q, Schorr P, Cutler AJ, Crosby WL, et al. (1998) ICK1, a cyclin-dependent protein kinase inhibitor from Arabidopsis thaliana interacts with both Cdc2a and CycD3, and its expression is induced by abscisic acid. Plant J 15: 501–510. PMID: 9753778

37. Bisbis B, Delmas F, Joubès J, Sicard A, Hernould M, et al. (2006) Cyclin-dependent kinase (CDK) inhibitors regulate the CDK-cyclin complex activities in endoreduplicating cells of developing tomato fruit. J Biol Chem 281: 7374–7383. PMID: 16407238

38. Nafati M, Fragne N, Hernould M, Chevalier C, Gévaudant F (2010) Functional characterization of the tomato cyclin-dependent kinase inhibitor SlKRP1 domains involved in protein-protein interactions. New Phytol 188: 136–149. doi: 10.1111/j.1469-8137.2010.03364.x PMID: 20618916

39. Chen H, Zhang J, Neff MM, Hong S-W, Zhang H, et al. (2008) Integration of light and abscisic acid signaling during seed germination and early seedling development. P Natl Acad Sci USA 105: 4495–4500 doi: 10.1073/pnas.0710778105 PMID: 18332440

40. Mäkelä P, Munns R, Colmer TD, Peltonen-Sainio P (2003) Growth of tomato and an ABA-deficient mutant (sitiens) under saline conditions. Physiol Plantarum 117: 58–63.

41. Aroca R, Del Mar Alguacil M, Vernieri P, Ruiz-Lozano JM (2008) Plant responses to drought stress and exogenous ABA application are modulated differently by mycorrhization in tomato and an ABA-deficient mutant (sitiens). Microb Ecol 56: 704–719. doi: 10.1007/s00248-008-9390-y PMID: 18443845

42. Sharp RE (2002) Interaction with ethylene: changing views on the role of abscisic acid in root and shoot growth responses to water stress. Plant Cell Environ 25: 211–222. PMID: 11841664

43. Taiz L, Zeiger E (2006) Plant Physiology, fourth edition. Sunderland, Massachusetts: Sinauer Associates, Inc., Publishers. Pp. 485–486. doi: 10.1016/j.jasu.2006.05.025 PMID: 19059154

44. Doležal K, Popa I, Hrynkiv V, Spichal L, Fojtíková M, et al. (2006) Preparation and biological activity of 6-benzylaminopurine derivatives in plants and human cancer cells. Bioorg Med Chem 14: 875–884. PMID: 16214355

45. Jones HG, Sharp CS, Higgs KH (1987). Growth and water relations of wilty mutants of tomato (Lycopersicon esculentum Mill.). J Exp Bot 38: 1846–1856.

46. Sindhu RK, Walton DC (1988) Xanthoxin metabolism in cell-free preparations from wild type and wilty mutants of tomato. Plant Physiol 88: 178–182. PMID: 16666262

47. Groot SP, Ypelaan II, Karssen CM (1991) Strongly reduced levels of endogenous abscisic acid in developing seeds of tomato mutant sitiens do not influence in vivo accumulation of dry matter and storage proteins. Physiol Plantarum 81: 73–78.

48. Leung J, Giraudat J (1998) Abscisic acid signal transduction. Annu Rev Plant Physiol Plant Mol Biol 49: 199–222. PMID: 15012233

49. Cutler SR, Rodriguez PL, Finkelstein RR, Abrams SR (2010) Abscisic acid: emergence of a core signaling network. Annu Rev Plant Biol 61: 651–679. doi: 10.1146/annurev-arplant-042809-112122 PMID: 20192755

50. Rushton DL, Tripathi P, Rabara RC, Lin J, Ringler P, et al. (2012) WRKY transcription factors: key components in abscisic acid signalling. Plant Biotechnol J 10: 2–11. doi: 10.1111/j.1467-7652.2011.00634.x PMID: 21696534

51. Finkelstein R (2013) Abscisic acid synthesis and response. Arabidopsis Book 11: e0166. doi: 10.1199/tab.0166 PMID: 24273463

52. Brocard-Gifford I, Lynch TJ, Garcia ME, Malhotra B, Finkelstein RR (2004) The Arabidopsis thaliana ABSCISIC ACID-INSENSITIVE8 locus encodes a novel protein mediating abscisic acid and sugar responses essential for growth. Plant Cell 16: 406–421. PMID: 14742875

53. Gonzalez-Guzman M, Pizzio GA, Antoni R, Vera-Sirera F, Merilo E, et al. (2012) Arabidopsis PYR/PYL/RCAR receptors play a major role in quantitative regulation of stomatal aperture and transcriptional response to abscisic acid. Plant Cell 24: 2483–2496. doi: 10.1105/tpc.112.098574 PMID: 22739828

54. Kraepiel Y, Rousselin P, Sotta B, Kerhoas L, Einhorn J, et al. (1994) Analysis of phytochrome- and ABA-deficient mutants suggests that ABA degradation is controlled by light in Nicotiana plumbaginifolia. Plant J 6: 665–672.

55. Weatherwax SC, Ong MS, Degenhardt J, Bray EA, Tobin EM (1996) The interaction of light in the regulation of plant gene expression. Plant Physiol 111: 363–370. PMID: 8787022

56. Symons GM, Reid JB (2003) Hormone levels and response during de-etiolation in pea. Planta 216: 422–431. PMID: 12520333

57. Nagel OW, Konings H, Lambers H (1994) Growth rate, plant development and water relations of the ABA deficient tomato mutant sitiens. Physiol Plantarum 92: 102–108.

58. Perrot-Rechenmann C (2010) Cellular responses to auxin: division versus expansion. Cold Spring Harb Perspect Biol. 2: a001446. doi: 10.1101/cshperspect.a001446 PMID: 20452959

59. Wen B, Nieuwland J, Murray JAH (2013) The Arabidopsis CDK inhibitor ICK3/KRP5 is rate limiting for primary root growth and promotes growth through cell elongation and endoreduplication. J Exp Bot 64: 1–13. doi: 10.1093/jxb/ers358 PMID: 23264638

60. del Castellano M, Boniotti MB, Caro E, Schnittger A, Gutierrez C (2004) DNA replication licensing affects cell proliferation or endoreplication in a cell type-specific manner. Plant Cell 16: 2380–2393. PMID: 15310110

61. Petke-Szandtner A, Meszaros T, Horvath GV, Bako L, Csordas-Toth E, et al. (2006) Activation of an alfalfa cyclin-dependent kinase inhibitor by calmodulin-like domain protein kinase. Plant J 46: 111–123. PMID: 16553899

62. Alabadí D, Gallego-Bartolomé J, García-Cárcel L, Orlando L, Rubio V, et al. (2008) Gibberellins modulate light signalling pathways to prevent Arabidopsis seedling de-etiolation in darkness. Plant J 53: 324–335. PMID: 18053005

63. Yamburenko MV, Zubo YO, Vankova R, Kusnetsov VV, Kulaeva ON, et al. (2013) Abscisic acid represses the transcription of chloroplast genes. J Exp Bot 64: 4491–4502. doi: 10.1093/jxb/ert258 PMID: 24078671

64. Guan C, Wang X, Feng J, Hong S, Liang Y, et al. (2014) Cytokinin antagonizes abscisic acid-mediated inhibition of cotyledon greening by promoting the degradation of ABSCISIC ACID INSENSITIVE5 protein in Arabidopsis. Plant Physiol 164: 1515–1526. doi: 10.1104/pp.113.234740 PMID: 24443524

65. Valente P, Tao W, Verbelen JP (1998) Auxins and cytokinins control DNA endoreduplication and deduplication in single cells of tobacco. Plant Sci 134: 207–215.

66. Scofield S, Dewitte W, Nieuwland J, Murray JA (2013) The Arabidopsis homeobox gene SHOOT MERISTEMLESS has cellular and meristem-organisational roles with differential requirements for cytokinin and CYCD3 activity. Plant J 75: 53–66. doi: 10.1111/tpj.12198 PMID: 23573875

67. Takahashi N, Kajihara T, Okamura C, Kim Y, Katagiri Y, et al. (2013) Cytokinins Control Endocycle Onset by Promoting the Expression of an APC/C Activator in Arabidopsis Roots. Curr Biol 23: 1812–1817. doi: 10.1016/j.cub.2013.07.051 PMID: 24035544

68. Brugière N, Jiao S, Hantke S, Zinselmeier C, Roessler JA, et al. (2003) Cytokinin oxidase gene expression in maize is localized to the vasculature, and is induced by cytokinins, abscisic acid, and abiotic stress. Plant Physiol 132: 1228–1240. PMID: 12857805

69. Rivero RM, Gimeno J, Van Deynze A, Walia H, Blumwald E (2010) Enhanced cytokinin synthesis in tobacco plants expressing PSARK::IPT prevents the degradation of photosynthetic protein complexes during drought. Plant Cell Physiol 51: 1929–1941. doi: 10.1093/pcp/pcq143 PMID: 20871100

70. Nambara E, Marion-Poll A (2005) Abscisic acid biosynthesis and catabolism. Annu Rev Plant Biol 56: 165–185.oamdg. PMID: 15862093

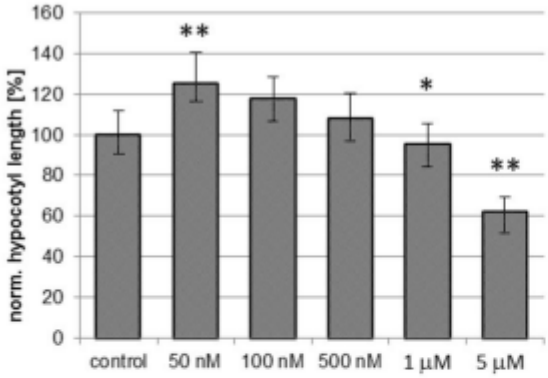

Supporting figure S1 The hypocotyl elongation of *not* mutant treated with various concentrations of ABA. Germinated seeds were transferred on basal media (control) or media supplemented with ABA and grown in the dark for 4 days. The results shown in the figure represent the medians of normalized length of hypocotyls from 1 independent experiment; the error bars represent the boundaries of the first and third quartiles. The sample "control" was set as 100% hypocotyl length and all other values (medians, quartiles) are expressed as percentage of this value. To prove significance the Kruskal-Wallis ANOVA with multiple post-hoc comparison was performed. Asterisks denote values that differ significantly from "control" sample (** $p < 0.01$, * $p < 0.05$; n=135).

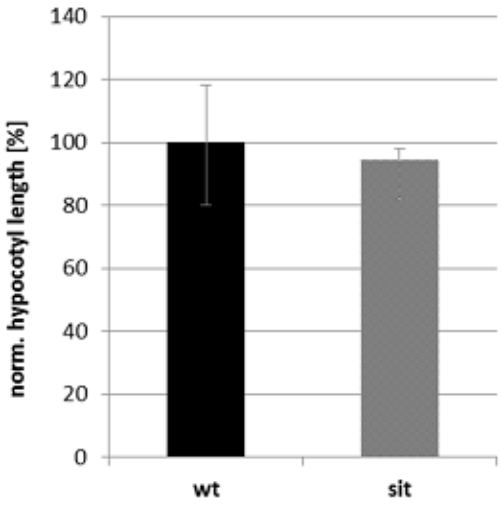

Supporting figure S2 The effect of the *sit* mutation on hypocotyl length in BL-grown seedlings. Seeds of the WT (cv. Rheinlands Ruhm) and *sit* mutant were germinated in darkness and then grown under continuous BL for 4 days. The results shown in the figure represent the medians of normalized length of hypocotyls from 1 independent experiment; the error bars represent the boundaries of the first and third quartiles. The sample "wt" was set as 100% hypocotyl length and all other values (medians, quartiles) are expressed as percentage of this value (Mann-Whitney test, $p > 0.05$, n=40).

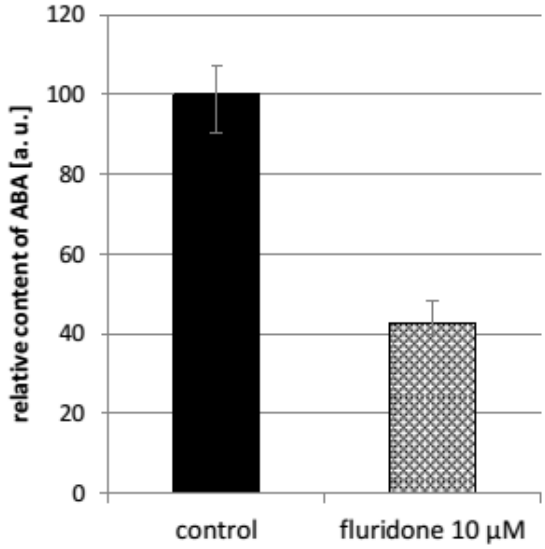

Supporting figure S3 The endogenous ABA content in fluridone treated WT hypocotyls (cv. Rutgers). Free ABA levels are reported as relative means [a.u.] ± SE based on two independent experiments. The control sample was assigned a value of 100 a.u.

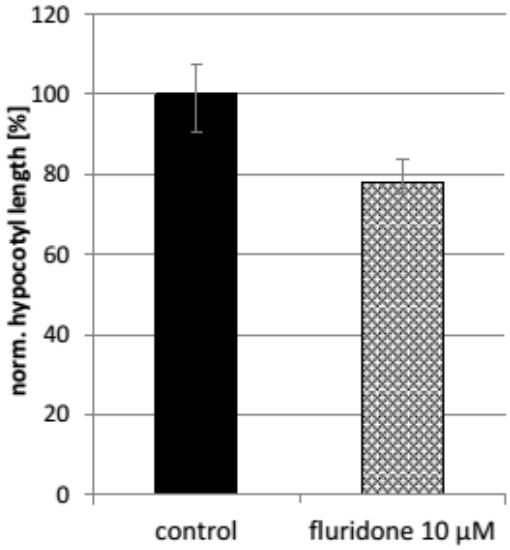

Supporting figure S4 The effect of fluridone on hypocotyl growth in dark-grown seedlings. Germinated seeds of WT (cv. Rutgers) were transferred to media supplemented with 10 µM fluridone and grown for 4 days in darkness. The results shown in the figure represent the medians of normalized length of hypocotyls from 2 independent experiments; the error bars represent the boundaries of the first and third quartiles. The control sample was set as 100% hypocotyl length. Other values (medians, quartiles) are expressed as percentage of these values. The statistical significance was evaluated by Mann-Whitney U test; $p < 0.02$.

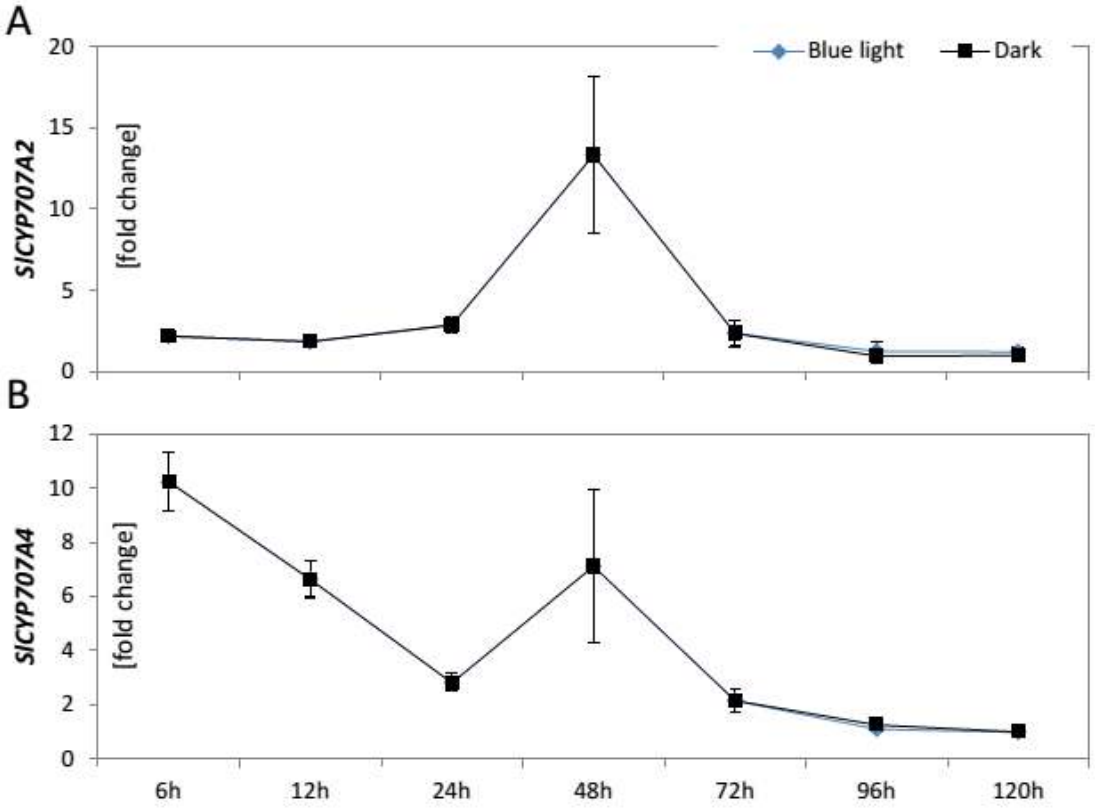

Supporting figure S5 The relative expression of the A) *SlCYP707A2* and B) *SlCYP707A4* ABA catabolic genes. Values shown are the geometric means of three biological replicates ± SE. *Tip41like* and *PP2ACs* were used as housekeeping genes. All values are expressed in arbitrary units relative to the expression of the corresponding gene in the 120h-Dark" sample.

S1 File:

Supporting table A Fold change in *LeNCED1* transcript expression based on three independent experiments.

	Set I.	Set II.	Set III.
Sample	Relative expression	Relative expression	Relative expression
6 h – D	**0.07**	**0.00**	**0.00**
12 h – D	**0.00**	**0.00**	**0.00**
24 h – D	**0.04**	**0.00**	**0.00**
48 h – D	**0.00**	**0.00**	**0.00**
72 h – D	**0.24**	**0.04**	**0.17**
96 h – D	**0.75**	**0.30**	**0.54**
96 h – BL	**0.32**	**0.12**	**0.23**
120 h – D	**1.00**	**1.00**	**1.00**
120 h – BL	**0.46**	**0.34**	**0.51**

Supporting Table B Fold change in *SlCYP707A3* transcript expression based on three independent experiments.

	Set I.	Set II.	Set III.
Sample	Relative expression	Relative expression	Relative expression
6 h – D	**0.60**	**1.13**	**0.72**
12 h – D	**1.33**	**1.36**	**1.72**
24 h – D	**1.42**	**2.29**	**1.22**
48 h – D	**3.64**	**1.90**	**2.14**
72 h – D	**1.33**	**2.21**	**0.73**
96 h – D	**0.91**	**1.17**	**0.82**
96 h – BL	**1.63**	**5.37**	**2.34**
120 h – D	**1.00**	**1.00**	**1.00**
120 h – BL	**1.73**	**1.02**	**1.88**

Supporting table C Fold change in *SlKRP1* and *SlKRP3* transcript expression based on three independent experiments.

		Set I.	Set II.	Set III.
Gene	Sample	Relative expression	Relative expression	Relative expression
SlKRP1	**wt control**	1.00	1.00	1.00
	wt ABA 100 nM	0.91	1.00	1.11
	***sit* control**	0.83	0.78	0.89
	***sit* ABA 100 nM**	0.95	0.89	1.04
SlKRP3	**wt control**	0.57	0.60	0.64
	wt ABA 100 nM	0.50	0.66	0.67
	***sit* control**	0.46	0.45	0.50
	***sit* ABA 100 nM**	0.55	0.50	0.62

S1 File continued:

Supporting table D Fold change in *SlLOG2* transcript expression based on three independent experiments.

	Set I.	**Set II.**	**Set III.**
Sample	**Relative expression**	**Relative expression**	**Relative expression**
wt control	1.00	1.00	1.00
wt ABA 100 nM	0.76	0.93	0.88
***sit* control**	1.39	2.49	1.98
***sit* ABA 100 nM**	1.12	1.57	1.35

Supporting table S1 The values of hypocotyl length used for data normalization. Medians, first and third quartiles are given. The control sample used for data normalization is marked as "norm."

Figure	Genotype and/or treatment	Median hypocotyl length [mm]	1st quartile [mm]	3rd quartile [mm]	
2A	WT control	98	91	104	norm.
	WT 100 nM ABA	101	98	103	
	sit control	80	72	84	
	sit 100 nM ABA	99	94	106	
2B	control	53	46	62	norm.
	50 nM	76	67	81	
	100 nM	83	78	87	
	500 nM	74	69	80	
	1 μM	74	64	80	
	5 μM	46	38	52	
2C	control	73	66	83	norm.
	50 nM	77	67	81	
	100 nM	80	71	92	
	500 nM	74	63	85	
	1 μM	69	56	78	
	5 μM	41	22	58	
2D	WT control	101	95	104	norm.
	WT 50 nM ABA	100	91	106	
	not control	91	86	96	
	not 50 nM ABA	103	99	112	
S1	control	52	46	64	norm.
	50 nM	81	75	81	
	100 nM	84	77	86	
	500 nM	71	67	76	
	1 μM	75	67	80	
	5 μM	40	36	45	
S2	WT	28	22	33	norm.
	sit	26	23	27	
S4	control	68	62	73	norm.
	fluridone 10 μM	53	51	57	

Supporting table S2 Absolute quantification of free ABA in tomato seedlings based on three independent experiments ± SE from three technical replicates.

Sample	Set I. ABA [pmol/g FW]	Set II. ABA [pmol/g FW]	Set III. ABA [pmol/g FW]
6 h – D	**29** ± 2.5	**9** ± 0.7	**45** ± 3.6
12 h – D	**18** ± 5.4	**6** ± 0.4	**25** ± 4.2
24 h – D	**5** ± 0.1	**4** ± 0.3	**n. a.**
48 h – D	**2** ± 0.2	**2** ± 0.3	**3** ± 0.3
72 h – D	**1** ± 0.2	**1** ± 0.1	**7** ± 1.4
96 h – D	**8** ± 1.7	**7** ± 0.9	**26** ± 1.0
96 h – BL	**5** ± 0.7	**3** ± 0.5	**8** ± 1.2
120 h – D	**11** ± 0.5	**15** ± 0.6	**32** ± 0.8
120 h – BL	**7** ± 0.2	**8** ± 0.6	**12** ± 1.6

n. a.: not analyzed - sample lost during the analysis

Supporting table S3 Absolute quantification of free ABA in hypocotyls of ABA-deficient mutants and corresponding WTs based on two biological repeats ± SE from two technical replicates.

Sample	Set I. ABA [pmol/g FW]	Set II. ABA [pmol/g FW]
sit	**0.8** ± 0.2	**0.8**±0.1
WT (cv. Rheinlands-Ruhm)	**17.9** ± 0.4	**18** ± 1.9
not	**2.6** ± 0.5	**2.9** ± 0.0
WT (cv. Lukullus)	**21.8** ± 0.6	**19.5** ± 1.4

Supporting table S4 Absolute quantification of CK levels in tomato seedlings ± SE based on three independent experiments. <LOD indicates that the levels of the corresponding compound were below the limit of detection; cZ *cis*-zeatin compounds, tZ *trans*-zeatin compounds, DHZ dihydrozeatin compounds, iP isopentenyladenine compounds, xR ribosides, xOG O-glucosides, x9G 9-glucosides, xMP monophosphates, x7G 7-glucosides.

	wt control			**wt 100 nM ABA**			***sit* control**			***sit* ABA 100 nM**		
CKs	[pmol/g FW]	±	SE	[pmol/g FW]	±	SE	[pmol/g FW]	±	SE	[pmol/g FW]	±	SE
cZ	**0.09**	±	0.03	**0.13**	±	0.01	**0.14**	±	0.02	**0.10**	±	0.01
cZR	**0.37**	±	0.04	**0.42**	±	0.05	**1.13**	±	0.40	**0.33**	±	0.05
cZOG	**0.09**	±	0.03	**0.13**	±	0.02	**0.14**	±	0.01	**0.08**	±	0.01
cZ9G	**0.15**	±	0.00	**0.14**	±	0.01	**0.11**	±	0.02	**0.10**	±	0.01
cZROG	**0.15**	±	0.01	**0.15**	±	0.02	**0.41**	±	0.15	**0.18**	±	0.04
cZRMP	**0.36**	±	0.01	**0.55**	±	0.20	**0.43**	±	0.14	**0.64**	±	0.23
cZ7G	**8.55**	±	0.59	**8.79**	±	0.26	**10.76**	±	0.35	**8.29**	±	0.65
tZ	**0.17**	±	0.02	**0.09**	±	0.02	**0.21**	±	0.04	**0.16**	±	0.01
tZR	**1.35**	±	0.09	**0.55**	±	0.02	**1.12**	±	0.17	**0.60**	±	0.08
tZOG	**0.10**	±	0.02	**0.07**	±	0.02	**0.13**	±	0.03	**0.08**	±	0.01
tZ9G	**0.28**	±	0.03	**0.18**	±	0.00	**0.46**	±	0.06	**0.28**	±	0.05
tZROG	**0.57**	±	0.06	**0.51**	±	0.09	**1.34**	±	0.07	**1.01**	±	0.10
tZRMP	**0.66**	±	0.08	**0.28**	±	0.02	**0.53**	±	0.06	**0.57**	±	0.05
tZ7G	**8.26**	±	0.47	**5.33**	±	0.43	**15.44**	±	0.50	**9.34**	±	1.88
DHZ	**0.01**	±	0.00	**0.01**	±	0.00	**0.02**	±	0.00	**0.01**	±	0.00
DHZR	**0.10**	±	0.01	**0.05**	±	0.01	**0.14**	±	0.02	**0.09**	±	0.05
DHZOG	**0.06**	±	0.00	**0.08**	±	0.01	**0.11**	±	0.03	**0.07**	±	0.02
DHZ9G	<LOD			<LOD			<LOD			<LOD		
DHZROG	**0.73**	±	0.08	**1.10**	±	0.38	**2.19**	±	0.17	**1.82**	±	0.50
DHZRMP	<LOD			<LOD			<LOD			<LOD		
DHZ7G	**23.29**	±	1.40	**26.91**	±	4.26	**73.61**	±	0.61	**44.07**	±	3.54
iP	**0.24**	±	0.02	**0.42**	±	0.09	**0.33**	±	0.06	**0.32**	±	0.12
iPR	**0.12**	±	0.03	**0.14**	±	0.04	**0.31**	±	0.07	**0.26**	±	0.06
iP9G	**0.12**	±	0.02	**0.15**	±	0.04	**0.13**	±	0.01	**0.15**	±	0.02
iPRMP	**0.40**	±	0.07	**0.31**	±	0.09	**0.49**	±	0.06	**0.41**	±	0.06
iP7G	**14.43**	±	0.94	**14.09**	±	1.02	**40.38**	±	3.59	**48.05**	±	1.12
SUMA	**60.64**	±	4.02	**60.58**	±	7.12	**150.07**	±	6.63	**117.00**	±	8.66

7. SPATIO-TEMPORAL CHANGES IN ENDOGENOUS ABSCISIC ACID CONTENTS DURING ETIOLATED GROWTH AND PHOTOMORPHOGENESIS IN TOMATO SEEDLINGS

Published as:

Humplík JF, Turečková V, Fellner M, Bergougnoux V. 2015. Spatio-temporal changes in endogenous abscisic acid contents during etiolated growth and photomorphogenesis in tomato seedlings. *Plant Signaling & Behavior.* 10:e1039213. doi: 10.1080/15592324.2015.1039213

ARTICLE ADDENDUM

Plant Signaling & Behavior 10:8, e1039213; August 2015; Published with license by Taylor and Francis Group, LLC

Spatio-temporal changes in endogenous abscisic acid contents during etiolated growth and photomorphogenesis in tomato seedlings

Jan F Humplík[1,*], Veronika Turečková[1], Martin Fellner[1], and Véronique Bergougnoux[2]

[1]Laboratory of Growth Regulators & Department of Chemical Biology and Genetics; Centre of the Region Haná for Biotechnological and Agricultural Research; Faculty of Science; Palacký University & Institute of Experimental Botany ASCR; Olomouc, Czech Republic; [2]Department of Molecular Biology; Centre of the Region Haná for Biotechnological and Agricultural Research; Faculty of Science; Palacký University; Olomouc, Czech Republic

The role of abscisic acid (ABA) during early development was investigated in tomato seedlings. The endogenous content of ABA in particular organs was analyzed in seedlings grown in the dark and under blue light. Our results showed that in dark-grown seedlings, the ABA accumulation was maximal in the cotyledons and elongation zone of hypocotyl, whereas under blue-light, the ABA content was distinctly reduced. Our data are consistent with the conclusion that ABA promotes the growth of etiolated seedlings and the results suggest that ABA plays an inhibitory role in de-etiolation and photomorphogenesis in tomato.

Keywords: abscisic acid, blue-light, etiolated growth, photomorphogenesis, tomato

*Correspondence to: Jan F Humplík; Email: jan.humplik@upol.cz

Submitted: 03/23/2015

Accepted: 03/30/2015

http://dx.doi.org/10.1080/15592324.2015.1039213

Light is an important signal regulating plant development. After germination in the dark (D), the seedling undergoes etiolated growth referred as skotomorphogenesis. This developmental step is characterized by rapid elongation of the hypocotyl topped by a hook with underdeveloped cotyledons. This is to ensure the seedling reaches a light environment before exhausting its reserves. As soon as the seedling perceives the light, photomorphogenesis starts. The transition from skoto- to photomorphogenesis, called deetiolation, represents the switch from heterotrophy to autotrophy.[1] On a cellular level, light is absorbed by photoreceptors specific to particular monochromatic light: phytochromes for red (RL) and far-red wavelengths, cryptochromes/phototropins for blue light (BL). Although other receptors have been identified, these 3 classes of photoreceptors represent the major light sensors. Even though all are implicated in the inhibition of hypocotyl growth,[2] at the same intensity, BL is a more efficient inhibitor of elongation than RL.[3,4] The phytohormones gibberellins, auxin, brassinosteroids, ethylene and cytokinin, regulate Arabidopsis hypocotyl growth both during skoto- and photomorphogenesis.[5] The establishment of skotomorphogenesis depends on interactions between hormones. Despite the fact abscisic acid (ABA) contributes to these complex hormonal networks in different physiological responses, its particular role during skoto- and photomorphogenesis has not been thoroughly investigated.

We recently studied the role of ABA in the growth of etiolated tomato hypocotyls using ABA-deficient *sitiens* and *notabilis* mutants.[5] Physiological experiments showed a significant reduction in hypocotyl growth in the mutants compared to wild-types (WTs). Low concentrations of ABA (nM) stimulated the mutant growth but not the WTs. Higher concentration of ABA led to growth inhibition in all genotypes. Our results suggested that in plants with physiological ABA concentrations (i.e. WTs), exogenous ABA leads to an "over-dose" effect responsible for the observed growth inhibition. In contrast, in the ABA-deficient plants that are "starving" for ABA, the response to exogenous ABA can be considered as closer to the "real physiological situation" of the plant. In summary, it appears that a fine-tuned regulation of endogenous ABA content is required to support hypocotyl growth. At the same time, we analyzed the endogenous ABA content in WT tomato plants (cv. Rutgers) during germination and

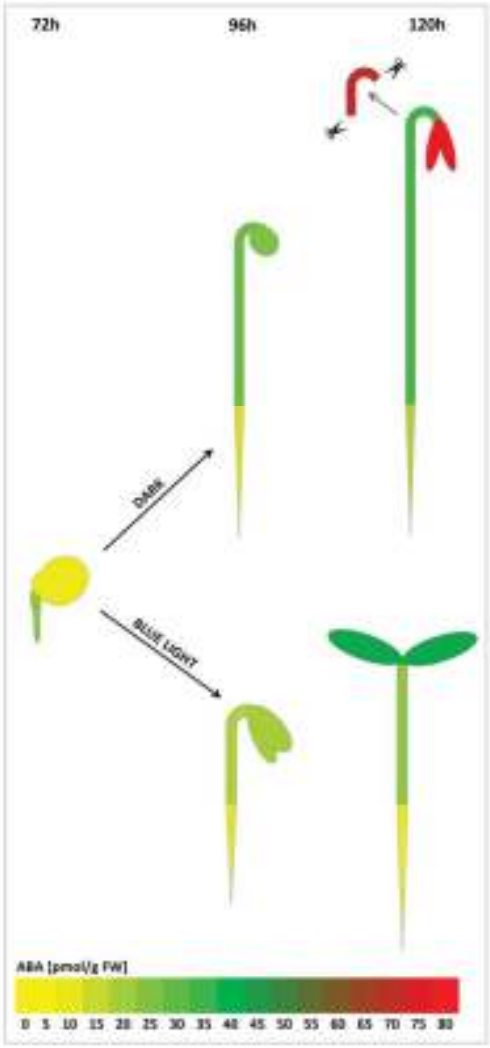

Figure 1. Spatiotemporal changes in ABA content presented in particular organs of tomato seedlings. ABA concentrations during germination in the D (72h) and etiolated growth in the D and during de-etiolation and photomorphogenesis in BL (96 h-120 h) are visualized as a "heat map" by color range. The colors represent median values of absolute ABA concentrations in given part of the seedling that were calculated from 3 biological repeats and correspond to the scale (0 – 80 pmol/g of fresh weight - FW).

seedling development. If the hypothesis that ABA inhibits plant growth in the light is true,[6,7] then ABA should be synthesized and accumulate during photomorphogenesis. Interestingly, the quantitative analysis of ABA content in whole D-grown and de-etiolated seedlings revealed ABA accumulated to a greater extent in D-grown seedlings. These physiological data are supported by the expression analysis of *LeNCED1* gene, encoding an enzyme involved in ABA synthesis. Indeed, *LeNCED1* transcripts accumulated significantly in the D-grown seedlings than in de-etiolated seedlings.[5] Altogether, our previously published results demonstrated ABA accumulation is required to stimulate the fast growth of tomato hypocotyl during skotomorphogenesis.

We further investigated the effect of BL on the spatio-temporal distribution of free ABA content in different organs of tomato (cv Rheinlands Ruhm) seedlings: radicles, cotyledons with endosperm, roots, whole hypocotyls or elongating zone of hypocotyl,[8] and cotyledons (**Fig. 1**). The extraction and quantification of ABA was performed as described by Turečková et al.[9] At the onset of germination, ABA accumulated more in the emerging radicle than in the rest of the seed. During the development of the seedling, ABA concentration increased in both hypocotyl and in cotyledons to a similar extent after 96 h of cultivation. One day later (120h), a significant increase in ABA content was observed in cotyledons but not in the intact hypocotyl. This result is in agreement with data from the Arabidopsis *abi3* (ABA insensitive 3) mutant. Indeed, ABI3, a component of the ABA signaling pathway, is required to maintain unfolded, yellowish cotyledons containing undifferentiated plastids.[10] ABA also controls the entry into stomatal-lineage development in Arabidopsis leaves.[11] Interestingly, there was marked great accumulation of free ABA in the elongating zone of hypocotyl, further supporting our published data.[5] Finally, the low concentration of free ABA in the root throughout the experimental period indicated that ABA probably has no or only a limited role during early root development in tomato seedling. However, a potential effect of artificial *in vitro* cultivation especially in root development cannot be excluded. When seedlings were grown under BL, ABA accumulation was significantly reduced in the hypocotyl and cotyledons (**Table 1**) showing similar proportional distribution in particular organs as in the D (**Fig. 1**).

Table 1. Quantification of free ABA in particular plant organs of tomato seedlings grown in the dark and under blue light. The data are presented as medians of 3 biological experiments, statistical significance was performed using Mann-Whitney test.

Time	Organ	DARK ABA (pmol/g FW)	BLUE LIGHT ABA (pmol/g FW)	p value
96 h	Cotyledon	25.27	19.37	<0.01
	Hypocotyl	28.44	17.86	<0.01
	Root	11.70	9.98	<0.07
120 h	Cotyledon	77.45	41.33	<0.01
	Hypocotyl	33.76	22.54	<0.01
	Root	18.26	8.87	<0.01

The regulation of endogenous ABA by light was described more than 20 y ago. In pea, deficiency in R/FR light perception resulted in accumulation of ABA in seeds and leaves.[12] RL also reduced ABA accumulation in etiolated *Lemna gibba* and D-treatment of previously light-grown Arabidopsis and *Lemna gibba* plants led to a significant accumulation of ABA.[13] The treatment of photoblastic lettuce seeds by RL decreased ABA content and down-regulated the ABA biosynthetic genes *LsNCED2* and *LsNCED4*.[14] All these data were obtained from plants grown in RL. As the same responses were observed in tomato seedlings grown in BL, we hypothesize that the different light signaling pathways converge to induce hormonal-regulated plant growth and development. Nevertheless, in barley grain, exposure to light induced expression of the *HvNCED* gene and accumulation of ABA.[15] The discrepancy between our data and the published literature can be explained by the fact that barley is differently regulated by light than other species. For example, whereas light induces germination of lettuce seeds,[14] it strengthens the dormancy of barley grains, i.e., inhibit their germination.[16]

To summarize, in tomato seedlings, ABA accumulates in elongation zone of hypocotyl to participate in cell expansion during skotomorphogenesis. Light reduces the ABA content to a minimum required to maintain the steady-state growth rate characteristic of photomorphogenesis. Moreover, ABA markedly accumulates in cotyledons during skotomorphogenesis. ABA might thus contribute to the inhibition of cotyledon development in particular, by maintaining unfolded cotyledons to protect the apical meristem from damage by soil particles, and restrict stomata initiation and maturation of plastids (Fig. 2).

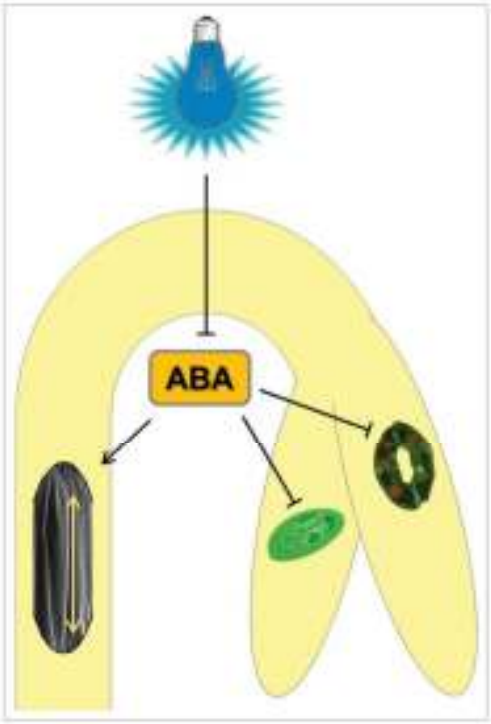

Figure 2. Hypothetical model of ABA action in etiolated growth of tomato seedlings. The abscisic acid content is reduced by BL exposure to promote de-etiolation. When the seedlings are kept in the D, ABA inhibits maturation of chloroplasts and development of stomata, but supports the cell elongation to maintain hypocotyl growth. (The part of the figure was adopted from Wikipedia free illustrations under CC license).

Disclosure of Potential Conflicts of Interest

No potential conflicts of interest were disclosed.

Acknowledgments

Authors thank Alex Outlon for proofreading of the manuscript.

Funding

This work was supported by the Ministry of Education, Youth and Sports

of the Czech Republic grant no. LO1204 (National Program of Sustainability) and internal grant from Palacký University IGA_PrF_2015_021. V. Bergougnoux and M. Fellner were supported by the Operational Programs Education for Competitiveness - European Social Fund, project no. CZ.1.07/2.3.00/20.0165 and project no. CZ.1.07/2.3.00/30.0004, respectively.

References

1. Arsovski AA, Galstyan A, Guseman JM, Nemhauser JL. Photomorphogenesis. Arabidopsis Book 2012; 10: e0147; PMID:22582028; http://dx.doi.org/10.1199/tab.0147
2. Casal JJ. Phytochromes, cryptochromes, phototropin: photoreceptor interactions in plants. Photochem Photobiol 2000; 71:1-11; PMID:10649883; http://dx.doi.org/10.1562/0031-8655(2000)071%3c0001:PCPPII%3e2.0.CO;2
3. Parks BM, Cho MH, Spalding EP. Two genetically separable phases of growth inhibition induced by blue light in Arabidopsis seedlings. Plant Physiol 1998; 118: 609-15; PMID:9765547; http://dx.doi.org/10.1104/pp.118.2.609
4. Parks BM, Spalding EP. Sequential and coordinated action of phytochromes A and B during Arabidopsis stem growth revealed by kinetic analysis. Proc Natl Acad Sci USA 1999; 96: 14142-6; PMID:10570212; http://dx.doi.org/10.1073/pnas.96.24.14142
5. Humplík JF, Bergougnoux V, Jandová M, Šimura J, Pěnčík A, Tomanec O, Rolčík J, Novák O, Fellner, M. Endogenous abscisic acid promotes hypocotyl growth and affects endoreduplication during dark-induced growth in tomato (*Solanum lycopersicum* L.). PloS One 2015; 10:e0117793; http://dx.doi.org/10.1371/journal.pone.0117793
6. Fellner M, Zhang R, Pharis RP, Sawhney VK. Reduced de−etiolation of hypocotyl growth in a tomato mutant is associated with hypersensitivity to, and high endogenous levels of, abscisic acid. J Exp Bot 2001; 52:725-38; PMID:11413209
7. Chen H, Zhang J, Neff MM, Hong S-W, Zhang H, Deng XW, Xiong L. Integration of light and abscisic acid signaling during seed germination and early seedling development. Proc Natl Acad Sci USA 2008; 105:4495-500; PMID:18332440; http://dx.doi.org/10.1073/pnas.0710778105
8. Bergougnoux V, Zalabák D, Jandová M, Novák O, Wiese-Klinkenberg A, Fellner M. Effect of blue light on endogenous isopentenyladenine and endoreduplication during photomorphogenesis and de-etiolation of tomato (*Solanum lycopersicum* L.) seedlings. PLoS One 2012; 7:e45255; http://dx.doi.org/10.1371/journal.pone.0045255
9. Turečková V, Novák O, Strnad M. Profiling ABA metabolites in *Nicotiana tabacum* L. leaves by ultra-performance liquid chromatography–electrospray tandem mass spectrometry. Talanta 2009; 80:390-9; http://dx.doi.org/10.1016/j.talanta.2009.06.027
10. Rohde A, De Rycke R, Beeckman T, Engler G, Van Montagu M, Boerjan W. ABI3 affects plastid differentiation in dark-grown Arabidopsis seedling. Plant Cell 2000; 12: 35-52; PMID:10634906; http://dx.doi.org/10.1105/tpc.12.1.35
11. Tanaka Y, Nose T, Jikumaru Y, Kamiya Y. 2013. ABA inhibits entry into stomatal-lineage development in Arabidopsis leaves. Plant J 2013; 74: 448-57; PMID:23373882; http://dx.doi.org/10.1111/tpj.12136
12. Kraepiel Y, Rousselin P, Sotta B, Kerhoas L, Einhorn J, Caboche M, Miginiac E. Analysis of phytochrome- and ABA-deficient mutants suggests that ABA degradation is controlled by light in *Nicotiana plumbaginifolia*. 1994; 6:665-72
13. Weatherwax SC, Ong MS, Degenhardt J, Bray EA, Tobin EM. The interaction of light and abscisic acid in the regulation of plant gene expression. Plant Physiol 1996; 111:363-70; PMID:8787022; http://dx.doi.org/10.1104/pp.111.2.363
14. Sawada Y, Aoki M, Nakaminami K, Mitsuhashi W, Tatematsu K, Kushiro T, Koshiba T, Kamiya Y, Inoue Y, Nambara E, et al. Phytochrome- and gibberellin-mediated regulation of abscisic acid metabolism during germination of photoblastic lettuce seeds. Plant Physiol 2008; 146:1386-96; PMID:18184730; http://dx.doi.org/10.1104/pp.107.115162
15. Gubler F, Hughes T, Waterhouse P, Jacobsen J. Regulation of dormancy in barley by blue light and after-ripening: effects on abscisic acid and gibberellin metabolism. Plant Physiol 2008; 147:886-96; PMID:18408047; http://dx.doi.org/10.1104/pp.107.115469
16. Bethke PC, Gubler F, Jacobsen JV, Jones RL. Dormancy of Arabidopsis seeds and barley grains can be broken by nitric oxide. Planta 2004; 219:847-55; PMID:15133666; http://dx.doi.org/10.1007/s00425-004-1282-x

8. INTERACTION OF ABA AND CYTOKININS DURING TOMATO HYPOCOTYL ELONGATION

In this chapter, we present data which aim to understand the specific role of ABA in tomato hypocotyl elongation during skotomorphogenesis. The results presented here shows data that are complementary to those that were published, or data that are intended for publication in close future. In addition to some physiological experiments and expression analysis, we present here detailed analysis of the interaction between ABA and CKs during etiolated growth, as well as a spatial repartition of CKs during photomorphogenesis of tomato seedlings. These data are presented as a chapter of the thesis as they were obtained after the publishing of the two above mentioned articles. The methodology for presented experiments is given in the chapter 4.

8.1. Results and Discussion

8.1.1. ABA and tomato hypocotyl elongation during skotomorphogenesis

In order to investigate the role of ABA during tomato hypocotyl elongation, the effect of low ABA concentrations on relative growth rate (RGR) was determined as described in Material and methods (chapter 4). Although not found significant, our data suggested that low concentrations of ABA stimulates WT hypocotyl elongation. This was seemingly the case for all tested concentrations, from 1 to 100 nM (see Fig. 3). When the exogenous treatment with ABA was performed on different WT cultivars, no significant stimulatory effect of ABA on final hypocotyl length could be observed, even if some light trend of stimulation could be suggested (Humplík et al. 2015a, *PloSONE*). It has to be noted that calculation of RGR represents different approach to the simple measurement of final hypocotyl length. The kinetics of growth response of control and treated variant could be different at certain time point, the temporal changes in endogenous plant hormone content and sensitivity may buffer the potential effect of the treatment leading to the similar final hypocotyl length in both variants. The measurement of RGR between 1 and 2 days of seedling growth describes part of this kinetics. However the measurement of RGR requires some non-invasive approach e.g. scanning of the Petri dishes with seedlings. This method is based on short-time application of strong light into the sample that is obviously not an optimal method for analyzing etiolated (fully dark grown) seedlings. Even the short-time application of the light could induce photomorphogenesis via cryptochrome signaling (Parks et al. 1998). Perhaps some special phenotyping system employing video camera in infrared part of light spectra could be used to avoid this problem. The difference between the data presented in the article and the data presented here could be also explained by the different cultivar used. It can be hypothesized that in a short time period of treatment, ABA will stimulate growth, which will be attenuated or inhibited after long exposure to ABA.

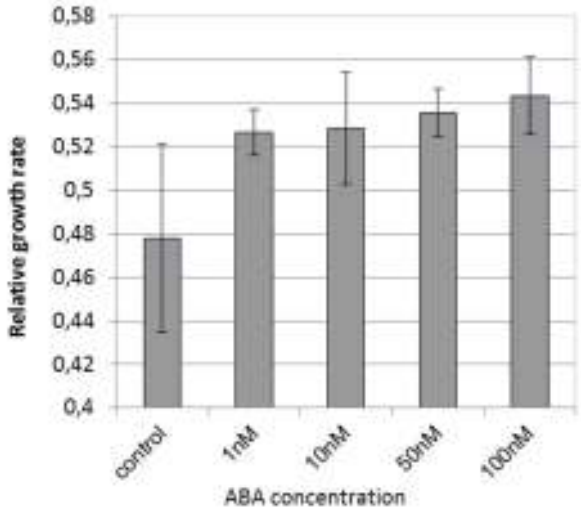

Figure 3. The effect of ABA on relative growth rate (RGR) of etiolated tomato hypocotyl.
Germinated seeds were transferred to Petri dish with new media supplemented with various concentration of abscisic acid. The Petri dished were scanned on flat-bad scanner in two time points (24 and 48 hours after transfer) and RGR was calculated. The columns represent mean RGR values calculated from 15 seedlings per one ABA concentration. Error bars represent ± SE. The data of one independent experiment are presented.

Recently, pyrabactin, a synthetic ABA analog was isolated (Cutler et al. 2010). In a recent study, it was demonstrated that this agonist of ABA is able to induce additive effects to ABA in stomatal responses and could be used instead of ABA to circumvent the supposed saturation of receptors by endogenous ABA in WT seedlings of pea (Puli and Raghavendra 2012). Thus, pyrabactin was used on tomato seedlings. For this purpose, germinated tomato seeds were transferred on media supplemented or not with pyrabactin; final hypocotyl length was measured after 3 days of growth. Our data showed that concentrations of pyrabactin from 25 to 200 nM had a stimulatory effect on hypocotyl growth (Fig. 4). Due to the absence of biological replicate and also to the low amount of seedlings measured per each concentrations tested, we cannot describe a dose-dependent response, neither a significant stimulation of the hypocotyl growth. In order to build a solid conclusion, the experiment will have to be repeated. Nevertheless, we can conclude that the use of an ABA agonist allowed us to affect hypocotyl growth in tomato.

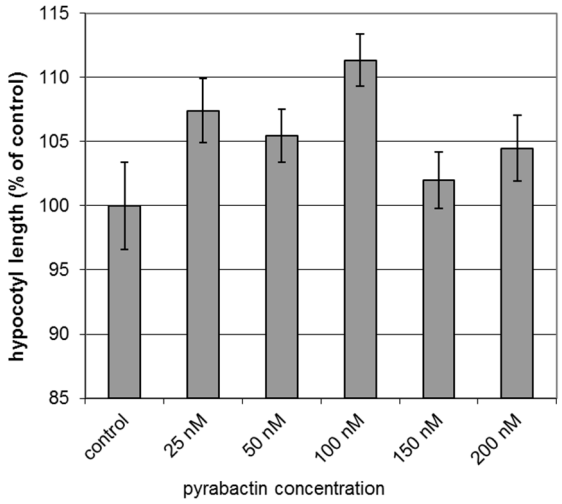

Figure 4. The effect of pyrabactin on the growth of etiolated tomato hypocotyl.
Germinated seeds were transferred to Petri dish with new media supplemented with various concentration of pyrabactin, cultivated in dark for 3 days and the length of hypocotyl was measured. The columns represent mean relative hypocotyl length (% of control sample) calculated from 15 seedlings per one pyrabactin concentration. Error bars represent ± SE. The data of two independent experiments are presented.

8.1.2. ABA and control of cell cycle

We demonstrated a clear relationship between hypocotyl elongation in the dark, ABA content and DNA endoreduplication (Humplík et al. 2015a, *PloSONE*). Although the role of endoreduplication in plant cell elongation is not fully elucidated (De Veylder et al. 2011), there are growing evidences for its stimulatory role in the plant growth (Bergougnoux et al. 2012; Wen et al. 2013). To onset the endoreduplication, the suppression of CDKB family of proteins is necessary. Inhibition of CDK activity is achieved through the availability of CYCD and CYCA proteins that are regulated by their selective degradation or rate of transcription (Maluszynska et al. 2013). Importantly, the activity of the CDK-CYC complexes could be blocked by the INHIBITOR OF CDK/KIP-RELATED PROTEIN (ICK/KRP) family. The high levels of over-expression of ICK/KRPs caused general inhibition of cell cycle progression in G1/S checkpoint, whereas lower level of expression stimulated endoreduplication, obstructing G2/M transition (Wen et al. 2013).

We specifically focused our attention on the elongating zone of the hypocotyl, situated beneath the cotyledons. Indeed, it has been demonstrated that this approximately 1 cm-long zone of hypocotyl is the zone where cell elongation takes place during skotomorphogenesis and responds to light in de-etiolation (Bergougnoux et al. 2012). The analysis of the expression in the elongating zone of the hypocotyls of *SlKRP2* and *SlKRP4*, encoding two other CDK inhibitors, showed that, similarly to *SlKRP1* and *SlKRP3* (Humplík et al. 2015a, *PloSONE*), both genes were less abundant in the *sit* mutant compared to WT and that exogenous ABA induced accumulation of these transcripts (Fig. 5). Interestingly, exogenous ABA induced also accumulation of *SlKRP4* transcript in the WT, which was not observed for other ICK/KRPs encoding genes. Based on their sequence, ICK/KRP proteins share very little similarities and are divided into two groups based on their C-term motifs, seemingly responsible for their sub-nuclear mode of action (Nafati et al. 2010). SlKRP1, SlKRP3 and SlKRP2 belong to the same subgroup, with the two first being closer relatives; SlKRP4 belongs to the second subgroup (Nafati et al. 2010). Thus the fact that SlKRP4 is also induced by exogenous ABA in the WT might reflect a different regulation and a different function in the cell of the elongating zone of hypocotyl. More detailed investigations on this specific SlKRP would be interesting in order to better understand the role of ABA in the control of endocycles.

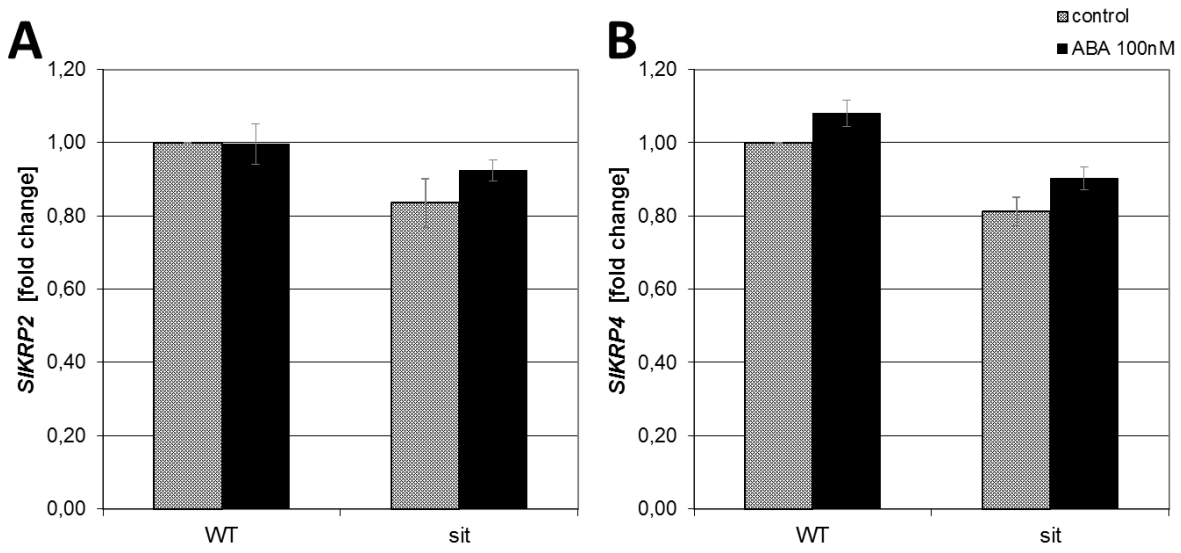

Figure 5. The effect of ABA-deficiency on the expression of CDK inhibitors *SlKRP2* and *SlKRP4*.
Analysis of the expression of the *SlKRP2* and *SlKRP4* genes based on the mean of three independent experiments ± SE. *Tip41like* and *PP2ACs* were used as housekeeping genes. All expression values are quoted relative to those for the "WT control" sample.

Cyclins are another group of proteins having an important role in the control of cell cycle. The role of specific cyclins (SlCycD3.1 and SlCycD3.3) during de-etiolation and inhibition of hypocotyl elongation upon exposure to blue light was recently suggested (Bergougnoux et al. 2012). Because SlCycD3.1 and SlCycD3.3 are known to be up-regulated by cytokinins, which are more accumulated in the *sit* mutant (Riou-Khamlichi et al. 1999; Humplík et al. 2015a, *PloSONE*; data presented beneath), we expect that these two genes will be upregulated in the mutant. For this purpose, the expression of *SlCycD3.1* and *SlCycD3.2* genes was analyzed in the elongating zone of hypocotyl of WT and *sit* mutant treated or not with ABA (Fig. 6). We did not observe a higher accumulation of these two transcripts in the mutant compared to the WT; even a slight, but non-significant decrease in the expression of *SlCycD3.3* could be observed. No significant difference in the expression of both genes could be observed when both WT and *sit* mutant were treated with exogenous ABA. From these results, we hypothesized that regulation of *SlCycD3.1* and *SlCycD3.3* transcription is ABA-independent. ABA might rather control cell cycle by stimulating *SlKRP* expression, consequently inhibiting CDKs.

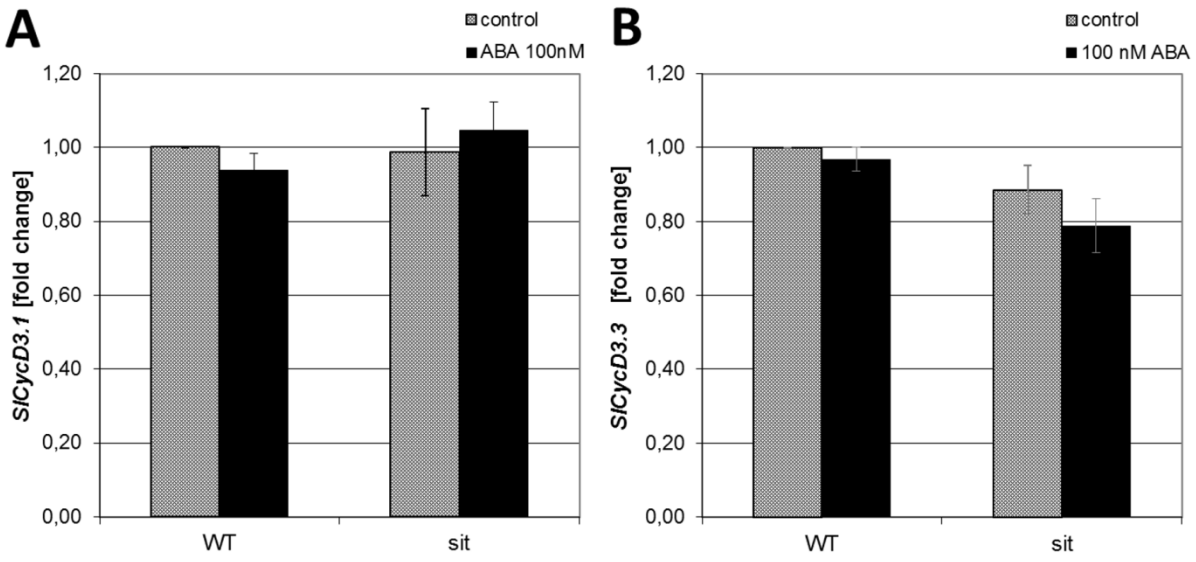

Figure 6. The effect of ABA-deficiency on the expression of genes encoding cyclin D3 *SlCycD3.1* and *SlCycD3.3*. Analysis of the expression of the *SlCycD3.1* and *SlCycD3.3* genes based on the mean of three independent experiments ± SE. *Tip41like* and *PP2ACs* were used as housekeeping genes. All expression values are quoted relative to those for the "WT control" sample.

8.1.3. Crosstalk between ABA and cytokinins

It was previously reported that CKs play a role in inhibition of hypocotyl elongation during BL induced de-etiolation of tomato seedlings (Bergougnoux et al. 2012). Therefore, we wondered whether a crosstalk exists between ABA and CKs in this process. For this purpose, we investigated the expression of genes encoding LONELY GUY (LOG) proteins, responsible for the direct synthesis of free, active CK from the riboside monophosphate precursor (reviewed in Zalabák et al. 2013). We already demonstrated that *SlLOG2* was upregulated in the *sit* mutant compared to WT (Humplík et al. 2015a, *PloSONE*). Here, we report the analysis of expression of 3 other *SlLOG* genes: *SlLOG1*, *SlLOG4* and *SlLOG6* (Fig. 7). No difference in *SlLOG1* gene expression could be detected between WT and *sit* mutant grown on medium not supplemented with ABA. While exogenous ABA induced reduction in *SlLOG1* transcript accumulation, no effect could be observed in WT. No difference in *SlLOG4* gene expression was observed in any of the genotype or depending on ABA treatment. Finally, the most interesting results were obtained for *SlLOG6* gene. Indeed, *SlLOG6* gene was found to be highly accumulated in *sit* mutant compared to WT and the ABA treatment induced a strong inhibition of *SlLOG6* transcription. It was already previously reported that *SlLOG2* is the most abundant member of the LOG family in the elongating zone of hypocotyl and the one which is having probably the most important role during BL-induced inhibition of hypocotyl elongation (Bergougnoux et al. 2012). It was also found that BL induced expression of *SlLOG6* and *SlLOG1* genes, but to lower amplitude compared to *SlLOG2* gene and that *SlLOG4* was probably not involved in the process (Bergougnoux et al. 2012). All data taken together tend to demonstrate

that SlLOG2 and SlLOG6 are the main enzymes in the elongating zone of hypocotyl involved in the synthesis of CKs which are required to restrain the cell elongation. We further demonstrated a control of ABA on the process.

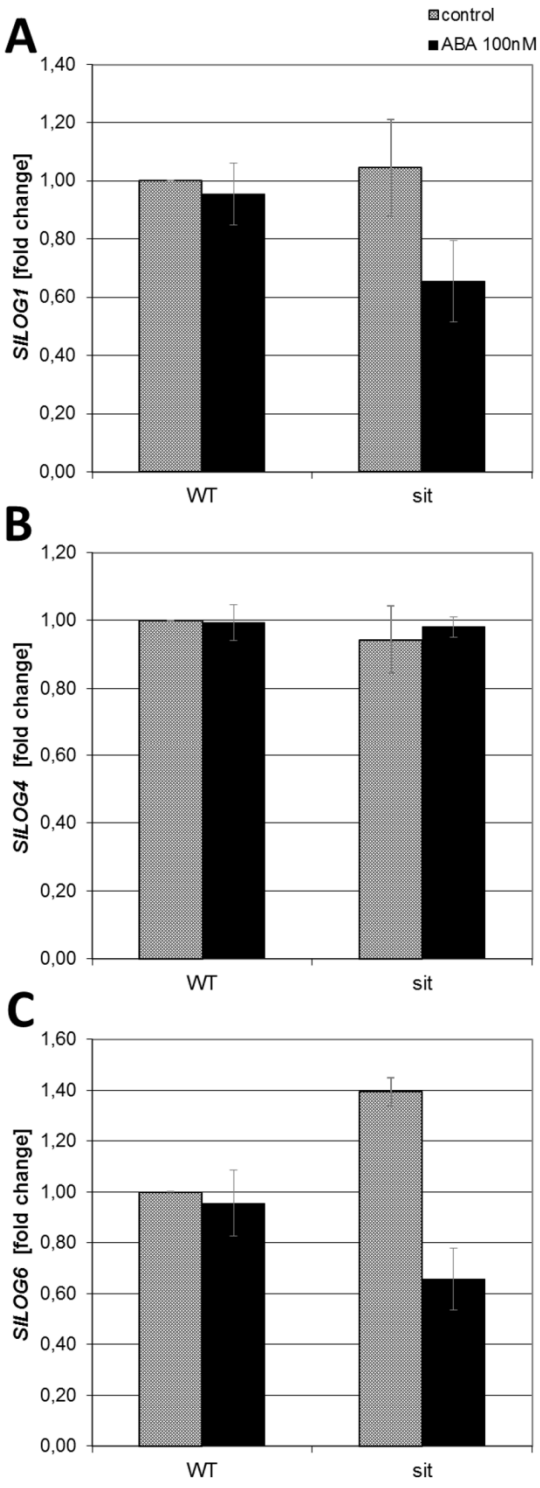

Figure 7. The effect of ABA-deficiency on the expression of genes encoding LOG enzyme *SlLOG1*, *SlLOG4* and *SlLOG6*.
Analysis of the expression of the *SlLOG1*, *SlLOG4* and *SlLOG6* genes based on the mean of three independent experiments ± SE. *Tip41like* and *PP2ACs* were used as housekeeping genes. All expression values are quoted relative to those for the "WT control" sample.

We previously reported a higher CKs content in whole *sit* mutant seedlings compared to the WT (Humplík et al. 2015a, *PloSONE*). In order to get a more precise picture of the control of ABA on the distribution of endogenous CKs, we analyzed CKs content in different organs of the *sit* mutant and WT grown in the dark for 2 and 3 days after sowing. CK metabolites were extracted and measured from cotyledons, full hypocotyl, elongating zone of hypocotyl and roots. Because the data presented in Table 2 are quite complex to interpret, we also present them as a heat map where data are summed up to the "functional groups" (active CKs – bases+ribosides, monophosphates, O- and N-glucosides). Colours represent ratios between sit (control or ABA treated) mean values divided by WT (control) mean values (Fig. 8). Thus the heat map indicates if the particular groups of CK metabolites are up-regulated, down-regulated or not-changed in the *sit* mutant and if those differences are influenced by exogenous treatment with ABA (100 nM). It should be noted that heat map serves only for better expression of observed trends, where no statistics was applied to test the significance. Particular compound mean values coupled with test of statistical significance based on three biological repeats are given in the Table 2.

In control conditions, the *sit* mutant accumulated also CK-conjugated glucosides, which are considered as storage forms of CKs. It has to be said that O-glucosylation is a reversible reaction that can be used as a source of free cytokinins, whereas 7-/9-(N-) glucosylation is an irreversible reaction. The reverse reaction from O-glucoside to the active CK is mediated by β-glucosidase. This enzyme was shown to be important in early seedling development where it hydrolyzes tZ-O-glucoside and DHZ-O-glucoside to free bases in developing embryo and coleoptiles (for the full names of CK metabolites please refer to list of abbreviations). Also the enormous amount of O-glucosides and ribosides was detected in the developing seeds suggesting their storage function (reviewed in Zalabák et al. 2013). When considering the overall quantity of the CK types, it is noticeable that iP-types represented the main group of CK metabolites in all organs. Moreover significant increases of iP-types were detected in all organs. Although some changes were observed also in other CK-types, it seems presumable that iP-types are the main regulators of shoot development during skotomorphogenesis. It has to be noted that absolutely main fraction of the overall pool of iP-types is formed by N-glucosides (Table 2). This seems to indicate tendency of the mutant seedling to alleviate the negative effects of boosted iP synthesis. Also the relative differences between ABA-deficient mutant and WT were detected within the group of iP- metabolites as shown in Figure 8. The highest relative differences, highest increases, in whole experiment were observed in the iP and iPR suggesting that they are major CK contributors to the *sitiens* phenotype.

If one considers active CKs (free bases and their corresponding ribosides), iP is the main CK to be relatively up-regulated in the *sit* mutant compared to the WT. The accumulation of active iP-derivatives correlated with phenotypes characteristic of CK-overproducer: shorter hypocotyl, smaller and greener cotyledons/leaves, roots. Indeed, CKs are known to be involved in the control of chloroplast biogenesis and function, influencing pigment accumulation (Zubo et al. 2008). As expectable ABA-deficient mutants in light conditions develop smaller

cotyledons compared to the WTs. Interestingly the effect of ABA-deficiency on the photosynthetic apparatus was observed in the cotyledons of the *sit, not* and *flc* mutants. The kinetic chlorophyll fluorescence imaging was performed in the cotyledons of one week old seedlings grown under white light. When compared to the WTs all three mutants exhibited higher maximal quantum yield of PSII photochemistry for a dark-adapted state (Φ_{Po}, also referred as F_V/F_M) together with higher quantum yield of regulatory light-induced non-photochemical quenching (Φ_{NPQ}). On the contrary the maximal quantum yield of PSII photochemistry for a light-adapted state (Φ_{PSII}, also referred as F_V'/F_M'), quantum yield of basic non-regulatory light-induced non-photochemical quenching ($\Phi_{f,D}$) and actual quantum yield of PSII photochemistry for a light adapted state (Φ_P) were equal or lower in all three ABA-deficient mutants (Fig 9). Very recently similar effect was found in Arabidopsis leaves to be characteristic of CKs treatment (Vylíčilová et al. 2015).

The elevated contents of iP and iPR in *sit* were efficiently lowered by exogenous ABA treatment (100 nM). However in elongating zone of hypocotyl (hypocotyl segments) not the up- but down-regulation was detected in the mutant seedlings and this effect was not affected by exogenous ABA. For this effect we have no explanation and further investigation will be necessary to understand it. However it can be postulated that in *sit* mutant, the absence of ABA results in the accumulation of CKs, mainly iP-types, disturbing the normal CK homeostasis. In order to maintain a proper homeostasis, active free CKs are stored as O-glucosides or degraded into N-glucoside derivatives.

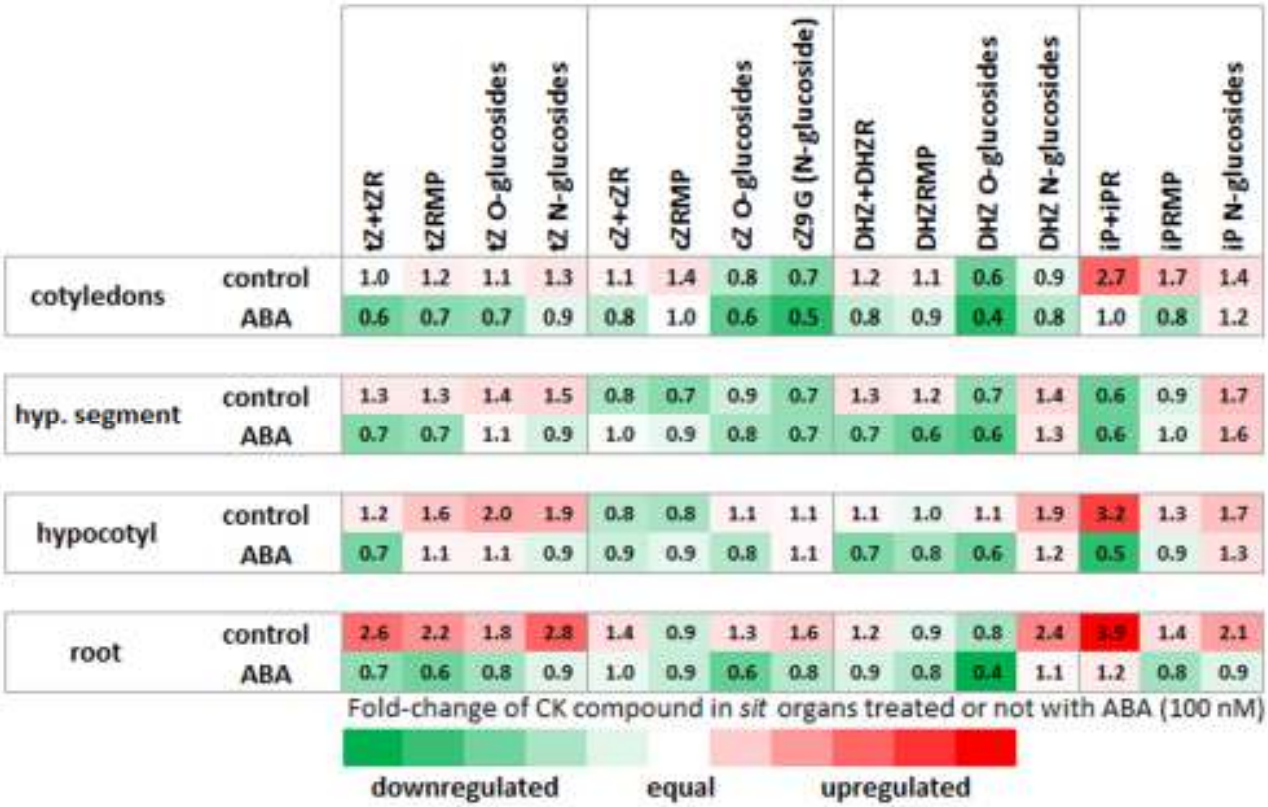

Figure 8. The relative comparison of changes in CK metabolites content in particular etiolated seedling organs in ABA-deficient mutant *sit* presented as a "heat map."

The mean values from CKs "functional-groups" were summed up in *sit* untreated and ABA-treated samples as well as in WT untreated samples. The values from *sit* were divided by values from WT showing the fold-changes in particular groups of compounds. The data from three biological repeats are presented. The full data of CKs analysis with statistical comparison are provided in Table 2.

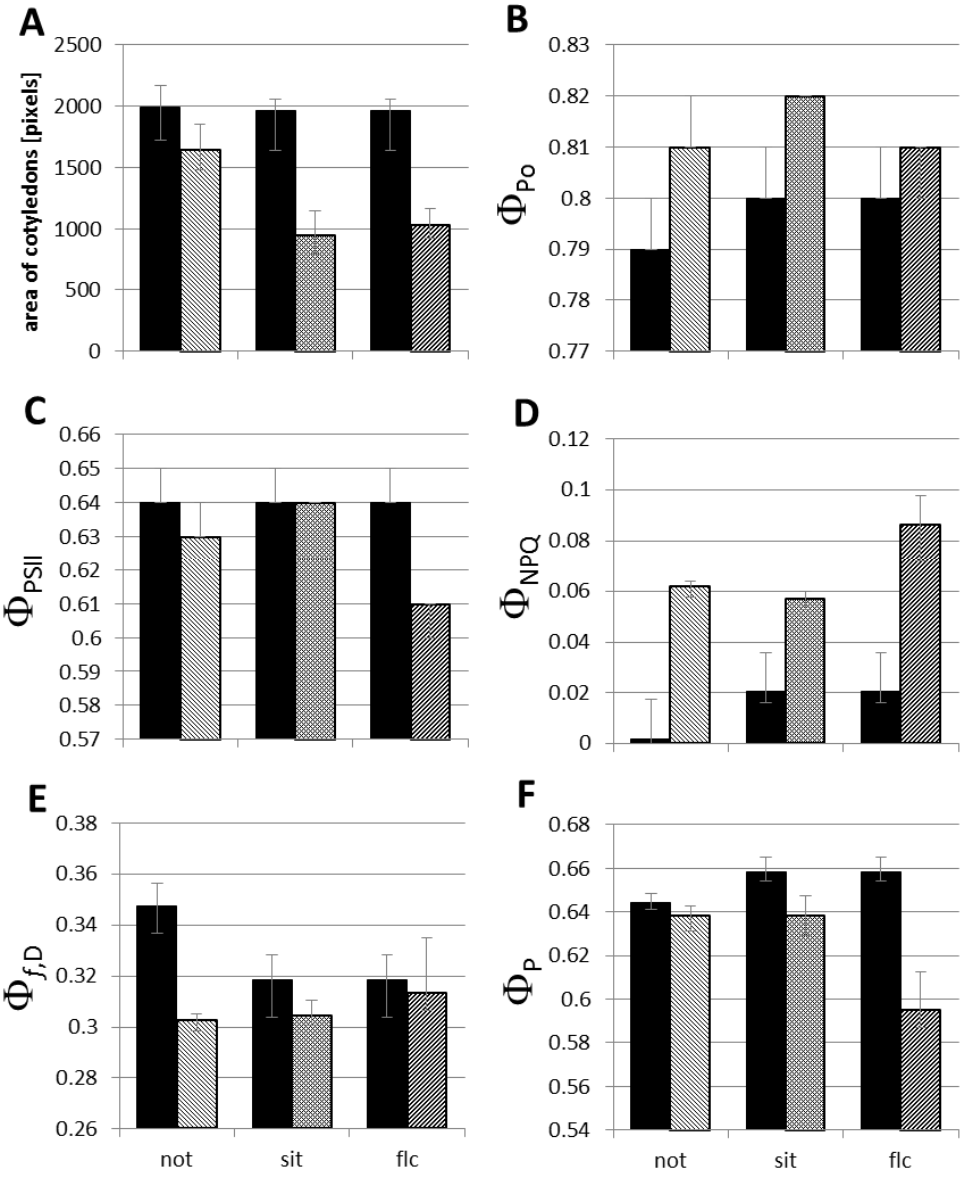

Figure 9. The effect of ABA-deficiency on the growth and photosynthetic efficiency of green cotyledons.
The seedlings of three ABA-deficient tomato mutants were grown in white-light conditions for one week. Than the measurement of leaf (cotyledon) area and photosynthetic efficiency was performed by fluorescence camera. The columns represent median values, error bars represent 25% and 75% quartiles for: A) cotyledon area, B) maximal quantum yield of PSII photochemistry, C) maximal quantum yield of PSII photochemistry for a light-adapted state, D) quantum yield of regulatory light-induced non-photochemical quenching, E) quantum yield of basic non-regulatory light-induced non-photochemical quenching, F) actual quantum yield of PSII photochemistry for light-adapted state. The shaded columns refer to the mutant samples, whereas the black columns show values of corresponding WTs. At least 15 seedlings per variant was analysed in one independent experiment.

8.1.4. Spatiotemporal distribution of cytokinins during blue-light induced photomorphogenesis

Once we observed that ABA content is lowered by BL-induced photomorphogenesis (see chapter 7) it seemed logical to investigate if the profile of CK metabolism in etiolated and BL-grown WT seedling organs is comparable to the profiles of WT and ABA-deficient mutants. Such a finding would suggest a direct link between ABA content and regulation of CK metabolism during de-etiolation and photomorphogenesis. However, the preliminary data that are presented here did not provide clear interpretation suggesting that regulation of CK metabolism is more complex in etiolated ABA-deficient seedlings and in WT seedlings undergoing photomorphogenesis. The WT seedlings were cultivated on MS media and after germination part of the seedlings was transferred to continuous BL to induce de-etiolation, whereas other part was kept in the dark. Subsequently, the seedlings were harvested after 24 and 48 hours of BL or dark cultivation that represent age of seedlings 96 and 120 hours after sowing. It this case the hypocotyl segments were not excised since it would be hardly possible to find a corresponding growing region in much shorter BL-grown hypocotyls – only entire cotyledons, hypocotyls and roots are compared particularly. It should be also considered that data from BL-grown roots were affected by un-natural lightning of roots on Petri dish. Because the data presented in Table 3 are quite complex to interpret, we also present them as a heat map where data are summed up to the "functional groups" (active CKs – bases+ribosides, monophosphates, O- and N-glucosides). Colours represent ratios between BL-grown seedlings mean values divided by dark-grown seedlings mean values. Thus the heat map indicates if the particular groups of CK metabolites are up-regulated, down-regulated or not-changed in the BL (Fig.10). It should be noted that heat map serves only for better expression of observed trends, where no statistics was applied to test the significance. But particular compound values coupled with test of statistical significance based on three biological repeats are given in the Table 3. In 96 hours old seedlings the BL induced elevation of certain *t*Z-types and iPRMP (for the full names of CK metabolites please refer to list of abbreviations). On the contrary *c*Z, *c*ZR, three metabolites from DHZ-group and iP and iPR decreased in BL-grown compared to the etiolated cotyledons. The hypocotyls of the same seedlings showed strongest upregulation in iPRMP (3.5) and then in *c*ZR (1.5) and slight increases in *t*ZRMP and *t*ZROG. Down-regulated was mainly DHZ (0.6) and slightly *t*Z and *t*Z9G. In roots most of the compounds were very slightly down-regulated by BL; only in *t*ZROG the strong effect was observed (0.1). The only higher fold-increase was observed in DHZ (1.6). In general, in one day older seedlings (120h after sowing) more upregulated metabolites were detected. The most dramatic changes occurred in 120h hypocotyls where important up-regulations in the three groups of metabolites were detected: in *c*Z-types, DHZ-types and iP-types (Fig. 10). In detail *c*ZR, *c*ZRMP, *c*Z-glucosides and in DHZ-types only glucosides were strongly elevated (maximum in DHZROG), from the iP-group iPRMP showed highest increase in whole experiment, others up-regulated iP-types were iP7G, iP9G. In roots of 120h old seedlings was again observed strong decrease of *t*ZROG, then slighter decreases in DHZRMP and two DHZ-glucosides. Elevations were detected for *t*Z7G and *c*Z (see Table 3).

The actual content of CKs in particular plant tissues/organs depends on the balance between *de novo* synthesis, transport, isoform conversion, conjugation and degradation (Sakakibara et al. 2006). Undoubtedly, light plays important role in the regulation of CK metabolism (Zdarska et al. 2015). Thus it was reported by Kraepiel et al. (1995) that in tobacco phytochrome mutants *pew1* and *pew2* the zeatin content was significantly reduced compared to the WT, but the levels of iP and other CK ribotides were not changed (Kraepiel et al. 1995). On the other hand, Bergougnoux et al. (2012) detected the important increase in iP, iPRMP and iP9G during BL-induced de-etiolation in tomato. Other CK-derivatives were found not to be involved in this process (Véronique Bergougnoux, personal communication). In our study the amount of iP-types was shown to be most abundant within the CK types. Indeed, the amount of iP-derivatives was 4-10 times higher in both D- and BL-grown seedlings compared to the other CK-types (Table 3.) Together with data of the changes of endogenous ABA in the same seedlings (see chapter 7) and data of CK analysis in ABA-deficient *sit* and WT seedlings, our results suggested that ABA promotes the etiolated hypocotyl growth via reduction of CKs, particularly iP-derivatives content. To fulfil the scheme of ABA – CKs interactions during skoto- and photo-morphogenesis it seems valuable to compare obtained analytical data with the expression of the CK metabolic genes in particular organs.

		tZ+tZR	tZRMP	tZ O-glucosides	tZ N-glucosides	cZ+cZR	cZRMP	cZ O-glucosides	cZ9 G (N-glucoside)	DHZ+DHZR	DHZRMP	DHZ O-glucosides	DHZ N-glucosides	iP+iPR	iPRMP	iP N-glucosides
96h	cotyledons	1.4	1.9	1.7	1.2	0.7	0.9	0.9	1.4	0.6	0.6	0.7	0.6	0.5	1.4	0.9
	hypocotyl	0.9	1.1	1.3	1.1	1.2	1.8	1.0	1.5	1.0	0.7	1.0	1.0	1.0	3.5	1.1
	root	1.2	1.8	0.1	1.1	0.7	0.7	0.9	0.9	1.1	1.0	0.8	0.8	0.9	1.2	1.0
120h	cotyledons	1.1	3.2	1.4	1.0	1.6	2.2	0.6	0.6	1.4	1.2	0.6	0.5	0.9	1.8	0.5
	hypocotyl	1.1	1.0	2.2	3.1	2.6	4.5	3.6	3.1	0.9	0.4	4.4	2.9	1.0	10.4	3.3
	root	1.0	0.8	0.1	1.2	1.2	1.2	0.8	0.9	1.0	0.7	0.9	0.8	1.1	1.1	1.0

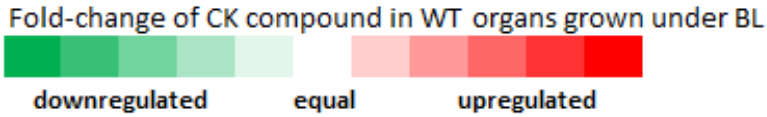

Figure 10. The relative comparison of changes in CK metabolites content in BL-grown WT seedlings presented as a "heat map."

The mean values from CKs "functional-groups" were summed up in BL-grown samples as well as in dark-grown samples. The values from BL were divided by values from dark showing the fold-changes in particular groups of compounds. The data from three biological repeats are presented. The full data of CKs analysis with statistical comparison are provided in Table 3.

Table 2. Quantification of CK metabolites in particular organs of *sit* and WT seedlings. Values are presented as a mean pmol.g^{-1} FW. Asterisks indicate statistically significant difference between marked sample and corresponding sample from WT 0 (control) group in t-test analysis (*, **, and *** correspond to p-values of 0.05 > p > 0.01, 0.01 > p > 0.001, and p < 0.001, respectively).

organ	genotype	treatment	tZ	tZR	tZRMP	tZOG	tZROG	tZ7G	tZ9G	cZ	cZR	cZRMP	cZOG	cZROG	cZ9G	DHZ	DHZR	DHZRMP	DHZOG	DHZROG	DHZ7G	DHZ9G
cotyledon	**WT**	**0**	0,50	0,14	0,38	0,42	2,32	25,56	1,71	0,19	0,30	2,40	0,33	1,00	1,06	0,05	0,09	0,06	1,00	6,46	233,79	10,96
	sit	**0**	0,45	0,18	0,46	0,61	2,50	34,20	1,25	0,16	0,40	3,25	0,34	0,77	0,74	0,05	0,11	0,06	0,80	3,89	221,20	10,03
		t-test				**			*			**		**	*				*	***		
	sit	**ABA**	0,34	0,07	0,27	0,32	1,71	24,66	1,00	0,17	0,24	2,42	0,28	0,51	0,49	0,05	0,07	0,05	0,45	2,86	191,40	10,21
		t-test	***	**	**	**	***		***				*	***	***				***	***		
hyp. segment	**WT**	**0**	0,41	0,76	1,85	0,18	0,62	8,02	0,98	0,08	0,23	1,63	0,13	0,24	0,45	0,04	0,12	0,17	0,17	1,78	50,49	2,23
	sit	**0**	0,48	1,00	2,35	0,23	0,89	12,07	1,11	0,07	0,18	1,16	0,16	0,16	0,33	0,07	0,15	0,20	0,16	1,25	73,57	2,87
		t-test			**		*	***			*	**	*	***	**	***		*		**	***	
	sit	**ABA**	0,39	0,42	1,38	0,11	0,74	7,25	0,85	0,12	0,19	1,54	0,14	0,14	0,33	0,05	0,07	0,11	0,09	1,02	63,35	2,90
		t-test		*	*	***		*		*				***	*	*	***	***	***	***	**	
hypocotyl	**WT**	**0**	0,22	0,48	0,57	0,06	0,20	2,09	0,26	0,08	0,24	1,09	0,04	0,08	0,18	0,02	0,05	0,06	0,04	0,38	10,94	0,41
	sit	**0**	0,24	0,60	0,94	0,09	0,41	4,01	0,49	0,05	0,21	0,85	0,06	0,08	0,19	0,02	0,05	0,06	0,05	0,41	20,22	0,88
		t-test			**	**	***	***	***	**		**	*						***		***	***
	sit	**ABA**	0,18	0,28	0,65	0,05	0,24	1,89	0,27	0,09	0,20	1,02	0,04	0,05	0,20	0,02	0,03	0,05	0,03	0,24	12,90	0,62
		t-test		*			*				**			***			**		***	***	**	**
root	**WT**	**0**	0,35	0,37	0,90	0,08	0,13	1,31	0,16	0,08	0,15	0,95	0,06	0,08	0,17	0,01	0,02	0,04	0,02	0,25	8,79	0,26
	sit	**0**	0,36	1,55	2,01	0,14	0,24	3,54	0,54	0,08	0,23	0,83	0,10	0,09	0,27	0,01	0,03	0,04	0,01	0,19	20,64	0,71
		t-test		***	**	**	**	***	***				**		*						**	***
	sit	**ABA**	0,21	0,32	0,59	0,06	0,10	1,13	0,23	0,07	0,15	0,81	0,04	0,05	0,14	0,01	0,02	0,03	0,01	0,09	9,38	0,44
		t-test	*		***	*	*						*	***				*	***	***		**

Table 2. continued

organ	genotype	treatment	iP	iPR	iPRMP	iP7G	iP9G	tZ-types	cZ-types	DHZ-types	iP-types	Total CK Bases	Total CK Ribosides	Total CK Nucleotides	Total CK O-glucosides	Total CK N-glucosides	Total CK
cotyledon	**WT**	**0**	0,15	0,13	0,30	96,85	0,48	5,48	5,29	18,60	97,84	0,88	0,59	3,14	11,54	370,41	386,56
	sit	**0**	0,41	0,34	0,52	132,98	0,41	5,45	5,66	14,94	134,38	0,98	0,86	4,29	8,90	400,80	415,83
		t-test	*	**	**	*				*	*			**	**		
	sit	**ABA**	0,17	0,10	0,24	115,21	0,51	3,71	4,11	13,68	116,18	0,73	0,43	2,98	6,12	343,48	353,74
		t-test			*	*		***	*	***	*	***			***		
hyp. segment	**WT**	**0**	0,18	0,15	0,23	25,49	0,72	4,80	2,76	4,51	26,68	0,72	1,18	3,87	3,12	88,36	97,25
	sit	**0**	0,15	0,05	0,21	44,46	0,49	6,06	2,06	4,70	45,29	0,73	1,35	3,92	2,86	134,89	143,74
		t-test		**		***	***	**	**		***					***	***
	sit	**ABA**	0,10	0,10	0,21	41,11	0,59	3,89	2,46	4,24	42,06	0,66	0,73	3,24	2,25	116,37	123,25
		t-test	***	**		***	**	*			***		**		**	**	**
hypocotyl	**WT**	**0**	0,36	0,15	0,08	7,32	0,26	1,78	1,71	0,96	7,88	0,50	0,85	1,76	0,79	21,46	25,36
	sit	**0**	0,30	1,31	0,11	12,58	0,43	2,78	1,45	1,48	13,93	0,47	1,52	1,96	1,11	38,80	43,86
		t-test		***		***	***	***	**	***	**				***	***	***
	sit	**ABA**	0,16	0,09	0,08	9,82	0,38	1,67	1,59	0,98	10,38	0,37	0,55	1,77	0,65	26,08	29,41
		t-test	*	*		***	**				***		***		*	**	*
root	**WT**	**0**	0,30	0,29	1,74	8,60	0,27	2,00	1,49	0,59	10,90	0,59	0,69	3,62	0,61	19,57	25,08
	sit	**0**	0,25	2,05	2,42	17,61	0,74	4,82	1,59	0,99	21,95	0,60	2,82	5,30	0,77	44,05	53,55
		t-test		**	*	**	***	***		**	***		**	*		**	***
	sit	**ABA**	0,19	0,54	1,34	7,81	0,36	1,50	1,26	0,60	9,87	0,38	0,75	2,77	0,34	19,49	23,74
		t-test			*			**				**		**	***		

Table 3. Quantification of CK metabolites in particular organs of D- or BL-grown seedlings. Values are presented as a mean pmol.g^{-1} FW. Asterisks indicate statistically significant difference in t-test analysis (*, **, and *** correspond to p-values of 0.05 > p > 0.01, 0.01 > p > 0.001, and p < 0.001, respectively).

organ	time after sowing	light conditions	tZ	tZR	tZRMP	tZOG	tZROG	tZ7G	cZ	cZR	cZRMP	cZOG	cZROG	cZ9G	DHZ	DHZR	DHZRMP	DHZOG	DHZROG	DHZ7G
96h	**cotyledon**	**D**	1,21	0,52	2,28	0,27	0,33	16,48	0,19	1,14	4,67	0,26	1,03	0,75	0,24	1,11	0,69	0,83	8,48	270,93
		BL	1,71	0,68	4,30	0,38	0,63	20,25	0,13	0,83	4,35	0,22	0,89	1,06	0,17	0,62	0,41	0,59	5,91	148,33
		t-test	*		***	*		*	*	**						**	*			***
	hypocotyl	**D**	1,10	1,67	3,64	0,25	0,90	10,23	0,14	0,22	1,35	0,19	0,48	0,66	0,11	0,19	0,23	0,22	3,31	74,83
		BL	0,87	1,54	3,87	0,27	1,27	11,12	0,10	0,32	2,43	0,20	0,48	0,97	0,07	0,22	0,17	0,22	3,35	75,24
		t-test	***						**	*	**			**	**		**			
	root	**D**	0,38	0,64	0,88	0,05	1,71	1,15	0,15	0,23	1,21	0,04	0,09	0,31	0,01	0,04	0,04	0,02	0,37	9,94
		BL	0,57	0,70	1,55	0,05	0,14	1,30	0,12	0,16	0,88	0,04	0,08	0,27	0,02	0,04	0,03	0,02	0,30	7,97
		t-test	**		***		***			*					*					
120h	**cotyledon**	**D**	0,53	0,11	0,39	0,41	0,94	26,89	0,16	0,13	2,41	0,23	0,95	0,91	0,04	0,05	0,05	0,92	6,09	221,98
		BL	0,56	0,15	1,26	0,51	1,31	28,32	0,15	0,31	5,25	0,15	0,61	0,54	0,06	0,08	0,06	0,73	3,62	121,05
		t-test			***					***	***	***	***	*	*	**		**	***	***
	hypocotyl	**D**	0,33	0,43	1,32	0,10	0,60	3,79	0,09	0,20	1,31	0,07	0,13	0,33	0,04	0,09	0,12	0,08	0,71	19,91
		BL	0,35	0,45	1,32	0,30	1,25	11,84	0,13	0,62	5,87	0,19	0,50	1,03	0,02	0,10	0,05	0,22	3,26	55,97
		t-test				***	*	***	**	***	***	***	***	***	***		***	***	***	***
	root	**D**	0,26	0,46	0,93	0,07	1,26	1,15	0,08	0,21	1,18	0,04	0,07	0,19	0,02	0,04	0,03	0,02	0,23	5,83
		BL	0,31	0,43	0,78	0,07	0,12	1,40	0,12	0,25	1,40	0,03	0,06	0,16	0,02	0,04	0,02	0,02	0,21	4,64
							***	*	**								**			*

Table 3. continued

organ	time after sowing	light conditions	iP	iPR	iPRMP	iP7G	iP9G	tZ-types	cZ-types	DHZ-types	iP-types	CK Bases	CK Ribosides	CK Nucleotides	CK O-glucosides	CK N-glucosides	Total CK
96h	**cotyledon**	**D**	1,44	0,59	1,00	77,53	0,52	6,18	8,03	23,29	80,78	3,07	3,06	8,65	11,20	379,70	405,68
		BL	0,62	0,34	1,43	70,70	0,49	9,27	7,49	16,77	73,41	2,63	2,30	10,50	8,62	251,47	275,51
		t-test	*	*	*			**					*			***	***
	hypocotyl	**D**	0,28	0,04	0,53	43,54	1,96	9,07	3,05	9,63	46,33	1,64	2,10	5,76	5,36	138,29	153,14
		BL	0,21	0,10	1,87	49,21	2,06	9,19	4,50	9,01	53,41	1,27	2,15	8,33	5,79	144,93	162,47
		t-test			***				**			***		**			
	root	**D**	0,26	0,34	2,33	7,54	0,36	3,87	2,02	0,99	10,66	0,80	1,08	4,46	2,28	20,01	28,64
		BL	0,21	0,35	2,85	7,65	0,32	3,17	1,54	0,97	11,38	0,91	1,25	5,31	0,64	18,21	26,33
		t-test			*										***		
120h	**cotyledon**	**D**	0,30	0,05	0,29	93,70	0,34	4,29	4,79	19,59	94,64	1,03	0,32	3,14	9,54	358,16	372,19
		BL	0,27	0,03	0,53	48,99	0,22	5,10	7,01	10,35	50,04	1,04	0,57	7,10	6,93	206,24	221,87
		t-test		*	***	***	**		**	***	***		**	***	**	***	***
	hypocotyl	**D**	0,15	0,06	0,15	11,78	0,35	3,25	2,12	2,22	12,45	0,61	0,74	2,90	1,68	37,83	43,76
		BL	0,16	0,05	1,53	39,00	1,42	5,04	8,33	8,30	42,15	0,66	1,21	8,77	5,73	115,26	131,62
		t-test			***	***	***	***	***	***	***		***	***	***	***	***
	root	**D**	0,16	0,23	1,55	6,75	0,19	3,15	1,77	0,71	8,76	0,52	0,83	3,68	1,69	14,65	21,36
		BL	0,22	0,19	1,75	6,46	0,21	1,87	2,02	0,58	8,80	0,64	0,90	3,95	0,51	13,31	19,30
		t-test						***							***		

9. CONCLUSIONS AND PERSPECTIVES

This thesis tries to bring an answer to the question on how ABA contributes to the seedling development especially to the elongation of hypocotyl. The literature review showed that the opinions on the role of ABA during plant growth are often contradictory. Indeed, whereas authors using exogenous ABA treatment or mutants in ABA signaling elements more often concluded that ABA is a growth inhibitor, studies employing ABA-deficient mutants rather suggest a growth-promotive effect of ABA. We would like to underline that simplified "labeling" of hormones as stimulators or inhibitors should be avoided to circumvent misunderstanding that is further "dogmatized" within the scientific community. Although, these facts sounds logical and easy to understand, in the mainstream community of plant biologist that is mostly educated in molecular and cellular biology, but less in plant physiology "the abbreviated views" on the hormone action are common. Every physiological response to exogenous hormone application is primarily question of compound concentration and tissue sensitivity (Trewavas 1982). Moreover, there is an important level of uncertainty of the relevance of correlation between effect of exogenous treatment and physiological role of endogenous hormone (Sharp 2002). Similar uncertainty has to be considered in relation with experiments using biosynthetic or signalling mutants, especially in those with constitutively expressed mutation effect. The plant that is for its whole life under pressure of mutation will respond by hardly-predictable network of backward regulatory mechanisms to alleviate the negative effects. We should have all these facts in our minds when interpreting a data from experiments in which plants are pushed into extremely artificial circumstances. From this point of view it seems to be very valuable to produce inducible transgenic plants with possibility of finely "tuning" of the mutation effect power. Such plants should allow switching on/off the mutation only in the particular physiological process avoiding the effects of pre-adaptation (including the epigenetic changes from maternal plant). Moreover, the gradual induction of the mutation should allow the analysis of the dose-response-like effects of the endogenous compound. Examples mentioned in the review part of the thesis demonstrate that artificial division of plant hormones to the regulators and inhibitors is only simplistic description of physiological reality. However, it does not exclude the fact that in particular physiological response one of the "poles" (inhibitor – stimulator) has to be preferred. In case of growth of etiolated tomato hypocotyl, the ABA-deficiency caused growth-inhibition. It strongly suggests that homeostatic concentration of endogenous ABA supports the hypocotyl growth during tomato skotomorphogenesis. We presented here further evidences that endogenous ABA accumulates in etiolated tomato seedlings and is degraded in response to the blue-light. In the context of our data, we hypothesized that during skotomorphogenesis, ABA promotes hypocotyl growth through the stimulation of CDK inhibitor family SlKRPs and through the inhibition of CKs biosynthesis and stimulation of CKs glucosylation leading to the stimulation of endoreduplication cell expansion. In the presence of light the ABA content is decreased allowing higher CKs synthesis and lower glucosylation leading to the mitosis and cell differentiation (Fig. 11). The obtained data demonstrated the importance of a proper regulation of ABA metabolism during tomato post-germination growth. Although the detailed

mechanism of ABA action remains challenging for the future, we believe that our observations provide a novel inspiring view on the role of ABA during young seedling development.

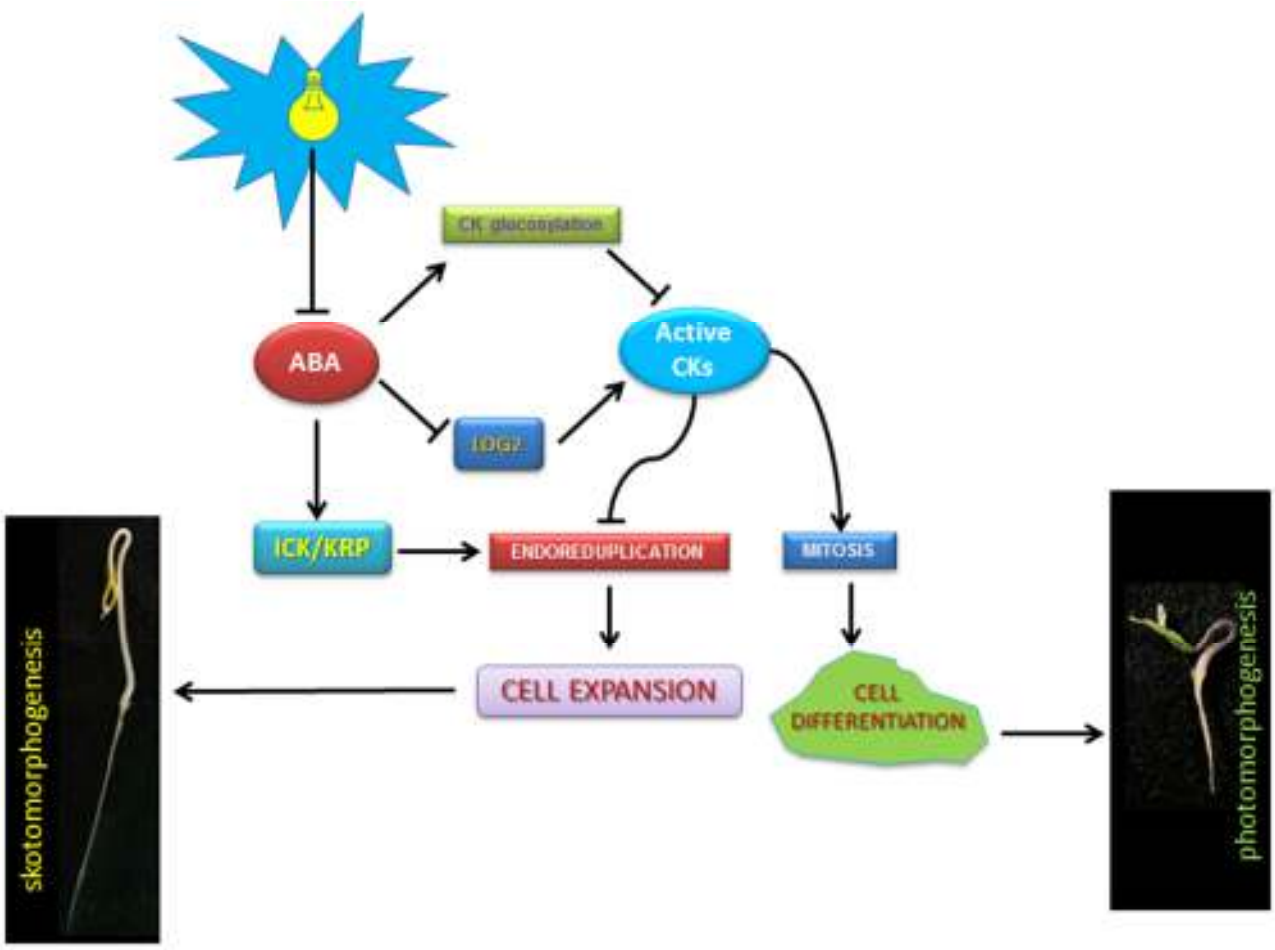

Figure 11. A simplified hypothetical model of ABA action during tomato seedling skotomorphogenesis and de-etiolation.

In absence of light the ABA biosynthesis is upregulated that leads to activation of ICK/KRPs proteins and downregulation of CKs content by inhibition of *LOG2* expression and stimulation of CK glucosylation. ICK/KRP proteins enhance DNA endoreduplication by inhibiting CDK that promote the cell expansion and etiolated growth (skotomorphogenesis). When the light is perceived the ABA synthesis is inhibited and decreased ABA content allows increase of CKs that stimulates cell division in favour of DNA endoreduplication that inhibits the hypocotyl growth and supports photomorphogenesis.

10. REFERENCES

Abe H, Yamaguchi-Shinozaki K, Urao T, Iwasaki T, Hosokawa D, Shinozaki K. 1997. Role of Arabidopsis MYC and MYB homologs in drought- and abscisic acid regulated gene expression. *Plant Cell.* 9:1859-168

Abe H, Urao T, Ito T, Seki M, Shinozaki K, Yamaguchi-Shinozaki K. 2003. Arabidopsis AtMYC2 (bHLH) and AtMYB2 (MYB) function as transcriptional activators in abscisic acid signaling. *Plant Cell.* 15:63–78

Addicott FT, Lyon JL. 1969. Physiology of Abscisic Acid and Related Substances. Annu. Rev. Plant Physiol. 20:139–64

Achard P, Herr A, Baulcombe DC, Harberd NP. 2004. Modulation of floral development by a gibbere lin-regulated microRNA. *Development.* 131:3357–65

Achard P, Baghour M, Chapple A, Hedden P, Van Der Straeten D, Genschik P, et al. 2007. The plant stress hormone ethylene controls floral transition via DELLA-dependent regulation of floral meristem-identity genes. *P Natl Acad Sci USA*. 104:6484–89

Alabadí D, Gallego-Bartolomé J, Orlando L, García-Cárcel L, Rubio V, et al. 2008. Gibberellins modulate light signaling pathways to prevent Arabidopsis seedling de-etiolation in darkness. *Plant J*. 53:324–35

Alabadí D, Blázquez MA. 2009. Molecular interactions between light and hormone signaling to control plant growth. *Plant Mol Biol.* 69:409–417

Ali-Rachedi S, Bouinot D, Wagner MH, Bonnet M, Sotta B, et al. 2004. Changes in endogenous abscisic acid levels during dormancy release and maintenance of mature seeds: studies with the cape verde islands ecotype, the dormant model of *Arabidopsis thaliana*. *Planta*. 219:479–88

Allan AC, Fricker MD, Ward JL, Beale MH, Trewavas AJ. 1994. Two transduction pathways mediate rapid effects of abscisic acid in Commelina guard cells. *Plant Cell* 6: 1319-28

Anderson JP, Badruzsaufari E, Schenk PM, Manners JM, Desmond OJ, Ehlert C, Maclean DJ, Ebert PR, Kazan K. 2004. Antagonistic interaction between abscisic acid and jasmonate-ethylene signaling pathways modulates defense gene expression and disease resistance in Arabidopsis. *Plant Cell.* 16:3460–79

Aroca R, Del Mar Alguacil M, Vernieri P, Ruiz-Lozano JM. 2008. Plant responses to drought stress and exogenous ABA application are modulated differently by mycorrhization in tomato and an ABA-deficient mutant (*sitiens*). *Microb Ecol*. 56:704–19

Arsovski AA, Galstyan A, Guseman JM, Nemhauser JL. 2012. Photomorphogenesis. *Arabidopsis Book*. 10:e0147

Barrero JM, Piqueras P, González-Guzmán M, Serrano R, Rodríguez PL, et al. 2005. A mutational analysis of the aba1 gene of Arabidopsis thaliana highlights the involvement of ABA in vegetative development. *J Exp Bot*. 56:2071–83

Barrero JM, Rodríguez PL, Quesada V, Alabadí D, Blázquez M a., et al. 2008. The aba1 gene and carotenoid biosynthesis are required for late skotomorphogenic growth in *Arabidopsis thaliana*. *Plant Cell Environ*. 31:227–34

Bauer D, Viczián A, Kircher S, Nobis T, Nitschke R, et al. 2004. Constitutive Photomorphogenesis 1 and multiple photoreceptors control degradation of Phytochrome Interacting Factor 3, a transcription factor required for light signaling in Arabidopsis. *Plant Cell*. 16:1433–45

Bauer H, Ache P, Lautner S, Fromm J, Hartung W, et al. 2013. The stomatal response to reduced relative humidity requires guard cell-autonomous ABA synthesis. *Curr Biol*. 23:53–57

Beaudoin N, Serizet C, Gosti F, Giraudat J. 2000. Interactions between abscisic acid and ethylene signaling cascades. *Plant Cell.* 12:1103–15

Belin C, Megies C, Hauserová E, Lopez-Molina L. 2009. Abscisic acid represses growth of the Arabidopsis embryonic axis after germination by enhancing auxin signaling. *Plant Cell*. 21:2253–68

Ben Haj Salah H, Tardieu F. 1997. Control of leaf expansion rate of droughted maize plants under fluctuating evaporative demand–asuperposition of hydraulic and chemical messages? *Plant Physiol.* 114:893–900

Bergougnoux V, Zalabák D, Jandová M, Novák O, Wiese-Klinkenberg A, Fellner M. 2012. Effect of blue light on endogenous isopentenyladenine and endoreduplication during photomorphogenesis and de-etiolation of tomato (*Solanum lycopersicum* L.) seedlings. *PLoS One*. 7:e45255

Bhaskara GB, Nguyen TT, Verslues PE. 2012. Unique drought resistance functions of the highly ABA-induced clade A protein phosphatase 2Cs. *Plant Physiol.* 160:379–95

Blazquez MA, Green R, Nilsson O, Sussman MR, Weigel D. 1998. Gibberellins promote flowering of Arabidopsis by activating the *LEAFY* promoter. *Plant Cell*. 10:791–800

Blum A. 2015. Towards a conceptual ABA ideotype in plant breeding for water limited environments. *Funct Plant Biol*. 42:502–13

Bouchabke O, Tardieu F, Simonneau T. 2006. Leaf growth and turgor in growing cells of maize (*Zea mays* L.) respond to evaporative demand under moderate irrigation but not in water-saturated soil. *Plant Cell Environ*. 29:1138–48

Bradford KJ. 1983. Water relations and growth of the *flacca* tomato mutant in relation to abscisic acid. *Plant Physiol*. 72:251–55

Burbidge A, Grieve TM, Jackson A, Thompson A, Mc-Carty DR, Taylor IB. 1999. Characterization of the ABA-deficient tomato mutant *notabilis* and its relationship with maize Vp 14. *Plant J.* 17:427–31

Carvalho RF, Campos ML, Pino LE, Crestana SL, Zsögön A, et al. 2011. Convergence of developmental mutants into a single tomato model system: "micro-tom" as an effective toolkit for plant development research. *Plant Methods*. 7:18

Cashmore AR, Jamarillo JA, Wu YJ, Liu D. 1999. Cryptochromes: blue light receptors for plants and animals. *Science*. 284:760–765

Chen JG, Zhou X. 1998. Involvement of abscisic acid in mesocotyl growth in etiolated seedlings of a foxtail millet dwarf mutant. *J Plant Growth Regul*. 17:147–51

Chen G, Shi Q, Lips SH, Sagi M. 2003. Comparison of growth of *flacca* and wild-type tomato grown under conditions diminishing their differences in stomatal control. *Plant Sci*. 164:753–57

Chen H, Zhang J, Neff MM, Hong SW, Zhang H, Deng XW, Xiong L. 2008. Integration of light and abscisic acid signaling during seed germination and early seedling development. *Proc Natl Acad Sci USA*. 105:4495–500

Cheng WH, Endo A, Zhou L, Penney J, Chen H-C, et al. 2002. A unique short-chain dehydrogenase/reductase in Arabidopsis glucose signaling and abscisic acid biosynthesis and functions. *Plant Cell*. 14:2723–43

Choi H, Hong J, Ha J, Kang J, Kim S. 2000. ABFs, a family of ABA-responsive element binding factors. *J. Biol. Chem.* 275:1723-30

Chory J, Reinecke D, Sim S, Washburn T, Brenner M. 1994. A role for cytokinins in de-etiolation in Arabidopsis (det mutants have an altered response to cytokinins). *Plant Physiol.* 104:339–47

Christmann A, Weiler EW, Steudle E, Grill E. 2007. A hydraulic signal in root-to-shoot signalling of water shortage. *Plant J*. 52:167–74

Clouse SD, Langford M, McMorris TC. 1996. A brassinosteroid-insensitive mutant in *Arabidopsis thaliana* exhibits multiple defects in growth and development. *Plant Physiol.* 111:671–78

Conti L, Galbiati M, Tobelli C. 2014. ABA Signal Perception and ABA Receptors. In: Zhang DP, editor. Abscisic Acid: Metabolism, Transport and Signaling. Dodrecht: Springer. pp. 365–84

Cornforth JW, Milborrow BV, Ryback G, Wareing PF. 1965. Chemistry and Physiology of Dormins In Sycamore: Identity of Sycamore Dormin with Abscisin II. *Nature* 205:1269–70

Cramer GR, Quarrie SA. 2002. Abscisic acid is correlated with the leaf growth inhibition of four genotypes of maize differing in their response to salinity *Funct Plant Biol*. 29:111–15

Creelman RA, Mason HS, Bensen RJ, Boyer JS, Mullet JE. 1990. Water deficit and abscisic acid cause differential inhibition of shoot versus root growth in soybean seedlings : analysis of growth, sugar accumulation, and gene expression. *Plant Physiol*. 92:205–14

Cutler SR, Rodriguez PL, Finkelstein RR, Abrams SR. 2010. Abscisic acid: emergence of a core signaling network. *Annu Rev Plant Biol*. 61:651–79

Dekkers BJW, Willems L, Bassel GW, Van Bolderen-Veldkamp RPM, Ligterink W, et al. 2012. Identification of reference genes for RT-qPCR expression analysis in Arabidopsis and tomato seeds. *Plant Cell Physiol*. 53:28–37

De Veylder L, Larkin JC, Schnittger A. 2011. Molecular control and function of endoreplication in development and physiology. *Trends Plant Sci*. 16:624–34

Ding Y, Kalo P, Yendrek C, Sun J, Liang Y, Marsh JF, Harris JM, Oldroyd GE. 2008. Abscisic acid coordinates nod factor and cytokinin signaling during the regulation of nodulation in *Medicago truncatula*. *Plant Cell.* 20:2681–95

Dodd IC, Davies WJ. 2010. Hormones and the regulation of water balance. In: Davies PJ, editor. Plant Hormones: Biosynthesis, Signal Transduction, Action!. Dodrecht: Springer. pp. 519–48

Domagalska MA, Sarnowska E, Nagy F, Davis SJ. 2010. Genetic analyses of interactions among gibberellin, abscisic acid, and brassinosteroids in the control of flowering time in *Arabidopsis thaliana*. *PLoS One*. 5:e14012

Dupeux F, Santiago J, Betz K, Twycross J, Park SY, Rodriguez L, Gonzalez-Guzman M, Jensen MR, Krasnogor N, Blackledge M, Holdsworth M, Cutler SR, Rodriguez PL, Marquez JA. 2011. A thermodynamic switch modulates abscisic acid receptor sensitivity. *EMBO J.* 30:4171–84

Ehlert C, Maurel C,Tardieu F, Simonneau T. 2009. Aquaporin-mediated reduction in maize root hydraulic conductivity impacts cell turgor and leaf elongation even without changing transpiration. *Plant Physiol.* 150:1093–104

El-Antably HMM. 1974. Important effect of ABA and other growth hormones on growth and yield of corn and Sorghum. *Biochemie und Physiologie der Pflanzen.* 166:351-56

Fambrini M, Vernieri P, Toncelli ML, Rossi VD, Pugliesi C. 1995. Characterization of a wilty sunflower (*Helianthus annuus* L.) mutant 3. Phenotypic interaction in reciprocal grafts from wilty mutant and wild-type plants. *J Exp Bot.* 46:525–30

Finch-Savage WE, Leubner-Metzger G. 2006. Seed dormancy and the control of germination. *New Phytol*. 171:501–23

Finkelstein RR. 1994. Mutations at two new Arabidopsis ABA response loci are similar to the abi3 mutations. *Plant J.* 5:765–71

Finkelstein RR, Wang ML, Lynch TJ, Rao S, Goodman HM. 1998. The Arabidopsis abscisic acid response locus ABI4 encodes an APETALA2 domain protein. *Plant Cell.* 10:1043–54

Finkelstein R, Lynch T. 2000. The Arabidopsis abscisic acid response gene ABI5 encodes a basic leucine zipper transcription factor. *Plant Cell.* 12:599–609

Finkelstein R. 2010. The role of hormones during seed development and germination. In: Davies PJ, editor. Plant Hormones: Biosynthesis, Signal Transduction, Action!. Dodrecht: Springer. pp. 549–73

Finkelstein R. 2013. Abscisic acid synthesis and response. *Arabidopsis Book*. 11:e0166

Folta KM, Spalding EP. 2001. Unexpected roles for cryptochrome 2 and phototropin revealed by high-resolution analysis of blue light-mediated hypocotyl growth inhibition. *Plant J.* 26:471–478

Frey A, Godin B, Bonnet M, Sotta B, Marion-Poll A. 2004. Maternal synthesis of abscisic acid controls seed development and yield in *Nicotiana plumbaginifolia*. *Planta*. 218:958–64

Fujii H, Verslues P, Zhu JK. 2011. Arabidopsis decuple mutant reveals the importance of SnRK2 kinases in osmotic stress responses in vivo*. Proc. Natl. Acad. Sci. USA.* 108:1717–22

Fujita Y, Nakashima K, Yoshida T, Katagiri T, Kidokoro S, Kanamori N, Umezawa T, Fujita M, Maruyama K, Ishiyama K, Kobayashi M, Nakasone S, Yamada K, Ito T, Shinozaki K, Yamaguchi-Shinozaki K. 2009. Three SnRK2 Protein Kinases are the Main Positive Regulators of Abscisic Acid Signaling in Response to Water Stress in Arabidopsis. *Plant Cell Physiol.* 50:2123–32

Ghassemian M, Nambara E, Cutler S, Kawaide H, Kamiya Y, McCourt P. 2000. Regulation of abscisic acid signaling by the ethylene response pathway in Arabidopsis. *Plant Cell.* 12:1117–26

Giraudat J, Hauge B, Valon C, Smalle J, Parcy F, Goodman H. 1992. Isolation of the Arabidopsis ABI3 gene by positional cloning. *Plant Cell* 4:1251–61

Goethe JW, 1790. Versuch die Metamorphose der Pflanzen zu erklären. Gotha: Carl Wilhelm Ettinger. English translation: Miller D, 1988. Goethe, Collected works, Scientific studies, Vol. 12. Princeton: Princeton University Press.

Golldack D, Li C, Mohan H, Probst N. 2013. Gibberellins and abscisic acid signal crosstalk: living and developing under unfavorable conditions. *Plant Cell Rep*. 32:1007–16

Gomez-Cadenas A, Verhey SD, Holappa LD, Shen Q, Ho THD, Walker-Simmons MK. 1999. An abscisic acid-induced protein ki- nase, PKABA1, mediates abscisic acid-suppressed gene expression in barley aleurone layers. *Proc. Natl. Acad. Sci. USA.* 96:1767–72

Gonzáles CV, Ibara SV, Piccoli PN, Botto JF, Boccalandro HE. 2012. Phytochrome B increases drought tolerance by enhancing ABA sensitivity in *Arabidopsis thaliana*. *Plant, Cell Environ.* 35:1958–68

Gowing DJG, Davies WJ, Jones HG. 1990. A positive root-sourced signal as a indicator of soil drying in ammple, *Malus domestica* B. *J Exp Bot.* 41:1535–40

Guan C, Wang X, Feng J, Hong S, Liang Y, et al. 2014. Cytokinin antagonizes abscisic acid-mediated inhibition of cotyledon greening by promoting the degradation of abscisic acid insensitive5 protein in Arabidopsis. *Plant Physiol*. 164:1515–26

Gubler F, Hughes T, Waterhouse P, Jacobsen J. 2008. Regulation of dormancy in barley by blue light and after-ripening: effects on abscisic acid and gibberellin metabolism. *Plant Physiol.* 147:886–96

Hall HK, McWha JA. 1981. Effects of abscisic acid on growth of wheat (*Triticum aestivum* L.). *Ann Bot.* 47:427-33

Hao Q, Yin P, Li W, Wang L, Yan C, Lin Z, Wu Jim Z, Wang J, Yan SF, Yan N. 2011. The molecular basis of ABA-independent inhibition of PP2Cs by a subclass of PYL proteins. *Mol Cell.* 42:662–72

Harrison E, Burbidge A, Okyere JP, Thompson AJ, Taylor IB. 2011. Identification of the tomato ABA-deficient mutant sitiens as a member of the ABA-aldehyde oxidase gene family using genetic and genomic analysis. *Plant Growth Regul*. 64:301–09

Hartung W, Slovik S. 1991. Physicochemical properties of plant growth regulators and plant tissues determine their distribution and redistribution. *New Phytol.* 119:361–82

Hauser F, Waadt R, Schroeder JI. 2011. Evolution of abscisic acid synthesis and signaling mechanisms. *Curr Biol*. 21:346–55

Hayashi Y, Takahashi K, Inoue SI, Kinoshita T. 2014. Abscisic acid suppresses hypocotyl elongation by dephosphorylating plasma membrane H^+-ATPase in *Arabidopsis thaliana*. *Plant Cell Physiol*. 55:845–53

Hoffmann WA, Poorter H. 2002. Avoiding bias in calculations of relative growth rate. *Ann Bot*. 90:37–42

Holbrook NM, Shashidhar VR, James RA, Munns R. 2002. Stomatal control in tomato with ABA-deficient roots: response of grafted plants to soil drying. *J Exp Bot.* 53:1503–14

Horton RF. 1971. Stomatal opening: the role of abscisic acid. *Can J Bot*. 49:583–85

Hoth S, Morgante M, Sanchez JP, Hanafey MK, Tingey SV, Chua NH. 2002. Genome-wide gene expression profiling in *Arabidopsis thaliana* reveals new targets of abscisic acid and largely impaired gene regulation in the *abi1-1* mutant. *J Cell Sci*. 115:4891–900

Humplík JF, Bergougnoux V, Jandová M, Šimura J, Pěnčík A, Tomanec O, Rolčík J, Novák O, Fellner M. 2015a. Endogenous Abscisic Acid Promotes Hypocotyl Growth and Affects Endoreduplication during Dark-Induced Growth in Tomato (*Solanum lycopersicum* L.). *PLoS One*. 10:e0117793

Humplík JF, Turečková V, Fellner M, Bergougnoux V. 2015b. Spatio-temporal changes in endogenous abscisic acid contents during etiolated growth and photomorphogenesis in tomato seedlings. *Plant Signal Behav*. 10:e1039213

Humplík JF, Lazár D, Husičková A, Spíchal L. 2015c. Automated phenotyping of plant shoots using imaging methods for analysis of plant stress responses – a review. *Plant Methods*. 11:29.

Humplík JF, Lazár D, Fürst T, Husičková A, Hýbl M, Spíchal L. 2015d. Automated integrative high-throughput phenotyping of plant shoots: a case study of the cold-tolerance of pea (*Pisum sativum* L.). *Plant Methods*. 11:20.

Imber D, Tal M. 1970. Phenotypic reversion of *flacca*, a wilty mutant of tomato, by abscisic acid. *Science*. 169:592–93

Jeannette E, Rona JP, Barda, F, Cornel D, Sotta B, Miginiac E. 1999. Induction of RAB18 gene expression and activation of K+ out- ward rectifying channels depend on extracellular perception of ABA in *Arabidopsis thaliana* suspension cells. *Plant J.* 18:13–22

Jeong DH, Lee S, Kim SL, Hwang I, An G. 2007. Regulation of brassinosteroid responses by phytochrome B in rice. *Plant Cell Environ.* 30:590–99

Jia HF, Chai YM, Li CL, Lu D, Luo JJ, Qin L, Shen YY. 2011. Abscisic acid plays an important role in the regulation of strawberry fruit ripening. *Plant Physiol.* 157:188–99

Johnston CA, Temple BR, Chen JG, Gao Y, Moriyama EN, Jones AM, Siderovski DP, Willard FS. 2007. Comment on 'A G protein coupled receptor is a plasma membrane receptor for the plant hormone abscisic acid'. *Science*. 318:914

Jones RJ, Mansfield TA. 1970. Suppression of stomatal opening in leaves treated with abscisic acid. *J Exp Bot*. 21:714–19

Jones H, Sharp C, Higgs K. 1987. Growth and water relations of wilty mutants of tomato (*Lycopersicon esculentum* Mill.). *J Exp Bot.* 38:1848–56

Kami C, Lorrain S, Hornitschek P, Fankhauser C. 2010. Light-regulated plant growth and development. *Curr Top Dev Biol.* 91:29–64

Kerchev PI, Pellny TK, Vivancos PD, Kiddle G, Hedden P, Driscoll S, Vanacker H, Verrier P, Hancock RD, Foyer CH. 2011. The Transcription factor ABI4 is required for the ascorbic acid-dependent regulation of growth and regulation of jasmonate-dependent defense signaling pathways in Arabidopsis. *Plant Cell.* 23:3319–34

Kim DH, Yamaguchi S, Lim S, Oh E, Park J, Hanada A, Kamiya Y, Choi G. 2008. SOMNUS, a CCCH- type zinc finger protein in Arabidopsis, negatively regulates light-dependent seed germination downstream of PIL5. *Plant Cell*. 20:1260–77

Kim W, Lee Y, Park J, Lee N, Choi G. 2013. HONSU, a protein phosphatase 2C, regulates seed dormancy by inhibiting ABA signaling in Arabidopsis. *Plant Cell Physiol.* 54:555–72

King RW, Evans LT. 1977. Inhibition of flowering in *Lolium temulentum* L. By water stress: a role for Abscisic acid. *Aust J Plant Physiol*. 4:225–33

Kitahata N, Asami T. 2011. Chemical biology of abscisic acid. *J Plant Res*. 124:549–57

Kochhar TS. 1980. Effect of abscisic acid and auxins on the growth of tobacco callus. *Zeitschrift für Pflanzenphysiologie*. 97:1–4

Koops P, Pelser S, Ignatz M, Klose C, Marrocco-Selden K, Kretsch T. 2011. EDL3 is an F-box protein involved in the regulation of abscisic acid signalling in *Arabidopsis thaliana*. *J Exp Bot*. 62:5547–60

Koornneef M, Rolff E, Spruit CJP. 1980. Genetic control of light-inhibited hypocotyl elongation in *Arabidopsis thaliana* (L) Heynh. *Zeitschrift für Pflanzenphysiologie*. 100:147–60

Koornneef M, Reuling G, Karssen C. 1984. The isolation and charac- terization of abscisic acid-insensitive mutants of Arabidopsis thaliana. *Physiol Plant.* 61:377–83

Koussevitzky S, Nott A, Mockler TC, Hong F, Sachetto-Martins G, Surpin M, Lim J, Mittler R, Chory J. 2007. Signals from chloroplasts converge to regulate nuclear gene expression. *Science*. 316:715–19

Kraepiel Y, Rousselin P, Sotta B, Kerhoas L, Einhorn J, et al. 1994. Analysis of phytochrome- and ABA-deficient mutants suggests that ABA degradation is controlled by light in *Nicotiana plumbaginifolia*. *Plant J.* 6:665–72

Kraepiel Y, Marree K, Sotta B, Caboche M, Miginiac E. 1995. In vitro morphogenic characteristics of phytochrome mutants in *Nicotiana plumbaginifolia* are modified and correlated to high indole-3-acetic acid levels. *Planta*. 197:142–46

Kravtsov AK, Zubo YO, Yamburenko MV, Kulaeva ON, Kusnetsov VV. 2011. Cytokinin and abscisic acid control plastid gene transcription during barley seedling de-etiolation. *Plant Growth Regul*. 64:173–83

Kriedemann PE, Loveys BR, Fuller GL, Leopold AC. 1972. Abscisic acid and stomatal regulation. *Plant Physiol*. 49:842–47

Kushiro T, Okamoto M, Nakabayashi K, Yamagishi K, Kitamura S, et al. 2004. The Arabidopsis cytochrome P450 CYP707A encodes ABA 8'-hydroxylases: key enzymes in ABA catabolism. *EMBO J*. 23:1647–56

Kusnetsov VV, Oelmüller R, Sarwat MI, Porfirova SA, Cherepneva GN, et al. 1994. Cytokinins, abscisic acid and light affect accumulation of chloroplast proteins in *Lupinus luteus* cotyledons without notable effect on steady-state mRNA levels. *Planta*. 194:318–27

Kusnetsov V, Herrmann RG, Kulaeva ON, Oelmüller R. 1998. Cytokinin stimulates and abscisic acid inhibits greening of etiolated *Lupinus luteus* cotyledons by affecting the expression of the light-sensitive protochlorophyllide oxidoreductase. *Mol Gen Genet*. 259:21–28

Lazár D. 2015. Parameters of photosynthetic energy partitioning. *J Plant Physiol*. 175:131–47

Lee KH, Piao HL, Kim HY, Choi SM, Jiang F, Hartung W, Hwang I, Kwak JM, Lee IJ, Hwang I. 2006. Activation of glucosidase via stress-induced polymerization rapidly increases active pools of abscisic acid. *Cell.* 126:1109–20

Lee SJ, Park J, Lee M, Yu JH, Kim S. 2010. Isolation and functional characterization of CE1 binding proteins. *BMC Plant Biol*. 10:277

LeNoble ME, Spollen WG, Sharp RE. 2004. Maintenance of shoot growth by endogenous ABA: genetic assessment of the involvement of ethylene suppression. *J Exp Bot*. 55:237–45

Leung J, Bouvier-Durand M, Morris PC, Guerrier D, Chefdor F, Giraudat J. 1994. Arabidopsis ABA response gene ABI1: Features of a calcium-modulated protein phosphatase. *Science* 264:1448–52

Leung J, Merlot S, Giraudat J. 1997. The Arabidopsis ABSCISIC ACID-INSENSITIVE2 (ABI2) and ABI1 genes encode homologous protein phosphatases 2C involved in abscisic acid signal transduction. *Plant Cell.* 9:759–71

Leung J, Giraudat J. 1998. Abscisic acid signal transduction. *Annu Rev Plant Physiol Plant Mol Biol*. 49:199–222

Li J, Assmann SM. 1996. An abscisic acid-activated and calcium-independent protein kinase from guard cells of fava bean. *Plant Cell.* 8:2359–68

Li J, Nagpal P, Vitart V, McMorris TC, Chory J. 1996. A role for brassinosteroids in light-dependent development of Arabidopsis. *Science.* 272:398–401

Li Z, Zhang L, Yu Y, Quan R, Zhang Z, Zhang H, Huang R. 2011. The ethylene response factor AtERF11 that is transcriptionally modulated by the bZIP transcription factor HY5 is a crucial repressor for ethylene biosynthesis in Arabidopsis. *Plant J.* 68:88–99

Liang X, Wang H, Mao L, Hu Y, Dong T, Zhang Y, et al. 2012. Involvement of COP-1 in ethylene- and light-regulated hypocotyl elongation. *Planta.* 236:1791–1802

Lim CW, Kim JH, Baek W, Kim BS, Lee SC. 2012. Functional roles of the protein phosphatase 2C, AtAIP1, in abscisic acid signaling and sugar tolerance in Arabidopsis. *Plant Sci*. 187:83–88

Lim S, Park J, Lee N, Jeong J, Toh S, Watanabe A, Kim J, Kang H, Kim DH, Kawakami N, Choi G. 2013. ABA-INSENSITIVE3, ABA-INSENSITIVE5, and DELLAs interact to activate the expression of SOMNUS and other high-temperature-inducible genes in imbibed seeds in Arabidopsis. *Plant Cell.* 25:4863–78

Lin C. 2000. Plant blue-light receptors. *Trends Plant Sci.* 5:337–342

Lin BL, Wang HJ, Wang JS, Zaharia LI, Abrams SR. 2005. Abscisic acid regulation of heterophylly in *Marsilea quadrifolia* L.: effects of R-(−) and S-(+) isomers. *Plant Physiol*. 106:135–42

Lin R, Tang W. 2014. Cross talk between light and ABA signaling. In: Zhang DP, editor. Abscisic Acid: Metabolism, Transport and Signaling. Dodrecht: Springer. pp 255–269

Liu X, Zhang H, Zhao Y, Feng Z, Li Q, Yang HQ, Luan S, Li J, He ZH. 2013. Auxin controls seed dormancy through stimulation of abscisic acid signaling by inducing ARF-mediated ABI3 activation in Arabidopsis. *Proc Natl Acad Sci USA*. 110:15485–90

Lockhart JA. 1965. An analysis of irreversible plant cell elongation. *J Theor Biol.* 8:264–75

Luerssen H, Kirik V, Herrmann P, Misera S. 1998. FUSCA3 encodes a protein with a conserved VP1/ABI3-like B3 domain which is of func- tional importance for the regulation of seed maturation in *Arabidopsis thaliana*. *Plant J*. 15:755-64

Ma Y, Szostkiewicz I, Korte A, Moes Dl, Yang Y, Christmann A, Grill E. 2009. Regulators of PP2C phosphatase activity function as abscisic acid sensors. *Science.* 324:1064–68

Mäkelä P, Munns R, Colmer TD, Peltonen-Sainio P. 2003. Growth of tomato and an ABA-deficient mutant (*sitiens*) under saline conditions. *Physiol Plant.* 117:58–63

Maluszynska J, Kolano B, Sas-Nowosielska H. 2013. Endopolyploidy in plants. In: Leitch IJ, Greilhuber J, Dolezel J, Wendel J. editors. Plant Genome Diversity Volume 2, Physical Structure, Behaviour and Evolution of Plant Genomes. Dodrecht: Springer. pp. 99–119

Mazzella MA, Arana MV, Staneloni RJ, Perelman S, Rodriguez Batiller MJ, et al. 2005. Phytochrome control of the Arabidopsis transcriptome anticipates seedling exposure to light. *Plant Cell*. 17:2507–16

McCourt P, Creelman R. 2008. The ABA receptors—we report you decide. *Curr Opin Plant Biol*. 11:474–78

McWha JA, Jackson DL. 1976. Some growth promotive effects of abscisic acid. *J Exp Bot* 27:1004–08

Merlot S, Mustilli AC, Genty B, North H, Lefebvre V, Sotta B, Vavasseur A, Giraudat J. 2002. Use of infrared thermal imaging to isolate Arabidopsis mutants defective in stomatal regulation. *Plant J*. 30:601–09

Meyer K, Leube M, Grill E. 1994. A protein phosphatase 2C involved in ABA signal transduction in *Arabidopsis thaliana*. *Science.* 264:1452–55

Michelena VA, Boyer JS. 1982. Complete turgor maintenance at low water potentials in the elongating region of maize leaves. *Plant Physiol.* 69: 1145–49

Milborrow BV. 1966. The effects of synthetic *dl*-dormin (abscisin ii) on the growth of the oat mesocotyl. *Planta*. 70:155–71

Monke G, Seifert M, Keilwagen J, Mohr M, Grosse I, Hahnel U, Junker A, Weisshaar B, Conrad U, Baumlein H, Altschmied L. 2012. Toward the identification and regulation of the *Arabidopsis thaliana* ABI3 regulon. *Nuc. Acids Res.* 40:8240–54

Moss GI, Hall KC, Jackson MB. 1988. Ethylene and the responses of roots of maize (*Zea mays* L.) to physical impedance. *New Phytol.* 109:303–11

Mulholland BJ, Black CR, Taylor IB, Roberts J a, Lenton JR. 1996. Effect of soil compaction on barley (*Hordeum vulgare* L.) growth .1. possible role for ABA as a root-sourced chemical signal. *J Exp Bot*. 47:539–49

Murashige T, Skoog A. 1962. A revised medium for rapid growth and bio assays with tobacco tissue cultures. *Physiol Plant.* 15:473–97

Nafati M, Frangne N, Hernould M, Chevalier C, Gévaudant F. 2010. Functional characterization of the tomato cyclin-dependent kinase inhibitor SLKRP1 domains involved in protein-protein interactions. *New Phytol*. 188:136–49

Nakabayashi K, Okamoto M, Koshiba T, Kamiya Y, Nambara E. 2005. Genome-wide profiling of stored mRNA in Arabidopsis thaliana seed germination: epigenetic and genetic regulation of transcription in seed. *Plant J*. 41:697–709

Nakashima K, Ito Y, Yamaguchi-Shinozaki K. 2009. Transcriptional regulatory metworks in response to abiotic stresses in Arabidopsis and grasses. *Plant Physiol.* 149:88–95

Nambara E, Marion-Poll A. 2005. Abscisic acid biosynthesis and catabolism. *Annu Rev Plant Biol*. 56:165–85

Neill SJ, Horgan R. 1985. Abscisic acid production and water relations in wilty tomato mutants subjected to water deficiency. *J Exp Bot*. 36:1222–31

Nemhauser JL. 2008. Dawning of a new era: photomorphogenesis as an integrated molecular network. *Curr Opin Plant Biol*. 11:4–8

Nešković M, Petrović J, Radojević LJ, Vujičić R. 1977. Stimulation of growth and nucleic acid biosynthesis at low concentration of abscisic acid in tissue culture of *Spinacia oleracea*. *Physiol Plant.* 39:148–54

Nishimura N, Sarkeshik A, Nito K, Park SY, Wang A, Carvalho PC, Lee S, Caddell DF, Cutler SR, Chory J, Yates JR, Schroeder JI. 2010. PYR/PYL/RCAR family members are major in-vivo ABI1 protein phosphatase 2C-interacting proteins in Arabidopsis. *Plant J*. 61:290–99

Oh E, Kim J, Park E, Kim JI, Kang C, Choi G. 2004. PIL5, a phytochrome-interacting basic helix-loop- helix protein, is a key negative regulator of seed germination in Arabidopsis thaliana. *Plant Cell.* 16:3045–58

Ohkuma K, Lyon JL, Addicott FT, Smith OE. 1963. Abscisin II, an Abscission-Accelerating Substance from Young Cotton Fruit. *Science* 142:1592–93

Osterlund MT, Hardtke CS, Wei N, Deng XW. 2000. Targeted destabilization of HY5 during light-regulated development of Arabidopsis. *Nature.* 405:462–66

Pandey S, Chen JG, Jones AM, Assmann SM. 2006. G-protein complex mutants are hypersensitive to abscisic acid regulation of germination and postgermination development. *Plant Physiol*. 141:243–56

Park SY, Fung P, Nishimura N, Jensen DR, Fujii H, Zhao Y, et al. 2009. Abscisic acid inhibits type 2C protein phosphatases via the PYR/PYL family of START proteins. *Science*. 324:1068–71

Parks BM, Cho MH, Spalding EP. 1998. Two genetically separable phases of growth inhibition induced by blue light in Arabidopsis seedlings. *Plant Physiol.* 118: 609–15

Parks BM, Spalding EP. 1999. Sequential and coordinated action of phytochromes A and B during Arabidopsis stem growth revealed by kinetic analysis. *Proc Natl Acad Sci USA*. 96:14142–46

Pilet PE. 1970. The effect of auxin and abscisic acid on the catabolism of RNA. *J Exp Bot.* 21:446–51

Pilet PE. 1975. Abscisic acid as a root growth inhibitor: physiological analyses. *Planta.* 122:299–302

Pilet PE, Saugy M. 1987. Effect on root growth of endogenous and applied IAA and ABA: a critical reexamination. *Plant Physiol*. 83:33–38

Puli MR, Raghavendra AS. 2012. Pyrabactin, an ABA agonist, induced stomatal closure and changes in signalling components of guard cells in abaxial epidermis of *Pisum sativum*. *J Exp Bot*. 63:1349–56

Quail PH. 2002a. Phytochrome photosensory signalling networks. *Nat Rev Mol Cell Biol*. 3:85–93

Quail PH. 2002b. Photosensory perception and signalling in plant cells: new paradigms? *Curr Opin Cell Biol*. 14: 180–188

Quarrie SA. 1987. Use of genotypes differing in endogenous abscisic acid levels in studies of physiology and development. In: Hoad GV, Lenton JR, Jackson MB, Atkin RK, editors. Hormone Action in Plant Development – a Critical Appraisal. London: Butterworths. pp. 89–105

Raz V, Bergervoet JHW, Koornneef M. 2001. Sequential steps for developmental arrest in Arabidopsis seeds. *Development.* 128:243–52

Reyes JL, Chua NH. 2007. ABA induction of miR159 controls transcript levels of two MYB factors during Arabidopsis seed germination. *Plant J.* 49:592–606

Riboni M, Galbiati M, Tonelli C, Conti L. 2013. *GIGANTEA* enables drought escape response via abscisic acid-dependent activation of the florigens and *SUPPRESSOR OF OVEREXPRESSION OF CONSTANS1*. *Plant Physiol*. 162:1706–19

Riou-Khamlichi C, Huntley R, Jacqmard A, Murray JAH. 1999. Cytokinin activation of Arabidopsis cell division through a D-type cyclin. *Science.* 283:1541–44

Ritchie S, Gilroy S. 2000. Abscisic acid stimulation of phospholipase D in the barley aleurone is G-protein-mediated and localized to the plasma membrane. *Plant Physiol.* 124:693–702

Rodriguez P, Benning G, Grill E. 1998. ABI2, a second protein phos- phatase 2C involved in abscisic acid signal transduction in Arabidopsis. *FEBS Lett.* 421:185–90

Rohde A, Van Montagu M, Boerjan W. 1999. The ABSCISIC ACID-INSENSITIVE 3 (*ABI3*) gene is expressed during vegetative quiescence processes in Arabidopsis. *Plant Cell Environ*. 22:261–70

Rohde A, De Rycke R, Beeckman T, Engler G, Van Montagu M, Boerjan W. 2000. ABI3 affects plastid differentiation in dark-grown Arabidopsis seedlings. *Plant Cell*. 12:35–52

Rubio S, Rodrigues A, Saez A, Dizon MB, Galle A, Kim TH, Santiago J, Flexas J, Schroeder JI, Rodriguez PL. 2009. Triple loss of function of protein phosphatases type 2C leads to partial constitutive response to endogenous abscisic acid. *Plant Physiol*. 150:1345–55

Rushton DL, Tripathi P, Rabara RC, Lin J, Ringler P, Boken AK, Langum TJ, Smidt L, Boomsma DD, Emme NJ, Chen X, Finer JJ, Shen QJ, Rushton PJ. 2011. WRKY transcription factors: key components in abscisic acid signalling. *Plant Biotech. J.* 10:2-11

Saab IN, Sharp RE, Pritchard J, Voetberg GS. 1990. Increased endogenous abscisic acid maintains primary root growth and inhibits shoot growth of maize seedlings at low water potentials*. Plant Physiol.* 93:1329–36

Sagi M, Scazzocchio C, Fluhr R. 2002. The absence of molybdenum cofactor sulfuration is the primary cause of the *flacca* phenotype in tomato plants. *Plant J*. 31:305–17

Sakakibara H. 2006. Cytokinins: activity, biosynthesis, and translocation. *Annu Rev Plant Biol*. 57:431–49

Sansberro PA, Mroginski LA, Bottini R. 2004. Foliar sprays with ABA promote growth of *Ilex paraguariensis* by alleviating diurnal water stress. *Plant Growth Regul.* 42: 105–11

Sawada Y, Aoki M, Nakaminami K, Mitsuhashi W, Tatematsu K, et al. 2008. Phytochrome- and gibberellin-mediated regulation of abscisic acid metabolism during germination of photoblastic lettuce seeds. *Plant Physiol*. 146:1386–96

Seo M, Hanada A, Kuwahara A, Endo A, Okamoto M, et al. 2006. Regulation of hormone metabolism in Arabidopsis seeds: phytochrome regulation of abscisic acid metabolism and abscisic acid regulation of gibberellin metabolism. *Plant J*. 48:354–66

Shackel KA, Matthews MA, Morrison JC. 1987. Dynamic relation between expansion and cellular turgor in growing grape (*Vitis vinifera* L.) leaves. *Plant Physiol.* 84:1166–71

Sharp RE, Wu Y, Voetberg GS, Saab IN, LeNoble ME. 1994. Confirmation that abscisic acid accumulation is required for maize primary root elongation at low water potentials. *J Exp Bot*. 45: 1743–51

Sharp RE, LeNoble ME, Else M a, Thorne ET, Gherardi F. 2000. Endogenous ABA maintains shoot growth in tomato independently of effects on plant water balance: evidence for an interaction with ethylene. *J Exp Bot*. 51:1575–84

Sharp RE. 2002. Interaction with ethylene: changing views on the role of abscisic acid in root and shoot growth responses to water stress. *Plant Cell Environ*. 25:211–22

Sheen J. 1998. Mutational analysis of protein phosphatase 2C involved in abscisic acid signal transduction in higher plants. *Proc. Natl. Acad. Sci. USA.* 95:975–80

Shen YY, Rose JKC. 2014. ABA metabolism and signaling in fleshy fruits. In: Zhang DP, editor. Abscisic Acid: Metabolism, Transport and Signaling. Dodrecht: Springer. pp.271–86

Shinomura T. 1997. Phytochrome regulation of seed germination. *J Plant Res*. 110:151–61

Shinozaki K, Yamaguchi-Shinozaki K, Mizoguchi T, Urao T, Katagiri T, et al. 1998. Molecular responses to water stress in *Arabidopsis thaliana*. *J Plant Res*. 111:345–51

Shkolnik-Inbar D, Bar-Zvi D. 2010. ABI4 Mediates abscisic acid and cytokinin inhibition of lateral root formation by reducing polar auxin transport in Arabidopsis. *Plant Cell.* 125:3560-73

Schneider CA, Rasband WS, Eliceiri KW. 2012. NIH Image to ImageJ: 25 years of image analysis. *Nat Methods.* 9:671–75

Schwartz SH, Zeevaart JAD. 2010. Abscisic Acid Biosynthesis And Metabolism. In: Davies PJ, editor. Plant Hormones: Biosynthesis, Signal Transduction, Action!. Dodrecht: Springer. pp. 137–155

Smalle J, Haegman M, Kurepa J, Van Montagu M, Van den Straeten D. 1997. Ethylene can stimulate *Arabidopsis* hypocotyl elongation in the light. *P Natl Acad Sci USA.* 94:2756-61

Smalle J, Kurepa J, Yang P, Emborg TJ, Babiychuk E, et al. 2003. The pleiotropic role of the 26S proteasome subunit RPN10 in Arabidopsis growth and development supports a substrate-specific function in abscisic acid signaling. *Plant Cell*. 15:965–80

Spollen WG, LeNoble ME, Samuels TD, Bernstein N, Sharp RE. 2000. Abscisic acid accumulation maintains maize primary root elongation at low water potentials by restricting ethylene production. *Plant Physiol*. 122:967–76

Stone SL, Kwong LW, Yee KM, Pelletier J, Lepiniec L, Fischer RL, Goldberg RB, Harada JJ. 2001. *LEAFY COTYLEDON2* encodes a B3 domain transcription factor that induces embryo development. *Proc. Natl. Acad. Sci. USA.* 98:11806-11

Stone SL, Williams LA, Farmer LM, Vierstra RD, Callis J. 2006. KEEP ON GOING, a RING E3 ligase essential for Arabidopsis growth and development, is involved in abscisic acid signaling. *Plant Cell*. 18:3415–28

Sun J, Li C. 2014. Cross Talk of Signaling Pathways Between ABA and Other Phytohormones. In: Zhang DP, editor. Abscisic Acid: Metabolism, Transport and Signaling. Dodrecht: Springer. pp.243–253

Suzuki M, Kao CY, Cocciolone S, McCarty DR. 2001. Maize *VP1* complements Arabidopsis *abi3* and confers a novel ABA/auxin interaction in roots. *Plant J.* 28:409–18

Suzuki M, Ketterling MG, Li QB, McCarty D. 2003. Viviparous1 alters global gene expression patterns through regulation of abscisic acid signaling. *Plant Physiol*. 132:1664–77

Suzuki M, Wang HHY, McCarty DR. 2007. Repression of the LEAFY COTYLEDON 1/B3 regulatory network in plant embryo development by VP1/ABSCISIC ACID INSENSITIVE 3-LIKE B3 Genes. *Plant Physiol.* 143: 902-911

Symons GM, Reid JB. 2003a. Hormone levels and response during de-etiolation in pea. *Planta*. 216:422–31

Symons GM, Reid JB. 2003b. Interactions between light and plant hormones during de-etiolation. *J Plant Growth Regul*. 22:3–14

Szostkiewicz I, Richter K, Kepka M, Demmel S, Ma Y, Korte A, Assaad FF, Christmann A, Grill E. 2010. Closely related receptor complexes differ in their ABA selectivity and sensitivity. *Plant J*. 61:25–35

Taiz L, Zeiger E. 2010. Plant Physiology, 5th International Edition. Sunderland: Sinauer Associates. pp. 494–520

Takahashi K. 1972. Abscisic acid as a stimulator of rice mesocotyl growth. *Nature New Biol.* 238:92–93

Tal M. 1966. Abnormal stomatal behavior in wilty mutants of tomato. *Plant Physiol*. 41:1387–91

Tan BC, Schwartz SH, Zeevaart JA, McCarty DR. 1997. Genetic control of abscisic acid biosynthesis in maize. *Proc Natl Acad Sci USA*. 94:12235–40

Tanaka Y, Sano T, Tamaoki M, Nakajima N, Kondo N, Hasezawa S. 2005. Ethylene inhibits abscisic acid-induced stomatal closure in Arabidopsis. *Plant Physiol*. 138:2337–43

Tanaka Y, Sano T, Tamaoki M, Nakajima N, Kondo N, Hasezawa S. 2006. Cytokinin and auxin inhibit abscisic acid-induced stomatal closure by enhancing ethylene production in Arabidopsis. *J Exp Bot*. 57:2259–66

Tanaka Y, Nose T, Jikumaru Y, Kamiya Y. 2013. ABA inhibits entry into stomatal-lineage development in Arabidopsis leaves. *Plant J*. 74:448–57

Tang AC, Boyer JS. 2002. Growth-induced water potentials and the growth of maize leaves. *J Exp Bot.* 53: 489–503

Tardieu F, Parent B, Simonneau T. 2010. Control of leaf growth by abscisic acid: hydraulic or non-hydraulic processes? *Plant, Cell Environ*. 33:636–47

Taylor HF, Burden RS. Xanthoxin, a new naturally occurring plant growth inhibitor. 1970. *Nature*. 227:302–04

Taylor IB, Tarr AR. 1984. Phenotypic interactions between abscisic acid deficient tomato mutants. *Theor Appl Genet*. 68:115–19

Taylor IB, Linforth RST, Al-Naieb RJ, Bowman WR, Marples BA. 1988. The wilty tomato mutants *flacca* and *sitiens* are impaired in the oxidation of ABA-aldehyde to ABA. *Plant Cell Environ.* 11:739–45

Teltscherová L, Seidlová F. 1977. The differential effect of abscisic acid on *Chenopodium rubrum* L. in dependence on growth and developmental state. *Biol Plant*. 19:377–80

Termaat A, Passioura JB, Munns R. 1985. Shoot turgor does not limit shoot growth of NaCl-affected wheat and barley. *Plant Physiol.* 77: 869–72

Thomas TH, Wareing PF, Robinson PM. 1965. Chemistry And Physiology of 'Dormins' In Sycamore: Action of the Sycamore 'Dormin' as a Gibberellin Antagonist. *Natur*e 205:1270–72

Thompson AJ, Thorne ET, Burbidge A, Jackson AC, Sharp RE, Taylor IB. 2004. Complementation of *notabilis*, an abscisic acid-deficient mutant of tomato: importance of sequence context and utility of partial complementation. *Plant Cell Environ*. 27:459–71

Todoroki Y. 2014. ABA and Its Derivatives: Chemistry and Physiological Functions. In: Zhang DP, editor. Abscisic Acid: Metabolism, Transport and Signaling. Dodrecht: Springer. pp. 1–20

Toyomasu T, Kawaide H, Mitsuhashi W, Inoue Y, Kamiya Y. 1998. Phytochrome regulates gibberellin biosynthesis during germination of photoblastic lettuce seeds. *Plant Physiol*. 118:1517–23

Trewavas AJ. 1982. Growth substance sensitivity: the limiting factor in plant development. *Physiol Plant*. 55:60–72

Uno Y, Furihata T, Abe H, Yoshida R, Shinozaki K, Yamaguchi-Shinozaki K. 2000. Arabidopsis basic leucine zipper transcription factors involved in an abscisic acid-dependent signal transduction pathway under drought and high-salinity conditions. *Proc. Natl. Acad. Sci. USA.* 97:11632-37

Urao T, Yamaguchi-Shinozaki K, Urao S, Shinozaki K. 1993. An Arabidopsis myb homolog is induced by dehydration stress and its gene product binds to the conserved MYB recognition sequence. *Plant Cell*. 5:1529-39

Van Staden J, Bornman CH. 1969. Inhibition and promotion by abscisic acid of growth in spirodela. *Planta*. 85:157–59

Van Volkenburgh E, Davies WJ. 1983. Inhibition of light stimulated leaf expansion by abscisic acid. *J Exp Bot*. 34:835–45

Vandenbussche F, Habricot Y, Condiff AS, Maldiney R, Van Der Straeten D, Ahmad M. 2007. HY5 is a point of convergence between cryptochrome and cytokinins sigalling pathways in *Arabidopsis thaliana*. *Plant J*. 49:428–41

Venis M. 1985. Methods in receptor research. In: Venis M, editor. Hormone binding sites in plants. New York: Longman. pp. 24–40

Vylíčilová H, Husičková A, Spíchal L, Srovnal J, Doležal K, Plíhal O, Plíhalová L. 2015. C2-substituted aromatic cytokinin sugar conjugates delay the onset of senescence via maintaining correct function of the photosynthetic apparatus. *in preparation*

Wang XQ, Ullah H, Jones A, Assmann S. 2001. G protein regulation of ion channels and abscisic acid signaling in Arabidopsis guard cells. *Science.* 292:2070–72

Wang L, Hua D, He J, Duan Y, Chen Z, Hong X, Gong Z. 2011a. Auxin response factor2 (ARF2) and its regulated homeodomain gene HB33 mediate abscisic acid response in Arabidopsis. *PLoS Genet*. 7:e1002172

Wang Y, Li L, Ye T, Zhao S, Liu Z, Feng YQ, Wu Y. 2011b. Cytokinin antagonizes ABA suppression to seed germination of Arabidopsis by downregulating ABI5 expression. *Plant J.* 68:249–61

Wang XF, Zhang DP. 2014. ABA Signal Perception and ABA Receptors. In: Zhang DP, editor. Abscisic Acid: Metabolism, Transport and Signaling. Dodrecht: Springer. pp. 89–116

Watanabe H, Takahashi K. 1997. Effects of abscisic acid, fusicoccin, and potassium on growth and morphogenesis of leaves and internodes in dark-grown rice seedlings. *Plant Growth Regul*. 21:109–14

Watanabe H, Takahashi K. 1999. Effects of abscisic acid and its related compounds on rice seedling growth. *Plant Growth Regul.* 28:5–8

Watanabe H, Takahashi K, Saigusa M. 2001. Morphological and anatomical effects of abscisic acid (ABA) and fluridone (FLU) on the growth of rice mesocotyls. *Plant Growth Regul*. 34:273–75

Weatherwax SC, Ong MS, Degenhardt J, Bray EA, Tobin EM. 1996. The interaction of light and abscisic acid in the regulation of plant gene expression. *Plant Physiol.* 111:363–70

Wen B, Nieuwland J, Murray J a H. 2013. The Arabidopsis CDK inhibitor ICK3/KRP5 is rate limiting for primary root growth and promotes growth through cell elongation and endoreduplication. *J Exp Bot*. 64:1135–44

White CN, Proebsting WM, Hedden P, Rivin CJ. 2000. Gibberellins and seed development in maize. I. evidence that gibberellin/abscisic acid balance governs germination versus maturation pathways. *Plant Physiol*. 122:1081–88

Wilkinson S, Davies WJ. 2008. Manipulation of the apoplastic pH of intact plants mimics stomatal and growth responses to water availability and microclimatic variation. *J Exp Bot.* 59:619–31

Wilmowicz E, Frankowski K, Glazinska P, Kesy J, Kopcewicz J. 2011. Involvement of ABA in flower induction of *Pharbitis nil*. *Acta Soc Bot Pol*. 80:21–26

Wong CE, Singh MB, Bhalla PL. 2009. Molecular processes underlying the floral transition in the soybean shoot apical meristem. *Plant J.* 57:832-45

Woodward AW, Bartel B. 2005. Auxin: regulation, action, and interaction. *Ann Bot*. 95:707–35

Xu ZY, Yoo YJ, Hwang I. 2014. ABA Conjugates and Their Physiological Roles in Plant Cells. In: Zhang DP, editor. Abscisic Acid: Metabolism, Transport and Signaling. Dodrecht: Springer. pp. 77–87

Yamburenko MV, Zubo YO, Vanková R, Kusnetsov VV, Kulaeva ON, Börner T. 2013. Abscisic acid represses the transcription of chloroplast genes. *J Exp Bot*. 64:4491–502

Yoshida T, Fujita Y, Sayama H, Kidokoro S, Maruyama K, Mizoi J, Shinozaki K, Yamaguchi-Shinozaki K. 2010. AREB1, AREB2, and ABF3 are master transcription factors that cooperatively regulate ABRE-dependent ABA signaling involved in drought stress tolerance and require ABA for full activation. *Plant J.* 61:672-85

Zalabák D, Pospíšilová H, Šmehilová M, Mrízová K, Frébort I, Galuszka P. 2013. Genetic engineering of cytokinin metabolism: prospective way to improve agricultural traits of crop plants. *Biotechnol Adv*. 31:97–117

Zdarska M, Dobisová T, Gelová Z, Pernisová M, Dabravolski S, Hejátko J. 2015. Illuminating light, cytokinin, and ethylene signalling crosstalk in plant development. *J Exp Bot*. 66:4913–31

Zhang J, Davies WJ. 1990. Does ABA in the xylem control the rate of leaf growth in soil-dried maize and sunflower plants? *J Exp Bot.* 41:1125–32

Zhang JH, Davies WJ. 1991. Antitranspirant activity in xylem sap of maize plants. *J Exp Bot.* 42:317–21

Zhang X, Zhang Q, Xin Q, Yu L, Wang Z, Wu W, Jiang L, Wang G, Tian W, Deng Z, Wang Y, Liu Z, Long J, Gong Z, Chen Z. 2012. Complex structures of the abscisic acid receptor PYL3/RCAR13 reveal a unique regulatory mechanism. *Structure.* 20:780–90

Zhang X, Jiang L, Wang G, Yu L, Zhang Q, Xin Q, Wu W, Gong Z, Chen Z. 2013. Structural insights into the abscisic acid stereospecificity by the ABA receptors PYR/PYL/RCAR. *PLoS ONE.* 8: e67477

Zheng Z, Xu X, Crosley RA, Greenwalt SA, Sun Y, et al. 2010. The protein kinase SnRK2.6 mediates the regulation of sucrose metabolism and plant growth in Arabidopsis. *Plant Physiol*. 153:99–113

Zubo YO, Yamburenko M V, Selivankina SY, Shakirova FM, Avalbaev AM, et al. 2008. Cytokinin stimulates chloroplast transcription in detached barley leaves. *Plant Physiol*. 148:1082–93

APPENDIX I.

DEVELOPMENT AND TESTING OF NEW HIGH-THROUGHPUT METHODS FOR EVALUATION OF PLANT GROWTH AND PHYSIOLOGY

This appendix describes other scientific outputs that were performed by the author of the thesis. Although this part is not directly connected to the main topic of the thesis, we believe that it should be noted since it represents piece of work that was done in parallel to the main research topic. Moreover, the main topic of the thesis is focused on the role of particular hormone in selected developmental window of a single species, but this part of work was intended to provide novel methodological tools for studying plant growth and physiology in more general frame. Aim of this work was to develop and optimize growing and measuring protocols for high-throughput plant phenotyping with respect to abiotic-stress studies. This could be seen as another linking point between ABA and this appendix, since the ABA is the most important plant hormone in plant stress research. The automated plant phenotyping is a new branch of approaches that allows the analysis of the plants on the large scale. In our university the prototype system for high-throughput plant analysis was set-up since 2013. However there were no optimized protocols for growing and measuring plants in this system. Moreover, the system was built as a hardware solution, but important part of software for plant image analysis has to be developed *de novo*. As a main operator, the author of the thesis was responsible for design and validation of measuring protocols, conducting the experiments, outputs analysis, testing of new software and design of problem solutions. The introduction to the issue is provided in the chapter 11.1 that was recently published as a short review in the Plant Methods journal (Humplík et al. 2015c). The second chapter 11.2 describes a pilot study performed in the cold acclimation of pea cultivars that was published in the same journal (Humplík et al. 2015d). In this study the cold-acclimation of two morphologically similar, but differently cold-sensitive cultivars of field pea (*Pisum sativum* L.) was performed. During the cold acclimation the non-invasive screening of plant growth and efficiency of photosynthesis was analyzed. The growth was measured by RGB cameras with newly developed software, whereas the photosynthetic parameters were measured by fluorescent camera with software provided by manufacturer. Integration of descriptive morphological trait (shoot growth) and physiological trait of photosystem II efficiency provided not only selection of differently sensitive variants, but also allowed insight into the differing strategies of cold acclimation.

APPENDIX I.A

Automated phenotyping of plant shoots using imaging methods for analysis of plant stress responses – a review.

Published as:

Humplík JF, Lazár D, Husičková A, Spíchal L. 2015c. Automated phenotyping of plant shoots using imaging methods for analysis of plant stress responses – a review. *Plant Methods*. 11:29. doi:10.1186/s13007-015-0072-8.

Humplík et al. Plant Methods (2015) 11:29
DOI 10.1186/s13007-015-0072-8

PLANT METHODS

REVIEW Open Access

Automated phenotyping of plant shoots using imaging methods for analysis of plant stress responses – a review

Jan F Humplík[1†], Dušan Lazár[2†], Alexandra Husičková[2] and Lukáš Spíchal[1*]

Abstract

Current methods of in-house plant phenotyping are providing a powerful new tool for plant biology studies. The self-constructed and commercial platforms established in the last few years, employ non-destructive methods and measurements on a large and high-throughput scale. The platforms offer to certain extent, automated measurements, using either simple single sensor analysis, or advanced integrative simultaneous analysis by multiple sensors. However, due to the complexity of the approaches used, it is not always clear what such forms of plant phenotyping can offer the potential end-user, i.e. plant biologist. This review focuses on imaging methods used in the phenotyping of plant shoots including a brief survey of the sensors used. To open up this topic to a broader audience, we provide here a simple introduction to the principles of automated non-destructive analysis, namely RGB, chlorophyll fluorescence, thermal and hyperspectral imaging. We further on present an overview on how and to which extent, the automated integrative in-house phenotyping platforms have been used recently to study the responses of plants to various changing environments.

Keywords: Plant phenotyping, RGB digital imaging, Chlorophyll fluorescence imaging, Thermal imaging, Hyperspectral imaging, Shoot growth, Biomass production

Introduction

Recently, a large number of reviews have been published on the advantages and possibilities of high-throughput plant phenotyping approaches [1-5]. Most focus on the potential of these approaches which use precise and sophisticated tools and methodologies to study plant growth and development. To review the state-of-the-art of phenotyping platforms, we present a list of recent publications in Table 1. Interestingly, in about a half of these, only one measuring tool, mostly RGB imaging, for plant phenotyping was used. In the other papers, integrative phenotyping, signifying two or more measuring tools but which are rarely automated, was used (Table 1). This illustrates that the integrative automated high-throughput phenotyping measurements/platforms are still rather rare. Greenhouse- and grow chamber-based plant phenotyping platforms are publically available and these offer their services and collaborative projects. Descriptions, methodological background and focus can be found at http://www.plant-phenotyping-network.eu/eppn/select_installation. As an example of the integrative automated high-throughput phenotyping platform, a grow chamber-based phenotyping facility installed at Palacký University in Olomouc, Czech Republic is presented in Figure 1.

High-throughput integrative phenotyping facilities provide an opportunity to combine various methods of automated, simultaneous, non-destructive analyses of plant growth, morphology and physiology, providing a complex picture of the plant growth and vigour in one run, and repeatedly during the plant's life-span. Particular methods used in integrative plant phenotyping are often not new and usually represent those which have already been used for a number of years in basic research, e.g. non-invasive methods that employ visible or fluorescence imaging (described in more detail further in the text). High-throughput then allows analysis of the plants on a

* Correspondence: lukas.spichal@upol.cz
†Equal contributors
[1]Department of Chemical Biology and Genetics, Centre of the Region Haná for Biotechnological and Agricultural Research, Faculty of Science, Palacký University, Šlechtitelů 11, Olomouc CZ-78371, Czech Republic
Full list of author information is available at the end of the article

Table 1 List of selected works describing automated high-throughput analysis to study plant stress responses

Study	Plant species	Type of stress	Type of the study	Type of automated analysis	Platform name/origin
Granier et al. 2006; [58]	*Arabidopsis*	drought-stress	methodology	RGB (top view)	PHENOPSIS
Skirycz et al. 2011; [59]	*Arabidopsis*	drought-stress	applied	RGB (top view)	WIWAM
Clauw et al. 2015; [60]	*Arabidopsis*	drought-stress	applied	RGB (top view)	WIWAM
Tisné et al. 2013; [61]	*Arabidopsis*	drought-stress	applied	RGB (top view)	PHENOSCOPE
Neumann et al. 2015; [26]	barley	drought-stress	methodology	RGB (multiple views)	LemnaTec
Pereyra-Irujo et al. 2012; [62]	soybean	drought-stress	methodology	RGB (two-views)	GlyPh (self-construction)
Honsdorf et al. 2014; [16]	barley, (wild species)	drought-stress	applied	RGB (multiple views)	LemnaTec
Coupel-Ledru et al. 2014; [63]	grapevine	drought-stress	applied	RGB (multiple views)	LemnaTec
Petrozza et al. 2014; [66]	tomato	drought-stress	applied	RGB (multiple views), hyperspectral NIR, SLCFIM	LemnaTec
Harshavardhan et al. 2014; [67]	*Arabidopsis*	drought-stress	applied	RGB (top view), hyperspectral NIR	LemnaTec
Bresson et al. 2013; [68]	*Arabidopsis*	drought-stress	applied	RGB (top view)	PHENOPSIS
Bresson et al. 2014; [69]	*Arabidopsis*	drought-stress	applied	RGB (top view), TLCFIM	PHENOPSIS
Chen et al. 2014; [64]	barley	drought-stress	methodology	RGB (multiple-views), hyperspectral NIR, SLCFIM	LemnaTec
Fehér-Juhász et al. 2014; [19]	wheat	drought-stress	applied	RGB (multiple views), thermoimaging	self-construction, semi-automated
Cseri et al. 2013; [65]	barley	drought-stress	methodology	RGB (multiple views), thermoimaging	self-construction, semi-automated
Vasseur et al. 2014 [71]	*Arabidopsis*	heat-stress, drought-stress	applied	RGB (top view)	PHENOPSIS
Rajendran et al. 2009; [73]	wheat	salt-stress	applied	RGB (multiple views)	LemnaTec
Harris et al. 2010; [74]	wheat, barley	salt-stress	applied	RGB (multiple views)	LemnaTec
Golzarian et al. 2011; [18]	barley	salt-stress	methodology	RGB (multiple views)	LemnaTec
Schilling et al. 2014; [75]	barley	salt-stress	applied	RGB (multiple views)	LemnaTec
Hairmansis et al. 2014; [76]	rice	salt-stress	applied	RGB (multiple views) SLCFIM	LemnaTec
Chaerle et al. 2006; [77]	tobacco	biotic-stress	methodology	thermoimaging, TLCFIM	self-construction
Poiré et al. 2014; [79]	*Brachypodium*	nutrient-deficiency	methodology	RGB (multiple views)	LemnaTec
Neilson et al. 2015; [80]	*Sorghum*	nutrient-deficiency	methodology	RGB (multiple views), hyperspectral NIR	LemnaTec
Chaerle et al. 2007; [81]	bean	nutrient-deficiency, biotic-stress	methodology	RGB (top view), thermoimaging, TLCFIM	self-construction
Jansen et al. 2009; [37]	*Arabidopsis*, tobacco	drought-stress, chilling-stress	methodology	RGB (top view), KCFIM	GROWSCREEN (self-construction)
Humplík et al. 2015; [20]	pea, field cultivars	cold-stress	methodology	RGB (multiple views), KCFIM	PlantScreen

large scale. This enables users to apply statistics to discover subtle but significant differences between the studied genotypes and treatment variants.

The potential users of such facilities, mostly biologists, are often not very familiar with the applied physical methods used in integrative plant phenotyping. Thus, in this mini-review, we present a simple introduction to the basis of various non-invasive sensors used in high-throughput phenotyping platforms, namely visible red-green-blue (RGB) imaging, chlorophyll fluorescence imaging (CFIM), thermoimaging, and hyperspectral imaging. Further, we describe potential applications of some of the phenotyping methods that have been used to study the responses of different plant species to various stresses.

Non-destructive analysis of growth and physiology of plant shoots

The methods for automated phenotyping and their aims have been reviewed in a number of recent reports [3,6,7]. In the following text we give a description of the basis of the automated non-invasive analysis of plant

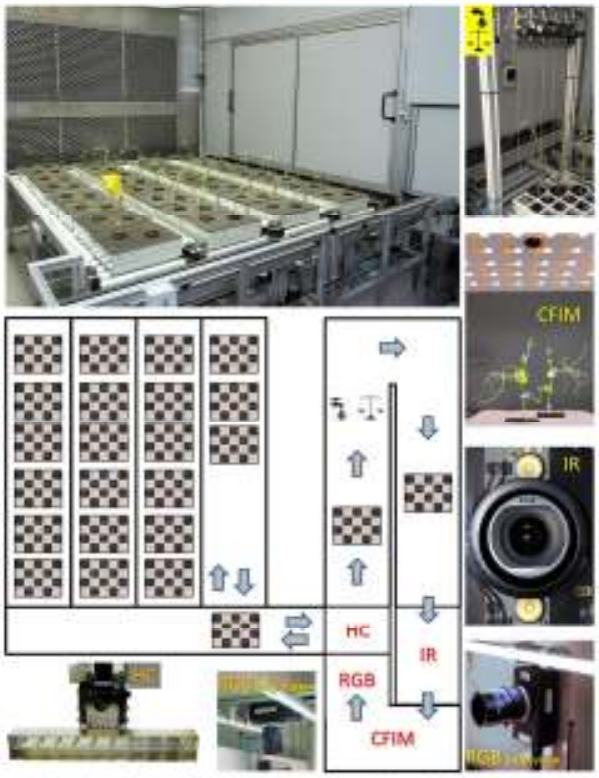

Figure 1 Scheme of the grow chamber-based automated high-throughput phenotyping platform PlantScreen™ (Photons Systems Instruments , Brno, Czech Republic), installed at Palacký University in Olomouc, Czech Republic [20]. The system is located in a growth chamber with white LED illumination (max. 1000 μmol photons m^{-2} s^{-1}) and controlled environment (10 – 40°C, 30 – 99% relative humidity). The growth area with roller conveyer has capacity of up to 640 *Arabidopsis*, cereals and other crops grown in standardized pots. The measuring cabinet contains acclimation chamber for dark adaptation of plants coupled with an automated weighting and watering area. The cabinet is equipped with KCFIM and RGB imaging (top and 2 side views), thermoimaging (IR) to measure stomata openness and SWIR hyperspectral imaging to determine water content. The platform can be controlled either from the place or via remote control software. The operating software enables automatic data evaluation.

shoots and appropriate sensors that have been used for studies of plant stress responses.

Visible RGB imaging of plant shoots

Apart from the importance of root-growth analysis, a key descriptive parameter in plant physiology is the growth of plant shoots. Although there are numerous secondary traits describing the morphology of shoots in particular species and their developmental stages, the primary and universal trait is biomass formation. Shoot biomass is defined as the total mass of all the above-ground plant parts at a given point in a plant's life [8]. This trait can be easily assessed by a simple weighing of the fresh (FW) and dry (DW) masses. However, this involves the destruction of the measured plant thus only allowing end-point analyses. Similarly, leaf area and consequently the plant growth rate are usually determined by manual measurements of the dimensions of plant leaves [9-11]. Such measurements are highly time consuming and thus cannot be used for large scale experiments. For this reason, plant phenotyping facilities prefer to evaluate the growth rate using imaging methods which employ digital cameras with subsequent software image analysis. This enables a faster and more precise determination of the leaf area [12-14] and other parameters called projected area (Figure 2), or hull area in the case of monocots [15,16]. In general, non-invasive techniques of shoot growth determination have proven very reliable, and high correlations between the digital area and the shoot fresh, or dry weights, respectively,

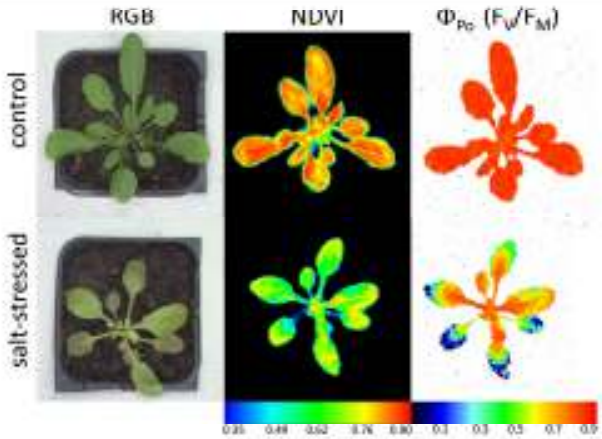

Figure 2 The illustrative figure presenting outcome of simultaneous analysis of control and salt-stressed *Arabidopsis* plants, using RGB, hyperspectral and Chl fluorescence imaging. The 18 DAS old soil-grown *Arabidopsis* plants were treated with 250 mM NaCl (salt-stressed) and water (control) and after 48 hours were analysed by different sensors for comparison. In morphology (top-view RGB imaging can be used for computation of rosette area or shape parameters), spatial distribution of vegetation index reflecting changes in the chlorophyll content (NDVI) provided by VIS/NIR hyperspectral camera, and the changes in maximal quantum yield of PSII photochemistry for a dark adapted state (Φ_{Po}, also referred as F_V/F_M) reflecting the photosynthetic activity of the plants obtained from KLFIM.

were reported in *Arabidopsis*, tobacco [17], cereals [18,19], and pea [20]. An example of a general shoot phenotyping protocol based on biomass estimation was reported by Berger et al. [21]. Similarly, other common morphometric parameters such as stem length, number of tillers and inflorescence architecture can be assessed non-destructively and manually, but again the time requirements, limit the number of plants analysed. High-throughput approaches for analyses of these rather species-specific traits would be very valuable [15], however, with the exception of *Arabidopsis* [22] the range of accessible solutions is still limited (for some emerging methods see [23-26]).

Correct determination of digital plant growth area can be distorted by overlapping leaves, leaf twisting and curling, and circadian movement, especially when the RGB image is taken only from one view (e.g. from top view). A new approach developed for *Arabidopsis* consisting of plant area estimation (which takes into account leaf overlapping), growth modelling and analysis, followed by application of a nonlinear growth model to generate growth curves, and subsequent functional data analysis, was shown to analyse the plant growth in high-throughput experiments more precisely [14]. However, due to the use of only a top-view RGB imaging, this approach cannot be applied for analyses of most of the agronomical important plants with vertical growth. A set-up that introduces more projections (e.g. side-views) into the phenotyping platforms thus can partially solve this problem. The three-views RGB imaging together with linear mathematical modelling was used for accurate estimation of plant shoot dry weight of wheat and barley from two dimensional images [18]. The accuracy of three-view approach has been recently validated in species with challenging shoot morphology such as field pea [20].

Chlorophyll fluorescence imaging (CFIM)

One of the chlorophyll (Chl) fluorescence methods is chlorophyll fluorescence induction (CFIN), i.e., the measurement of the Chl fluorescence signal during illumination of the sample following prior dark adaptation. Since the first paper on CFIN by Kautsky and Hirsch [27], CFIN has been one of the most common methods used in photosynthesis and plant physiology research: it is inexpensive, non-destructive, and above all, provides a great deal of information about the photosynthetic function of the sample (reviewed, e.g., by Lazár [28,29]). Use of pulse amplitude modulation (PAM) techniques for the measurement of CFIN together with the application of the saturation pulse (SP) method enables the separation of photochemical and non-photochemical events occurring in the sample [30]. Chl fluorescence is excited and measured with the help of weak measuring flashes, whereas photosynthesis is maintained by actinic illumination and saturation of photosynthesis is achieved by the SPs. Since Chls absorb in blue (Chl *a* at 436 nm and Chl *b* at 470 nm, respectively) and red (at about 650 nm for

both Chls *a* and *b*) regions of visible spectrum, the measuring and actinic light is the light with one of the above wavelengths, usually 650-nm. The SPs are usually generated by white light. On the other hand, Chl fluorescence emission spectrum at room temperature shows two peaks centred at about 680 and 735 nm. To avoid a possible overlap of the 650-nm excitation light with Chl fluorescence emission, the Chl fluorescence signal is detected at wavelengths longer than 700 nm. To reveal spatial heterogeneity of the fluorescence signal during CFIN, imaging Chl fluorometers were developed [31,32]. In the images (for illustration see Figure 2), different colours are used to show different fluorescence intensities according to a chosen false colour scale (as mentioned above, fluorescence emission is always above 700 nm, red light). An additional advantage of the CFIM is that it provides a huge amount of data which can be thoroughly analysed and used for early detection of plant stress as shown, e.g., by Lazár et al. [33]. At present, modern CFIM instruments adopt PAM and SP methods/techniques and are thus highly suitable for high-throughput plant phenotyping (reviewed, e.g., by Gorbe and Calatayud [34], Harbinson et al. [35]). However, over the course of time, too many Chl fluorescence parameters were defined and claimed to reflect particular functions of photosynthetic apparatus. Hence, there is a problem over which parameter should be measured/evaluated and presented. Values of most of the parameters cannot be mutually compared. It is only possible to compare relative changes (caused, e.g., by a stress treatment) of a given parameter. The parameters of the so-called energy partitioning, i.e., quantum yields of processes responsible for the use of the absorbed light energy, are the best choice (reviewed by Lazár [36]) as they are all defined on the same basis and can be directly compared. Since all quantum yields sum to unity, the quantum yields express fractions of absorbed excitation light that are used for given processes (photochemical and various types of non-photochemical energy dissipations).

It is also worth mentioning here that kinetic types of CFIM (KCFIM) that measure whole CFIN and also apply the SPs which then allow computation of various Chl fluorescence parameters, and integrate signal from the whole leaf or shoot, are the most valuable for physiological studies. However, integration of KCFIM into high-throughput systems [20,37] is not very common and in the majority of recent reports, imaging systems measuring either single Chl fluorescence level (SLCFIM) or two Chl fluorescence levels (usually the minimal and maximal Chl fluorescence levels for the dark-adapted state; TLCFIM) were used (see Table 1). As intensity of Chl fluorescence depends on the amount of chlorophylls, the SLCFIM might be used, e.g. to distinguish between non-stressed and senescent leaves (when the amount of Chls is decreased) at the later stages of stress progression but it does not provide any information about early processes in photosytem II (PSII) that are not necessarily linked to the later senescence events. Further, the usual output of the TLCFIM, the F_V/F_M ratio, which estimates the maximum quantum yield of photosystem II photochemistry, provides only a limited information about photosynthetic function compared with the outputs of the KCFIMs, which also allow determination of the other quantum yields and parameters (see [36] for a review).

Thermoimaging

Plants are cooled by transpiration and when the stomata are closed, plant temperature increases. Based on this principle, thermal imaging was used for the first time to detect the changes in the temperature of sunflower leaves caused by water deficiency [30]. In addition to transpiration, stomata also drive water vapour, both parameters being typically determined by leaf gas exchange measurements. However, leaf gasometry involves contact with leaves which often interferes with their function. Further, leaf gasometry is time-consuming, limited by sample size and/or large number of samples required. In addition to heat emission, plants can lose heat by conduction and convection, which in fact represent mechanisms of a non-photochemical quenching of excited states. For this reason, it is not unexpected that an increased thermal signal correlates with an increase in non-photochemical quenching as shown by Kaňa and Vass [39]. Given the foregoing, thermoimaging is a very suitable method for plant phenotyping [19,40,41]. Like CFIM, it uses cameras to measure spatial heterogeneity of heat emissions, usually from leaves: the heat is electromagnetic radiation in the infrared region, usually between 8 – 13 μm. Generally, thermal imaging has been successfully used in a wide range of conditions and with diverse plant species. The technique can be applied to different scales, e.g., from single seedlings/leaves through whole trees or field crops to regions. However, researchers have to keep in mind that environmental variability, e.g., in light intensity, temperature, relative humidity, wind speed, etc. affects the accuracy of thermal imaging measurements and therefore the measurements and their interpretations must be done with care. Although thermal imaging sensors have been integrated into the in-house phenotyping platforms with controlled-environment (see section *The use of phenotyping methods to study plant stress responses*) the majority of studies have been performed so far in field conditions [42-44]. All aspects of thermal imaging used for the exploration of plant-environment interactions, as well as an overview of the application of thermoimaging in field phenotyping, were recently reviewed by Costa et al. [45].

Hyperspectral imaging (VIS-NIR, SWIR)

The absorption of light by endogenous plant compounds is used for calculations of many indices which reflect the composition and function of a plant. Such indices are, for example, the normalized difference vegetation index (NDVI) [46], an estimator of the Chl content, and the photochemical reflectance index (PRI) [47], an estimator of the photosynthetic efficiency. The absorption of a compound (e.g., water) at a given wavelength [48] can also be used for direct estimation of the compound contents in the plant. For practical reasons, measurement of absorbance is replaced here by measurements of reflectance. Depending on the measured wavelengths of reflected signal, various detectors are used, usually VIS-NIR (visible-near infrared region (400–750) - (750–1400 nm)) and SWIR (short wavelength infrared region; 1400–3000 nm). Measurements of the reflectance signal in VIS-NIR and SWIR regions originate from methods of remote sensing [49-51]. However, due to the high value of the information they carry, they are very suitable methods for plant phenotyping [52-54]. The reflectance signal can be detected at selected wavelengths or separated spectral bands (so-called multispectral detection). The whole spectral region can also be measured even for each pixel when cameras are applied and the hyperspectral imaging is carried out (Figure 2). Whereas the hyperspectral imaging in the VIS-NIR spectral region is used for evaluation of several indices as mentioned above, the SWIR spectral region is mainly used for the estimation of the plant's water content. Several aspects of plant reflectance were recently reviewed by Ollinger [55]. Despite the many indices that have been defined so far, based on the reflectance measurements, it is difficult to assess them accurately, similar to the situation with CFIN parameters (see above). For this reason, critical revision of all of the reflectance indices is needed to evaluate which of them provide the required information in the best way.

The use of phenotyping methods to study plant stress responses

One of the most important applications of automated plant phenotyping methods is in studies of plants' responses to various types of environmental stresses. In Table 1 we listed recent reports describing phenotyping protocols developed for indoor automated shoot phenotyping used in stress-related studies. Since the integrative approaches are a logical but rather new step in the development of phenotyping platforms, there are limited reports on the use of simultaneous analysis by multiple sensors. For this reason, we included here "single-sensor" experiments as well, that were performed in the automated platforms.

Perhaps the most widely used application of high-throughput phenotyping is in the search for drought-tolerant varieties. Objectives, traits and approaches related to automated plant selection for drought stress resistance were recently reviewed in Mir et al. [56], and Berger et al. [57]. Here, we add information from examples of the use of non-invasive plant phenotyping in this field. One of the early reports on the use of the high-throughput phenotyping platform describes the employment of the commercial-prototype system for evaluation of drought tolerance in nine *Arabidopsis* accessions [58]. The screening was based on RGB imaging, estimating rosette-leaf area and automated pot weighing and watering to assess transpiration rates. A very similar approach was later used by Skirycz et al. also in *Arabidopsis* [59]. The same platform was further used in a recent physiological study of Clauw and co-authors in which the impact of mild-drought on various *Arabidopsis thaliana* accessions was evaluated [60]. Another study on *Arabidopsis* employing top-view RGB imaging, pot weighing and automated rotation of pots was performed by Tisné et al. [61]. The phenotyping platform was designed to prevent position effect on water evaporation and authors demonstrated important improvement in the evaporation homogeneity [61].

Although these studies represent an important contribution to the development of automated phenotyping, the design of the platform for top-view experiments has limited their use to analyses of plants with leaf rosette. Further progress thus lay in development of platforms allowing RGB imaging from multiple positions. The most recent advances in the use of multiple-view RGB imaging followed by software analysis were demonstrated in a study by Neumann et al. [26]. The authors were able to automatically extract from the images of the barley plants, the plant height and width, and also leaf colours to evaluate the impact of drought on the degradation of chlorophyll. Earlier, Pereyra-Irujo et al. [62], reported a study that employed a self-constructed high-throughput platform for the RGB screening of growth and water-use efficiency (WUE) in two soybean (*Glycine max* L.) genotypes. The system with automated weighing and watering placed in the greenhouse was used to analyse the projected area of the shoots and the mass of the pots [62]. An impressive number of plants was analysed for similar traits in the study by Honsdorf et al. [16]. These authors searched for drought-tolerance QTLs in 48 wild barley introgression lines, using a commercial greenhouse based platform with multiple-view RGB imaging and automated weighing and watering [16]. A similar approach utilising estimation of shoot biomass based on RGB imaging was used by Coupel-Ledru et al., to screen thousands of grapevine plants for drought tolerance [63]. In these studies, the plant water

management was automatically analysed by simple weighing of the pots. This approach, however, begs several questions about the homogeneity of evaporation from the soil of the pots placed in different positions of the growing area. The solution to this issue usually requires an exhaustive validation process with numerous control pots and artificial plant-like objects randomly distributed throughout the growing area (Mark Tester, personal communication). A more elegant solution could be the use of the specific sensors controlling directly the plant water content [64] or transpiration [65] of each plant. Even this approach, however, requires appropriate validation.

An integrative way of analysis was employed in the study of Petrozza et al. [66]. Here, the effect of Megafol treatment on drought-stressed tomatoes was assessed using RGB imaging to distinguish shoot area, SLCFIM measurement to calculate "stress index" and NIR camera for water content estimation. Repeated measurements by NIR camera throughout the experiment allowed visualizing the drop of the high water content index that precedes the growth limitation caused by drought stress [66]. A combination of RGB and NIR imaging techniques was also used by Harshavardhan et al. for analysis of the drought-tolerance of transgenic *Arabidopsis* plants [67]. The RGB imaging was employed by Bresson et al. to study the effect of plant-bacteria interactions on plant tolerance to drought stress [68]. The integration of F_V/F_M measurement by TLCFIM provided complementary information to the growth rate and WUE analysis obtained by pot weighing [69]. A combination of RGB, SLCFIM and NIR imaging techniques was used by Chen et al. [64] to study different phenotypic traits of 18 barley genotypes. The authors used sophisticated statistics and mathematical modelling to classify genotypes based on their response to drought stress [64].

Another important trait in drought studies is the leaf surface temperature that reflects the transpiration rate of the plant (as discussed above in the section *Thermoimaging*). A combination of shoot digital imaging, thermoimaging and automated weighing and watering to study WUE was used by Fehér-Juhász et al. [19]. These authors employed a self-constructed greenhouse-based platform for the selection of drought-tolerant transgenic wheat plants. The platform allows monitoring of the mature cereal plants' growth by multiple-view RGB imaging and assessment of the leaf surface temperature by side-view thermal camera recording the differences in temperatures of plant shoots [19]. The same platform and a similar phenotyping experimental design were used for evaluation of drought tolerance in barley. The system provides integrative analysis of plant growth and physiology, but its use for large-scale analysis is limited by a semi-automated regime requiring manual loading of the plants into the system [65].

Given that physiological responses to drought and high temperature stresses are tightly connected, similar approaches can be used to study the tolerance of plants to both drought and high temperature. The use of high-throughput phenotyping for high temperature tolerance and a description of the appropriate sensors can be found in a review by Gupta et al. [70]. More recently, the effects of the high temperature on the *Arabidopsis* plants were studied by Vasseur et al. [71]. The authors used commercial-prototype platform allowing the top-view RGB imaging and WUE analysis followed by highly-sophisticated statistical approach to reveal contrasting adaptive strategies to the high temperature and drought stresses [71].

The salinization of soil is another phenomenon often associated with drought and high temperature stress. The example of the protocol for salt stress study in various cereals combining RGB imaging with destructive leaf sampling to measure Na^+ concentration was described by Berger et al. [72]. The effect of salt stress was studied by Rajendran et al. [73] using digital RGB imaging in a greenhouse-based commercial system. This study provided deep insight into the physiological processes connected with salinity in wheat. The authors used the multiple-view RGB imaging to estimate a digital area of shoot, and to visualize changes in leaf colour for quantification of the senescent area. Using non-invasive plant phenotyping and analysis of Na^+ concentration in 4th leaf, the authors predicted a plant salinity tolerance index that showed a good correlation with the results obtained from conventional salt-tolerance measurements [73]. Simple RGB imaging in wheat and barley was carried out in the physiological study of Harris et al. [74], and described in the methodological report of Golzarian et al. [18]. Recently, Schilling et al. applied a similar approach to select a salt-tolerant line of transgenic barley [75]. The combination of digital RGB imaging (used to measure shoot growth rate) with SLCFIM (used for the assessment of senescent areas) was used for the selection of salt-tolerant cultivars of rice by Hairmansis et al. [76]. These studies of salt-stress tolerance were performed using the same commercial platform involving SLCFIM sensor. As mentioned in the section *Chlorophyll fluorescence imaging (CFIM)* this type of CFIM in fact provides only estimation of a senescent area that can be obtained using an older way of estimation based on colour detection by RGB imaging. Thus, to increase the value of the physiological evaluation, the use of KCFIM is necessary for quantification of the quantum yield of photochemistry and of the other competitive processes [36].

Combination of RGB imaging, thermoimaging and TLCFIM was used in the pioneer work of Chaerle et al. who evaluated the effects of mild mottle virus infection on tobacco and bean plants [77]. The use of high-

throughput techniques in the nutrient starving stress studies have been already reported too. The principle of the method based on RGB imaging of leaf expansion was described by Moreau et al. [78]. A comprehensive study on the phenotypic effects of nitrogen and phosphorus nutrient statuses of *Brachypodium* was carried out by Poire et al. employing RGB imaging to estimate growth rate [79]. A similar approach was used in a study of Neilson et al. [80] where the responses to nitrogen deficiency and drought were evaluated by RGB imaging, NIR imaging and automated weighing, respectively. The authors also developed software that extracted from the images, additive traits such as projected plant height and the height to the ligule of the youngest fully expanded leaf, which showed very good correlations with standard manually measured agronomical parameters [80]. The multiple-sensor approach was described earlier in beans by Chaerle et al., who used RGB imaging, thermoimaging and TLCFIM to evaluate the phenotypes related to magnesium deficiency and biotic stress [81]. The impact of cold stress on plant growth and physiology is routinely studied using non-invasive methods through the analysis of Chl fluorescence, but not using fluorescence sensors integrated into complex growth-analysing platforms [82-84]. Jansen et al. studied the effects of chilling stress in *Arabidopsis* and tobacco plants using a growth chamber based system equipped with digital top-view RGB screening and KCFIM [37]. Very recently an automated screening approach based on RGB imaging and KCFIM analysis for selection of pea cultivars with different cold-sensitivity was developed by Humplík et al. [20]. The reported study was not intended only for selection of cold-sensitive/tolerant varieties of pea but also for studies of plant cold-response strategies in general. Since the CFIM analysis is not limited to plant morphology and the image analysis was sensitive enough to detect tiny tendrils of pea, the described procedure should be theoretically employed for shoot analyses of other plant species [20].

Conclusions

This mini-review focuses on recent advances towards development of integrative automated platforms for high-throughput plant phenotyping that employ multiple sensors for simultaneous analysis of plant shoots. In both basic and applied science, the recently emerging approaches have found importance as tools in unravelling complex questions of plant growth, development, responses to environment, as well as selection of appropriate genotypes in molecular breeding strategies. As far as phenotype is an interactive network of responses by the plant to its environment that affects in turn, the expression of the genotype it is worth pointing out that attention to the way the analyses are done, under precisely controlled conditions allowing for direct linking the huge amount of complex phenotyping data obtained to the particular conditions. It would also help the end user – the biologist – to narrow his/her view on the importance of various parameters and indices available from the specialized measurements (specifically CFIN and reflectance measurements) and evaluate which of them provide the required information in the best way and hence thus the most suitable for high-throughput plant phenotyping. Such information and standardized protocols applicable for the particular phenotyping methodologies should be available in the near future due to the phenotyping community efforts.

Abbreviations

Chl: Chlorophyll; CFIM: Chlorophyll fluorescence imaging; CFIN: Chlorophyll fluorescence Induction; DW: Dry weight; F_M: Maximal chlorophyll fluorescence levels for dark- adapted state; FW: Fresh weight; F_V: variable chlorophyll fluorescence level for a dark-adapted state; ϕ_{P_0}: The maximal quantum yield of photosystem II photochemistry for a dark-adapted state; KCFIM: Kinetic chlorophyll fluorescence imaging; NDVI: Normalized difference vegetation index; PAM: Pulse amplitude modulation; PRI: Photochemical reflectance index; PSII: Photosystem II; RGB: Red-green-blue; SLCFIM: Single-level chlorophyll fluorescence imaging; SP: Saturation pulse; SWIR: Short wavelength infrared; TLCFIM: Two-level chlorophyll fluorescence imaging; VIS-NIR: Visible-near infrared; WUE: Water-use efficiency.

Competing interests

The authors declare that they have no competing interests.

Authors' contributions

JFH, DL, AH and LS drafted the manuscript. All authors read and approved the final manuscript.

Acknowledgment

This work was supported by the grant No LO1204 (Sustainable development of research in the Centre of the Region Haná from the National Program of Sustainability I, Ministry of Education, Youth and Sports, Czech Republic.

Author details

[1]Department of Chemical Biology and Genetics, Centre of the Region Haná for Biotechnological and Agricultural Research, Faculty of Science, Palacký University, Šlechtitelů 11, Olomouc CZ-78371, Czech Republic. [2]Department of Biophysics, Centre of the Region Haná for Biotechnological and Agricultural Research, Faculty of Science, Palacký University, Šlechtitelů 11, Olomouc CZ-78371, Czech Republic.

Received: 5 February 2015 Accepted: 9 April 2015
Published online: 17 April 2015

References

1. Araus JL, Cairns JE. Field high-throughput phenotyping: the new crop breeding frontier. Trends Plant Sci. 2014;19:52–61.
2. Granier C, Vile D. Phenotyping and beyond: modelling the relationships between traits. Curr Opin Plant Biol. 2014;18:96–102.
3. Fiorani F, Schurr U. Future scenarios for plant phenotyping. Annu Rev Plant Biol. 2013;64:267–91.
4. Fiorani F, Rascher U, Jahnke S, Schurr U. Imaging plants dynamics in heterogenic environments. Curr Opin Biotech. 2012;23:227–35.
5. Walter A, Studer B, Kölliker R. Advanced phenotyping offers opportunities for improved breeding of forage and turf species. Annals Bot. 2012;110:1271–9.
6. Jansen M, Flood P, Knopp KA, van Dusschoten D, Fiorani F, Rascher U, et al. Non-invasive phenotyping methodologies enable the accurate characterization of growth and performance of shoots and roots. In: Tuberosa R, Graner A, Frison E, editors. Genomics of Plant Genetic Resources. Volume 1st ed. Netherlands: Springer; 2014. p. 173–206.

7. Pieruschka R, Poorter H. Phenotyping plants: genes, phenes and machines. Funct Plant Biol. 2012;39:813–20.
8. Roberts MJ, Long SP, Tieszen LL, Beadle CL. Measurement of plant biomass and net primary production of herbaceous vegetation. In: Hall DO, Scurlock JMO, Bolhar-Nordenkampf HR, Leegood RC, Long SP, editors. Photosynthesis and Production in a Changing Environment. Netherlands: Springer; 1993.
9. Rouphael Y, Mouneimne AH, Ismail A, Mendoza-De Gyves E, Rivera CM, Colla G. Modeling individual leaf area of rose (Rosa hybrida L.) based on leaf length and width measurement. Photosynthetica. 2010;48:9–15.
10. Cemek B, Unlukara A, Kurunc A. Nondestructive leaf-area estimation and validation for green pepper (Capsicum annuum L.) grown under different stress conditions. Photosynthetica. 2011;49:98–106.
11. Misle E, Kahlaoui B, Hachicha M, Alvarado P. Leaf area estimation in muskmelon by allometry. Photosynthetica. 2013;51:613–20.
12. Green JM, Appel H, MacNeal Rehrig E, Harnsomburana J, Chang J-F, Balint-Kurti P, et al. PhenoPhyte: a flexible affordable method to quantify 2D phenotypes from imagery. Plant Methods. 2012;8:45.
13. Zhang X, Hause RJ, Borevitz JO. Natural genetic variation for growth and development revealed by high-throughput phenotyping in Arabidopsis thaliana. G3-Genes Genom Genet. 2012;2:29–34.
14. Tessmer OL, Jiao Y, Cruz JA, Kramer DM, Chen J. Functional approach to high-throughput plant growth analysis. BMC Syst Biol. 2013;7 Suppl 6:S17.
15. Furbank RT, Tester M. Phenomics–technologies to relieve the phenotyping bottleneck. Trends Plant Sci. 2011;16:635–44.
16. Honsdorf N, March TJ, Berger B, Tester M, Pillen K. High-throughput phenotyping to detect drought tolerance QTL in wild barley introgression lines. PLoS One. 2014;9:e97047.
17. Walter A, Scharr H, Gilmer F, Zierer R, Nagel KA, Ernst M, et al. Dynamics of seedling growth acclimation towards altered light conditions can be quantified via GROWSCREEN: a setup and procedure designed for rapid optical phenotyping of different plant species. New Phytol. 2007;174:447–55.
18. Golzarian MR, Frick RA, Rajendran K, Berger B, Roy S, Tester M, et al. Accurate inference of shoot biomass from high-throughput images of cereal plants. Plant Methods. 2011;7:1–11.
19. Fehér-Juhász E, Majer P, Sass L, Lantos C, Csiszár J, Turóczy Z, et al. Phenotyping shows improved physiological traits and seed yield of transgenic wheat plants expressing the alfalfa aldose reductase under permanent drought stress. Acta Physiol Plant. 2014;36:663–73.
20. Humplík JF, Lazár D, Fürst T, Husičková A, Hýbl M, Spíchal L. Automated integrative high-throughput phenotyping of plant shoots: a case study of the cold-tolerance of pea (Pisum sativum L.). Plant Methods. 2015;11:1–11.
21. Berger B, de Regt B, Tester M. High-throughput phenotyping of plant shoots. In: Normanly J, editor. High-Throughput Phenotyping in Plants. New York City: Humana Press; 2012. p. 9–20.
22. Camargo A, Papadopoulou D, Spyropoulou Z, Vlachonasios K, Doonan JH, Gay AP. Objective definition of Rosette shape variation using a combined computer vision and data mining approach. PLoS One. 2014;9, e96889.
23. Crowell S, Falcão AX, Shah A, Wilson Z, Greenberg AJ, McCouch SR. High-resolution inflorescence phenotyping using a novel image-analysis pipeline, PANorama. Plant Physiol. 2014;165:479–95.
24. Paulus S, Dupuis J, Riedel S, Kuhlmann H. Automated analysis of barley organs using 3d laser scanning: an approach for high throughput phenotyping. Sensors. 2014;14:12670–86.
25. Fanourakis D, Briese C, Max JF, Kleinen S, Putz A, Fiorani F, et al. Rapid determination of leaf area and plant height by using light curtain arrays in four species with contrasting shoot architecture. Plant Methods. 2014;10:9.
26. Neumann K, Klukas C, Friedel S, Rischbeck P, Chen D, Entzian A, Stein N, Graner A, Kilian B. Dissecting spatio-temporal biomass accumulation in barley under different water regimes using high-throughput image analysis. Plant Cell Environ. 2015. doi: 10.1111/pce.12516, in press.
27. Kautsky H, Hirsch A. Neue Versuche zur Kohlensäureassimilation. Naturwissenschaften. 1931;19:964.
28. Lazár D. Chlorophyll a fluorescence induction. Biochim Biophys Acta. 1999;1412:1–28.
29. Lazár D. The polyphasic chlorophyll a fluorescence rise measured under high intensity of exciting light. Funct Plant Biol. 2006;33:9–30.
30. Schreiber U, Schliwa U, Bilger W. Continuous recording of photochemical and non-photochemical chlorophyll fluorescence quenching with a new type of modulation fluorometer. Photosynth Res. 1986;10:51–62.
31. Omasa K, Shimazaki K-I, Aiga I, Larcher W, Onoe M. Image analysis of chlorophyll fluorescence transients for diagnosing the photosynthetic system of attached leaves. Plant Physiol. 1987;84:748–52.
32. Daley PF, Raschke K, Ball JT, Berry JA. Topography of photosynthetic activity of leaves obtained from video images of chlorophyll fluorescence. Plant Physiol. 1989;90:1233–8.
33. Lazár D, Sušila P, Nauš J. Early detection of plant stress from changes in distributions of chlorophyll a fluorescence parameters measured with fluorescence imaging. J Fluoresc. 2006;16:173–6.
34. Gorbe E, Calatayud A. Applications of chlorophyll fluorescence imaging technique in horticultural research: A review. Sci Hortic. 2012;138:24–35.
35. Harbinson J, Prinzenberg AE, Kruijer W, Aarts MGM. High throughput screening with chlorophyll fluorescence imaging and its use in crop improvement. Curr Opin Biotech. 2012;23:221–6.
36. Lazár D. Parameters of photosynthetic energy partitioning. J Plant Physiol. 2015;175:131–47.
37. Jansen M, Gilmer F, Biskup B, Nagel KA, Rascher U, Fischbach A, et al. Simultaneous phenotyping of leaf growth and chlorophyll fluorescence via GROWSCREEN FLUORO allows detection of stress tolerance in Arabidopsis thaliana and other rosette plants. Funct Plant Biol. 2009;36:902–14.
38. Hashimoto Y, Ino T, Kramer PJ, Naylor AW, Strain BR. Dynamic analysis of water stress of sunflower leaves by means of a thermal image processing system. Plant Physiol. 1984;76:266–9.
39. Kaňa R, Vass I. Thermoimaging as a tool for studying light-induced heating of leaves Correlation of heat dissipation with the efficiency of photosystem II photochemistry and non-photochemical quenching. Environ Exp Bot. 2008;64:90–6.
40. Siddiqui ZS, Cho J-I, Park S-H, Kwon T-R, Ahn B-O, Lee G-S, et al. Phenotyping of rice in salt stress environment using high-throughput infrared imaging. Acta Bot Croat. 2014;73:149–58.
41. Virlet N, Lebourgeois V, Martinez S, Costes E, Labbé S, Regnard J-L. Stress indicators based on airborne thermal imagery for field phenotyping a heterogeneous tree population for response to water constraints. J Exp Bot. 2014;65:5429–42.
42. Jones HG, Serraj R, Loveys BR, Xiong L, Wheaton A, Price AH. Thermal infrared imaging of crop canopies for the remote diagnosis and quantification of plant responses to water stress in the field. Funct Plant Biol. 2009;36:978–89.
43. Costa JM, Ortuño MF, Lopes CM, Chaves MM. Grapevine varieties exhibiting differences in stomatal response to water deficit. Funct Plant Biol. 2012;39:179–89.
44. Grant OM, Davies MJ, James CM, Johnson AW, Leinonen I, Simpson DW. Thermal imaging and carbon isotope composition indicate variation amongst strawberry (Fragaria x ananassa) cultivars in stomatal conductance and water use efficiency. Environ Exp Bot. 2012;76:7–15.
45. Costa JM, Grant OM, Chaves MM. Thermography to explore plant–environment interactions. J Exp Bot. 2013;64:3937–49.
46. Rouse JW, Haas RH, Schell JA, Deering DW. Monitoring vegetation systems in the Great Plains with ERTS. In: Freden SC, Mercanti EP, Becker MA, editors. NASA SP-351. Proceedings of the 3rd Earth Resources Technology Satellite-1Symposium, Washington DC: NASA Scientific and Technical Information Office; 1974. p. 309–17.
47. Gamon JA, Peñuelas J, Field CB. A narrow-waveband spectral index that tracks diurnal changes in photosynthetic efficiency. Remote Sens Environ. 1992;41:35–44.
48. Carter GA. Primary and secondary effects of water content on the spectral reflectance of leaves. Am J Bot. 1991;78:916–24.
49. Huber S, Tagesson T, Fensholt R. An automated field spectrometer system for studying VIS, NIR and SWIR anisotropy for semi-arid savanna. Remote Sens Environ. 2014;152:547–56.
50. Lamb DW, Schneider DA, Stanley JN. Combination active optical and passive thermal infrared sensor for low-level airborne crop sensing. Precis Agric. 2014;15:523–31.
51. Saberioon MM, Amin MSM, Anuar AR, Gholizadeh A, Wayayok A, Khairunniza-Bejo S. Assessment of rice leaf chlorophyll content using visible bands at different growth stages at both the leaf and canopy scale. Int J Appl Earth Observ Geoinform. 2014;32:35–45.
52. Garriga M, Retamales JB, Romero-Bravo S, Caligari PDS, Lobos GA. Chlorophyll, anthocyanin, and gas exchange changes assessed by spectroradiometry in *Fragaria chiloensis* under salt stress. J Integr Plant Biol. 2014;56:505–15.

53. Mahajan GR, Sahoo RN, Pandey RN, Gupta VK, Kumar D. Using hyperspectral remote sensing techniques to monitor nitrogen, phosphorus, sulphur and potassium in wheat (Triticum aestivum L.). Precis Agric. 2014;15:499–522.
54. Petach AR, Toomey M, Aubrecht DM, Richardson AD. Monitoring vegetation phenology using an infrared-enabled security camera. Agri Forest Meteorol. 2014;195–196:143–51.
55. Ollinger SV. Sources of variability in canopy reflectance and the convergent properties of plants. New Phytol. 2011;189:375–94.
56. Mir RR, Zaman-Allah M, Sreenivasulu N, Trethowan R, Varshney RK. Integrated genomics, physiology and breeding approaches for improving drought tolerance in crops. Theor Appl Genet. 2012;125:625–45.
57. Berger B, Parent B, Tester M. High-throughput shoot imaging to study drought responses. J Exp Bot. 2010;61:3519–28.
58. Granier C, Aguirrezabal L, Chenu K, Cookson SJ, Dauzat M, Hamard P, et al. PHENOPSIS, an automated platform for reproducible phenotyping of plant responses to soil water deficit in. New Phytol. 2006;169:623–35.
59. Skirycz A, Vandenbroucke K, Clauw P, Maleux K, De Meyer B, Dhondt S, et al. Survival and growth of Arabidopsis plants given limited water are not equal. Nat Biotechnol. 2011;29:212–4.
60. Clauw P, Coppens F, De Beuf K, Dhondt S, Van Daele T, Maleux K, et al. Leaf Responses to Mild Drought Stress in Natural Variants of Arabidopsis thaliana. Plant Physiol. 2015;114:254–84.
61. Tisné S, Serrand Y, Bach L, Gilbault E, Ben Ameur R, Balasse H, et al. Phenoscope: An automated large-scale phenotyping platform offering high spatial homogeneity. Plant J. 2013;74:534–44.
62. Pereyra-Irujo GA, Gasco ED, Peirone LS, Aguirrezábal LA. GlyPh: a low-cost platform for phenotyping plant growth and water use. Funct Plant Biol. 2012;39:905–13.
63. Coupel-Ledru A, Lebon E, Christophe A, Doligez A, Cabrera-Bosquet L, Péchier P, et al. Genetic variation in a grapevine progeny (Vitis vinifera L. cvs Grenache x Syrah) reveals inconsistencies between maintenance of daytime leaf water potential and response of transpiration rate under drought. J Exp Bot. 2014;65:6205–218.
64. Chen D, Neumann K, Friedel S, Kilian B, Chen M, Altmann T, et al. Dissecting the Phenotypic Components of Crop Plant Growth and Drought Responses Based on High-Throughput Image Analysis. Plant Cell. 2014;26:4636–55.
65. Cseri A, Sass L, Törjék O, Pauk J, Vass I, Dudits D. Monitoring drought responses of barley genotypes with semi-robotic phenotyping platform and association analysis between recorded traits and allelic variants of some stress genes. Aust J Crop Sci. 2013;7:1560–70.
66. Petrozza A, Santaniello A, Summerer S, Di Tommaso G, Di Tommaso D, Paparelli E, et al. Physiological responses to Megafol® treatments in tomato plants under drought stress: A phenomic and molecular approach. Sci Hortic (Amsterdam). 2014;174:185–92.
67. Harshavardhan VT, Van Son L, Seiler C, Junker A, Weigelt-Fischer K, Klukas C, et al. AtRD22 and AtUSPL1, Members of the Plant-Specific BURP Domain Family Involved in Arabidopsis thaliana Drought Tolerance. PLoS One. 2014;9, e110065.
68. Bresson J, Varoquaux F, Bontpart T, Touraine B, Vile D. The PGPR strain Phyllobacterium brassicacearum STM196 induces a reproductive delay and physiological changes that result in improved drought tolerance in Arabidopsis. New Phytol. 2013;200:558–69.
69. Bresson J, Vasseur F, Dauzat M, Labadie M, Varoquaux F, Touraine B, et al. Interact to survive: Phyllobacterium brassicacearum improves Arabidopsis tolerance to severe water deficit and growth recovery. PLoS One. 2014;9, e107607.
70. Gupta PK, Balyan HS, Gahlaut V, Kulwal PL. Phenotyping, genetic dissection, and breeding for drought and heat tolerance in common wheat: status and prospects. Plant Breeding Reviews. 2012;36:85–147.
71. Vasseur F, Bontpart T, Dauzat M, Granier C, Vile D. Multivariate genetic analysis of plant responses to water deficit and high temperature revealed contrasting adaptive strategies. J Exp Bot. 2014;65:6457–69.
72. Berger B, de Regt B, Tester M. Trait dissection of salinity tolerance with plant phenomics. In: Shabala S, Cuin TA, editors. Plant Salt Tolerance. New York City: Humana Press; 2012. p. 399–413.
73. Rajendran K, Tester M, Roy SJ. Quantifying the three main components of salinity tolerance in cereals. Plant, Cell Environ. 2009;32:237–49.
74. Harris BN, Sadras VO, Tester M. A water-centred framework to assess the effects of salinity on the growth and yield of wheat and barley. Plant Soil. 2010;336:377–89.
75. Schilling RK, Marschner P, Shavrukov Y, Berger B, Tester M, Roy SJ, et al. Expression of the Arabidopsis vacuolar H⁺-pyrophosphatase gene (AVP1) improves the shoot biomass of transgenic barley and increases grain yield in a saline field. Plant Biotechnol J. 2014;12:378–86.
76. Hairmansis A, Berger B, Tester M, Roy SJ. Image-based phenotyping for non-destructive screening of different salinity tolerance traits in rice. Rice. 2014;7:16.
77. Chaerle L, Pineda M, Romero-Aranda R, Van Der Straeten D, Barón M. Robotized thermal and chlorophyll fluorescence imaging of pepper mild mottle virus infection in Nicotiana benthamiana. Plant Cell Physiol. 2006;47:1323–36.
78. Moreau D, Schneider C, Huguet T, Salon C, Munier-Jolain N. Can differences of nitrogen nutrition level among Medicago truncatula genotypes be assessed non-destructively? Probing with a recombinant inbred lines population. Plant Signal Behav. 2009;4:30–2.
79. Poiré R, Chochois V, Sirault XRR, Vogel JP, Watt M, Furbank RT. Digital imaging approaches for phenotyping whole plant nitrogen and phosphorus response in Brachypodium distachyon. J Integr Plant Biol. 2014;56:781–96.
80. Neilson EH, Edwards AM, Blomstedt CK, Berger B, Møller BL, Gleadow RM. Utilization of a high-throughput shoot imaging system to examine the dynamic phenotypic responses of a C4 cereal crop plant to nitrogen and water deficiency over time. J Exp Bot. 2015;66:1817–32.
81. Chaerle L, Hagenbeek D, Vanrobaeys X, Van Der Straeten D. Early detection of nutrient and biotic stress in Phaseolus vulgaris. Int J Remot Sens. 2007;28:3479–92.
82. Devacht S, Lootens P, Baert J, Van Waes J, Van Bockstaele E, Roldán-Ruiz I. Evaluation of cold stress of young industrial chicory (Cichorium intybus L.) plants by chlorophyll a fluorescence imaging. I. Light induction curve. Photosynthetica. 2011;49:161–71.
83. Lootens P, Devacht S, Baert J, Van Waes J, Van Bockstaele E, Roldán-Ruiz I. Evaluation of cold stress of young industrial chicory (Cichorium intybus L.) by chlorophyll a fluorescence imaging. II. Dark relaxation kinetics. Photosynthetica. 2011;49:185–94.
84. Mishra A, Mishra KB, Höermiller II, Heyer AG, Nedbal L. Chlorophyll fluorescence emission as a reporter on cold tolerance in Arabidopsis thaliana accessions. Plant Signal Behav. 2011;6:301.

APPENDIX I.B

Automated integrative high-throughput phenotyping of plant shoots: a case study of the cold-tolerance of pea (*Pisum sativum* L.)

Published as:

Humplík JF, Lazár D, Fürst T, Husičková A, Hýbl M, Spíchal L. 2015d. Automated integrative high-throughput phenotyping of plant shoots: a case study of the cold-tolerance of pea (*Pisum sativum* L.). *Plant Methods*. 11:20. doi:10.1186/s13007-015-0063-9.

Humplík et al. Plant Methods (2015) 11:20
DOI 10.1186/s13007-015-0063-9

PLANT METHODS

METHODOLOGY Open Access

Automated integrative high-throughput phenotyping of plant shoots: a case study of the cold-tolerance of pea (*Pisum sativum* L.)

Jan F Humplík[1†], Dušan Lazár[2†], Tomáš Fürst[3], Alexandra Husičková[2], Miroslav Hýbl[4] and Lukáš Spichal[1*]

Abstract

Background: Recently emerging approaches to high-throughput plant phenotyping have discovered their importance as tools in unravelling the complex questions of plant growth, development and response to the environment, both in basic and applied science. High-throughput methods have been also used to study plant responses to various types of biotic and abiotic stresses (drought, heat, salinity, nutrient-starving, UV light) but only rarely to cold tolerance.

Results: We present here an experimental procedure of integrative high-throughput in-house phenotyping of plant shoots employing automated simultaneous analyses of shoot biomass and photosystem II efficiency to study the cold tolerance of pea (*Pisum sativum* L.). For this purpose, we developed new software for automatic RGB image analysis, evaluated various parameters of chlorophyll fluorescence obtained from kinetic chlorophyll fluorescence imaging, and performed an experiment in which the growth and photosynthetic activity of two different pea cultivars were followed during cold acclimation. The data obtained from the automated RGB imaging were validated through correlation of pixel based shoot area with measurement of the shoot fresh weight. Further, data obtained from automated chlorophyll fluorescence imaging analysis were compared with chlorophyll fluorescence parameters measured by a non-imaging chlorophyll fluorometer. In both cases, high correlation was obtained, confirming the reliability of the procedure described.

Conclusions: This study of the response of two pea cultivars to cold stress confirmed that our procedure may have important application, not only for selection of cold-sensitive/tolerant varieties of pea, but also for studies of plant cold-response strategies in general. The approach, provides a very broad tool for the morphological and physiological selection of parameters which correspond to shoot growth and the efficiency of photosystem II, and is thus applicable in studies of various plant species and crops.

Keywords: Plant phenotyping, RGB digital imaging, Chlorophyll fluorescence imaging, Shoot growth, Biomass production, Cold adaptation, Pea (*Pisum*)

Introduction

In plants, acclimation to cold, causes reduced growth, increase in antioxidant content, reduced water content, and changes in gene regulation, hormone balance, membrane composition, osmotic regulation, and photosynthetic function [1]. The adaptability and productivity of legumes (chickpea, faba bean, lentil, and pea) are limited by abiotic stresses in general [2], and their high sensitivity to chilling and freezing temperatures is well described [3].

Since cold tolerance is an important agronomical problem in Central and Northern Europe and geographically similar regions, we aimed to develop a routine measuring procedure for automated integrative high-throughput screening for selection of potentially cold tolerant cultivars. Pea (*Pisum sativum* L.) was chosen as a model crop because its tolerance to cold stress is one of the limiting factors in autumn sowings which allows for the enhanced productivity of pea plants. Overwintering plants have developed adaptive responses to seasonal weather changes. For example, overwintering evergreens

* Correspondence: lukas.spichal@upol.cz
†Equal contributors
[1]Department of Chemical Biology and Genetics, Centre of the Region Haná for Biotechnological and Agricultural Research, Faculty of Science, Palacký University, Šlechtitelů 11, Olomouc CZ-78371, Czech Republic
Full list of author information is available at the end of the article

have developed so-called sustained non-photochemical quenching (reviewed, e.g., by Verhoeven [4]) as a protection mechanism against absorbed light which is in excess with respect to the capacity of the carbon photosynthetic reactions and which is decreased during winter. These plants sense the upcoming cold period through the perception of environmental impulses, mainly temperature and day length. However, the sustained non-photochemical quenching does not work in modern pea cultivars. For this reason, we chose two modern cultivars and investigated their reaction to cold stress. We employed digital RGB imaging to study shoot growth, and chlorophyll (Chl) fluorescence imaging (CFIM) to analyze various parameters of plant photosystem II (PSII) efficiency. The cultivars used in this study were morphologically similar which facilitated the validation of sensitivity and resolution of our visible imaging analysis.

There is a paucity of information on the acclimation of pea plants to cold. An extensive study was published by Markarian et al. [5]. These authors evaluated 26 pea lines based on their winter survival. Further physiological parameters (total dry matter and photosynthetic area) of autumn- and spring-sown pea plants were evaluated by Silim et al. [6]. Autumn-sown plants produced similar seed yields to spring sowings when the winter survival was adequate, and autumn sowings matured 2–4 weeks before the spring-sown crops, depending on the variety and season [6]. The effects of short term acclimation (four days) of pea plants to cold temperatures (5°C) were explored by Yordanov et al. [7] who measured the rate of oxygen production and CO_2 assimilation, and Chl fluorescence parameters in order to evaluate photochemical activity and functional heterogeneity of PSII. They found that cold-acclimated plants showed higher photosynthetic rates and better Chl fluorescence parameters than non-acclimated plants [7]. The effects of short term cold acclimation (three days, 4°C) and subsequent recovery (2 days) of standard pea plants were studied by Chl fluorescence measurements in more detail by Georgieva and Lichtenthaler [8]. The Chl fluorescence parameters reflecting photosynthetic function decreased during cold acclimation but were reversible in the subsequent recovery [8]. A similar study was later carried out with three different pea cultivars by Georgieva and Lichtenthaler [9].

These studies revealed the importance of two potential traits that could be used to distinguish between pea cultivars with different cold-sensitivity: rate of shoot growth and values of Chl fluorescence parameters. Both traits can now be studied by non-invasive high-throughput platforms to provide integrative insight into plant physiology during cold acclimation. The spatio-temporal changes in shoot biomass or leaf area can be assessed using automated RGB imaging and image-analysis software, as has been shown for many species such as cereals, tomatoes, soybean and beans [10-13]. The Chl fluorescence parameters are routinely analyzed by non-imaging fluorometres (NICF) or the imaging system (CFIM). For physiological studies, kinetic types of CFIM that allow computation of various Chl fluorescence parameters on the whole leaf or shoot are the most valuable. However, the kinetic type CFIM has not been commonly integrated into high-throughput systems [14] and in recent reports only systems measuring a single Chl fluorescence level have been employed [11,15]. The intensity of Chl fluorescence depends on the amount of chlorophylls; thus, a single Chl fluorescence level can be used, e.g., to distinguish between non-stressed and senescent leaves (when amount of Chls is decreased) at late stages of stress. However, this does not provide any information about earlier processes in PSII that are not necessarily linked to later senescence events.

In this report, we describe a procedure employing an automated integrative high-throughput platform suitable for studies of the physiological basis of cold-stress adaptation and selection of pea cultivars with cold sensitivity/tolerance. The platform measures shoot area and Chl fluorescence to provide a complex analysis of plants during cold-acclimation. For this purpose, we developed new software for automatic RGB image analysis and we evaluated various parameters of Chl fluorescence obtained from CFIM. The data from the automated phenotyping platform were validated through estimation of shoot biomass by manual weighing of the shoots and by measurement of Chl fluorescence by a NICF hand operated fluorometer. Despite the complexity of pea shoots, very good correlation between pixel based shoot area and fresh biomass were obtained. Similarly, the Chl fluorescence parameters measured by NICF fully confirmed the reliability of the automated CFIM analysis.

Results and discussion

Visible imaging used for shoot growth

To compare the influence of cold acclimation on biomass production, two putative cold-resistant cultivars of pea Terno and Enduro were selected (labeled as TER and END, respectively). After germination, the seedlings were grown in a growth chamber at 22/20°C (see Materials and methods) and after the development of the first true leaf, the cold stress conditions were established. The seedlings continued growing in 5°C for 21 days and were screened twice per week in the automated platform. The green area of each individual seedling was extracted from particular projections (Figure 1) and combined to account for the overall shoot biomass. As shown in Figure 2, the total green area of the plants was calculated at 7 time-points. The cultivar TER showed a significantly higher (for p values see Table 1) increase in the total green area compared to the cultivar END

Figure 1 The example images of three optical projections of single END seedling used for calculation of total green area on 8th day of cold acclimation. The green area that was digitally extracted from the images is marked by white border line.

(Figure 3A). Because the green area of the cultivars was different at the beginning of the experiment, the normalized green area (NGA) was calculated, where the green area on the n^{th} (5, 8, ... 21) day of measurement was divided by the green area obtained on the 1st measuring day. The TER cultivar showed higher shoot growth which on the 21st day was almost a 3.5 fold increase in the green area, whereas END multiplied its projected area by only about 2.5-times (Figure 3B). To analyze how the cultivars differed in their growth rates, the relative growth rate (RGR) was used according to Hoffmann and Poorter [16]. We used the following formula:

$$RGR = \frac{\overline{lnW_2} - \overline{lnW_1}}{t_2 - t_1}$$

where $\overline{lnW_1}$ and $\overline{lnW_2}$ are the means of the natural logarithms of the plant's green areas and t_1 and t_2 are the times at which the green areas were measured. The TER cultivar relative growth rate was significantly higher (for p values see Table 1) during the whole period of cold acclimation. Moreover, at the beginning of the cold stress, the TER cultivar tended to speed-up its growth, then reached a steady state and finally decreased its RGR by the end of the experiment. The second cultivar, END, was very stable, slightly decreasing its growth rate during the experiment (Figure 3C). To examine the statistical significance of the differences between obtained TER and END growth-related parameters, the non-parametric Mann–Whitney *U* test was performed for each measuring day. The p values obtained for each measuring day are shown in Table 1.

It has been reported that cold-treatment affects total shoot biomass production and growth-rate in spring-sown and overwintering pea cultivars [6,17]. Besides shoot growth cold-treatment affects also growth of the root as showed in work by Bourion et al. [17]. However, the effect on the root is less severe compared to the above ground parts of the plants [17]. Due to this fact and due to the technical set up of our automated platform in this study we focused only on the analyses of cold-treatment effects on shoot growth. We describe here the development of the measuring setup for automated screening of pea cultivars with different cold-sensitivity through analysis of the shoot growth by RGB imaging followed by precise image-analysis. A similar approach has been shown for different species and different types of stresses. Considering crop species alone, most of the protocols for automated phenotyping using RGB imaging were designed for cereals, most often to

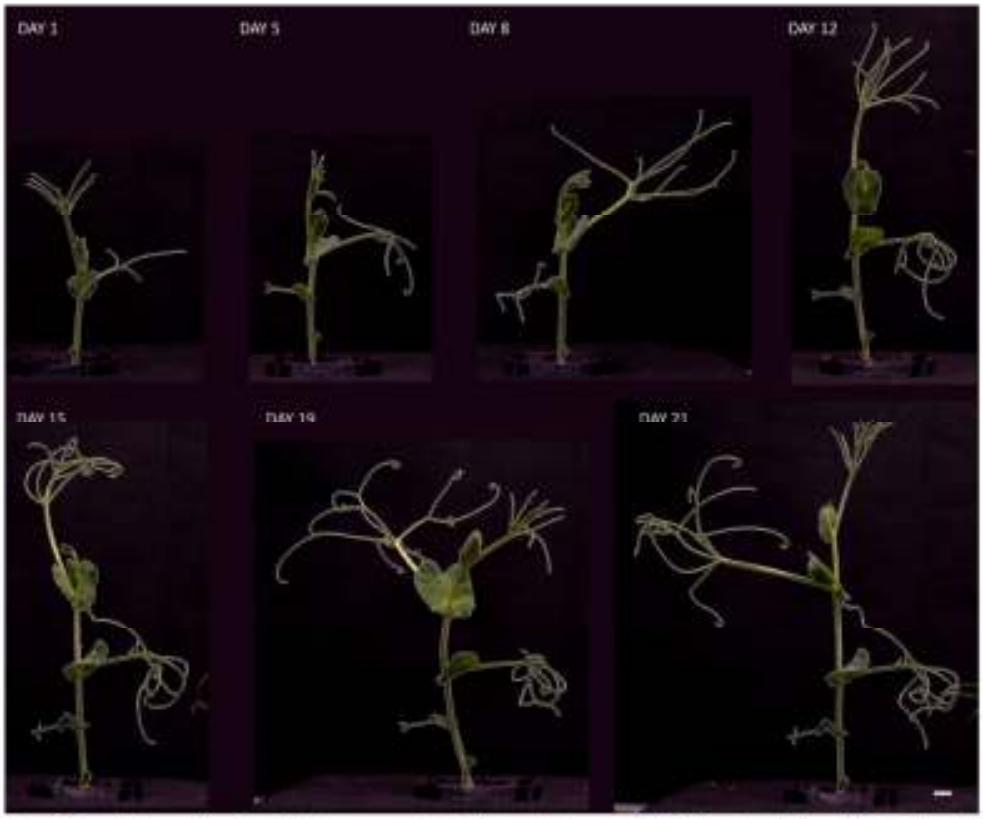

Figure 3 Example images taken from front view camera showing the growth progress of the TER seedling during cold acclimation for 21 days. The green area that was digitally extracted from the images is marked by white border line. The white bar in the right bottom site represents length of 1 cm.

Table 1 The p values of the Mann–Whitney test of statistical significant difference of growth parameters based on RGB imaging

Measuring day	Green area p value	NGA p value	Growth rate p value
1	<0.001	n. a.	n. a.
5	<0.001	<0.003	<0.003
8	<0.001	<0.001	<0.001
12	<0.001	<0.001	<0.001
15	<0.001	<0.001	<0.001
19	<0.001	<0.001	<0.001
21	<0.001	< 0.001	< 0.001

For each day the comparisons between TER and END datasets were tested in all three parameters respectively.

screen for drought, or salt tolerant plants [10,15,18-23]. Surprisingly, use of such a method has not been presented so far for any crops studied for cold-acclimation. Although there was no presumed effect of cold-treatment on the reliability of RGB imaging, the complicated morphology of field pea cultivars could potentially affect the accuracy of the automated measurements. For this reason, we tested our method of the green area (or projected area) estimation from automated RGB imaging by its comparison with a method of manual weighing of the shoots. The shoots of both cultivars were harvested on the last measuring day and FW of individual plant shoots was measured. Subsequently, correlations between the green area and FW were calculated using the non-parametric Spearman correlation coefficient. A similar approach has been reported recently by Hairmansis et al. [15] for rice. These authors found a

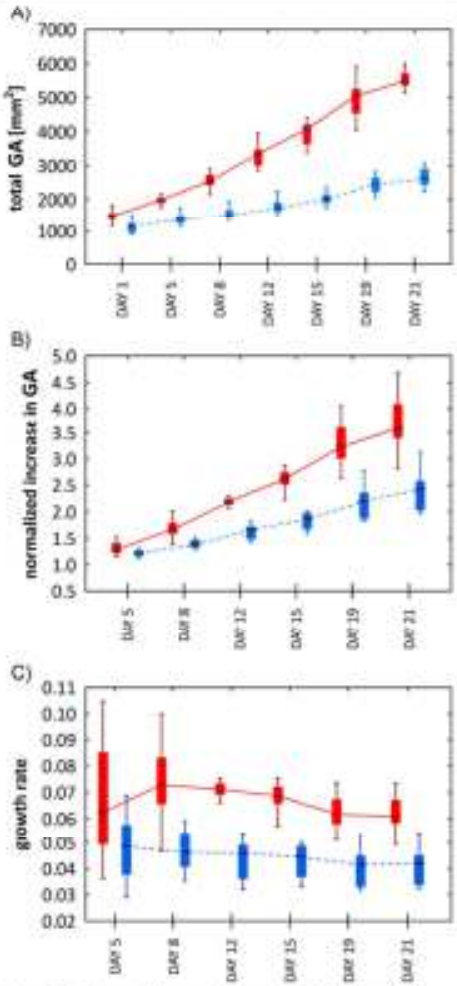

Figure 3 Analyses of the growth progress of shoots of TER (red boxes – full line) and END (blue boxes – dashed line) pea cultivars. The values derived from the green area on n^{th} days (1, 5, 8, ..., 21) are presented as medians (black bars) and quartiles (boxes). For better readability, the boxes are shifted in x-axis to not to overlap, but still represent the values measured on the same days. **A)** A total green area. **B)** A normalized green area. **C)** A relative growth rate. The error bars show minimal and maximal values.

correlation of projected area and FW ranging from 0.96 to 0.97. A more sophisticated calculation was developed by Golzarian et al. [22] who used estimated shoot area as a function of plant area and plant age. This method was applied by Pereyra-Irujo et al. [12] in experiments with soybean, providing a correlation of 0.97 in dry mass. Shoots of cereals and soybean have relatively low spatial-complexity. In contrast, shoots of field pea cultivars TER and END are formed mainly by stem and tiny tendrils (Figures 1, 2) requiring very precise identification by image-analysis software. Despite the challenging pea shoot morphology, Spearman correlation coefficients of 0.91 and 0.96 for TER and END cultivars, respectively, were found in our analysis ($p < 0.05$; Figure 4). This is fully comparable with the phenotyping protocols designed for other crop species and provides an efficient and reliable tool for the evaluation of pea growth.

Chlorophyll fluorescence imaging used for determination of photosynthetic function

Further variables used for phenotyping of the two pea cultivars were those obtained from measurements of Chl fluorescence induction (CFIN), which reflects photosynthetic function, mainly of PSII. Based on our knowledge of the parameters that can be determined from CFIN (reviewed in Lazár [24]), we selected the following parameters: i) the maximal quantum yield of PSII photochemistry for a dark-adapted state, $\Phi_{P0} = (F_M - F_0)/F_M = F_V/F_M$, where F_0, F_M, and F_V are the minimal, maximal, and variable fluorescence levels, respectively, for a dark-adapted state; ii) the actual quantum yield of PSII photochemistry for a light-adapted state, $\Phi_P = (F_M' - F(t))/F_M'$ where F_M' and $F(t)$ are the maximal and actual (at time t; usually in the steady state) fluorescence levels for a light-adapted state; iii) the quantum yield of constitutive non-light induced (basal or dark) dissipation processes consisting of Chl fluorescence emission and heat dissipation, $\Phi_{f,D} = F(t)/F_M$; and iv) the quantum yield of regulatory light-induced heat dissipation, $\Phi_{NPQ} = F(t)/F_M' - F(t)/F_M$. It is worth mentioning here that $\Phi_P + \Phi_{f,D} + \Phi_{NPQ} = 1$; further that $\Phi_P = q_P\Phi_{PSII}$, where q_P (= $(F_M' - F(t))/(F_M' - F_0')$) is the coefficient of photochemical quenching which estimates a fraction of the so-called open PSII reaction centers; and that Φ_{PSII} (= $(F_M' - F_0')/F_M'$) is the maximal quantum yield of the PSII photochemistry for a light-adapted state. The F_0' in the last two equations is the minimal fluorescence level for a light-adapted state which was estimated from: $F_0' = F_0/((F_M - F_0)/F_M) + (F_0/F_M')$ (for details see [24]).

The changes in these Chl fluorescence parameters measured during acclimation of TER and END cultivars to 5°C for 21 days are shown in Figure 5. Φ_{P0} is affected very little by the cold acclimation of TER but there is a continual decrease in Φ_{P0} of END (Figure 5A). Φ_P initially decreases more in TER than in END but after 6 days it maintains its value in TER but continues to decrease in END (Figure 5B). The continual decrease in Φ_P in END is mostly caused by a continual decrease in Φ_{PSII}; q_P slightly increasing in the last two measurements in END (Figure 5B). On the other hand, the initial decrease in Φ_P in TER is mostly caused by decrease in

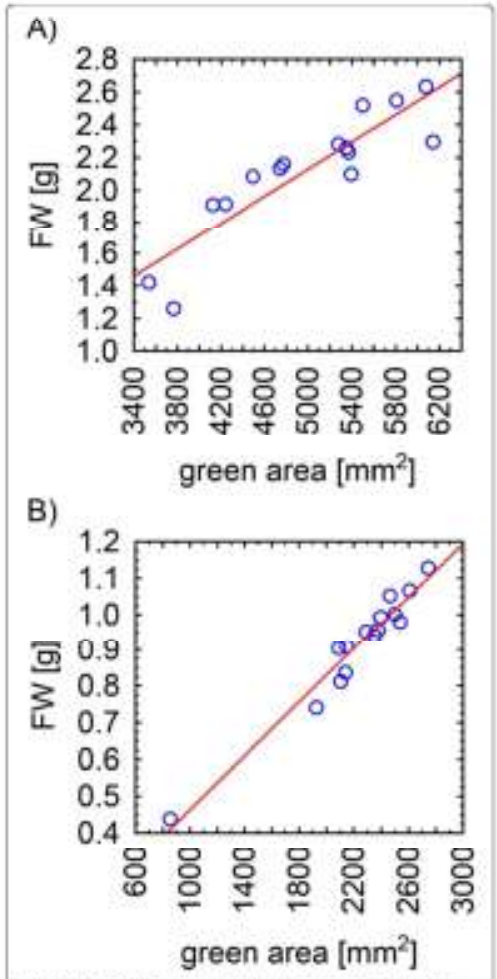

Figure 4 The correlation of the green area and biomass. The Spearmann correlation coefficients of FW and green area of TER cultivar **A)** and END cultivar **B)** were 0.91 and 0.96, respectively (p-value = 0.05).

q_p but the almost unchanged value of Φ_F in TER after 6 days is caused by the counter action of q_p which increases, and of Φ_{PSII}, which decreases (Figure 5B). Therefore, it can be concluded that photosynthesis of the two pea cultivars uses different strategies for cold acclimation. Whereas in END, the number of open reaction centers as well as their maximal photosynthetic quantum yield in light generally decrease with prolonged cold acclimation, in TER, a decrease of the maximal quantum yield of PSII photochemistry in light (Φ_{PSII}) is compensated by an increase of number of the open PSII reaction centers (q_p) (Figure 5B). Furthermore, END shows an increased quantum yield of constitutive non-light induced dissipation processes ($\Phi_{f, D}$) at the end of the cold acclimation compared to TER (Figure 5C), whereas the rise of the quantum yield of regulatory light-induced heat dissipation (Φ_{NPQ}) during the acclimation is faster in TER than in END (Figure 5D).

It is interesting to note that cold-induced changes of the Chl fluorescence parameters for given cultivar and differences (or about the same values) of the parameters between the cultivars (Figure 5) are not accompanied by expected changes and differences of green areas and growth rates (Figure 3). Even when the photosynthetic function was decreased by cold treatment (decrease of the Φ_{PSII}, Φ_F, q_p and Φ_{PSII} parameters; Figure 5A and 5B), the total and normalized green area of both cultivars was still increased (Figure 3A and 3B). It might show that the grow rate changed (for TER; Figure 3C) or decreased (for END; Figure 3C) with increasing duration of the cold treatment, however, these changes were not statistically significant (data not shown). The uncorrelated behavior of photosynthetic and growth parameters reflects different temperature dependences of photosynthesis and processes hidden behind the plant growth. While photosynthetic function was decreased by treatment of the cultivars at 5°C, probably much lower temperatures would be needed to stop plant growth. Therefore, FCIM data and RGB imaging data carry different and complementary information about acclimation of plants to lower temperatures. To take advantage of the high-throughput capacity of our phenotyping platform, we used a relatively short protocol to measure CFIN. This set up, however, did not allow for determination of photoinactivated centers which might be formed during a joint action of light and cold [25–28]. Depending on the theory used, the formation of the photoinactivated PSII centers can influence all quantum yields of the light-adapted state (for a review see [24]) used in this work. Therefore, in the next study we aim to modify the CFIN measuring protocol in order to determine the quantum yield of photoinsactivated PSII centers as well.

Furthermore, we tested the reliability and accuracy of the Chl fluorescence parameters measured by the automated CFIM in a high-throughput set up by comparing the selected parameter (Φ_{Fv}) with the same parameter measured by a hand-operated non-imaging Chl fluorometer. For this purpose the overall Chl fluorescence images were separated into images of the second and third leaves and their Φ_{Fv} were evaluated. On the other hand, Φ_{Fv} was evaluated from the fast Chl fluorescence rise as measured by the non-imaging Chl fluorometer with a different set of leaves (see Materials and methods). The results of these comparisons are presented in Figure 6A for the second leaves and in Figure 6B for the third leaves, respectively.

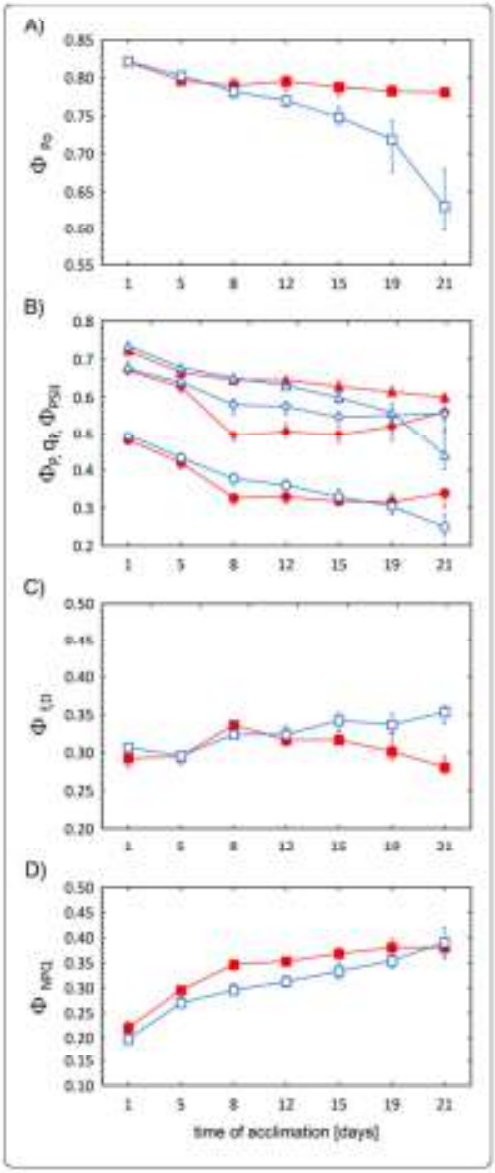

Figure 5 Changes of CFIN parameters of TER (full symbols) and END (open symbols) pea cultivars measured during the 21 days of cold acclimation. Changes in **A)** the maximal quantum yield of PSII photochemistry for a dark-adapted state (Φ_{P_0}); **B)** the maximal and the actual quantum yield of photosystem II photochemistry for a light-adapted state (Φ_{P_m}, Φ_P respectively), the coefficient of photochemical quenching (q_P); **C)** the quantum yield of constitutive non-light induced dissipation processes ($\Phi_{f,D}$); **D)** the quantum yield of regulatory light-induced heat dissipation (Φ_{NPQ}) are shown. The values represent medians from 15 measurements. The error bars represent quartiles. The medians of all the TER and END parameters at the end of measurements were statistically significant (p value < 0.05), except of q_P and Φ_{NPQ}.

A representative image of the spatial distribution of Chl fluorescence is presented in Figure 6C. Not surprisingly, the data show that there is no statistically significant difference (at $p < 0.05$) between Φ_{P_0} measured for given leaves by the two different approaches. Moreover, Figure 6C documents another advantage of using the CFIM in automated high-throughput platforms. Although the software is primarily adjusted to calculate the mean value of fluorescence from the total surface of every plant, if needed, the CFIN images can be later separated for subsequent calculation of the Chl fluorescence parameters taken from the individual selected areas which represent individual plant parts (Figure 6C).

To the best of our knowledge, only one study was published reporting on use of CFIM integration into a high-throughput phenotyping platform to analyze cold- or chilling-stress. Using an automated phenotyping platform Jansen et al. [14] evaluated only the F_V/F_M parameter (Φ_{P_0}) for two different *Arabidopsis* plants (wild-type and a mutant), and wild-type tobacco plants. Φ_{P_0} decreased in the wild-type tobacco plants during the cold treatment, and the same decreasing trends were found with *Arabidopsis* plants. however, the differences between the wild-type and a mutant were not convincing. Using a CFIM system, Lootens et al. and Devacht et al. [25,29] studied the effect of different cold temperatures on industrial chicory plants. In agreement with our results, the authors found again only a small decrease of Φ_{P_0} after 10-day incubation at 4°C and the values of the Φ_P and Φ_{PSII} parameters caused by the incubation were similar to those obtained in our study. Mishra et al. [30,31] used CFIM to study the effect of a two-week incubation at 4°C on nine *Arabidopsis thaliana* accessions differing in cold tolerance. In addition to evaluation of standard Chl fluorescence parameters, like Φ_{P_0}, Φ_P, and q_P, the authors also showed that combinatorial imaging of Chl fluorescence transients combined with classifier and feature selection methods could discriminate between detached leaves from cold sensitive and cold tolerant accessions.

Materials and methods

Plant material

Two morphologically similar field pea (*P. sativum* subsp. *sativum* var. *sativum*) cultivars Terno (TER) and Enduro

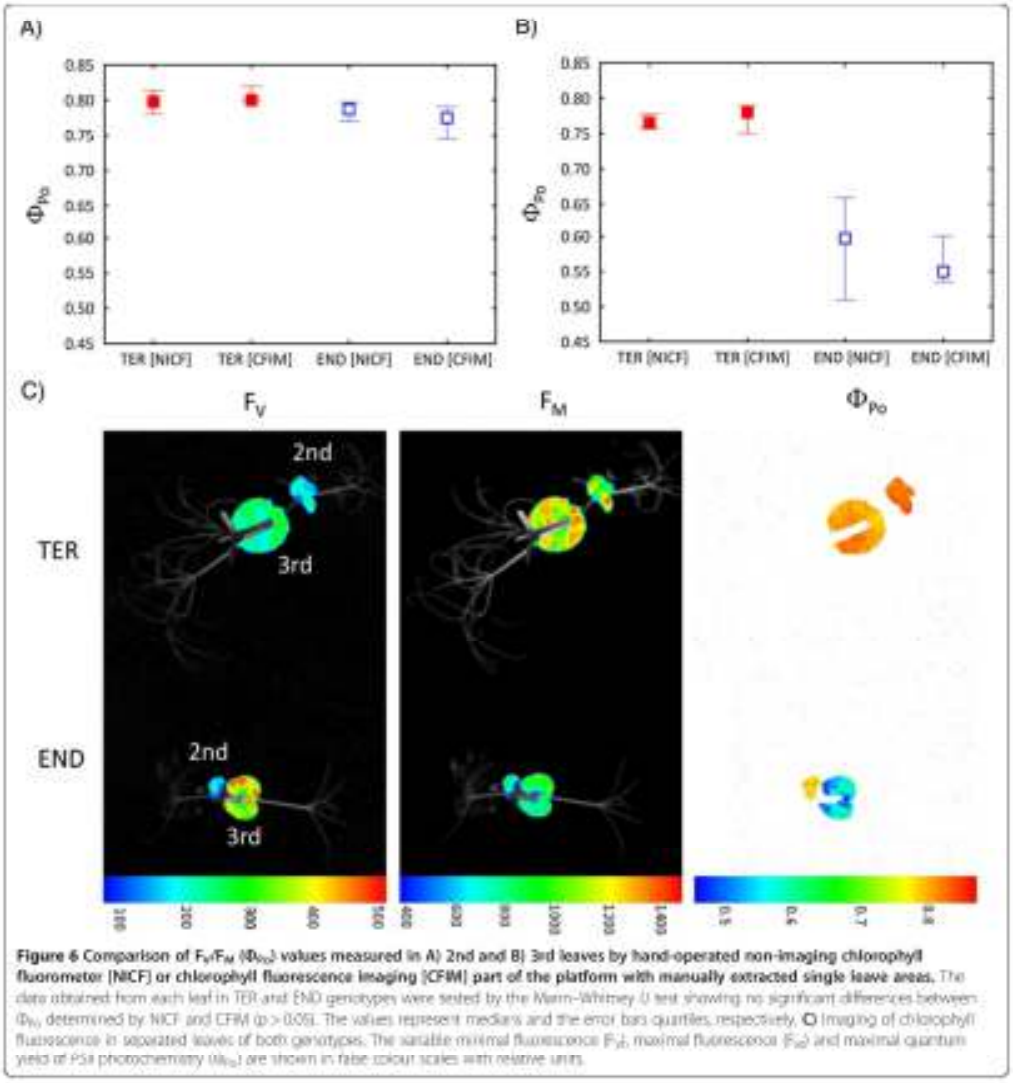

Figure 6 Comparison of F_V/F_M (Φ_{Po}) values measured in A) 2nd and B) 3rd leaves by hand-operated non-imaging chlorophyll fluorometer [NICF] or chlorophyll fluorescence imaging [CFIM] part of the platform with manually extracted single leave areas. The data obtained from each leaf in TER and END genotypes were tested by the Mann–Whitney *U* test showing no significant differences between (Φ_{Po} determined by NICF and CFIM ($p > 0.05$). The values represent medians and the error bars quartiles, respectively. **C** Imaging of chlorophyll fluorescence in separated leaves of both genotypes. The variable minimal fluorescence (F_V), maximal fluorescence (F_M) and maximal quantum yield of PSII photochemistry (Φ_{Po}) are shown in false colour scales with relative units.

(END) were used in the experiment. TER is pea cultivar, used for spring sowing term with a certain capacity to cold-acclimation, whereas END is a cold-tolerant over-wintering cultivar. The END cultivar was obtained from the Selgen a.s. company (Prague, Czech Republic). The TER cultivar was taken from the Czech collection of pea genetic resources kept in Agritec Ltd., Šumperk, Czech Republic. The collection is run according to the general rules of the National Programme for Plant Genetic Resources of the Czech Republic and the passport data are available on http://genbank.vurv.cz/genetic/resources/.

Cultivation conditions and experimental setup

The TER and END pea cultivars were sown into standardized pots (65 x 65 x 95 mm, Plant-It-Rite, Australia) filled with 100 g of soil (Substrate 2, Klasmann-Deilmann

GmbH, Germany) and watered to full water capacity. The seeds were germinated in mini-greenhouses (50 x 32 x 6 cm with clear plastic lid) in a growth chamber with white LED lighting (150 μmol photons of PAR m^{-2} s^{-1}). The conditions were set-up to simulate a long day (16 h day, 8 h night) with temperatures of 22°C during the light period and 20°C in the night. The relative humidity was set to 60%. After the development of the first true leaves, the temperature was decreased to 5°C for the entire experiment, the other parameters remained unchanged. The plants were regularly watered with the same amount of water. Fifteen seedlings from each cultivar were used for the automated phenotyping, and another fifteen plants were used for control measurements of maximal quantum yield of PSII photochemistry through the use of a hand-operated non-imaging Chl fluorometer. For measurements in PlantScreen™ phenotyping platform (Photon Systems Instruments, Brno, Czech Republic), the pots with the seedlings were placed in standardized trays; two pots per tray and automatically loaded and measured by the platform. The movement of the trays was performed by a robotic-driven conveyor belt that routinely transferred experimental plants between the growing and measuring areas according to a user-defined protocol. A single measuring round of 8 trays consisted of 20 minutes of dark-adaptation, followed by the measurement of Chl fluorescence and digital RGB imaging from three optical projections. Approximately 16 plants per hour were analyzed, due to the length of the measuring round that is dependent on the length of the dark adaptation and CFIM measurement. In the case of RGB imaging the platform throughput increases to about 60 experimental trays (120 plants) per hour. The data from Chl fluorescence and RGB imaging were stored in a database server, and analyzed either by the software provided by the manufacturer or by the software developed by the authors of this study as described below.

RGB software image analysis

The plants were automatically loaded into the measuring cabinets of the PlantScreen™ platform where the three RGB images – the top, front, and side views – (Figure 1) of each experimental tray containing two plants were taken. To assess the total green area, the green mask of the individual plants has to be found in the image. To this end, we used a combination of automatic thresholding procedures and automatic edge detection techniques. First, the image was converted from the RGB colour space into the HSV colour space. It is much easier to find the green mask in the H channel of the HSV colour space because the S and V channels only contain information on the saturation and brightness of the colour but not the hue itself. The region in the three dimensional RGB space which defines the 'plant green' colour may have a rather complicated shape, however, it is reduced to a line-segment in the one-dimensional H space as the S and V coordinates can be ignored. For thresholding in the H channel, several standard automatic algorithms can be used, e.g., the most popular Otsu method [32] that calculates the optimum threshold separating the foreground and background pixels so that their combined intra-class variance is minimal. In our case, we used an even simpler technique - foreground (i.e., the plant) was predefined as a particular line segment in the H channel. This was possible due to the standardized image acquisition setting.

The thresholding step usually provides very good discrimination between the plant and its background and no further processing is necessary. However, the pea plants possess very thin offshoots (only one or two pixels thick) that may be difficult to find by thresholding alone. If the thresholding routine makes a single-pixel mistake, which often happens due to noise in the image, the entire offshoot is lost, which is undesirable. We solved this problem by exploiting the Canny automatic edge detection algorithm which tracks the contours of the plant image [33]. The thin offshoots were tracked particularly well because the edge detection algorithm focused on such thin structures. The results of the thresholding step were then combined with the edge detection step and the final green mask of the object was found. Finally, a couple of post processing steps were performed (e.g. median filtering and image opening and/or closing) to enhance the quality of the mask.

It only took several seconds on a standard PC to find the green mask of a single pea plant. The mask provided information about the projection of the plant surface area onto the three image planes. The projections can be expressed in square millimeters because the RGB camera had been calibrated beforehand. The calibration proceeded as follows. Two bars covered by millimeter paper were placed in the pots instead of the pea plants. The bars were approximately the same height as the plants. Three images (top, front, side) of the two bars were acquired with the same camera setting used for the entire experiment. These images served as the standard for converting the leaf area from pixels to square millimeters. The total green area of the plant is then estimated as $A = \sqrt{(A_x^2 + A_y^2 + A_z^2)}$, where A_x, A_y, and A_z are the respective projections onto the three image planes. This procedure is naturally not precise but it gives an estimate which is in good correlation (Figure 4) with the fresh biomass of the above ground plant parts.

CFIM and non-imaging Chl fluorescence measurements

A standard protocol was used for the measurement of Chl fluorescence quenching using the CFIM part of the PlantScreen™ platform. The plants underwent 20 – 40 minutes of dark adaptation before CFIM measurements. During all signal recordings, short (33.3 μs) red (650 nm) "measuring" flashes were applied and a Chl fluorescence signal was detected a few microseconds before the measuring flash and

during the flash, and then the two signals were substracted. This is a pulse amplitude modulation (PAM) type of measurement. To measure the minimal fluorescence for a dark-adapted state, F_0, only the measuring flashes were applied for an initial 5 seconds. Then, a saturation pulse of 800 ms duration (white light, intensity of 1000 μmol photons of PAR m^{-2} s^{-1}) was applied and the maximal fluorescence for a dark-adapted state, F_M, was measured. After the F_M measurement, fluorescence was kept relaxed in darkness for 17 seconds. Red actinic light (650 nm, intensity of 100 μmol photons m^{-2} s^{-1}) was then switched on for 70 seconds to drive photosynthesis. It was visually checked so that a steady state fluorescence signal was attained at 70 s of illumination. During the actinic illumination, saturation pulses were applied at 8, 18, 28, 48, and 68 seconds from the beginning of the actinic illumination. The value of the maximal fluorescence measured during the last saturation pulse was taken as the maximal fluorescence signal for the light-adapted state, F_M'. The fluorescence signal caused by the actinic illumination measured just before the last saturation pulse was taken as the steady state fluorescence for a light-adapted state, F (t). The four fluorescence levels (F_0, F_M, F (t), F_M') were used for calculation of the minimal fluorescence level for a light-adapted state, F_0', the quantum yields, and the other fluorescence parameters as defined and described in the Results section.

A hand-operated FluorPen fluorometer (Photon Systems Instruments, Brno, Czech Republic) was used for control measurements in order to compare the results obtained using automatized CFIM with hand-operated non-imaging Chl fluorescence measurements. Blue light (455 nm) of intensity 1000 μmol photons m^{-2} s^{-1} and a duration of 1 second was used by FluorPen for illumination of the sample and a whole fast fluorescence rise (the O-J-I-P curve) was recorded. However, only the minimal and maximal fluorescence levels, F_0 and F_M, respectively, for the dark adapted state, were evaluated from the curve using built-in routines. The two fluorescence levels were used for calculation of the maximal quantum yield of PSII photochemistry (see Results). The data for Chl fluorescence measurements are presented as medians and lower and upper quartiles [34].

Conclusion

In this proof-of-concept study, the high-throughput method for automated screening of cold-tolerant pea (*Pisum sativum* L.) cultivars was designed. TER and END cultivars were screened simultaneously in an automated way with throughput of 16 plants per hour for i) growth of the aerial parts by RGB imaging and ii) for the efficiency of photosynthesis by chlorophyll fluorescence imaging. We demonstrated that the presented integrative approach based on analyses of differences in relative growth rate and selected CFIM parameters can provide deeper insight into the physiological base of cold-acclimation. Data from both analytical tools pointed to significant differences in the growth and photosynthesis of TER and END cultivars, and indicated that the two pea cultivars use different strategies for cold acclimation differing in number of open PSII reaction centers, their maximal photosynthetic quantum yield in light and quantum yield of constitutive non-light induced dissipation processes. The reliability of the screening was verified by independent measuring of the fresh weight of the shoots and by Chl fluorescence measurement by hand fluorometer. Since the CFIM analysis is not limited to plant morphology and our image analysis was sensitive enough to detect tiny tendrils of pea, we believe that the described procedure can be easily employed for shoot analyses of other different plant species.

Abbreviations

Chl: Chlorophyll; CFIM: Chlorophyll fluorescence imaging; CFIN: Chlorophyll fluorescence induction; END: Endura; F_0 and F_0': Minimal chlorophyll fluorescence levels for dark- and light-adapted states, respectively; F_M and F_M': Maximal chlorophyll fluorescence levels for dark- and light-adapted states, respectively; FW: Fresh weight; F (t): Actual (at time t; usually in the steady state) fluorescence level for light-adapted state; F_v: Variable chlorophyll fluorescence level for a dark-adapted state; Φ_{PSII}: The maximal quantum yield of photosystem II photochemistry for a dark-adapted state; Φ_F: The actual quantum yield of photosystem II photochemistry for a light-adapted state; Φ_{PSII}': The maximal quantum yield of photosystem II photochemistry for a light-adapted state; Φ_{NPQ}: The quantum yield of constitutive non-light induced (basal or dark) dissipation processes consisting of fluorescence emission and heat dissipation; Φ_{NPQ}: The quantum yield of regulatory light-induced heat dissipation; GA: Green area; NIDF: Non-imaging chlorophyll fluorescence fluorometer; NGA: Normalized green area; RGB: Red-green-blue; RGR: Relative growth rate; PAM: Pulse-amplitude modulation; PAR: Photosynthetic active radiation; PSII: Photosystem II; q_P: The coefficient of photochemical quenching; TER: Terno.

Competing interests

The authors declare that they have no competing interests.

Authors' contributions

JH and OL carried out the visible and fluorescence imaging analysis, data processing and interpretation, participated in the design of the study and drafted the manuscript. TF developed and carried out the software image analysis, data processing, performed the statistical analysis, and drafted the manuscript. AH carried out the visible and fluorescence imaging analyses, data processing and interpretation, participated in the design of the study and drafted the manuscript. MH contributed to the design of the study, and helped to draft the manuscript. LS conceived the study, participated in its design and coordination and drafted the manuscript. All authors read and approved the final manuscript.

Acknowledgments

This work was supported by the grant No LO1204 (Sustainable development of research in the Centre of the Region Haná) from the National Program of Sustainability I, Ministry of Education, Youth and Sports, Czech Republic. AH. was supported by the Operational Program Education for Competitiveness - European Social Fund (project CZ.1.07/2.3.00/20.0165).

Author details

[1]Department of Chemical Biology and Genetics, Centre of the Region Haná for Biotechnological and Agricultural Research, Faculty of Science, Palacký University, Šlechtitelů 11, Olomouc CZ-78371, Czech Republic. [2]Department of Biophysics, Centre of the Region Haná for Biotechnological and Agricultural Research, Faculty of Science, Palacký University, Šlechtitelů 11, Olomouc CZ-78371, Czech Republic. [3]Department of Mathematical Analysis and Applications of Mathematics, Faculty of Science, Palacký University, 17. listopadu 12, Olomouc CZ-77146, Czech Republic. [4]Department of Genetic

Resources for Vegetables, Medicinal and Special Plants, Centre of the Region Haná for Biotechnological and Agricultural Research, Crop Research Institute, Šlechtitelů 11, Olomouc CZ-78371, Czech Republic.

Received: 15 October 2014 Accepted: 2 March 2015
Published online: 19 March 2015

References

1. Xin Z, Browse J. Cold comfort farm: the acclimation of plants to freezing temperatures. Plant Cell Environ. 2000;23:893–902.
2. Stoddard FL, Balko C, Erskine W, Khan HR, Link W, Sarker A. Screening techniques and sources of resistance to abiotic stresses in cool-season food legumes. Euphytica. 2006;147:167–86.
3. Maqbool A, Shafiq S, Lake L. Radiant frost tolerance in pulse crops – a review. Euphytica. 2010;172:1–12.
4. Verhoeven A. Sustained energy dissipation in winter evergreens. New Phytol. 2014;201:57–65.
5. Markarian D, Harwood RR, Rowe PR. The inheritance of winter hardiness of Pisum. II. Description and release of advance generation breeding lines. Euphytica. 1968;17:110–3.
6. Silim SN, Hebblethwaite PD, Heath MC. Comparison of the effects of autumn and spring sowing date on growth and yield of combining peas (Pisum sativum L.). J Agri Sci. 1985;104:35–46.
7. Yordanov I, Georgieva K, Tsonev T, Velikova V. Effect of cold hardening on some photosynthetic characteristics of pea (Pisum sativum L. CV. RAN 1) plant. Bulg J Plant Physiol. 1996;22:13–21.
8. Georgieva K, Lichtenthaler HK. Photosynthetic activity and acclimation ability of pea plants to low and high temperature treatment as studied by means of chlorophyll fluorescence. J Plant Physiol. 1999;155:416–23.
9. Georgieva K, Lichtenthaler HK. Photosynthetic response of different pea cultivars to low and high temperature treatments. Photosynthetica. 2006;44:569–78.
10. Berger B, de Regt B, Tester M. High-throughput phenotyping of plant shoots. In: Normanly J, editor. High-throughput phenotyping in plants. New York City: Humana Press; 2012. p. 9–20.
11. Petrozza A, Santaniello A, Summerer S, Di Tommaso G, Di Tommaso D, Paparelli E, et al. Physiological responses to Megafol® treatments in tomato plants under drought stress: a phenomic and molecular approach. Sci Hortic (Amsterdam). 2014;174:185–92.
12. Pereyra-Irujo GA, Gasco ED, Peirone LS, Aguirrezábal LA. GlyPh: a low-cost platform for phenotyping plant growth and water use. Funct Plant Biol. 2012;39:905–13.
13. Chaerle L, Hagenbeek D, Vanrobaeys X, Van Der Straeten D. Early detection of nutrient and biotic stress in Phaseolus vulgaris. Int J Remote Sens. 2007;28:3479–92.
14. Jansen M, Gilmer F, Biskup B, Nagel KA, Rascher U, Fischbach A, et al. Simultaneous phenotyping of leaf growth and chlorophyll fluorescence via GROWSCREEN FLUORO allows detection of stress tolerance in Arabidopsis thaliana and other rosette plants. Funct Plant Biol. 2009;36:902–14.
15. Hairmansis A, Berger B, Tester M, Roy SJ. Image-based phenotyping for non-destructive screening of different salinity tolerance traits in rice. Rice. 2014;7:16.
16. Hoffmann WA, Poorter H. Avoiding bias in calculations of relative growth rate. Ann Bot London. 2002;90:37–42.
17. Bourion V, Lejeune-Hénaut I, Munier-Jolain N, Salon C. Cold acclimation of winter and spring peas: carbon partitioning as affected by light intensity. Eur J Agron. 2003;19:535–48.
18. Honsdorf N, March TJ, Berger B, Tester M, Pillen K. High-throughput phenotyping to detect drought tolerance qtl in wild barley introgression lines. PLoS One. 2014;9:e97047.
19. Fehér-Juhász E, Majer P, Sass L, Lantos C, Csiszár J, Turóczy Z, et al. Phenotyping shows improved physiological traits and seed yield of transgenic wheat plants expressing the alfalfa aldose reductase under permanent drought stress. Acta Physiol Plant. 2014;36:663–73.
20. Rajendran K, Tester M, Roy SJ. Quantifying the three main components of salinity tolerance in cereals. Plant Cell Environ. 2009;32:237–49.
21. Harris BN, Sadras VO, Tester M. A water-centred framework to assess the effects of salinity on the growth and yield of wheat and barley. Plant Soil. 2010;336:377–89.
22. Golzarian MR, Frick RA, Rajendran K, Berger B, Roy S, Tester M, et al. Accurate inference of shoot biomass from high-throughput images of cereal plants. Plant Methods. 2011;7:1–11.
23. Schilling RK, Marschner P, Shavrukov Y, Berger B, Tester M, Roy SJ, et al. Expression of the Arabidopsis vacuolar H+-pyrophosphatase gene (AVP1) improves the shoot biomass of transgenic barley and increases grain yield in a saline field. Plant Biotechnol J. 2014;12:378–86.
24. Lazár D. Parameters of photosynthetic energy partitioning. J Plant Physiol. 2015;175:131–47.
25. Lootens P, Devacht S, Baert J, Van Waes J, Van Bockstaele E, Roldán-Ruiz I. Evaluation of cold stress of young industrial chicory (Cichorium intybus L.) by chlorophyll a fluorescence imaging. II. Dark relaxation kinetics. Photosynthetica. 2011;49:185–94.
26. Somersalo S, Krause GH. Reversible photoinhibition of unhardened and cold-acclimated spinach leaves at chilling temperatures. Planta. 1990;180:181–7.
27. Liu P, Meng QW, Zou Q, Zhao SJ, Liu QZ. Effects of cold hardening on chilling induced photoinhibition of photosynthesis and on xanthophyll cycle pigments in sweet pepper. Photosynthetica. 2001;39:467–72.
28. Hogewoning SW, Harbinson J. Insights on the development, kinetics, and variation of photoinhibition using chlorophyll fluorescence imaging of a chilled, variegated leaf. J Exp Bot. 2007;58:453–63.
29. Devacht S, Lootens P, Baert J, Van Waes J, Van Bockstaele E, Roldán-Ruiz I. Evaluation of cold stress of young industrial chicory (Cichorium intybus L.) plants by chlorophyll a fluorescence imaging. I. Light induction curve. Photosynthetica. 2011;49:161–71.
30. Mishra A, Mishra KB, Höermiller II, Heyer AG, Nedbal L. Chlorophyll fluorescence emission as a reporter on cold tolerance in Arabidopsis thaliana accessions. Plant Signal Behav. 2011;6:301.
31. Mishra A, Heyer AG, Mishra KB. Chlorophyll fluorescence emission can screen cold tolerance of cold acclimated Arabidopsis thaliana accessions. Plant Methods. 2014;10:38.
32. Otsu N. A threshold selection method from gray-level histograms. IEEE T Syst Man Cyb. 1979;9:62–6.
33. Canny JA. Computational approach to edge detection. IEEE T Pattern Anal. 1986;8:679–98.
34. Lazár D, Nauš J. Statistical properties of chlorophyll fluorescence parameters. Photosynthetica. 1998;35:121–7.